

DAILY RAINFALL-RUNOFF MODELING USING ARTIFICIAL NEURAL NETWORK

A THESIS

*Submitted in fulfilment of the
requirements for the award of the degree*

of

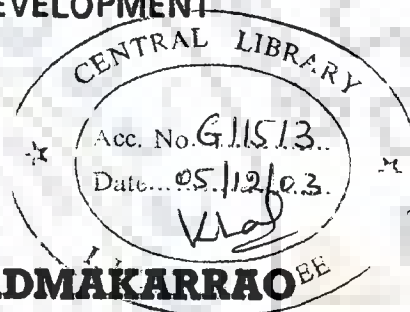
DOCTOR OF PHILOSOPHY

in

WATER RESOURCES DEVELOPMENT

By

RAJURKAR MILIND PADMAKARRAO



WATER RESOURCES DEVELOPMENT TRAINING CENTRE
INDIAN INSTITUTE OF TECHNOLOGY ROORKEE
ROORKEE-247 667 (INDIA)

DECEMBER, 2002

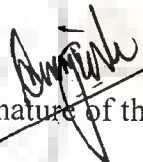


INDIAN INSTITUTE OF TECHNOLOGY
ROORKEE, ROORKEE – 247 667

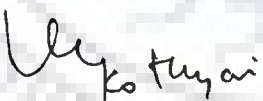
CANDIDATE'S DECLARATION


I hereby certify that the work which is being presented in the thesis entitled **DAILY RAINFALL-RUNOFF MODELING USING ARTIFICIAL NEURAL NETWORK** in fulfillment of the requirement for the award of the Degree of Doctor of Philosophy and submitted in the Water Resources Development and Training Centre of the Institute is an authentic record of my own work carried out during a period from July 1999 to December 2002 under the supervision of Dr. U.C. Chaube, Professor, Water Resources Development and Training Centre and Dr. U.C. Kothiyari, Associate Professor, Department of Civil Engineering.

The matter presented in this thesis has not been submitted by me for the award of any other degree of this or any other Institute/University.

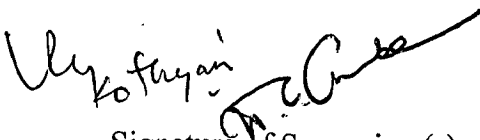

Signature of the Candidate

This is to certify that the above statement made by the candidate is correct to the best of my (our) knowledge.

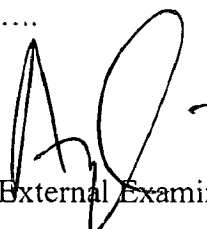
Date: Dec. 10, 2002

Signature of Supervisor
(Dr. U.C. Kothiyari)
Associate Professor
Dept. of Civil Engg.,
IIT Roorkee, Roorkee


Signature of Supervisor
(Dr. U.C. Chaube)
Professor
W.R.D.T.C.,
IIT, Roorkee, Roorkee

The Ph.D. Viva-Voce examination of **RAJURKAR MILIND PADMAKARRAO**,
Research Scholar, has been held on 27th May 2003


Signature of Supervisor(s)


Signature of H.O.D.


Signature of External Examiner

ABSTRACT

The models developed to simulate the rainfall-runoff process can be broadly grouped under three categories, with increasing order of complexities involved as: i) empirical; ii) conceptual; and iii) physically based distributed models. The first category of models, namely the empirical models treat the hydrologic system (*e.g.* a catchment) as a black box and try to find relationship between historical inputs and the outputs without considering the physical laws operating within it. The conceptual models, on the other hand, attempt to represent the known physical process occurring in the rainfall-runoff transformation in a simplified manner by way of linear/nonlinear mathematical formulations. The third category of models *i.e.* the physically based models, are too complex, data intensive and cumbersome to use. Typically, they involve solution of partial differential equations that represent the flow processes within the catchment. The kind of data required for use of the physically based distributed models is rarely available, even in the heavily instrumented research catchments. The physically based models and the conceptual models generally involve use of a number of parameters many of which are difficult to ascertain for catchments from different geographical and climatic regions.

Even though many types of models are presently available for representing rainfall-runoff process, the problem still remains unresolved and it is perhaps for this reason that the alternative modeling approaches are still being sought. The system theoretic modeling approach has been added with a new dimension through adoption of the Artificial Neural Network (*ANN*) technique in rainfall-runoff modeling. Many studies utilizing *ANNs* are reported in literature because they possess desirable attributes of universal approximation and have the ability to learn from examples without the need for explicit physics. An *ANN* is a massively parallel distributed information processing system, capable of learning any nonlinear relationship and because of which it has emerged as a viable tool for the simulation and control of complicated, nonlinear dynamic systems. Different types of *ANN* structures are developed for solving various types of problems.

The rainfall-runoff modeling using *ANNs* would have to be classified as the empirical modeling. The application of the *ANN* for rainfall-runoff modeling on various time scales has been carried out by many researchers. In most of these studies, the *ANN*

was used as an independent model and results obtained through its application were compared with those produced by the conventional models. In these studies the inputs to the *ANN* consisted of combinations of variable like current and antecedent rainfall and runoff values, temperature, snowmelt *etc.*

It is very well established from these studies that, the rainfall information alone is not sufficient to estimate the runoff accurately from a catchment, as the state of the catchment *i.e.* the antecedent soil moisture condition in a catchment plays an important role in determining the amount of runoff generated from the given rainfall. While, it is well established that the inclusion of the recently observed discharges with the current and antecedent rainfalls as inputs to the *ANN* greatly enhances the forecasting ability of the neural networks in the updating case, the present study investigates whether good estimates of observed discharges enhance the flow simulation efficiency in the non-updating case.

The inclusion of discharges observed in the past as input to the *ANN* based rainfall-runoff models makes it difficult to treat these models as cause-and-effect models. Such models are useful in forecasting problems but are not so useful in conceptualizing the catchment. The objective of the present study is to propose a modeling approach, which combines the linear/nonlinear models with the *ANN* so as to overcome the difficulties cited above, and explore the application of the neural networks for the non-updating flow simulation. The *ANN* model is therefore coupled with the system theoretic linear/nonlinear models such that output from these models forms an input to the *ANN*. The present study presents the *ANN* as a flexible nonlinear rainfall-runoff black box model, which is useful in sparse data scenario for the non-updating simulation of discharge from rainfall, using daily data for the case of isolated runoff events. An attempt is made to incorporate, as far as possible; the understanding of the physical process of runoff generation over a catchment in the *ANN* based rainfall-runoff modeling. The study also provides a viable alternative for the discharges observed in the past time periods, being used as one of the inputs to the *ANN* in most of the existing studies.

A methodology is developed using the *ANN* for rainfall-runoff modeling over a catchment when the hydrologic applications require that the runoff be predicted with the help of rainfall information alone and without much understanding of the hydrologic dynamics of the catchment being investigated. The capability and effectiveness of the proposed methodology in sparse data scenarios is demonstrated. The daily rainfall and

runoff data from seven catchments located in different parts of the world, two of which are relatively large in size, are used in the present study. These catchments are i) Bird Creek (USA), ii) Brosna (Ireland), iii) Garrapatas (Colombia), iv) Kizu (Japan), v) Pampanga (Philippines), vi) Krishna (India), and vi) Narmada (India).

Daily runoff and the corresponding rainfall data of the runoff events that occurred during the flood period only are modeled in the study as during flood period (monsoon season) high flows are experienced and modeling of which is important for flood forecasting, design and operation of water resources structures *etc.* The consideration of losses due to evaporation and evapotranspiration is important as the rainfall-runoff modeling carried out is on daily scale and the runoff events are spread over several days. The observed rainfall subtracted with the losses due to evaporation and evapotranspiration is called here as the *Effective Rainfall*, which is the actual rainfall that is contributing into the process of runoff generation over any catchment. Determination of the catchment memory length is the critical part of the system based rainfall-runoff modeling in which current and antecedent rainfall values are used as input. The memory of a catchment is determined adopting the two-step procedure consisting of i) correlation analysis, and ii) determination of ordinates of response function of the catchment. Appropriate linear/nonlinear model depending upon the size of the catchment is employed for determining the response function ordinates. The method of least squares and the smoothed least squares method are used in deriving the response functions for the different catchments.

Two of the catchments being relatively large in size involve sub-divisions into smaller hydrologically homogeneous areas to account for the heterogeneity in the spatial distribution of rainfall. The application of the neural networks in case of large size catchments in the context of incorporating the distributed nature of input, *i.e.* the areal disaggregation of the rainfall is also demonstrated in the present study.

An *ANN* model based on a feedforward neural network; with the logistic sigmoid function as the transfer function, and single hidden layer is used for modeling the daily rainfall-runoff relationship. The application of the three layer feedforward *ANN* is specifically made to account for the non-linearity present in the rainfall-runoff process. The non-linearity of the runoff distribution over all the catchment is verified by using the measure of non-linearity introduced by Rogers, known as the Standardized Peak

Discharge Distribution (*SPDD*). The *ANN* application involves two different input combinations:

Case-I: Only the output of the linear/nonlinear model computed through the convolution of the derived response functions with the current and antecedent rainfalls is given as input to the *ANN*.

Case-II: The current and antecedent rainfall values for the length equal to memory of the catchment are also supplied as input to the *ANN* in addition to the input used in Case-I.

The output of the system based linear model is denoted by *RIL* and that of a nonlinear model by *RIN*. The total number of runoff events identified in a catchment are divided into two sets. About 70% of the data is used in training and the remaining values of the data (approximately 30% of data) are used as the testing set. A data normalization procedure is adopted before presenting the data to the *ANN* because, the logistic sigmoid used as the transfer function for neurons in the hidden and the output layers has bounded output range in the interval $[0, 1]$. The backpropagation algorithm involving a forward and the backward pass is used for training the network. The *TRAINGDX* function in *MATLAB* routines, which works on gradient descent method and uses the adaptive learning and momentum parameter, is used for training. The various input combinations to the *ANN* consisted of (i) Only rainfall (*P*); (ii) Output of linear model (*RIL*); (iii) Output of the nonlinear model (*RIN*); (iv) *P* in combination with *RIL*; (v) *P* in combination with *RIN*; and (vi) *P* in combination with runoff observed in the previous time period (Q_{t-1}). The *ANN* with these different inputs is applied to each of the catchment. It was ensured that the trial and error process of training the *ANN* leads to an optimal network configuration having the best possible performance without the network getting overtrained.

The performance of the models applied in the present study (the linear/nonlinear and the *ANN* models) is evaluated based on the various statistical and graphical criteria, which are indicative of the model performance.

The results obtained demonstrate that the proposed alternative for discharges observed in the past in the form of the output of the linear/nonlinear models provides better system theoretical representation of the rainfall-runoff relationship on catchments from different parts of the world investigated in the study. The results of the *ANN* model application in case of large size catchments prove that it is worthwhile to consider separate

inputs into the sub-catchments (to a point) in order to improve the model efficiency. The input scenarios of P in combination with RIL or RIN are clearly superior to the RIL alone or RIN alone input scenario. Replacing the linear model with a nonlinear model did not result in any substantial improvement in the final results of the ANN , thus validating the claim that ANN completely takes care of the non-linearity existing in the rainfall-runoff relationship. The coupled $SLM - ANN$ model with input scenario involving P in combination with RI is capable of producing reasonably satisfactory non-updated estimates of the outflows on most of the catchments.

The response functions obtained for different catchments studied have physically realistic shapes. Parameterization of these response functions by using the discrete gamma function leads to the establishment of relations, albeit qualitatively, between these parameters and the catchment characteristics. So the proposed approach can possibly be extended to the catchments for which the gauge and discharge records are nonexistent. The $ANNs$ trained on similar catchments can possibly be used for predicting the runoff over an ungauged catchment as the response function derived as above when convoluted with current and antecedent rainfalls in an ungauged catchment results in the estimates of runoff from a system based model which forms the input to a trained ANN as both are coupled. However, application of the proposed approach for runoff estimation could not be tested in an ungauged catchment in the present study because of non-availability of elaborate data.

ACKNOWLEDGEMENTS

I would like to acknowledge all the people who have been of help and assisted me throughout my research.

I remain indebted with gratitude to my supervisor Dr. U.C. Chaube, Professor, Water Resources Development and Training Centre, for his guidance, encouragement, and valuable suggestions throughout the course of this research work. My other supervisor Dr. U.C. Kothyari, Associate Professor, Department of Civil Engineering has been of great help during the study. His guidance at each step, meticulous observations, pinpointed suggestions from time to time enabled in carrying out the research in more systematic manner. I acknowledge with gratitude the wholehearted support provided by him during this research work.

I sincerely thank both of my supervisors for their critical observations and suggestions during the finishing stages, which were extremely helpful in giving the final shape to the thesis.

I am extremely grateful to Prof. B.M. Naik (Ex.) Principal of my parent Institute for sponsoring me to pursue my Ph.D. studies and for his encouragement for pursuing higher studies. I also gratefully acknowledge the cooperation extended by Principal Dr. T.R. Sontakke and Dr. P.S. Charpe, Head, Department of Civil (W.M.) of my parent Institute.

I wish to express my indebtedness to Mr. Sunil Sharma and Mrs. Sharma Bhabhi for their help, encouragement and moral support during my stay at Roorkee.

I thankfully acknowledge the help by the fellow research scholars Dr. Bala Prasad, Mr N.K. Khullar, and Dr. M.K. Jain, Scientist C, NIH, Roorkee at various stages of the study. Special thanks are due to Mr. M.D. Patil, Mrs. and Mr. Harne, Mrs. and Mr. Lalit Awasthi, Mrs. and Mr. Ashwini Kumar, from Roorkee and my colleagues at S.G.G.S. College of Engineering and Technology, Nanded; Dr. A.U. Digraskar, Dr. M.L. Waikar, Dr. P.D. Dahe, and Shri Rajesh Jamkar, for their encouragement and moral support.

Shri Kaka Selukar had relieved me from the worries of Tax calculations during these years; I sincerely thank him for his help.

The assistance provided by the staff of W.R.D.T.C. is thankfully acknowledged. I need to have a special mention of Mr. Mohd. Furqan Ullah, Librarian, NIH, Roorkee who provided access to the literature collected during various stages of study. I extend my wholehearted thanks to him.

My parents, brothers, sister, in-laws, and all the near and dear family members have provided me unfailing moral support and constant encouragement in pursuing higher studies. The continued blessings received from them are acknowledged with deep sense of gratitude.

The continued loving care, emotional support and suggestions by my wife Sow. Archana, who pursued her Ph.D. simultaneously are my profound lasting memories. I would not have completed this work successfully without her help, and support in managing day-to-day activities. My only daughter Aishwarya who is eight years old needs a special mention. Time spent with her was helpful in reducing the mental stress to a great extent. She was a source of energy during the stay at Roorkee and the driving force to carry on the work.

I dedicate this thesis to Parampujya Swami Varanand Bharati (Lovingly called as Appa) a visionary, who was my mentor, inspiration, and a steering force in my life. I joined IIT Roorkee only because of him. His inner desire and continuous motivation in bringing out the best of every individual made me to sustain the hardship faced during the research work. His discourse and advise had a deep impact on my life and inculcated a sense of honesty in me. I remain indebted to him forever.

The acknowledgement would be incomplete without mention of the blessings of The Almighty, which helped me in keeping high moral during difficult period. I shall remain obliged to the Almighty forever.

(Milind Padmakarrao Rajurkar)

TABLE OF CONTENTS

	Page No.
<i>Candidate's Declaration</i>	
<i>Abstract</i>	<i>i</i>
<i>Acknowledgements</i>	<i>vi</i>
<i>Table of Contents</i>	<i>viii</i>
<i>List of Figures</i>	<i>xii</i>
<i>List of Tables</i>	<i>xv</i>
<i>List of Notations and Symbols</i>	<i>xvii</i>
Chapter –1 INTRODUCTION	1
1.1 GENERAL	1
1.2 THE RAINFALL-RUNOFF PROCESS	2
1.3 MODELING OF THE RAINFALL-RUNOFF PROCESS	3
1.4 THE ARTIFICIAL NEURAL NETWORK	5
1.5 BACKGROUND OF THE STUDY	6
1.6 OBJECTIVES OF THE PRESENT STUDY	7
1.7 PRESENTATION OF THE STUDY	8
Chapter –2 REVIEW OF LITERATURE	10
2.1 PHYSICALLY BASED OR PROCESS BASED MODELS	11
2.2 CONCEPTUAL MODELS FOR RAINFALL-RUNOFF PROCESS	12
2.3 LINEAR MODELS FOR EXCESS RAINFALL-DIRECT RUNOFF PROCESS	14
2.3.1 Methods of Deriving UH for Single Storm Event	16
2.3.2 Methods of Deriving UH for Multi Storm Event	16
2.3.3 Relating UH Parameters with the Catchment Characteristics	17
2.4 LINEAR MODELS FOR TOTAL RAINFALL-TOTAL RUNOFF PROCESS	18
2.5 CATCHMENT NON-LINEARITY	20
2.6 NONLINEAR BLACK BOX MODELS FOR RAINFALL- RUNOFF PROCESS	22
2.7 ARTIFICIAL NEURAL NETWORK THEORY	23

2.8	MATHEMATICAL ASPECTS OF <i>ANN</i>	24
2.9	CLASSIFICATION OF <i>ANN</i>	26
2.9.1	Feedforward Backpropagation Network	26
2.9.2	Recurrent Neural Networks	29
2.9.3	Radial Basis Function Network	29
2.9.4	Cascade Correlation Algorithm	30
2.9.5	Self-Organizing Feature Maps	30
2.10	IMPORTANT ASPECTS OF <i>ANN</i> MODELING	31
2.10.1	Selection of Input and Output Variables	31
2.10.2	Data Normalization	32
2.10.3	Designing a Network	32
2.10.4	Training the Network	32
2.10.5	Strengths and Limitations	33
2.11	<i>ANN</i> APPLICATIONS IN HYDROLOGY AND WATER RESOURCES ENGINEERING	35
2.12	<i>ANN</i> APPLICATIONS IN RAINFALL-RUNOFF MODELING	37
2.13	CONCLUDING REMARKS	52
Chapter -3	HYDROLOGIC DATA	58
3.1	INTRODUCTION	58
3.2	EVENT IDENTIFICATION	59
3.3	THE NARMADA CATCHMENT	61
3.3.1	Catchment Representation	63
3.4	THE KRISHNA CATCHMENT	66
3.4.1	Catchment Representation	67
3.5	OTHER CATCHMENTS	69
3.5.1	The Bird Creek Catchment	69
3.5.2	The Brosna Catchment	69
3.5.3	The Garrapatas Catchment	71
3.5.4	The Kizu Catchment	71
3.5.5	The Pampanga Catchment	71
3.6	DETERMINATION OF EFFECTIVE RAINFALL	72

Chapter –4	MODELING APPROACH	76
4.1	INTRODUCTION	76
4.2	METHODOLOGY	78
4.3	DETERMINATION OF MEMORY OF THE CATCHMENT	79
4.3.1	Correlation Analysis	80
4.3.2	Determination of the Response Function	81
4.4	ASSESSMENT OF THE CATCHMENT NON-LINEARITY	85
4.5	PROPOSED COUPLING OF AUXILIARY LINEAR/NONLINEAR MODELS AND THE <i>ANN</i>	86
4.5.1	Normalization of Inputs for <i>ANN</i>	88
4.5.2	Proposed Inputs to the <i>ANN</i>	89
4.5.3	Training the Network	91
4.6	ALTERNATE INPUTS TO THE <i>ANN</i>	93
4.6.1	Only Rainfall (<i>P</i>)	94
4.6.2	Q_{t-1} and Rainfall	94
4.6.3	RI_t , RI_{t-1} , and Rainfall	94
4.7	PARAMETERIZATION OF THE RESPONSE FUNCTIONS	94
4.8	PERFORMANCE EVALUATION CRITERIA	96
4.9	CONCLUDING REMARKS	99
Chapter –5	LINEAR AND NONLINEAR MODEL APPLICATION – RESULTS AND DISCUSSIONS	100
5.1	INTRODUCTION	100
5.2	IDENTIFICATION OF THE HYDROLOGIC NON-LINEARITY	100
5.3	DETERMINATION OF THE RESPONSE FUNCTION	105
5.3.1	Response Functions For Catchments Without Sub-Divisions	105
5.3.2	Response Functions For Catchments Involving Sub-Divisions	106
5.4	APPLICATION OF THE LINEAR AND NONLINEAR MODELS	108
5.4.1	Linear and Nonlinear Model Application to Catchments Without Sub-Divisions	113
5.4.2	Application of Linear and Nonlinear Models to Catchments With Sub-Divisions	126
5.5	PARAMETERIZATION OF THE RESPONSE FUNCTIONS	137
5.6	CONCLUDING REMARKS	141

Chapter –6	ANN MODEL APPLICATION – RESULTS AND DISCUSSIONS	142
6.1	INTRODUCTION	142
6.2	APPLICATION OF THE ANN MODEL	142
6.2.1	The Bird Creek Catchment	144
6.2.2	The Brosna Catchment	145
6.2.3	The Garrapatas Catchment	147
6.2.4	The Kizu Catchment	147
6.2.5	The Pampanga Catchment	147
6.2.6	Results For The Individual Runoff Events	150
6.2.7	The Krishna Catchment	155
6.2.8	The Narmada Catchment	156
6.3	GRAPHICAL PRESENTATION OF THE RESULTS OF ANN APPLICATIONS	165
6.3.1	Results Obtained in Catchments Without Sub-Divisions	165
6.3.2	Results Obtained For The Krishna Catchment	167
6.3.3	Results Obtained For The Narmada Catchment	169
6.4	PERFORMANCE OF ANN WITH OTHER INPUTS	170
6.5	STUDY ON POSSIBLE USE OF THE ANN BASED MODELING IN THE UNGAUGED CATCHMENTS	171
6.6	CONCLUDING REMARKS	172
Chapter –7	CONCLUSIONS	203
7.1	INTRODUCTION	203
7.2	BROAD CONCLUSIONS	203
7.3	SPECIFIC CONCLUSIONS	204
7.4	SCOPE FOR FUTURE WORK	206
	REFERENCES	207

LIST OF FIGURES

FIGURE NO.	TITLE	PAGE NO.
1.1	The Process of Rainfall-Runoff Transformation Over a Catchment (Kulandaiswamy, 1964)	3
1.2	Configuration of Three Layer Feedforward <i>ANN</i>	6
2.1	Schematic Diagram of a Node	25
2.2	Different Transfer Functions Used in <i>ANN</i>	26
2.3	Descent to The Global Minimum	28
2.4	Recurrent Neural Network	28
2.5	Comparison Between Observed Runoff and the Runoff Computed by <i>ANN</i> Based Model of Halff <i>et al.</i> (1993)	39
2.6	Comparison of Observed and One-Step-Ahead Predicted Hydrographs for Five-Year Validation Period: a) <i>ANN</i> (5,4,3,1); b) <i>ARMAX</i> (2,4,3); c) <i>SAC-SMA</i> (Hsu <i>et al.</i> , 1995)	39
2.7	Performance of <i>TDNN</i> , <i>RNN</i> and <i>SOLO</i> Models for Evaluation Year 1980 (Hsu <i>et al.</i> , 1998)	44
2.8	Scatter Plots Demonstrating the Importance of Information on Water Level for Previous Time Period a) No Water Level Information; b) Water Level 4 Hours Before; c) Water Level 4 and 2 Hours Before (Campolo <i>et al.</i> , 1999)	45
2.9	Scatter Plots for <i>ANN</i> Model for Data of Namakan Lake (a) 1-Week Ahead Forecast; (b) 4-Weeks Ahead Forecast (Zealand <i>et al.</i> , 1999)	47
3.1	Definition Diagram Showing Identification of The Runoff Event	60
3.2	Index Map of The Narmada Catchment up to Jamtara G&D Site	62
3.3	Index Map of The Krishna Catchment up to Galgali G&D Site	64
4.1	Flowchart Depicting The Steps Involved in The Modeling Process	77
4.2	A Sample Cross Correlogram	80
4.3	Structure of the Rainfall Matrix For Multiple (Three) Input Scenario (Linear Model)	82
4.4	Structure of the Rainfall Matrix For Nonlinear Model (Eq. 2.10)	82
4.5	Schematic Showing Linkages between the Auxiliary Model and the <i>ANN</i>	88
5.1(a)	Plots between $\log(Q_p)$ and $\log(V)$ for Bird Creek, Brosna, and Garrapatas Catchments	102

FIGURE NO.	TITLE	PAGE NO.
5.1(b)	Plots between $\log(Q_p)$ and $\log(V)$ for Kizu and Pampanga Catchments	103
5.1(c)	Plots between $\log(Q_p)$ and $\log(V)$ for Krishna and Narmada Catchments	104
5.2	Response Functions For the Catchments Without Sub-Divisions (Linear Model)	107
5.3	Response Function For Catchments With Sub-Divisions (Linear Model)	109
5.4	Map of Krishna Catchment Showing Three Sub-Divisions (A), (B), and (C)	110
5.5	The Response Functions for Three Sub-Divisions Scenario in The Krishna Catchment	112
5.6	Scatter Plots For the Catchments With No Sub-Divisions (Linear Model - Validation)	119
5.7	Scatter Plots For the Catchments With No Sub-Divisions (Nonlinear Model - Validation)	120
5.8(a)-(c)	Linear Scale Plots For Linear and Nonlinear Models For Catchments With No Sub-Divisions (Calibration Events)	121-123
5.9(a)-(c)	Linear Scale Plots For Linear and Nonlinear Models For Catchments With No Sub-Divisions (Validation Events)	123-125
5.10	Scatter Plots For Validation in The Krishna Catchment	132
5.11	Scatter Plots For Validation in The Narmada Catchment	133
5.12	Linear Scale Plots For Calibration Event in Krishna Catchment (Linear/Nonlinear Model)	134
5.13	Linear Scale Plots For Validation Event in Krishna Catchment (Linear/Nonlinear Model)	135
5.14	Linear Scale Plots For Validation Event in Narmada Catchment (Linear/Nonlinear Model)	136
5.15(a)	Match between the Derived and the Fitted Response Function for Bird Creek, Brosna, and Garrapatas Catchments	138
5.15(b)	Match between the Derived and the Fitted Response Function for Kizu and Pampanga Catchments	139
5.15(c)	Match between the Derived and the Fitted Response Function for Krishna and Narmada Catchments	140
6.1(a)-(c)	Linear Scale Plots For Calibration Event For Catchment Without Sub-Divisions (Linear Model + ANN)	174-176
6.2(a)-(c)	Linear Scale Plots For Validation Event For Catchment Without Sub-Divisions (Linear Model + ANN)	176-178
6.3(a)-(b)	Scatter Plots For Catchments Without Sub-Divisions (Validation – Linear Model + ANN)	179-180

FIGURE NO.	TITLE	PAGE NO.
6.4(a)-(c)	Linear Scale Plots For Calibration Event For Catchment Without Sub-Divisions (Nonlinear Model + <i>ANN</i>)	181-183
6.5(a)-(c)	Linear Scale Plots For Validation Event For Catchment Without Sub-Divisions (Nonlinear Model + <i>ANN</i>)	183-185
6.6(a)-(b)	Scatter Plots For Catchments Without Sub-Divisions (Validation – Nonlinear Model + <i>ANN</i>)	186-187
6.7(a)	Linear Scale Plots For Calibration Event in Krishna Catchment (Linear Model + <i>ANN</i>)	188
6.7(b)	Linear Scale Plots For Validation Event in Krishna Catchment (Linear Model + <i>ANN</i>)	189
6.8	Scatter Plots For Validation in Krishna Catchment (Linear Model + <i>ANN</i>)	190
6.9(a)	Linear Scale Plots For Calibration Event in Krishna Catchment (Nonlinear Model + <i>ANN</i>)	191
6.9(b)	Linear Scale Plots For Validation Event in Krishna Catchment (Nonlinear Model + <i>ANN</i>)	192
6.10	Scatter Plots For Validation in Krishna Catchment (Nonlinear Model + <i>ANN</i>)	193
6.11	Linear Scale Plots For Validation Event in Narmada Catchment (Linear Model + <i>ANN</i>)	194
6.12	Scatter Plots For Validation in Narmada Catchment (Linear Model + <i>ANN</i>)	195
6.13	Linear Scale Plots For Validation Event in Narmada Catchment (Nonlinear Model + <i>ANN</i>)	196
6.14	Scatter Plots For Validation in Narmada Catchment (Nonlinear Model + <i>ANN</i>)	197
6.15(a)	The <i>ANN</i> Structures For Bird Creek and Brosna Catchments	198
6.15(b)	The <i>ANN</i> Structures For Garrapatas and Kizu Catchments	199
6.15(c)	The <i>ANN</i> Structures For Pampang Catchment and Narmada Catchment (No Sub-Division)	200
6.15(d)	The <i>ANN</i> Structures For Narmada Catchment (Two and Three Sub-Divisions)	201
6.15(e)	The <i>ANN</i> Structures For Krishna Catchments (One and Two Sub-Divisions)	202

LIST OF TABLES

TABLE NO.	TITLE	PAGE NO.
2.1	Results Obtained in Terms Coefficient of Determination by Lorrai and Sechi (1995)	41
2.2	Statistics of Model Predictions (Fernando and Jayawardena, 1998)	43
2.3	Model Performance in Terms of R^2 for Different Models Obtained by Anmala <i>et al.</i> , (2000)	49
2.4	Comparative Statement of the <i>ANN</i> Applications for Rainfall-Runoff Modeling	55-57
3.1	Runoff Events Selected For The Narmada Catchment	65
3.2	Runoff Events Selected For The Krishna Catchment	65
3.3	Runoff Events Selected For The Bird Creek Catchment	68
3.4	Runoff Events Selected For The Brosna Catchment	68
3.5	Runoff Events Selected For The Garrapatas Catchment	70
3.6	Runoff Events Selected For The Kizu Catchment	70
3.7	Runoff Events Selected For The Pampanga Catchment	72
3.8	Details of Runoff Events Selected in All The Catchments	73
3.9	Brief Description of The Data Used	75
3.10	The Value of The Coefficient (C)	75
5.1	Results of The Non-Linearity Analysis	101
5.2	Memory Length and Ridge Parameter For Catchments Without Sub-Divisions (Linear Model)	106
5.3	Response Function Ordinates For The Nonlinear Model ($n = 1$)	111
5.4	Memory Length and Ridge Parameter For Catchments With Sub Divisions (Linear Model)	112
5.5	Results of the Linear Model Application to Catchments Without Sub-Divisions	116
5.6	Results of the Nonlinear Model Application to Catchments Without Sub-Divisions	116
5.7	Performance of Linear and Nonlinear Models For Catchments Without Sub-Divisions (Calibration Events)	117
5.8	Performance of Linear and Nonlinear Models For Catchments Without Sub-Divisions (Validation Events)	118
5.9	Results of the Linear Model Application to Catchments With Sub-Divisions	129

TABLE NO.	TITLE	PAGE NO.
5.10	Results of the Nonlinear Model Application to Catchments With Sub-Divisions	129
5.11	Results of Linear and Nonlinear Model Application to The Krishna Catchment	130
5.12	Results of Linear and Nonlinear Model Application to Narmada Catchment	131
5.13	Parameter Values For The Discrete Gamma Function	137
6.1	Results of <i>ANN</i> Applications for The Bird Creek Catchment	145
6.2	Results of <i>ANN</i> Applications for The Brosna Catchment	148
6.3	Results of <i>ANN</i> Applications for The Garrapatas Catchment	148
6.4	Results of <i>ANN</i> Applications for The Kizu Catchment	149
6.5	Results of <i>ANN</i> Applications for The Pampanga Catchment	149
6.6	Linear Model + <i>ANN</i> Results For Catchments Without Sub-Divisions (Calibration Events)	151
6.7	Linear Model + <i>ANN</i> Results For Catchments Without Sub-Divisions (Validation Events)	152
6.8	Nonlinear Model + <i>ANN</i> Results For Catchments Without Sub-Divisions (Calibration Events)	153
6.9	Nonlinear Model + <i>ANN</i> Results For Catchments Without Sub-Divisions (Validation Events)	154
6.10	<i>ANN</i> Model Application Results for The Krishna Catchment	157
6.11	<i>ANN</i> Models Application to Krishna Catchment (<i>RIL</i> , <i>RIN</i> ($n = 1, 2$))	158
6.12	<i>ANN</i> Models Application to Krishna Catchment (<i>RIL</i> + <i>P</i> , <i>RIN</i> + <i>P</i> ($n = 1, 2$))	159
6.13	<i>ANN</i> Model Application Results for The Narmada Catchment	162
6.14	<i>ANN</i> Models Application to Narmada Catchment (Linear Model + <i>ANN</i>)	163
6.15	<i>ANN</i> Models Application to Narmada Catchment (Nonlinear Model + <i>ANN</i>)	164

LIST OF NOTATIONS AND SYMBOLS

B	Intercept where $\text{Log}(V)$ is Zero
b_j	Threshold Value or Bias Associated with Node
C	Coefficient of Multiplication for Determining the AET
E^2	Nash-Sutcliffe Efficiency Coefficient
e_t	Model Error
$f(\cdot)$	Activation or Transfer Function of Node
F_o	Measure of Variability of Observed and Their Mean
F	Measure of Association Between Predicted and Observed Flow
$I(t)$	Volume of Inflow
K	Scale Parameter
l	Linear Part of Memory
m	Memory Length of the Catchment
mse	Mean Square Error
n	Nonlinear Part of Memory
N	Shape Parameter
P	Rainfall
\bar{Q}	Mean of Observed Runoff
\hat{Q}	Estimated Runoff
Q_o	Observed Runoff
Q_p	Peak discharge
Q_s	Value of Runoff at Starting Point of an Event
R^2	Coefficient of Determination
RIL	Output of Linear Model
RIN	Output of Nonlinear Model
R_p	Ridge Parameter
S_0	Initial Storage
S_j	Storage Volume in the Time Interval j

<i>SW</i>	Snowmelt Equivalent
<i>T</i>	Temperature
<i>U</i>	Pulse Response Function
<i>V</i>	Volume of Runoff
<i>VE</i>	Percentage of Volume Error
(W_{ij}, \dots, W_{nj})	Weight Vector
(X_1, \dots, X_n)	Input Vector
α	Momentum Factor
ε	Adaptive Learning Rate
τ	Dummy Variable

ABBREVIATIONS

<i>AET</i>	Actual Evapotranspiration
<i>AMC</i>	Antecedent Moisture Condition
<i>ANN</i>	Artificial Neural Network
<i>API</i>	Antecedent Precipitation Index
<i>ART</i>	Adaptive Resonance Theory
<i>CPN</i>	Counter Propagation Network
<i>DR</i>	Direct Runoff
<i>DRH</i>	Direct Runoff Hydrograph
<i>EBP</i>	Error Back Propagation
<i>EFR</i>	Effective Rainfall
<i>ER</i>	Excess Rainfall
<i>G&D</i>	Gauge and Discharge
<i>IHDM</i>	Institute of Hydrology Distributed Model
<i>IUH</i>	Instantaneous Unit Hydrograph
<i>LLSSIM</i>	Linear Least Squares Simplex
<i>LO</i>	Linear Output
<i>LP</i>	Linear Programming
<i>LPM</i>	Linear Perturbation Model
<i>LS</i>	Least Squares

<i>MISO</i>	Multiple Input Single Output
<i>MLP</i>	Multi Layer Perceptron
<i>MNN</i>	Modular Neural Network
<i>MOLS</i>	Method Of Least Squares
<i>msl</i>	Mean Sea Level
<i>NLP</i>	Non-Linear Programming
<i>NAM</i>	Nedbør-Afstrømnings Model
<i>NN</i>	Neural Network
<i>NNLPM</i>	Nearest Neighbor Linear Perturbation Model
<i>OLS</i>	Orthogonal Least Squares
<i>PERSIANN</i>	Precipitation Estimation From Remotely Sensed Information Using Artificial Neural Network
<i>PET</i>	Potential Evapotranspiration
<i>PMSE</i>	Pooled Mean Square Error
<i>PSR</i>	Phase Space reconstruction
<i>RBF</i>	Radial Basis Function
<i>RDNN</i>	Range Dependent Neural Network
<i>RFO</i>	Response Function Ordinates
<i>RMSE</i>	Root Mean Square Error
<i>RNN</i>	Recurrent Neural Network
<i>SAC-SMA</i>	Sacramento Soil Moisture Accounting
<i>SHE</i>	Syste'me Hydrologique Europe'en
<i>SLM</i>	Simple Linear Model
<i>SOFM</i>	Self Organizing Feature Maps
<i>SOLO</i>	Self Organizing Feature Map with Linear Output
<i>SPDD</i>	Standard Peak Discharge Distribution
<i>SSARR</i>	Stream Flow Synthesis and Reservoir Regulation
<i>TBP-NN</i>	Temporal Back Propagation Neural Network
<i>TDNN</i>	Time Delay Neural Network
<i>UH</i>	Unit Hydrograph
<i>VIS</i>	Volterra Integral Series

Chapter - 1

INTRODUCTION

1.1 GENERAL

The subject of hydrology pertains to scientific study of water, its properties, distribution, and effects on the earth's surface, soil, and atmosphere (McCuen, 1997). The hydrologic cycle is enormously complex and intricate, as it involves various interlinked physical processes such as precipitation, evaporation, infiltration, runoff *etc.*, most of which occur simultaneously. These processes also exhibit a high degree of spatial and temporal variability. Study of the hydrologic cycle has been a challenging task faced by the hydrologists over the years. In the absence of perfect knowledge about these processes due to the complexity involved, these processes are often represented in a simplified manner using systems concept (Chow *et al.*, 1988). A system may be considered to be an ordered assembly of interconnected elements that transform, in a given time reference, certain measurable inputs into measurable outputs, both of which are expressed as a function of time (McCuen and Snyder, 1986). A physical or conceptual boundary separates a system from the rest of the world, which is referred to as the environment.

Surface water hydrology deals with a part of the total hydrologic cycle, namely the catchment subsystem. The details of this subsystem are shown in Fig. 1.1. Unlike the hydrologic cycle, runoff generation process in a catchment is visualized as an open system, receiving the input and producing output (Dooge, 1973). Study of the rainfall-runoff process occurring in a catchment is the main aim of the present study. The problem addressed in the present work is the development of a model for daily rainfall-runoff modeling employing the *ANN* technique, wherein explicit water balance components are not necessary to be considered.

Many distinct decompositions of the rainfall-runoff process in a catchment are possible but the one represented in Fig. 1.1 has attracted more attention of the hydrologists, as it is helpful in finding relationship between the variables characterizing the input *i.e.* rainfall and the output *i.e.* runoff. Only rainfall input to the catchment is considered in the present study. The systems approach is one of the most popular methods of forecasting flows resulting from known rainfall over a catchment, as the true

mathematical representation of the natural process is very difficult, particularly in sparse data scenarios.

1.2 THE RAINFALL-RUNOFF PROCESS

Catchment is a hydrologic system which, when applied with input in the form of rainfall generates its response in the form of storm runoff. The transformation of rainfall into runoff over a catchment is a complex hydrologic phenomenon on account of underlying nonlinear sub-processes. A proper understanding of the rainfall-runoff relationship at the catchment scale is important for water management studies, safe yield computation, and design of flood control structures (Anmala *et al.*, 2000). When the rainfall occurs over an area, the following processes take place. (see Fig. 1.1)

- i) *Interception*: This is that part of rainfall which is held back on the leaves of plants and over the vegetation on ground and later evaporates into the atmosphere.
- ii) *Surface Retention*: Another part of the rainfall that is stored in the depressions on the earth surface or is retained under the vegetal cover, is called as the surface retention. In due course of time, it infiltrates into the ground and/or evaporates into the atmosphere.
- iii) *Overland Flow*: It is that portion of rainfall, which flows over the ground surface and meets the stream through gullies and rivulets.
- iv) *Infiltration*: It is the part of rainfall that immediately enters the soil surface, a portion of which is transpired into the atmosphere through the deep-rooted plants. The infiltrated water follows various paths.
 - a) *Soil Moisture*: A portion of the infiltrated water is retained in the upper layer of the soil. Later a part of this is evaporated and the remaining part is transpired into the atmosphere through the plants.
 - b) *Interflow*: Another portion of the infiltrated water moves towards streams without reaching the ground water table and is called as the interflow.
 - c) *Base flow*: Some part of the infiltrated water meets the groundwater table. A portion of this groundwater moves towards the streams and seeps into it

through the banks and bed and thus it also become runoff under favorable conditions called as the base flow.

Each of this process varies in space and time, which makes the process of rainfall-runoff transformation a complex one.

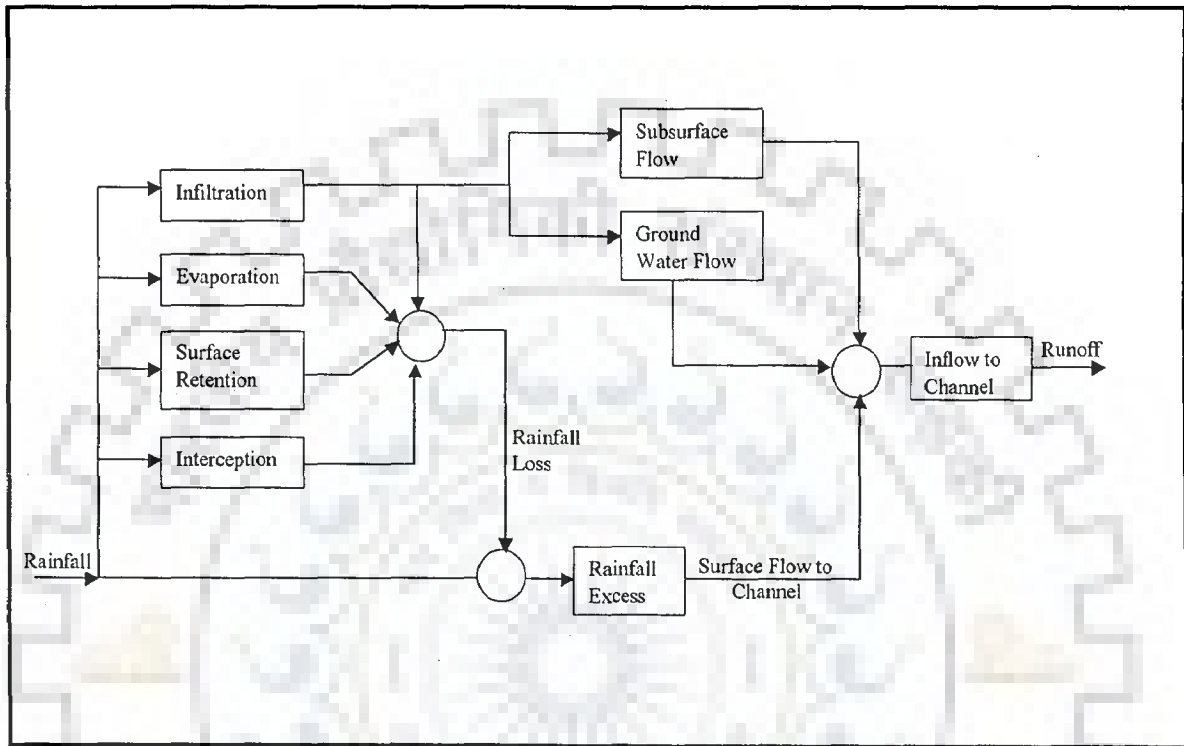


Fig. 1.1 The Process of Rainfall-Runoff Transformation Over a Catchment (Kulandaiswamy, 1964)

1.3 MODELING OF THE RAINFALL-RUNOFF PROCESS

A model represents the system by a set of relationships amongst parameters and variables contemplating the similarity of the prototype with the model, but without identity (Singh, 1988). The models developed to simulate the rainfall-runoff process can be broadly grouped under three categories, with increasing order of complexities involved as: i) empirical; ii) conceptual; and iii) physically based distributed models (Dooge, 1977). The first category of models, namely the empirical models treat hydrologic system (*e.g.* a catchment) as a black box and try to find relationship between historical inputs and the outputs (Singh, 1988). In this approach, the continuity equation is expressed in a spatially lumped form without considering the physical laws operating within the catchment and

instead a general but simple relationship is assumed between rainfall amount and the discharges at the outlet of the catchment. In operational hydrology many situations exist, which demand the use of such simple, system theoretic models.

The conceptual models, on the other hand, attempt to represent the known physical process occurring in the rainfall-runoff transformation in a simplified manner by way of linear/nonlinear mathematical formulations. The total process is divided into sub-processes, which are conceptualized assuming quasi-physical relationships, with the model parameters representing the catchment characteristics. While conceptual models have proved their importance in understanding the hydrological processes, their implementation and calibration presents various difficulties. As a result the model prediction accuracy is found to be user dependent (Klemes, 1982). The third category of models *i.e.* the physically based or process based models, are too complex, data intensive and cumbersome to use. Typically, they involve solution of a system of partial differential equations that represents the flow processes within the catchment (Beven, 1985; Loague and Freeze, 1985). The kind of data required for use of the physically based distributed models is rarely available, even in heavily instrumented research catchments. Even by using current advanced computing capabilities the representation of a catchment in the physically based model is, at best, an approximation (Beven, 1987, 1989). Despite these limitations, the physically based models have proved to be very useful for many hydrologic problems when utilized appropriately and are currently undergoing large scale advancements.

Even though many types of models are presently available for representing rainfall-runoff process, the problem still remains unresolved and it is perhaps for this reason that the alternative modeling approaches are still being sought. The system theoretic modeling approach has been added with a new dimension through adoption of the Artificial Neural Network (*ANN*) technique in rainfall-runoff modeling. The rainfall-runoff modeling using *ANNs* would have to be classified as the empirical modeling. This approach is called a *model* as it has many features in common with other modeling approaches in hydrology. The process of determination of appropriate neural network architecture can be considered equivalent to the model selection in the conventional way. Similarly, the conventional steps of model calibration and validation can be identified with

network training and testing in the context of *ANN* applications (ASCE, 2000 *a*). The *ANNs* are more versatile because there is a freedom in selecting the number of hidden layers and the number of nodes in each of these layers (Fausette, 1994). The advantages of *ANN* applications in hydrology are discussed by French *et al.* (1992). In the following paragraphs a brief review of *ANNs* and their application in modeling the rainfall-runoff process is presented.

1.4 THE ARTIFICIAL NEURAL NETWORK

An artificial neural network is a massively parallel distributed information processing system that has certain performance characteristics resembling biological neural networks of the human brain (Haykin, 1994). It is an interconnected assembly of simple processing elements, nodes, or neurons, which emulates the functioning of neurons in human brain. The processing of information takes place at these processing elements. The *ANN* is also described as a mathematical structure, which is capable of representing the arbitrary complex nonlinear process relating the input and the output of any system (Fausette, 1994). Therefore, the *ANN* has emerged as a viable tool for the simulation and control of complicated, nonlinear dynamic systems (Hsu *et al.*, 1997 *b*). The connection weights, threshold and the number of neurons in hidden layer can be termed as the parameters of an *ANN* model, which are adjusted during training process (Campolo *et al.*, 1999). The network consists of an input layer, an output layer, and one or more number of hidden layers. The input layer receives the input variables whereas the output layer consists of model outputs *i.e.* values predicted by the network. The number of hidden layers and the number of neurons in each hidden layer are usually determined by a trial and error procedure. A typical three layer feedforward neural network, which is the most widely used, is shown in Fig. 1.2. All connections shown in the figure are feedforward *i.e.* they allow information to pass from one layer to the next layer. Nodes within a layer are not interconnected. The connection links run from one layer to the other but do not leapfrog layers.

Many studies utilizing *ANNs* are reported in literature because they possess desirable attributes of universal approximation and have the ability to learn from examples without the need for explicit physics (Bishop, 1994; Hsu *et al.*, 1995). Although several studies indicating the potential of *ANN* as a useful tool in hydrology are reported, the

disadvantages of *ANNs* should not be ignored. A major limitation of *ANNs* is the lack of physical concepts and relations. The successful application of an *ANN* depends both on the quality and the quantity of data available. A detailed description about *ANN* and its application to rainfall-runoff modeling is given in the next chapter.

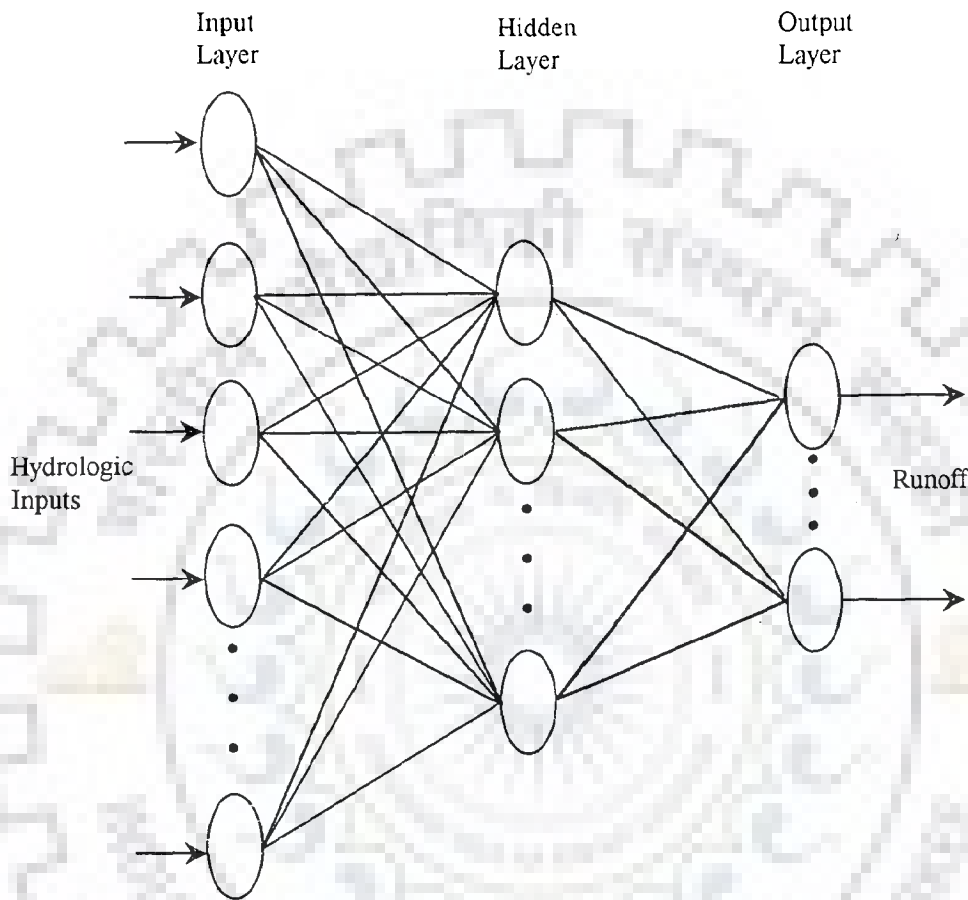


Fig.1.2 Configuration of Three Layer Feedforward ANN

1.5 BACKGROUND OF THE STUDY

The physically based models and the conceptual models generally involve use of a number of parameter of which many are either not yet readily available in the literature or are difficult to ascertain for catchments from different geographical and climatic regions. Also, such models become less reliable in their application for the scarce data scenarios. The catchments are found mostly to be hydrologically nonlinear. Serious error in hydrologic design can occur when a catchment instead is assumed to be linear. The widespread usage of the unit hydrograph approach (Sherman, 1932) and other linear models cited in literature makes more intensive the need for checking the applicability of

linear models. The *ANN* based models are supposed to effectively account for the non-linearity present in the process. Several studies on application of the *ANN* for rainfall-runoff modeling on various time scales are reported in literature. A detailed review of these studies is presented in chapter 2. In most of these studies, the *ANN* was used as an independent model and results obtained through its application were compared with those produced by the conventional models. In these studies the inputs to the *ANN* consisted of combinations of variable such as current and antecedent rainfall and runoff values, temperature, snowmelt *etc.* It is well established from these studies that, the rainfall information alone is not sufficient to estimate the runoff accurately from a catchment as the state of the catchment *i.e.* the antecedent soil moisture condition plays an important role in determining the amount of runoff generated from the given rainfall.

The studies carried out in the past involving use of *ANN* for runoff analysis have mainly dealt with flow updating and can be divided into two categories. The first category involves use of the observed discharge in the past as the only input to the *ANN* and runoff for next time step is forecasted. In the second category discharge observed in the past and other meteorological parameters such as current and antecedent rainfall, temperature, snowmelt *etc.* are used as input for forecasting the runoff in the next time step.

Inclusion of discharge observed in the preceding time intervals as input to the *ANN* based rainfall-runoff models makes it difficult to treat these models as cause-and-effect models. Such models are useful in the forecasting but are not so useful in conceptualizing the catchment and synthesis of daily flow data series.

1.6 OBJECTIVES OF THE PRESENT STUDY

The objective of the present study is to propose a modeling approach which couples the system theoretic linear/nonlinear models with the *ANN* so as to overcome the difficulties cited above and explore the application of the neural networks for the non-updating flow simulation. The *ANN* model is proposed to be coupled with the system theoretic linear/nonlinear models such that output from linear/nonlinear models forms one of the inputs to the *ANN*. The study presents the *ANN* as a flexible nonlinear rainfall-runoff black box model for the simulation of isolated runoff events with single or multiple peaks, spread over several days.

The specific objectives of the present study are:

- To apply the *ANN* in its true context *i.e.* as a nonlinear model.

- To incorporate, as far as possible, the understanding of the physical process of runoff generation in *ANN* based rainfall-runoff modeling over a catchment.
- To provide a viable alternative for the discharges observed in the previous time periods, being used as one of the inputs to the *ANN* in most of the existing studies.
- To develop a methodology for rainfall-runoff modeling when the hydrologic applications require that the runoff be predicted with the help of rainfall information alone and without much analysis on the hydrologic dynamics of the catchment being investigated.
- To demonstrate the capability and effectiveness of the proposed methodology in sparse data scenarios.
- To demonstrate application of the neural networks in case of large size catchments in the context of incorporating the distributed nature of input, *i.e.* the areal disaggregation of the rainfall.

1.7 PRESENTATION OF THE STUDY

Chapter 1: Describes various approaches including *ANN* used for rainfall-runoff modeling. A brief description about the *ANN* is provided and the scope and objectives of the study are outlined.

Chapter 2: First, a brief review of literature about the conventional approaches used for rainfall-runoff modeling is given in this chapter. It is followed by reviewing the application of *ANN* for various types of problems encountered in hydrology and water resources engineering. Then the studies involving application of *ANN* technique for rainfall-runoff modeling are reviewed in detail. The concluding remarks based on the review carried out are presented at the end.

Chapter 3: Provides the description about all the catchments studied and duration of the data used. The steps involved in identification of a runoff event are outlined. The runoff events identified in case of each catchment and their corresponding durations in days are given in tabular form. The computation of the effective rainfall as adopted in the present study is also described in this chapter.

Chapter 4: Presents various steps involved in the proposed methodology for daily rainfall-runoff modeling using the *ANN*. The steps involve correlation analysis, application

of linear/nonlinear model for determination of the response function of the catchment, and finally the application of the feedforward backpropagation *ANN* such that the output of the system based model forms one of the inputs to the *ANN*. The other inputs combinations given to the *ANN* are described and the procedure adopted for identification of the hydrologic non-linearity of the catchment and for parameterization of the response functions is outlined. Finally, various performance evaluation criteria used in the present study are described.

Chapter 5: In this chapter first the results of the analysis for ascertaining the hydrologic non-linearity of the catchments are presented. This is followed by presentation the results of the linear and nonlinear models employed in the study as the auxiliary models, are presented in tabular and graphical form separately for, i) the catchments without sub-divisions; and ii) the catchments involving sub-divisions. The discussions on the results obtained are provided. Finally, the results of the parameterization of the response function are given.

Chapter 6: This chapter presents the results of the coupled *SLM-ANN* and nonlinear-*ANN* models. The results of these *ANN* models along with results of the *ANN* with other input combinations are provided in tabular and graphical form. This is followed by presentation of the discussions on these results and the inferences drawn from the analysis of the results. The structures of the best performing *ANNs* with some of the input combinations are depicted at the end.

Chapter 7: The conclusions drawn from the study are summarized and the scope for future work is outlined in this chapter.

REVIEW OF LITERATURE

A vast amount of literature exists describing the rainfall-runoff process and various approaches adopted for its modeling. The models available for simulating the rainfall-runoff process vary considerably in their overall purpose, time base involved, size and nature of area that can be modeled, their conceptual basis, and in the mathematical strategies involved in their development. A critical review of literature related to the rainfall-runoff modeling is presented in this chapter. This encompasses review of various types of models applied for simulating the rainfall-runoff relationship along with the application of the artificial neural network technique for various types of problems encountered in hydrology in general and for rainfall-runoff modeling in particular.

The transformation of rainfall into runoff over a catchment is a complex hydrologic phenomenon on account of variation of the parameters and the sub-processes involved over space and time. A number of models have been developed to simulate this process. These models are grouped into following categories based on decreasing order of the complexity of physical laws involved.

- i) The physically based distributed or process based models
- ii) The conceptual models
- iii) The empirical or black box models.

The second and third category of models can be combined as the *lumped models* in which rainfall averaged over the catchment area is mostly used as the model input. Equation (2.1) expresses the relation between input, output, and the change in storage in the spatially lumped form of continuity equation for continuous time. A discrete time representation of Eq. (2.1) is given by Eq. (2.2) and the same is necessary, as the hydrologic data are available only at discrete time intervals.

$$\frac{ds}{dt} = I(t) - Q(t) \quad (2.1)$$

$$S_j = S_0 + \sum_{i=1}^j (I_i - Q_i) \quad (2.2)$$

where I and Q are the volumes of inflow and outflow respectively during a time interval. S_0 is the initial storage and S_j is the storage volume in j^{th} time interval (Chow *et al.*, 1988).

In these equations, the physical laws operating within the catchment are not considered; instead a simple relationship between catchment rainfall and the discharge at the outlet of the catchment is assumed and the responses are derived on basin wide scale.

2.1 PHYSICALLY BASED OR PROCESS BASED MODELS

Ideally the rainfall-runoff process should be modeled by the physics based models, which account for the variation in parameter values over space and time by discretizing the catchment into smaller units. This process of discretization makes them spatially distributed and in turn such models are capable of predicting the model outputs at any point within the catchment unlike the lumped models, which provide the results only at the outlet of the catchment. The basis of these models is to use equations of conservation of mass, energy, and momentum to describe the movement of water over the land surface and through the unsaturated and saturated zones of soil and represent various processes involved in transforming the system input to the output. The resulting system of nonlinear partial differential equations is required to be solved numerically at all the computational grid points (Wood and O'Connell, 1985). These types of models are developed based on highest degree of physical information. The development of physically based distributed models is relatively recent, which mainly took place due to the developments in the field of computer technology and in the areas of remote sensing and the geographical information system. Some of the physically based models developed are: *TOPMODEL* (Beven and Kirkby, 1979), The Systeme Hydrologique Europe'en (*SHE*) model (Abbott *et al.*, 1986 *a* and *b*); The Institute of Hydrology Distributed Model (*IHDM*) (Beven *et al.*, 1987); and some other models like those proposed by Smith and Woolhiser (1971), Engman and Rogowski (1974), Ross *et al.* (1979), and Kutchment (1980). An historical perspective of the development of the catchment scale models is presented by Singh and Woolhiser (2002). They have provided a comprehensive review of the distributed as well as conceptual models dealing with integration of hydrologic process on the catchment to determine the catchment response. The components of the physically based distributed model, some of which also require calibration, are based on basic physical laws governing the different processes (Refsgaard *et al.*, 1992). However, Beven (1989) emphasized that physically based models being process based, should be able to make prediction without calibration. Nevertheless, the application of such models in practice poses many kinds of

problems. The limitations of the process-based models were highlighted amongst others by Beven (1985, 1989) and Loague and Freeze (1985). Major limitations are listed below.

- i) **Data intensive:** Proper application of the physically based model requires use of vast amount of data, which may not be available for many catchments particularly for large catchments in developing countries.
- ii) **Lumping at small scale:** The application of distributed model over a catchment involves division of catchment into sub-areas, and lumping of the model parameters at this scale. Such a model is viewed as a lumped conceptual model rather than a distributed model.
- iii) **Difficulty in calibration:** As many parameters are involved, these interact with each other posing tremendous difficulties in model calibration.
- iv) **Unknown boundary conditions:** The initial and the boundary conditions particularly those related to soil moisture conditions are not known correctly and are also difficult to ascertain.
- v) **Expensive to run:** Short time steps may be necessary to maintain stable solution, and as the solution is found at each computational node at each time step, the number of calculations required can be very large. These models also require considerable expenditure in terms of programming, data preparation, and field experimentation.

The limitations outlined above make the physically based models presently unsuitable for practical applications. Successful application of the physically based models in the field is also hampered due to the scale problems associated with the immeasurable spatial variability of rainfall and hydraulic properties of soil.

2.2 CONCEPTUAL MODELS FOR RAINFALL-RUNOFF PROCESS

The conceptual models for rainfall-runoff are based on hypothetical conceptualization of catchment by linear/nonlinear reservoirs. The main aim of such models is to simplify and simulate the major processes that contribute to the response of the catchment to the rainfall input. The complex physical process of rainfall-runoff transformation is conceptualized through semi-empirical processes involving interlinked storages and simple budgeting procedures. The mass balance between inputs and outputs is attempted at all times in these types of models. The level of representation of physical

information in such a model lies between that of the physical process based model and the black box model (Wood and O'Connell, 1985).

Several conceptual models exist in literature simulating the rainfall-runoff process. Among the first were the models developed by Clarke (1945) and O'Kelly (1955), who proposed that the time area diagram if routed through a linear reservoir produces the unit hydrograph (*UH*) for the catchment. Nash (1957, 1959, 1960) developed a model based on a cascade of equal linear reservoirs for finding the instantaneous unit hydrograph (*IUH*) of a catchment. Dooge (1959) developed a general unit hydrograph theory assuming the catchment to be composed of parallel chains of linear reservoirs and linear stream channels. Kulandaiswamy (1964) gave a general storage equation governing the operation of the system, assuming that the catchment behavior can be described by analytical functions. In some of the conceptual models, the mathematical formulation of the physical processes involved is cumbersome resulting into a large number of parameters, and the interactions of these parameters is highly complicated *e.g.* Stanford Watershed Model (Crawford and Linsely, 1966). The conceptual rainfall-runoff models having varying degree of complexity are employed for modeling the rainfall-runoff relationship on daily basis. Some of these models are Streamflow Synthesis And Reservoir Regulation (*SSARR*) model developed by U.S. Army Corps of Engineers (Rockwood, 1982); Tank model, (Sugawara *et al.*, 1983); *ARNO* (Arno river) model, (Todini, 1988), Sacramento Soil Moisture Accounting (*SAC-SMA*) model of National weather service river forecast system (Burnash *et al.*, 1973).

The conceptual models have proved their importance in understanding the hydrological processes. Successful application of these models depends on how well they are calibrated. Their calibration and implementation presents various difficulties. The difficulties with conceptual models are pointed out by Klemes, (1982); Duan *et al.*, (1992) and others. Some of the limitations of the conceptual rainfall-runoff models are highlighted below.

- This type of models require significant amount of data.
- The unique optimal values for their parameters are difficult to obtain.
- It is difficult to determine the sensitivity of the parameters and hence the sensitivity of model forecasts to factors such as errors in input and output data, model error, objective function used *etc.*

- The nonlinear structural characteristics of conceptual rainfall-runoff models lead to the existence of multiple optima *i.e.* more than one solutions.
- These models also face problems like parameter interaction, non-convexity of response surface, and discontinuous derivatives.
- The model prediction accuracy is found to be user dependent as its use requires some degree of expertise and experience with the model.
- Very often the users are tempted to fit the model without seriously considering the parameter values, resulting in poor model performance during verification phase.

Although, conceptual models provide results with reasonable accuracy, their use is restricted due to the above mentioned difficulties experienced in their calibration and implementation.

2.3 LINEAR MODELS FOR EXCESS RAINFALL-DIRECT RUNOFF PROCESS

The empirical or black box type of models establish a relationship between input and the output functions, without considering the complex physical laws governing the process of rainfall-runoff transformation. The limitations of the physically based distributed models and the conceptual models outlined above make it difficult to employ these models in many practical situations which is one of the reasons for the development of many black box or empirical models. The black-box type models, which have minimum computational requirements, are used for getting the solutions to the practical problems.

The rational method was the first linear black box rainfall-runoff model (Mulvaney, 1850). The rational method presents the concept of time of concentration and its relation to peak flow but it fails to give time development of discharge. The development of empirical models gained a boost with the proposition of unit graph theory by Sherman (1932). He defined a unit graph or a unit hydrograph as:

"A direct runoff hydrograph (DRH) resulting from unit amount of excess rainfall generated uniformly over the catchment area at a constant rate for an effective duration."

A *UH* is a linear model that relates the excess rainfall (*ER*) to the direct runoff (*DR*), describing the response of a catchment. The assumptions regarding spatial and temporal uniformity of rainfall, validity of the principles of proportionality and superposition, and time invariance are basic in the concept of the *UH* theory.

The principles of linear system analysis form the basis for the *UH* method. Analysis based upon the *UH* concept has played an important role in rainfall-runoff modeling. The operation of a system, following the *UH* principles, in converting precipitation excess $P(t)$ into the direct storm runoff $Q(t)$ is expressed by the following convolution integral;

$$Q(t) = \int_{\tau=0}^{\tau=t} P(\tau) U(t-\tau) d\tau \quad (2.3)$$

where τ is the dummy variable of integration and $U(t)$ is the unit impulse response function ordinate at time t . This impulse response function is also known as the *IUH* of the catchment, which although a theoretical concept, is useful as it characterizes the response of the catchment to the rainfall without reference to the duration of rainfall. Due to this fact the *IUH* has been related to the geomorphological characteristics of the catchment (Rodrigue-Iturbe and Valdes, 1979; Gupta *et al.*, 1980).

When the input function is expressed as a series of pulses over successive short time intervals T , the linear input-output relationship given by Eq. (2.3) is expressed in the discrete form, in terms of the sampled pulse response by the following discrete convolution summation equation;

$$Q_t = \sum_{i=1}^m P_{t-i+1} U_i + e_t \quad (2.4)$$

where U_i refers to the i^{th} ordinate of the of pulse response, m is the memory length of the system which implies that the effect of any rainfall input P lasts only through m intervals of duration t and e_t is the model error term or the residuals. Above equation when written for each of input-output values in a series yields n linear equations, which in vector-matrix form can be written as;

$$[\mathbf{Q}] = [\mathbf{P}] [\mathbf{U}] + [\mathbf{E}] \quad (2.5)$$

where \mathbf{Q} is a $(n, 1)$ column vector of the output runoff series, \mathbf{P} is a (n, m) matrix of the input rainfall values, \mathbf{U} is a $(m, 1)$ column vector of the pulse response ordinates which are to be determined, and \mathbf{E} is a $(n, 1)$ column vector of model errors. When the data for calibration period are considerably longer than the memory of the length of the system the above equation represents an over determined system of linear equations and the vector \mathbf{U} of the pulse response ordinates can be estimated by the method of ordinary least squares

(Snyder, 1955). Conventionally, the Eq. (2.5) is used without the inclusion of the error term and solved using the matrix inversion methods given by

$$[U] = [P^T P]^{-1} [P^T][Q] \quad (2.6)$$

Several techniques of determination of optimal values of response function ordinates using various mathematical techniques have appeared in literature. A very exhaustive description of these methods is available in Singh (1988). These methods can be categorized as: i) methods of deriving UH for single storm event, and ii) methods of deriving UH from multistorm events. A brief review of these methods is presented in following paragraphs.

2.3.1 Methods of Deriving UH for Single Storm Event

Collin's method (1939), a trial and error procedure, was probably the first method to derive UH from a single complex storm. Various studies employing different mathematical techniques for determination of UH followed this and are widely reported, such as, method of least squares (*MOLS*), (Snyder, 1955; Newton and Vinyard, 1967); Harmonic analysis (O'Donnell, 1960); Fourier transform (Levi and Valdes, 1964; Blank *et al.*, 1971; Sarma *et al.*, 1973); Z-transform (Turner *et al.*, 1989); Successive approximation (Bender and Roberson, 1961); Laplace transform (Chow, 1964); system of progressive ordinate estimating (Linsley *et al.*, 1958).

Use of meixner function, which is a discrete time analog of Laguerre polynomials for determination of UH was suggested by Dooge (1965). Linear Programming (*LP*) with minimum sum of deviations was first applied by Eagleson *et al.* (1966) to obtain optimum UH . The use of Nonlinear Programming (*NLP*) for the same was demonstrated by Mays and Taur (1982) and was extended by Unver and Mays (1984) to find optimal values of parameter relating to loss rate function and the UH .

2.3.2 Methods of Deriving UH for Multi Storm Event

A catchment should have only one and unique UH for given unit duration but separate analysis of record from several rainfall-runoff events produced different UH s due to the limitations of the UH technique and the noise in the *ER* data as argued by Diskin and Boneh (1975). Deininger (1969); Singh (1976); Diskin and Boneh (1980); and Mays

and Coles (1980) demonstrated the application of *LP* method for multistorm events. Non-negativity constraint using least squares objective function in case of multistorm events was applied by Diskin and Boneh (1975). Mawdesley and Tagge (1981) used the Householder method proposed by Wilkinson (1965) to overcome difficulties encountered in the matrix inversion.

Bree (1978), and Kitanidis and Bras (1979) presented technique to tackle the problem of collinearity encountered in identification of system parameters when multievents are analyzed. The oscillations in recession part of *UH* were also observed by Delleur and Rao, (1971); Papazafiriou, (1976). Bruen and Dooge (1984) tackled the problem of sensitivity of *UH* ordinates using the concept of ridge regression, which is same as adding uncorrelated white noise component to the inflow series. This methodology was suggested by Kutchment (1967), and is an efficient and robust method of estimating *UH* ordinates, which takes advantage of symmetric Toplitz structure of the coefficient matrix. Dooge and Bruen (1989) explored the feasibility of using the concept of condition number of the matrix as a basis for deciding the situations under which data error causes unacceptable instability in derived *UH*s. This condition number depends on the shape of the input time series and the method used for deriving the *UH*. In their study various methods of deriving *UH* were compared. Bruen and Dooge (1992 *a* and *b*) demonstrated the use of a priori information about *UH* shape in addition to rainfall-runoff data in determination of *UH*. Zhao *et al.* (1995) described a methodology to obtain an optimal ridge parameter for use in the least square (*LS*) method to estimate *UH* considering the unit volume constraint. The other method of estimating oscillation free *UH* with non-negative ordinates is the Bayesian method investigated by Rao and Tirtotjondro (1995), who used both real and synthetic data.

2.3.3 Relating *UH* Parameters with the Catchment Characteristics

Many researchers have worked on establishing the relationship between parameters of the *UH* or the *IUH* and the catchment characteristics. Clarke (1944), Snyder (1938) and Gray (1961) presented empirical methods of deriving synthetic *UH* using lag for streamflow forecasting and related the hydrograph characteristics to catchment characteristics. The method of finding a synthetic *UH* based on dimensionless *UH* was given by SCS (1972). Dooge (1959) presented a general theory for the *UH* and used the

concept of linear channels and reservoirs in deriving a general equation for the UH . Nash (1959) used moments of IUH and related it with catchment characteristics. This methodology popularly known as the '*Nash Model*', has been widely applied in generating UH for ungauged catchments from varying climatic regions of the world.

Later on, some studies comparing the performance of the methods for determination of UH ordinate values have also been reported in the literature. Laurenson and O'Donnell (1969) discussed sensitivity of four methods of finding UH to data errors. Clarke (1973) reviewed the mathematical models used in hydrology and categorized them into four groups. Sarma *et al.* (1973) compared performance of five linear conceptual models for prediction of runoff from urban areas. Todini (1988) grouped the models on the basis of justification of approach for intended use. These studies have put forth the relative merits and demerits of various methods of deriving UH under different circumstances.

2.4 LINEAR MODELS FOR TOTAL RAINFALL-TOTAL RUNOFF PROCESS

Difficulties are encountered while deriving the effective rainfall and making the base flow separation for determination of the direct runoff in the analysis based on the UH theory. Alternative modeling approaches are available in literature which relate total rainfall and total runoff of a catchment in a manner similar to the UH procedure. Simplest of this type of model is called the Simple Linear Model (SLM) introduced in discrete form by Nash and Foley (1982). The form of the SLM is algebraically identical to that of UH concept [Eq. (2.4)] except for the difference that P is the total rainfall instead of the effective rainfall and U is the pulse response function of the catchment. Some differences arise due to larger time duration of the input and output functions (*e.g.* days) relative to the memory time of the system in SLM whereas, the event modeling is carried out in UH analysis (Kachroo, 1992). Such modeling approach overcomes the subjectivity involved in and the efforts required for determining the effective rainfall and the direct runoff.

Ahsan and O'Connor (1994) used the output of a SLM as an index of the soil moisture state of the catchment. They termed it to be an elaborate form of the Antecedent Precipitation Index (API), which is the classic index of recent history of rainfall occurring over a catchment. The simulated output of the SLM was called by them as the rainfall index. The use of SLM alone is found to overestimate the low flows and underestimate the high flows. As per Ahsan and O'Connor (1994), the SLM , though naive and primitive, is convenient starting point in rainfall-runoff modeling.

Linear modeling of the departure of normal seasonal values of rainfall and discharge series was found to be an attractive method by Nash and Barsi, (1983); Kachroo *et al.* (1992) and many others. This modeling approach was termed as Linear Perturbation Model (*LPM*) (Nash and Barsi, 1983) and it is found to be successful for catchments exhibiting a high degree of seasonal variation. In the catchment having a relatively predictable seasonal variation, a considerable improvement over the conventional rainfall-runoff models could be achieved by considering the relationship between the departures from the seasonal behavior of rainfall and discharge as input and output respectively, rather than using the total rainfall series as input and total runoff series as output (Kachroo *et al.*, 1992). This technique was also applied by Liang and Nash (1988); and Kothyari *et al.* (1993) for flow forecasting.

A major weakness of the above types of rainfall-runoff models is their inability to incorporate the spatial variation of rainfall over a catchment. Chow (1964) proposed that the catchment be divided into smaller sub-catchments. Each of which is subjected to separate hydrograph analysis and the catchment hydrograph can be obtained by routing the hydrographs for different tributaries. This methodology later gave rise to new type of models called as multiple input single output (*MISO*) models, which partially compensate the weakness cited above. The *MISO* models represent a catchment as an assembly of sub-catchments of approximately uniform rainfall distribution. In such models the rainfall occurring in each hydrologically homogeneous sub-area of the catchment is treated as a separate input received in parallel by the overall catchment system. The *MISO* linear and nonlinear black box models have been studied in detail by Liang, (1988); Liang and Nash, (1988); Papamichail and Papazafiriou, (1992); Liang *et al.*, (1994) among others. These models have been applied for flow forecasting at the outlet of medium and large size catchments. The linear *MISO* model for the catchment divided into J sub-areas can be given using the following equation.

$$Q_t = \sum_{j=1}^J \sum_{i=1}^m P_{t-i+1}^{(j)} U_i^{(j)} + e_t \quad (2.7)$$

where, $j = 1, 2, \dots, J$ designates the sub-area.

The models based on *UH* theory, the *SLM* and the *LPM* can be categorized as time invariant models, which is the simplest possible representation of a casual relationship between input and output function of time. The obvious complexities of the rainfall-runoff process, which involves infiltration and is affected by soil moisture condition,

imply that such a representation is not adequate in describing the nonlinear transformation of rainfall into runoff. The concept of nonlinearity is discussed next.

2.5 CATCHMENT NON-LINEARITY

If a hydrograph is analyzed, it can be deduced that a strong nonlinearity exists during rising limb, the peak, and the initial part of falling limb of the hydrograph. The recession, on the other hand, is more readily predictable by a linear operation on the antecedent input as it is less dependent on the distribution of input (Agorocho, 1963). Agorocho represented the hydrologic system using the functional series, considering the system to be nonlinear and suggested the absolute and unit linearity of hydrologic systems. The absolute linearity is defined as the ratio of linear term of the functional series to the summation of full series and should be equal to one for a system to be linear.

Chow (1964) reviewed most of the earlier research on nonlinear runoff. Later Clarke (1971) showed that, linearity in system theory sense is not necessarily equivalent to linearity in statistical sense. Most hydrologists used linearity in system theory sense with the exception of Agorocho (1963) whose model is linear in statistical regression sense but nonlinear in system theory sense. Rogers (1980, 1982) introduced a new way of measuring nonlinearity of a system known as the Standardized Peak Discharge Distribution (*SPDD*). As per him the slope of line that best fits the standardized peak discharge data is an indicator of nonlinearity of runoff distribution.

$$\log(Q_p) = B + M \log(V) \quad (2.8)$$

where, Q_p is the peak discharge in ft³/sec, V is the volume of runoff in inches, and the log inverse of B is the peak discharge when runoff volume is one unit. Alternatively, following second order relation between peak and volume of runoff is also given.

$$\log(Q_p/V^2) = B + \beta \log(V) \quad (2.9)$$

where $\beta = M - 2$. The regression slope of this *SPDD* model [Eq. (2.8)] is a catchment characteristic. A catchment is said to be linear if the value of $M = 1.0$ or alternatively if the value of $\beta = -1.0$. The values of slope less than this indicate the non-linearity of runoff

distribution or in other words the hydrologic non-linearity of the catchment. The catchments with similar values of slope could be homogeneous. This nonlinear *SPDD* relationship is applicable for any duration and no base flow separation is necessary. It is related to non-uniform distribution of infiltration capacities and storage conditions in a catchment. There is an assumption involved in *SPDD* relationship that the stage discharge relation of a gauge is consistent.

Rogers and Zia (1982) applied this relation to large sized catchments. Mimikou (1983) attempted to relate slope and intercept of this relation to the catchment characteristics and found that the intercept was highly correlated with the catchment area, main stream length and average bed slope whereas, the slope M had a weak relationship. He stated that hydrologic non-linearity exists when runoff volumes are not directly proportional to rainfall volumes. As per Mimikou (1983) the R^2 values of Eq. (2.8) reflect the degree of accuracy of peak discharge prediction from runoff volume. Singh and Aminian (1986) extended this study to large number of catchments from USA, Australia, Greece, and Italy using the direct runoff instead of total runoff as in case of Rogers (1980, 1982). As per Mimikou, (1983) only peak discharge distribution [Eq. (2.8)] is necessary and sufficient for checking the hydrologic non-linearity of a catchment. The *UH* based procedures cannot be applied to catchments with value of $M < 1.0$ (Rogers and Zia, 1982).

One more study discussing linearity vs. nonlinearity, which also gave alternative definitions for the same was carried out recently by Sivapalan *et al.*, (2002). As per them two hydrologically different definitions of non-linearity exist in literature. The first definition is with respect to the dynamical property such as rainfall-runoff response of the catchment and the second definition is with respect to dependence of catchment statistical property, such as mean annual flood on the area of the catchment. They have recommended that the term nonlinearity should be used for dynamical response of the catchment *i.e.* the nonlinear dependence of dynamical hydrological response on rainfall inputs rather than the second definition.

Various other measures of nonlinearity exist, such as Correlation Function, Coherence Function *etc.* (Singh, 1988). These concepts of non-linearity of runoff distribution existing in the catchment system have led to the development of nonlinear empirical models, which are discussed in brief in the next section.

2.6 NONLINEAR BLACK BOX MODELS FOR RAINFALL-RUNOFF PROCESS

As early as in 1960, Minshall found that one UH could not adequately define the shape of hydrograph derived from a storm of unit duration and noted the variations in storage characteristics of the catchment with flood magnitude. The procedure of nonlinear analysis using the functional series was investigated by Amorocho and Orlob (1961) who applied the Volterra integral series (VIS) for analyzing the $ER-DR$ relationship in a hydrologic system. Singh (1964) presented theory of nonlinear IUH to account for variations in IUH derived from different storms over a catchment. Amorocho and Brandstetter (1971) used meixner function to find nonlinear functional response function for a single storm event. Whereas, Diskin and Boneh (1973) developed computational technique for determining optimal kernel functions from multiple storms in discrete time. Many studies followed later taking the study by Amorocho and Orlob (1961) as base, such as, studies by Amorocho (1963); Amorocho and Hart (1965); Diskin and Boneh (1973); Papazafiriou (1976); Diskin *et al.* (1984), which considered various aspects of $ER-DR$ relationship. A detailed discussion on methodology of functional series as applied to hydrologic system is available in Amorocho (1973). The improvement suggested by Helweg *et al.* (1982) in the functional series model by Amorocho and Brandstetter (1971) eliminated the trial and error procedure required for estimation of parameters.

The kernel functions of the functional series model do not have any physical meaning and cannot assure physically realizable response. Muftuoglu (1984) proposed two nonlinear functional models that accounted for nonlinear storage and translation effects in a catchment, the kernel functions of which have physically realizable responses. The second order functional part (first term) and linear part (the second term) in his model given in Eq. (2.10) represent the direct runoff process and delayed flows respectively. The corresponding response functions are called two-dimensional finite period UH and the finite period UH . Muftuoglu (1984) used the nonlinear relation between total rainfall and total runoff instead of effective rainfall and direct runoff for modeling monthly flows in the model proposed by him.

$$Q_t = \sum_{i=1}^n \sum_{k=i}^n U_{i,k} P_{t-i+1} P_{t-k+1} + \sum_{i=1}^l U_{i+n} P_{t-(i+n)+1} + e_t \quad (2.10)$$

This model was later modified and extended by Kothyari and Singh (1999) for large size catchment as a nonlinear *MISO* model. This model has the form given in the following equation.

$$Q_t = \sum_{j=1}^J \sum_{i=1}^{n(j)} \sum_{k=i}^{n(j)} U_{i,k}^{(j)} P_{t-i+1}^{(j)} P_{t-k+1}^{(j)} + \sum_{j=1}^J \sum_{i=1}^{l(j)} U_{i+n}^{(j)} P_{t-(i+n)+1}^{(j)} + e_t \quad (2.11)$$

The notations have the same meaning as in earlier equations. Liang *et al.* (1994) also developed a nonlinear *MISO* model using the concept of linearly varying gain factor. The functional series is a universal mathematical model for nonlinear black box systems, which produces a single output from a serial input (Muftuoglu, 1991). The nonlinear model of the kind of functional series has not been sought for *MISO* system; instead the hydrologists have resorted to conceptual modeling approach (Kachroo and Liang, 1992). The system theoretic modeling approach has been added with a new dimension through the application of artificial neural network (*ANN*) technique for rainfall-runoff modeling. The systems approach in general and nonlinear functional analysis in particular has recently undergone a renaissance largely due to adoption of techniques like *ANN* and genetic algorithms (Minns and Hall, 1996). The applications of *ANN* for modeling the process of conversion of rainfall in to runoff will be discussed in detail next, but before that a brief account of the *ANN* technique and its application in for the problems other than rainfall-runoff modeling in the area of hydrology and water resources engineering is presented.

2.7 ARTIFICIAL NEURAL NETWORK THEORY

The development of *ANNs* began approximately 50 years ago with the progress in neurobiology, which promoted research in simulating the neural behavior by building the mathematical models of neurons in the human brain. The first abstract model of a single idealized biological neuron was presented by McCulloch and Pitts, (1943). A law explaining the learning of a network of neurons was proposed by Hebb (1949). The first *ANN* namely the perceptron created by Rosenblatt (1958), consisted of neurons arranged within one active layer. Many *ANN* structures have been proposed and explored since then. The *ANN* technique has experienced a huge resurgence in last two decades after Hopfield (1982) introduced the idea of energy minimization in physics into neural networks. The *ANN* has an ability to identify the relationship among the input patterns, by

virtue of which it can solve large-scale complex problems such as pattern recognition, nonlinear modeling *etc.* The applications of *ANNs* can be seen in such diverse areas as image processing, biomedical engineering, electrical engineering, chemical engineering, computer science, physics, and others.

As mentioned in chapter 1, the *ANN* is an interconnected assembly of simple neurons or nodes. It consists of an input layer, an output layer and one or more number of hidden layers. The input layer receives the input whereas the output layer produces model outputs through nonlinear operation carried out at different nodes. Each neuron in a layer operates in logical parallelism. Information is transmitted from one layer to other in serial operation (Hecht-Nielsen, 1990). A neural network is characterized by its architecture that represents the pattern of connection between nodes, its method of determining the connection weights, and the activation function (Fausett, 1994). The operation of an *ANN* is based on certain rules. A three layer feedforward *ANN* is shown in Fig. 1.2 as an illustrative example. The passing of signals between nodes in such a network takes place through connection links, which run from one layer to the next but do not leapfrog layers. Each connection link has an associated weight that represents its connection strength. Each node typically applies a nonlinear transformation to the input through an activation function and the output is derived (Caudill, 1987).

2.8 MATHEMATICAL ASPECTS OF *ANN*

A schematic diagram of a typical node of an *ANN* is depicted in Fig. 2.1. At each node in a layer of *ANN* the information is received, stored, processed, and communicated further to nodes in the next layer. The inputs to the *ANN* form an input vector $X = (x_1, \dots, x_n)$. The sequence of weights leading to the node form a weight vector $W_j = (w_{1j}, \dots, w_{nj})$, where w_{ij} represents the connection weight from the i^{th} node in the preceding layer to the j^{th} node. The weights can be positive or negative. The positive weights are called excitory connections whereas negative weights are termed as inhibitory connections. The output of node j is obtained by computing the value of function $f(\cdot)$.

This operation is defined as

$$Y_j = f(X \cdot W_j - b_j) \quad (2.12)$$

where b_j is the threshold value or the bias associated with node which must be exceeded before the node can be activated. In other words, unless the strength of input (weighted sum) received by a node exceeds the threshold value, the output of the neuron is zero. The function $f(.)$ is called an activation function or a non-linearity function, which ensures conditioning or dampening of the actual response of a neuron. This function can be of different forms *e.g.*, linear, step, ramp, logistic sigmoid, or bipolar sigmoid that determines the response of a node to the total input signal. The most commonly used form of $f(.)$ in Eq. (2.12) is the sigmoid function, given by

$$f_j = \frac{1}{1 + e^{-\sum w_{ij}x_i}} \quad (2.13)$$

The sigmoid (shown in Fig. 2.2) is a bounded, monotonically increasing function that provides a graded, nonlinear response enabling the *ANN* to map any nonlinear process. It is continuous and differentiable everywhere (Hecht-Nielsen, 1990). This is particularly useful in the feedforward backpropagation *ANN* as the change in weights is accomplished using the derivative of the transfer function. The popularity of the sigmoid function is partially attributed to the simplicity of its derivative that is used during the training process. Figure 2.2 also shows the other transfer or activation functions used in the *ANNs*.

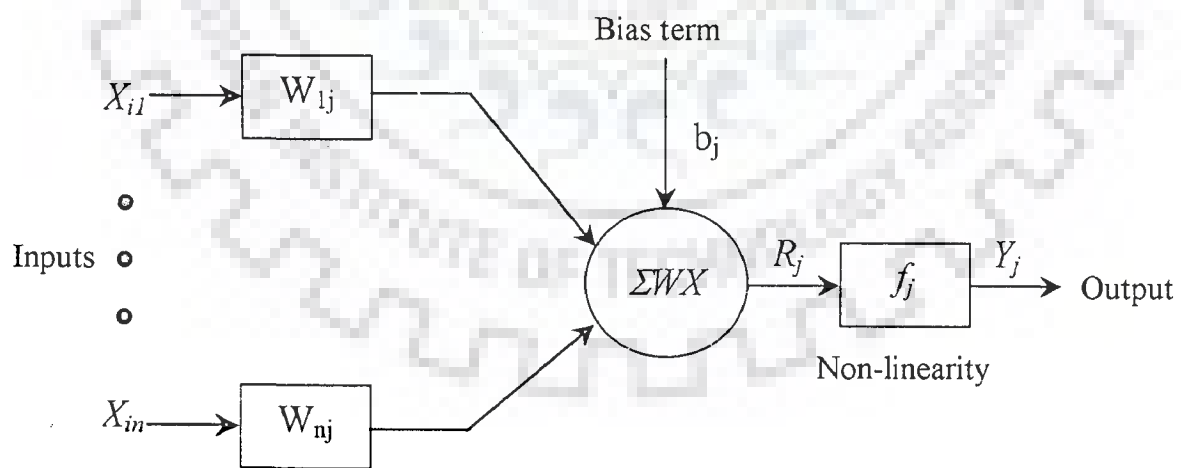


Fig. 2.1 Schematic Diagram of a Node

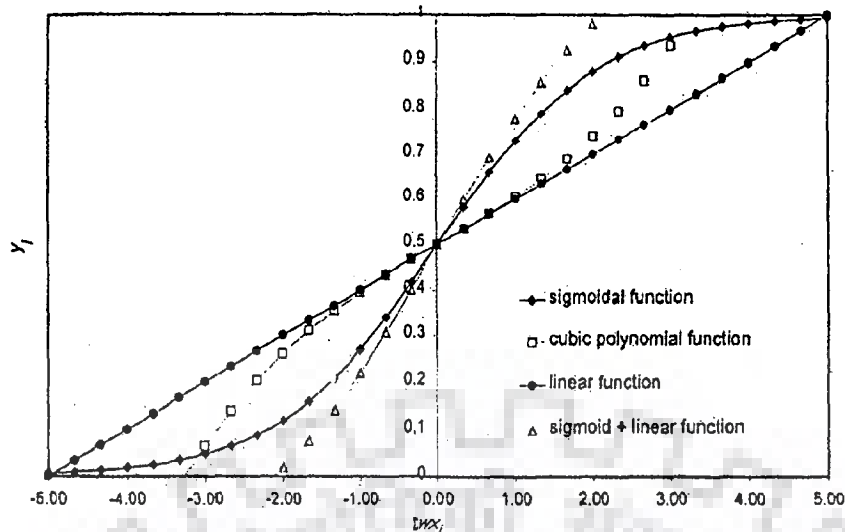


Fig. 2.2 Different Transfer Functions Used in ANN

2.9 CLASSIFICATION OF ANN

The ANN can be classified in different ways such as

- (i) Based on the number of layers
 - a) Single Layer Network (Hopfield nets)
 - b) Bilayer Network (Carpenter/Grossberg Adaptive Resonance Networks)
 - c) Multilayer network (Most Backpropagation Networks).
- (ii) Based on the direction of information flow
 - a) Feedforward Networks
 - b) Recurrent Networks

The important ones among the above types of networks are reviewed below.

2.9.1 Feedforward Backpropagation Network

A feedforward ANN can have many layers. This type of network is most widely used along with the backpropagation (BP) algorithm employed for its training. The BP algorithm is a supervised learning algorithm in which the output error is fed back through the network. These types of networks are considered as universal approximator as they do not require any explicit mathematical relationship between the inputs and the outputs. The results of Hornik *et al.* (1989) show that the standard multilayer feedforward network with a single hidden layer with an arbitrary number of sigmoidal hidden nodes can approximate

any measurable function to any degree of accuracy. In addition, De Villars and Bernard (1993) showed that the *ANN* comprised of two hidden layers tend to be less robust and converges with less accuracy than its single layer counterpart. Due to these reasons feedforward networks find applications in a wide variety of problems, such as classifying patterns, grouping similar patterns, or finding solutions to constrained optimization problems *etc.* A three layer feedforward network along with *BP* algorithm is employed in the present study because such feedforward *ANNs* are found to have the best performance with regard to input-output function approximation (Hsu *et al.*, 1995).

The backpropagation algorithm was originally developed by Werbos (1974), but its powerfulness was not recognized and appreciated for many years. Rumelhart *et al.* (1986) rediscovered the algorithm and made it popular by demonstrating how to train the hidden neurons for a complex mapping problems. It is essentially a gradient descent technique that minimizes the network error function. To start the backpropagation learning process we need i) set of training patterns, input, and target; ii) value of learning rate; iii) termination criterion for the algorithm; iv) methodology for updating weights; v) the nonlinear transfer function; and vi) initial weight values (Kartalopoulos, 2000). The *BP* algorithm involves two steps. In the first step the process begins with application of the first input pattern and the corresponding target output. The input pattern is passed from the input layer to the output layer. The response at the output layer is compared with the target response and error (E) for this pattern is calculated. The algorithm now steps back and the weights are updated or modified iteratively using the steepest-gradient descent principle and the computed error is propagated backwards to each node. The connection weights are adjusted based on the following equation

$$\Delta w_{ij}(n) = -\varepsilon \times \frac{\partial E}{\partial w_{ij}} + \alpha \times \Delta w_{ij}(n-1) \quad (2.14)$$

where,

$\Delta w_{ij}(n)$ and $\Delta w_{ij}(n-1)$ = weight increments between node i and j during the n^{th} and $(n-1)^{th}$ epoch.

ε = learning rate

α = momentum factor

The momentum factor speeds up training in very flat regions of the error surface and helps in preventing the oscillations in the weights. A learning rate is used to increase the chance of avoiding the training process being trapped in local minima instead of the

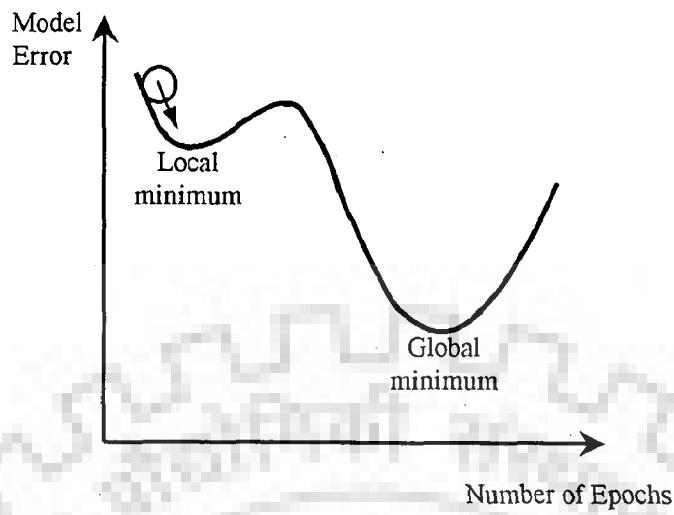


Fig. 2.3 Descent to The Global Minimum

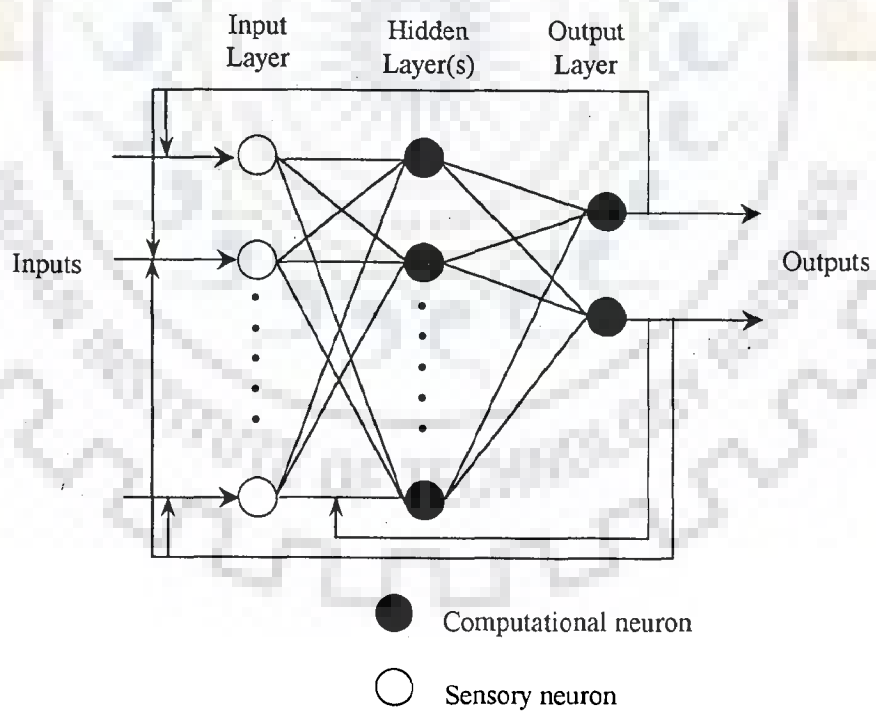


Fig. 2.4 Recurrent Neural Network

global minima. The descent of the training process towards global minima along with the local minima present on the error surface is shown in Fig. 2.3.

2.9.2 Recurrent Neural Networks

Recurrent neural network (*RNN*) distinguishes itself from feedforward *ANN* in that it has at least one feedback loop, which could be local or global (Haykin, 1994). Fig. 2.4 illustrates the structure of a *RNN*. The *RNN* architecture incorporates a multilayer perceptron (*MLP*) or a part of it and uses its mapping capability. Basically there are two functional uses of recurrent networks: i) associative memories and ii) input output mapping networks (Haykin, 1994). Such networks typically use a spatial-temporal variant of backpropagation for training. Essentially, there are three ways by which memory can be introduced into static neural networks (Islam and Kothari, 2000). These are; i) Tapped delay line model: In these type of network past inputs are explicitly available to determine its response at a given point in time by virtue of which a temporal pattern is converted to a spatial pattern, which can then be learned through classic backpropagation, ii) Partial recurrent models: These models retain the past output of nodes, e.g. the output of the hidden layer neurons of a feedforward network can be used as inputs to the network along with the true input, iii) Fully recurrent models: These models employ full feedback connections between nodes (ASCE, 2000 *a*). The *RNN* structure requires less time for training due to the reduced number of network weights.

2.9.3 Radial Basis Function Network

Developed by Powell (1985), a Radial Basis Function (*RBF*) network is used for classification and approximation problems. It is a three-layer network in which, the only hidden layer performs a fixed nonlinear transformation with no adjustable parameters. The standard Euclidean distance is used to measure relative distance between input vector and the center at each node. The computed Euclidean distance is then transformed by a nonlinear function that determines the output of the nodes in the hidden layer (ASCE, 2000 *a*). The primary difference between the *RBF* network and a backpropagation network is in the non-linearity associated with the hidden nodes (Fernando and Jaywardena, 1998).

The non-linearity in the error backpropagation (*EBP*) networks is implemented by a fixed activation function whereas in the *RBF* network, non-linearity is based on the training data (Mason *et al.*, 1996). Learning in *RBF* network is carried out in two phases, first for hidden layer and then for output layer. However, the *RBF* network usually requires more data to achieve the same accuracy as the backpropagation networks (Hassoun, 1995). One more problem with the *RBF* networks is that, when the input patterns fall within close proximity to each other the basis functions may have overlapping receptive fields.

2.9.4 Cascade Correlation Algorithm

The cascade correlation algorithm, developed by Fahlman and Lebiere (1991), differs from other approaches in that it starts without any hidden nodes and the network grows during the training by adding new hidden units one by one, maximizing the impact of the new node and creating a multilayer structure (Karunanithi *et al.*, 1994). Once a new hidden node has been added to the network, its input-side weights are frozen. A training cycle is divided into two phases. First, the output nodes are trained to minimize the total output error. Then a new node is inserted and connected to every output node and all previous hidden nodes. The addition of new hidden nodes is continued until maximum correlation between the hidden nodes and error is attained. The network architecture is determined as a part of the training process.

2.9.5 Self-Organizing Feature Maps

Unlike feedforward and recurrent neural networks that are primarily used for approximation and classification, Self-Organizing Feature Maps (*SOFMs*) are typically used for projecting patterns from high dimensional to low-dimensional space. *SOFM* were originally proposed by Kohonen (1989, 1990). The neurons in this networks are placed at the nodes of lattice that is usually one or two-dimensional. The synaptic weights in the network are first initialized. This is followed by the processes such as: i) competition, ii) cooperation, iii) synaptic adaptation (Haykin, 1994). When an input pattern is presented, it computes a matching value for each node in the competitive layer. The node that has the closest match to the input is identified as a winning unit (Hsu *et al.*, 1998).

2.10 IMPORTANT ASPECTS OF ANN MODELING

Although there are no fixed rules for developing an ANN, a general framework for its design is very well described in ASCE (2000 *a*) and (Kartalopoulos, 2000). Some of the points to be considered in the development of an ANN are:

1. Selection of Input and Output Variables
2. Data Normalization
3. Designing a Network
4. Training of the Network
5. Strengths and Limitations

The above points are reviewed in brief in the following paragraphs.

2.10.1 Selection of Input and Output Variables

The objective of an ANN is to generalize relationship given by the following equation

$$Y^m = f(X^n) \quad (2.15)$$

Where, X^n is an n -dimensional input vector consisting of variables $x_1, \dots, x_i, \dots, x_n$; and Y^m is an m -dimensional output vector consisting of resulting variables of interest $y_1, \dots, y_i, \dots, y_m$. In hydrological context the values of inputs x_i can be causal variables such as rainfall, temperature, discharges or water levels for previous time period, evaporation, basin area, elevation, slopes, meteorological data, and so on. The values of outputs y_i can be hydrological responses such as runoff, streamflow or ordinates of a hydrograph *etc.*

Proper selection of input variables is very important, so that an ANN is able to map to the desired output vector successfully. In ANN modeling the set of variables that influence the system are not known *a priori* as in case of physically based models. So, in this sense of nonlinear process identification, an ANN should not be considered as a mere black box. Proper understanding of the physical process being modeled is an important prerequisite for successful application of ANNs (ASCE, 2000 *a*). A sensitivity analysis can be used to determine the relative importance of a variable when sufficient data is available (Maier and Dandy, 1996). The learning process slows down due to unnecessary patterns in the training dataset.

2.10.2 Data Normalization

The data used in the hydrological studies are obtained either from field or through remote sensing. The data need to be normalized before being applied to an *ANN*. The applications involving use of *ANN* have stressed the importance of scaling the input/output quantities before presenting them to the network. For problems exhibiting high non-linearity, the variables are scaled between range of [0, 1] or some other suitable range. This kind of scaling tends to smooth the solution space and averages out some of the noise effects (ASCE, 2000 *a*).

2.10.3 Designing a Network

Design of the *ANN* is nothing but determination of the topology of the network and selecting a proper algorithm for its training. This is an important part of the process, which aims at providing an optimal *ANN* architecture such that it gives the best performance in terms of error minimization, and has minimum complexity (Kartalopoulos, 2000). Minimal network can offer better generalized performance than more complex networks (Rumelhart *et al.*, 1994). The numbers of neurons in the input and output layer are defined by the problem. The flexibility lies in selecting the number of hidden layers and the number of neurons in each of these hidden layers. This is a trial and error procedure aimed at deriving optimal architecture. Bishop (1995) provides an excellent review of approaches used for determining the network architecture with acceptable performance on the training and the generalization data. The algorithms used in deciding the size of network are categorized as follows.

- 1) Pruning algorithms: These generally start with a large network and proceed by removing weights to which sensitivity of the error is minimal.
- 2) Growing methods: Typically start with a small network and add nodes with full connectivity to nodes in the existing network (Haykin, 1994).

2.10.4 Training the Network

Training the network is very much similar to the calibrating the hydrologic model. The main objective of training is to produce desired set of outputs when a set of inputs is given to the *ANN*. The available data set is partitioned into training and testing datasets. It is important that the training dataset should contain sufficient patterns so that the network

can mimic the underlying relationship between input and output variables adequately. Each pass through the training data is called an epoch and during training process the *ANN* learns through overall change in weights accumulated over many epochs. Finally, the optimal weight matrices and bias vectors are found which minimize a predetermined error function, such as sum of squares of errors (Bishop, 1994). After proper training is accomplished, the *ANN* generates reasonable results given unknown inputs. The training process is stopped when no appreciable change in the values associated with the connection links is observed or some termination criterion is satisfied.

However, there is the danger of overtraining a network in this fashion, which is also termed as overfitting. This happens when the network parameters are too fine-tuned to the training dataset. The network, in the process of trying to "learn" the underlying rule, has started to fit the "noise" component of the dataset. In other words, overtrained network memorizes the individual examples, rather than trends in the dataset as a whole. When this happens, the network performs very well during training, but fails to generalize when given an unknown input (Haykin, 1994). To prevent this, help of the testing dataset is taken to stop the training when the network begins to overtrain. Initially, error for both the training and testing datasets reduces. After an optimal amount of training has been achieved, the error for the training set continues to decrease, but that for the testing dataset begins to rise. This is an indication that further training may result in overfitting the training data by a network. The process of training is stopped at this time, and the set of weights are assumed to be optimal (ASCE, 2000 *a*). The *ANN* is now ready to be used as a predictive tool.

2.10.5 Strengths and Limitations

The following are some of the reasons why *ANNs* have become an attractive computational tool (ASCE, 2000 *a*):

1. The *ANNs* are capable of recognizing the relation between the input and output variables without explicit physical consideration.
2. The *ANNs* performance is not affected even if the training sets contain noise and errors.
3. The *ANNs* are adaptable to solutions over time to compensate for changing circumstances.

One of the reasons that made *ANNs* an attractive tool for solving the problems in hydrology is the fact that the knowledge about these problems is far from perfect and many a times the problem is ill defined. Even the analysis using physically based models is not meaningful, as it has to rely on many assumptions. The *ANNs* model the non-linearity in the underlying process without having to solve complex partial differential equations. There is no need to make assumptions about the mathematical form of the relationship between input and output, which is an inherent part of regression-based techniques. The *ANNs* perform with almost same accuracy even in the presence of noise in the inputs and outputs because of distributed processing taking place within the network. This, along with the nonlinear nature of the activation function, truly enhances the generalizing capabilities of *ANNs* and makes them desirable for a large class of problems in hydrology.

There are three primary situations where *ANNs* are advantageous.

1. Situations where only a few decisions are required to be taken from a massive amount of data.
2. Situations where nonlinear mapping must be automatically acquired.
3. Situations where a near optimal solution to an optimization problem is required very quickly.

The successful application of the *ANN* for solving various problems encountered in hydrology has proved its potential. Nevertheless, its disadvantages should not be ignored. The *ANN* application may fail to produce satisfactory results as the success of an *ANN* application depends both on the quality and the quantity of data. Representing temporal variations is often achieved by including past inputs/outputs, which makes the resulting *ANN* structure more complicated. One of the major limitations of *ANNs* is that it lacks physical concepts and relations, which has been the point of criticism and the reasons for the skeptical attitude towards this methodology. Many times selection of the network architecture and training algorithm is dependent on the preference of the user, rather than on the physical aspects of the problem being studied. *ANNs* fail to predict out of range values indicating that they are also not well suited for extrapolation. In addition to that determination of the network architecture and its parameters is trial and error process, which consumes a lot of time.

2.11 ANN APPLICATIONS IN HYDROLOGY AND WATER RESOURCES ENGINEERING

Hydrologists are often confronted with the problems of prediction and estimation of runoff, precipitation, contaminant concentration, water stages, and many others. They attempt to provide rational answers to these problems. The process of problem solving becomes more complicated due to the fact that the understanding in many areas is far from perfect, paving way for empiricism to play an important role in modeling of these processes. The issues of spatial and temporal variation, errors in data *etc.* make the situation even worse.

ANNs have been applied to solve large-scale complex problems like pattern recognition, nonlinear modeling, and others. Researchers in hydrology and water resources engineering have shown serious interest in using this technique only during the last decade. *ANNs* have the ability to extract relation between the inputs and outputs of a process without need of knowing explicitly the physics involved. This property of *ANN* has attracted many researchers and a significant growth in the interest of this computational mechanism took place due to the work by Rumelhart *et al.* (1986). An exhaustive review investigating the applications of *ANN* in various branches of hydrology and a comparison of the *ANN* and other modeling philosophies in hydrology is available in ASCE (2000 *b*). Since the early nineties, *ANNs* have been successfully used in problems in hydrology such as rainfall-runoff modeling, streamflow forecasting, ground water modeling, water quality, precipitation forecasting, hydrologic time series, reservoir operations, and others. In the following paragraphs, first various applications of *ANN* in the field of hydrology and water resource engineering other than rainfall-runoff modeling will be reviewed in brief and this will be followed by a detailed review of *ANN* applications for rainfall-runoff modeling.

Among the first reported study in the field of hydrology employing *ANN* was by French *et al.* (1992) who used a three layer feedforward *ANN* to forecast rainfall. Navone and Ceccatto (1994) used *ANN* to predict monsoon rainfall over India. Rainfall prediction was also accomplished by Hsu *et al.* (1997 *a*, 1999) using the counter propagation network (*CPN*) developed by Hecht-Nielsen (1987). They transformed the satellite infrared images to corresponding rainfall rates with the use of *CPN*. A multilayer network with

backpropagation algorithm and *SOFM* were employed by Burian *et al.* (2000) for disaggregation of hourly rainfall data into sub-hourly time increments. Sorooshian *et al.* (2000) evaluated the automated Precipitation Estimation from Remotely Sensed Information using Artificial Neural Networks (*PERSIANN*) system of estimation of tropical rainfall using satellite data.

Applications of *ANN* for water quality modeling are also reported in literature. As the variable estimation in such problems is quite complex, the problem is suitable for *ANN* application. The *ANN* used by Rogers and Dowla (1994) was trained by a solute transport model for performing optimization studies in groundwater remediation. Maier and Dandy (1996) and Zhang and Stanley (1997) used the *ANN* for prediction of water quality parameters. Multiobjective optimization of water management in a river basin with *ANN* quality approach was studied by Wen and Lee (1998). *ANN* based identification of microbial contamination sources was carried out by Brion and Lingireddy (1999).

Ranjithan *et al.* (1993) used a three layer feedforward network for groundwater reclamation. A new approach for nonlinear groundwater management using *ANN* was presented by Rogers and Dowla (1994) while, Johnson and Rogers (1995) applied *ANN* for locational analysis in groundwater remediation.

A feedforward *ANN* was used for reservoir operation by Raman and Chandramouli (1996) and Jain *et al.* (1999). Coulibaly *et al.* (2000) introduced stopped training approach in training feedforward *ANN* whereas, Chandramouli and Raman (2001) analyzed a multireservoir system with dynamic programming and the *ANN*.

ANN has been successfully applied by Zhu and Fujitha (1994) to forecast hourly flood discharges. Karunanithi *et al.* (1994); and Muttiah *et al.* (1997) used the cascade correlation neural network for the prediction of river flow. Imrie *et al.* (2000) also used the same type of *ANN* but added with a guidance system so as to improve its generalization. Sudheer *et al.* (2000) employed the *ANN* to forecast daily runoff from an Indian river as a function of daily precipitation and some previous day's runoff values. The study by Thirumalaiah and Deo (2000) demonstrates the application of a feedforward *ANN* trained with the *BP* algorithm, the conjugate gradient, and the cascade correlation algorithm for real time forecasting of hourly flood runoff, daily river stage, and for predicting rainfall sufficiency over India.

Some typical applications of *ANN* for other problems encountered in hydrology are also reported. Raman and Sunilkumar (1995) employed *ANN* to model multivariate water resources time series and obtained comparable results with that of *ARMA* model. Hall and Minns (1998) and Hall *et al.* (2000) carried out the regional flood frequency analysis using *MLP* type neural networks. They also used *ANNs* to model relationships between catchment characteristics and parameters of flood frequency distributions at gauged sites and obtained superior results to those provided by traditional method. Hall and Minns (1999) employed a Kohonen network and C-means method for the classification of hydrologically homogeneous regions. Whereas, the classification of river basins in India was carried out using adaptive resonance theory (*ART*) network by Thandaveswara and Sajikumar (2000). The *ART* is an unsupervised competitive network used for clustering and follows incremental learning (Carpenter and Grossberg, 1987). Islam and Kothari (2000) examined the utility of three types of *ANNs* for characterization, estimation, and prediction of remotely sensed hydrologic processes and data found in multiple sources. Jain and Chalisgaonkar (2000) employed a three layer feedforward *ANN* for setting up stage discharge relations at two sites in the Narmada river basin in India. Ray and Klindworth (2000) applied the neural networks for assessing the contamination of private wells due to pesticide and nitrate. Analysis and quantification of spatial and temporal patterns of meteorological drought based on *ANN* was carried out by Shin and Salas (2000). Khalil *et al.* (2001) used the *ANN* based on the concepts and properties of groups for infilling the missing hydrological records whereas, Kumar *et al.* (2002) estimated the evapotranspiration by using the *ANN*.

2.12 ANN APPLICATIONS IN RAINFALL-RUNOFF MODELING

Determining the relationship between rainfall and runoff in a catchment is one of the most important problems faced by hydrologists and engineers. In addition to rainfall, runoff is dependent on numerous factors such as initial soil moisture, land use, catchment topography and geomorphology, evaporation, infiltration, distribution and duration of the rainfall, and so on.

A number of researchers have investigated the potential of neural networks in modeling the runoff based on rainfall and other meteorological inputs. The summarized description of the studies involving application of *ANN* in rainfall-runoff modeling is provided in Table 2.4. This table provides in nutshell the information about the type of *ANN* employed in these studies, the input parameters to the *ANN* considered, the output(s) predicted/forecasted, the scale of study, and the size of the catchment(s) studied. These studies are critically reviewed in the following paragraphs.

Among the first was a preliminary study by Halff *et al.* (1993) who used a three layer feedforward *ANN* to predict the hydrograph of storms using the observed rainfall hyetographs on the same basin. A total of five storm events were considered. Figure 2.5 shows the results obtained by Halff *et al.* (1993) when first four events were used for training and the last event was used for testing the performance of the *ANN* used in their study. This study opened up several possibilities of application of neural networks for rainfall-runoff modeling.

Hjelmfelt and Wang (1993) developed a neural network based on the unit hydrograph theory. They derived a composite runoff hydrograph for a catchment using the linear superposition. The resulting network reproduced the unit hydrograph better than the one obtained through the standard gamma function representation. Later, Hjelmfelt and Wang (1996) compared this method with a regular three layered feedforward backpropagation *ANN*.

Smith and Eli (1995) investigated the potential of *ANN* to map different rainfall patterns into various runoff measures. They applied a *BP* neural network model to predict peak discharge and time to peak over a synthetic catchment, overlaid with tree-type drainage pattern, using simulated data generated by either a linear or a nonlinear reservoir model. A stochastic rainfall pattern generator was used to generate rainfall patterns required for the study. A rainfall depth of one unit was applied instantaneously at several cells on a random basis. The peak discharge and the time to peak were predicted well by the neural network, both during training and testing.

Hsu *et al.* (1995) presented a procedure called Linear Least Squares Simplex (*LLSSIM*) for identifying the structure and parameters of a three layer feedforward *ANN*.

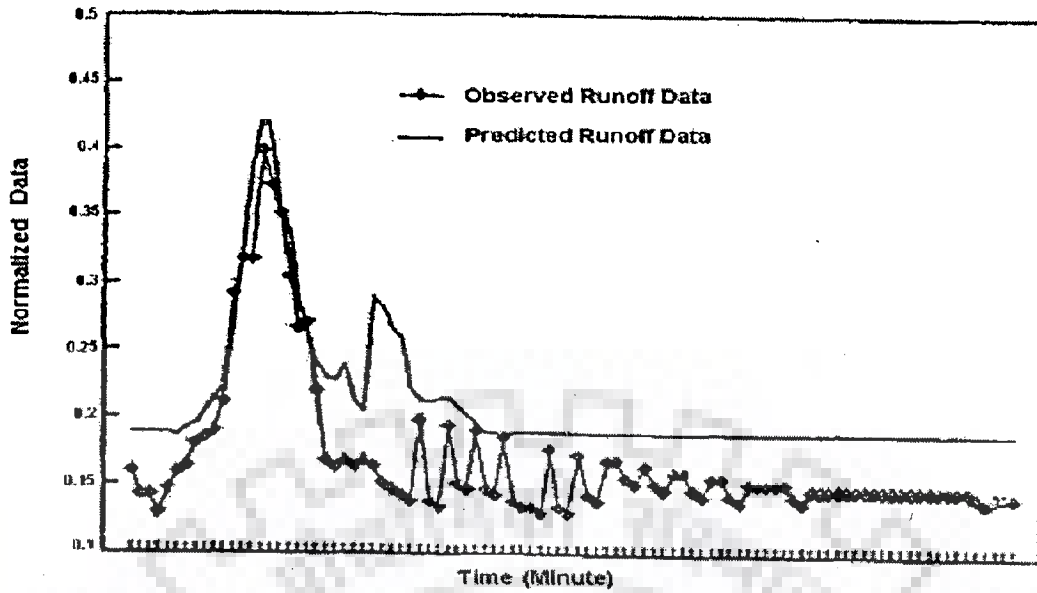


Fig. 2.5 Comparison Between Observed Runoff and the Runoff Computed by ANN Based Model of Halff *et al.* (1993)

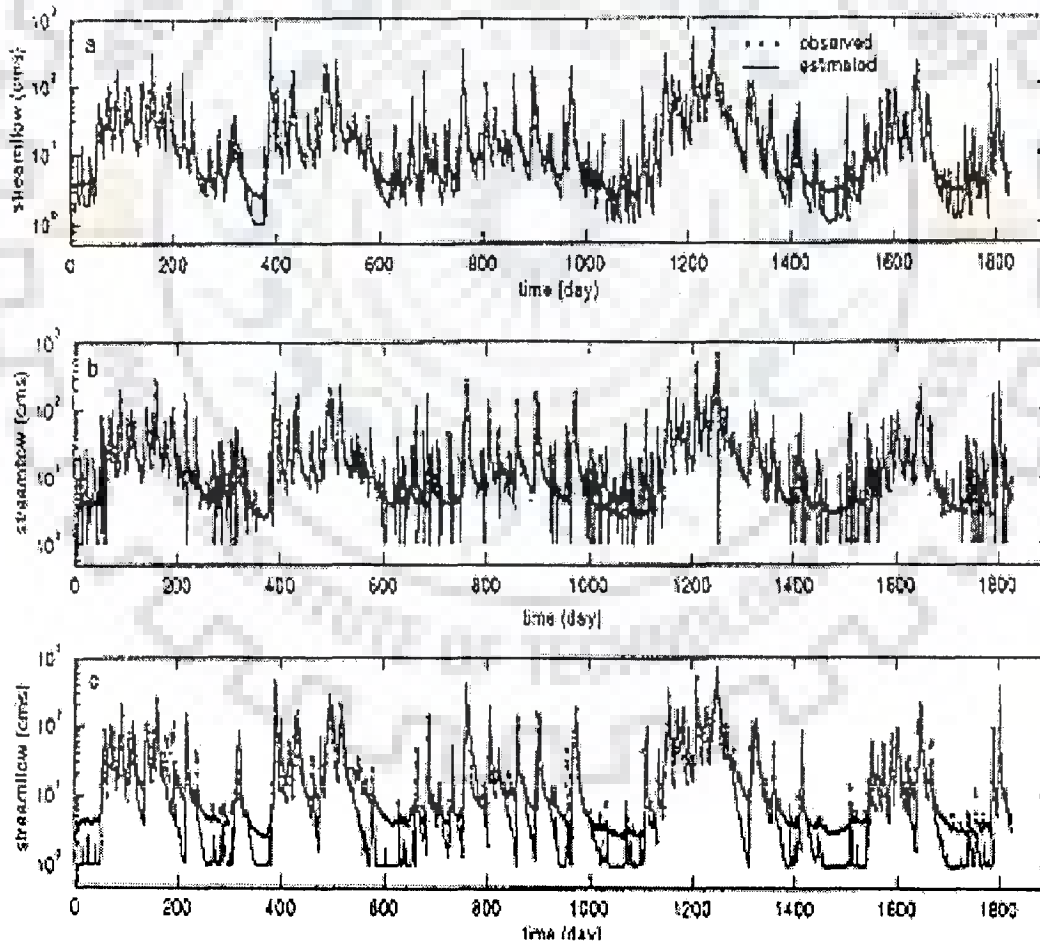


Fig. 2.6 Comparison of Observed and One-Step-Ahead Predicted Hydrographs for Five-Year Validation Period: (a) ANN (5,4,3,1); (b) ARMAX (2,4,3); (c) SAC-SMA (Hsu *et al.*, 1995)

They have attempted to enhance the training speed of the network by partitioning the weight space. The input hidden layer weights were estimated using a multistart downhill simplex nonlinear optimization algorithm, while the hidden output layer weights were estimated using optimal linear least squares estimation. The nonlinear portion of search is thereby confined to a smaller dimension space, resulting in acceleration of the training process and eliminating the probability of finding local minima. The performance of *ANN* was compared with the linear *ARMAX* time series model and the conceptual *SAC-SMA* model. The comparison of results obtained by them using the different models for one event is shown in Fig. 2.6. The *LLSSIM* is claimed to be a better algorithm than backpropagation or conjugate gradient techniques, especially in the absence of a good initial guess of weights. Though the study used data of rainfall and runoff on daily scale their main objective was to present a new algorithm for training the feedforward *ANN*. The inputs to the *ANN* consisted of the runoff observed in the past time periods.

Lorrai and Sechi (1995) applied a two hidden layer network with the aim of reproducing river flows using both mean aerial and point rainfall, and temperature data from a catchment in Italy on monthly scale. The data for different 10 years period was used for training and testing. The results obtained by them are given in Table 2.1. It can be observed that the performance of the feedforward *ANN* applied, in terms of the coefficient of determination, is poor if the testing period is different than that of training. This could be due to the fact that no data for the runoff observed in the past time periods was used in the study.

Carriere *et al.* (1996) developed a virtual runoff hydrograph system using a backpropagation *RNN*. The data from 45 laboratory experiments over a simulated catchment in the form of a tank under different conditions of slope and cover were used for this.

The *RBF* networks were employed for rainfall-runoff modeling by Mason *et al.* (1996). They used the *RBF* network for accelerating the training procedure as compared with regular backpropagation techniques and found that, though *RBF* networks provided faster training such networks require solution of a the linear system of equations that may become ill conditioned, especially if a large number of cluster centers are chosen.

Table 2.1 Results Obtained in Terms Coefficient of Determination by Lorrai and Sechi (1995)

Training Period	Evaluation/Testing Period		
	1946-55	1956-65	1966-75
1946-55	0.899	0.480	0.685
1956-65	0.597	0.699	0.472
1966-75	0.559	0.454	0.864

In their study, Minns and Hall (1996) point out the importance of standardization. The training data used by them consisted of model results from one storm sequence, and two such sequences were generated for testing using the Monte Carlo procedure. For each such storm sequence, the corresponding runoff sequence was constructed using a simple nonlinear model for flood estimation that allowed for different levels of non-linearity in the response. Minns and Hall used a three layer network with *BP* algorithm and found that *ANNs* performance was hardly influenced by the level of non-linearity. The performance of *ANN* dropped significantly whenever the network was required to predict out of range of the standardized values, suggesting that *ANNs* are not very good extrapolators.

In another study, Hsu *et al.* (1997 *b*) compared a three layer feedforward *ANN* with a *RNN* for daily rainfall-runoff modeling. They have observed that the feedforward *ANN* needs a trial and error procedure to find the appropriate number of time delayed input variables to the model whereas the *RNN* was able to provide a representation of the dynamic internal feedback loops in the system, eliminating need for lagged inputs, resulting in a compact weight space.

Shamseldin (1997) used the conjugate gradient method to train the feedforward network using daily average rainfall and runoff data from six catchments from different climatic conditions around the world. The *ANN* was given the same input as that of a simple linear model (*SLM*); a season based linear perturbation model (*LPM*), and a nearest neighbor linear perturbation model (*NNLPM*). The performance of *ANNs* was found to be better than the corresponding models during calibration and validation. The two parameter

gamma function was chosen to represent the impulse response of the rainfall series and its parameters were also estimated as part of the training process in his study.

Dawson and Wilby (1998) also used a three layer backpropagation network to determine runoff over two flood prone catchments in UK. They were successful in constructing a robust model using *ANN* for predicting 15-minute flows with 6-hour lead time. Their results show that *ANNs* performance was almost same as that of the existing forecasting system, which required more information. The *ANNs* appeared to overestimate low flows compared with actual flows. Dawson and Wilby emphasized upon the need for deciding upon the optimum training period for using the *ANN* in real-time mode. They used the continuous record of runoff. As per them accurate flood forecasting using *ANNs* requires, i) training of the *ANN* against selected events (*i.e.* individual flood hydrographs) contained in the total flow data set rather than the use of continuous record and ii) input variables which contain some memory of the antecedent catchment conditions.

Fernando and Jayawardena (1998) used a different type of *ANN* namely the *RBF* network for flood forecasting on hourly basis. They illustrated the application of *RBF* networks using an orthogonal least squares (*OLS*) algorithm to model the rainfall-runoff process. The parameters of a *RBF* model are linear and the advantage of *OLS* algorithm is that, it is capable of synthesizing suitable network architecture and thus eliminates the time consuming trial and error procedure required in the *MLP*. The hourly data for 12 high flow events occurred in a very small sized Kamihonsha catchment in Japan were used in the study. The one-hour predictions of *RBF* network were compared with the backpropagation *ANN* and the *ARMAX* model. The *RBF* network with *OLS* algorithm approach produced forecasts with comparable accuracy to those by a backpropagation algorithm in terms of mean discharge predicted by the models and the root mean square error (*RMSE*), as can be seen from the results obtained by Fernando and Jayawardena (1998) reproduced in the Table 2.2.

Hsu *et al.* (1998) tested a new type of neural network structure called self-organizing feature map with linear output (*SOLO*) for forecasting daily streamflow from rainfall measurements. The *SOLO* structure is a hybrid structure linking *SOFM* with a locally linear output (*LO*) mapping and requires hundred fold less computational efforts

Table 2.2 Statistics of Model Predictions (Fernando and Jayawardena, 1998)

Event No.	Predicted Duration (Hr.)	Mean Discharge (m ³ /s)				RMS Error (% of Observed Mean)		
		Observed	RBF/OLS	MLP/BP	ARMAX	RBF/OLS	MLP/BP	ARMAX
1 ^a	58	0.2643	0.2623	0.2686	0.2601	8.11	7.61	15.61
2 ^a	82	0.3508	0.3519	0.3520	0.3480	3.89	10.36	20.69
3	41	0.2233	0.2244	0.2315	0.2234	11.99	9.61	15.57
4	41	0.2368	0.2382	0.2459	0.3435	4.40	4.90	7.64
5	36	0.3744	0.3641	0.3714	0.3648	11.31	14.49	21.11
6	57	0.2886	0.2877	0.2914	0.2866	4.33	3.41	7.14
7	51	0.2794	0.2763	0.2833	0.2787	7.25	7.17	12.35
8	51	0.2779	0.2774	0.2837	0.2865	3.80	2.18	6.05
9	98	0.3268	0.3267	0.3277	0.3239	4.85	4.06	7.84
10	30	0.2328	0.2366	0.2430	0.2385	9.29	12.78	20.58
11	96	0.2340	0.2322	0.2401	0.2332	3.51	4.25	8.16
12	57	0.3324	0.3304	0.3334	0.3304	6.27	6.05	10.26

a – Event used in training, RMS- Root Mean Square

than Time Delay Neural Network (*TDNN*) and *RNN* models. Both *TDNN* and *RNN* require the solution of a nonlinear global optimization problem for accurate training of network parameters. The *SOLO* structure overcomes these difficulties. Its performance was compared with the *TDNN* and *RNN* structures. The *RMSE* performance of these different models is plotted in Fig. 2.7 against the total annual flow. It can be seen that the *RMSE* increases with the increasing total annual flow. The results indicated superior or equivalent performance of *SOLO* structure. The earlier studies (Hsu *et al.*, 1995; Gupta *et al.*, 1997) demonstrated the superior performance of *TDNN* in streamflow forecasting compared to complex physically based conceptual models. It can be seen from Fig. 2.7 that the *SOLO* model is able to consistently match all streamflow while the *TDNN* and *RNN* models tend to underestimate the low flows.

Campolo *et al.* (1999) made use of distributed rainfall data observed at different raingauge stations for the prediction of water levels at the catchment outlet. The neural network was applied over a sub-basin of the river Tagliamento in Italy. The data used was rainfall observed at five raingauge stations and the hydrometer data at the outlet of the sub-basin for twenty flooding events. The scatter plots in Fig. 2.8 (a) show that the model results obtained by them were poor when only rainfall observations were used as the input. The main reason for this was stated to be the fact that the input information represented by zero rainfalls during the recession part is mapped into varying water levels, which could

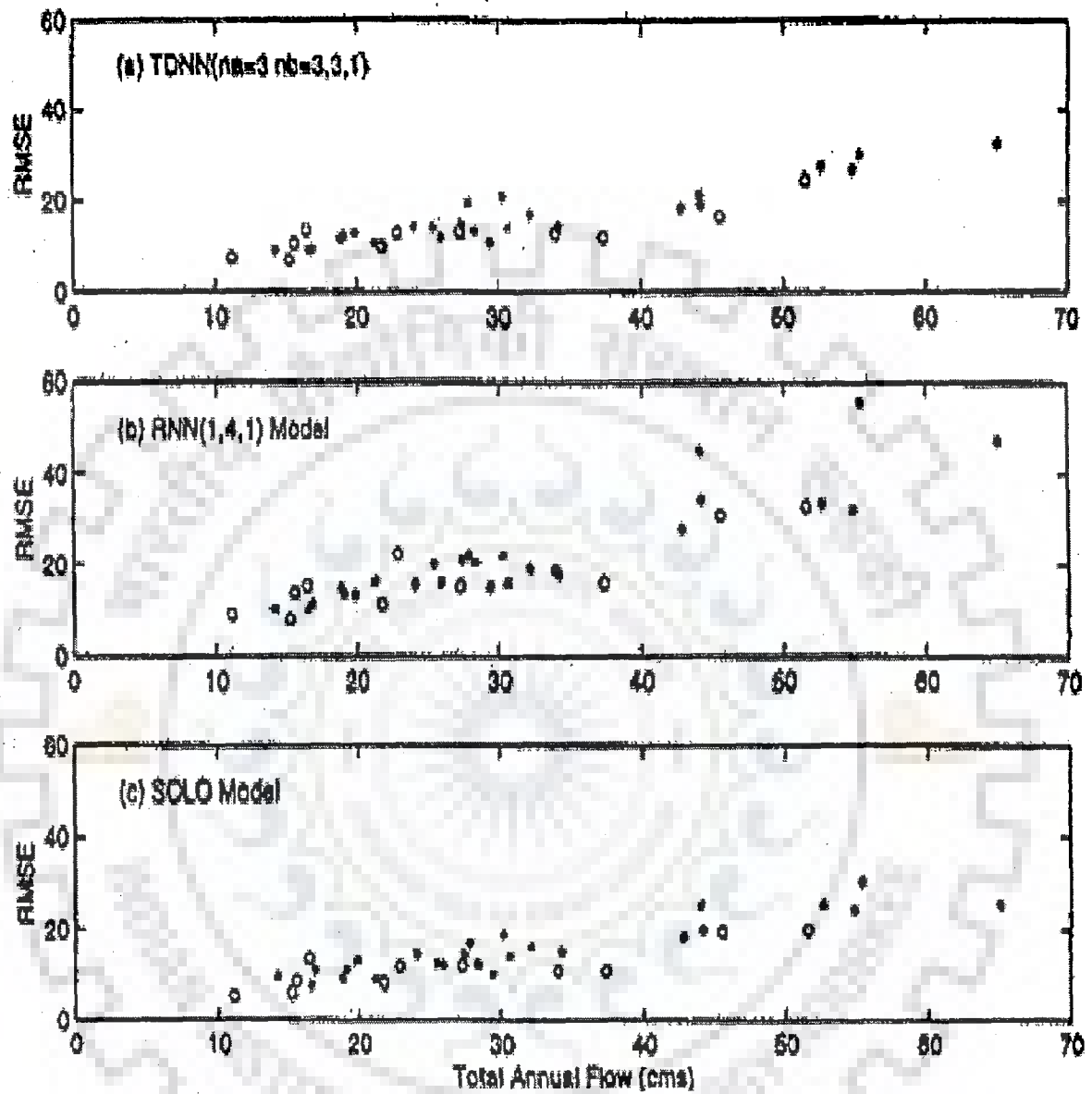


Fig. 2.7 Performance of *TDNN*, *RNN* and *SOLO* Models for Evaluation Year 1980 (Hsu *et al.*, 1998)

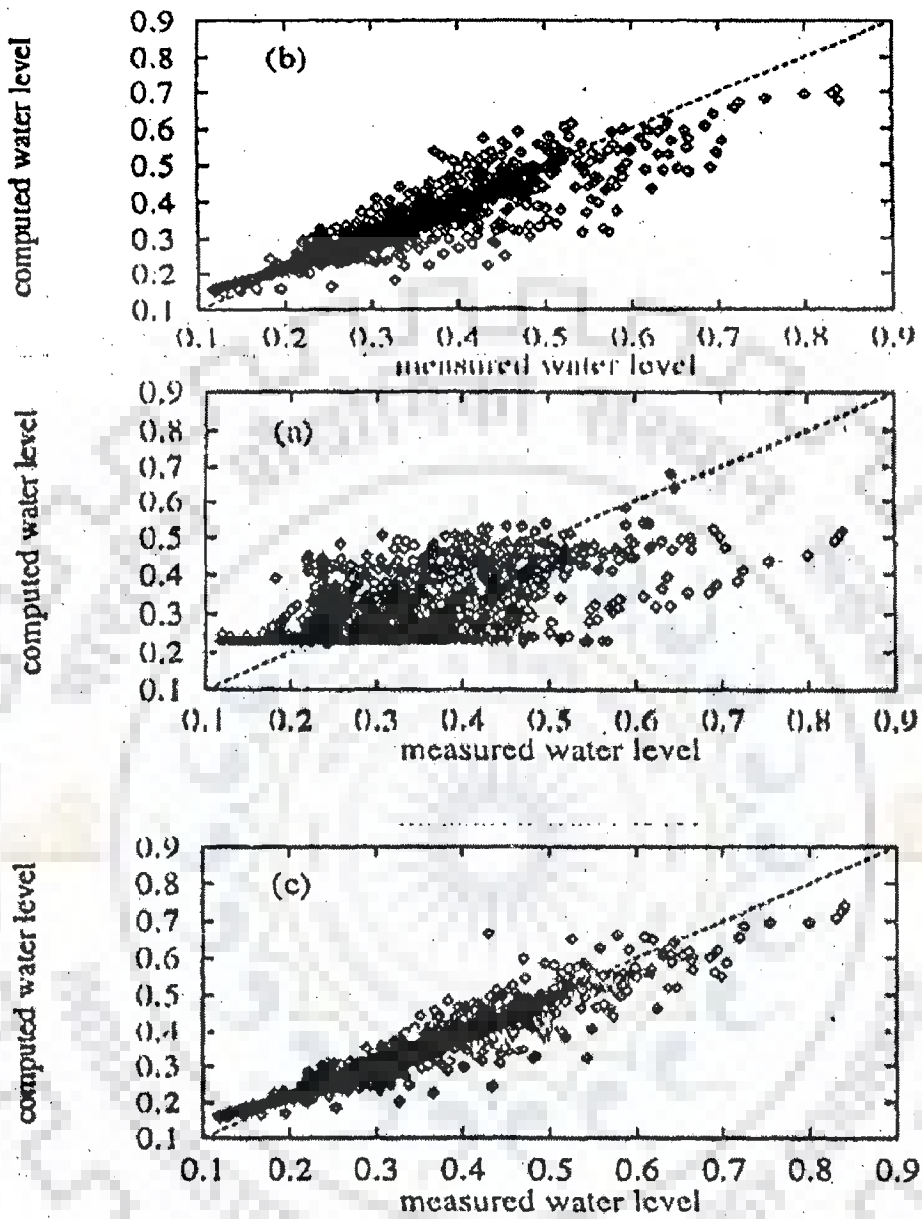


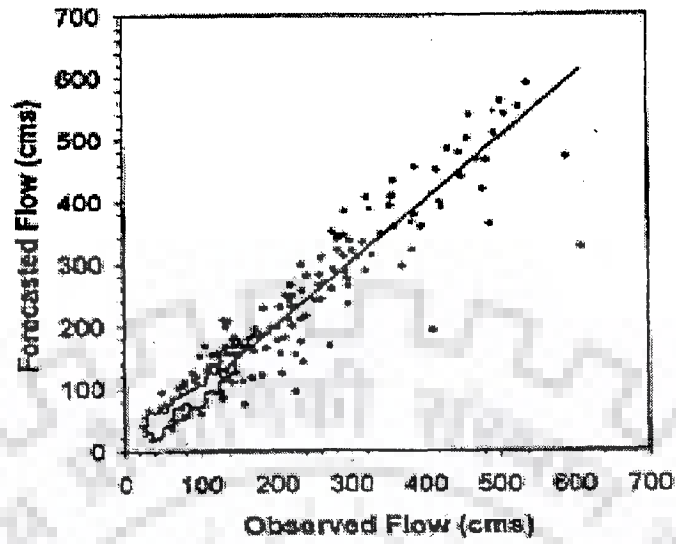
Fig. 2.8 Scatter Plots Demonstrating the Importance of Information on Water Level for Previous Time Period a) No Water Level Information; b) Water Level 4 Hours Before; c) Water Level 4 and 2 Hours Before (Campolo *et al.*, 1999)

not be learnt by the *ANN* model. The model accuracies were found to improve when the water levels observed in the recent past were also used as input as can be seen from Figs. 2.8 (b) and (c) which show respectively the scatter plots when the water level information 4 hours before and both, 4 and 2 hours before is also given as input to the *ANN*. The model predictions were accurate over 1 hour time horizon and the prediction accuracy of model decreased with increase in the prediction time horizon. This study demonstrates that for obtaining results with higher accuracy in rainfall-runoff modeling, the *ANN* must be provided with inputs, which correctly represent the soil moisture state of the catchment.

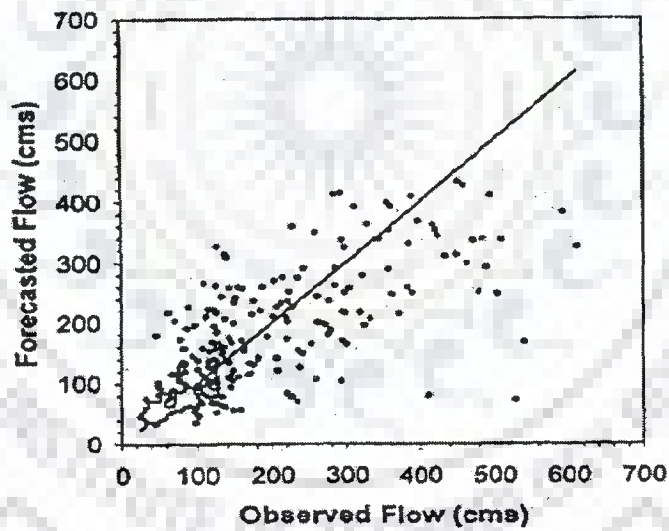
Zealand *et al.* (1999) applied *ANN* model for streamflow forecasting over a catchment of area 19,270 km² in Canada and used data for weekly averaged precipitation, temperature, and streamflow during 1965-85 for training and data from 1960-64 and 1986-88 was used for testing. The streamflow was forecasted with one week and four weeks lead-time. The *ANN* proved to be a better model than the conventional one for both forecast lead times. Figures 2.9 (a) and (b) show the scatter plots for *ANN* model applied by Zealand *et al.*, (1999) to the Namakan Lake with 1-week and 4-weeks lead-time. It can be seen from Fig. 2.9 (a) that the scatter for 1-week ahead forecast is less and all the points fall relatively close to the 45° line whereas, the scatter is more for 4-weeks ahead forecast in Fig. 2.9 (b).

Sajikumar and Thandaveswara (1999) used the temporal backpropagation neural network (*TBP-NN*) for monthly rainfall-runoff modeling in scarce data conditions. The *TBP-NN* resembles the standard backpropagation network except for having a linear finite impulse response filter for each connection. They used data from river Lee (U.K.) and river Thuthapuzha in Kerala (India). The *ANN* model was trained for different length of data. The input layer had only one neuron with the rescaled effective rainfall as input. The sum of delays used was equal to the memory length of the catchment studied. The results indicated improved performances of *ANN* in terms of accuracy and consistency over the Volterra type functional series model.

Tokar and Johnson (1999) reported that *ANN* models had better predicting accuracy and flexibility in daily rainfall-runoff modeling compared with regression and simple conceptual models. They used *ANN* with daily data of precipitation, temperature and snowmelt equivalent (*SW*) as input to forecast daily runoff for the Little Patuxent river



(a)



(b)

Fig. 2.9 Scatter Plots for ANN Model for Data of Namakan Lake (a) 1-Week Ahead Forecast; (b) 4-Weeks Ahead Forecast (Zealand *et al.*, 1999)

in Maryland (USA). The selection of training data had a large impact on accuracy of prediction of the *ANN* used. Tokar and Johnson found that, the type of training data is more important than the length of the data for neural network to perform better. An interesting feature observed by them was that the *ANN* model predictions were poor when Q_{t-1} was added as input in addition to the P_{t-1} . The reason for this was stated to be the fact that there existed very high correlation between Q_{t-1} and P_{t-1} values. Later Tokar and Markus (2000) extended this study for two more catchments and compared the *ANN*'s performance with that of conceptual models in predicting catchment runoff. The results obtained by them indicated that *ANNs* are more powerful tools in modeling the rainfall-runoff process for various time scales, topography, and climatic conditions than the other models studied. Modeling with *ANN* provided a systematic approach and reduced time spent on training as compared to the conceptual models. The performance of the *ANN* with Q_{t-1} as input was found to be best in one case study.

Anmala *et al.* (2000) carried out comparison of the feedforward network, the *RNN*, and the empirical models for predicting runoff over three medium sized catchments in Kansas (USA). Their study is on monthly basis and only the data for rainfall and temperature was used as input to the *ANN*. No data for runoff observed in the past time periods was used. Various experiments by varying the size of data for training and testing were carried out. Also, various network architectures were tested and it was observed that *RNN* performed better in prediction mode due to the dynamic feature embedded in the recurrent neural networks architecture. Table 2.3 shows the results obtained by them in terms of coefficient of determination (R^2) for different models employed by them. It can be seen from this table that the value of R^2 for the feedforward *ANN* in validation is very poor because the state of the catchment is not getting reflected in the inputs given to the network.

Tingsanchali and Gautam (2000) compared the performance of feedforward *ANN* model with Q_{t-1} , P_{t-1} and T_{t-1} as inputs in flood forecasting with the performance of two lumped conceptual hydrological models namely, the tank model and the Nedbøf-Afstrømning Model (*NAM*) and the *ARMA* model and found it to be superior. The models were applied to the two river basins in Thailand having area of 6,250 and 2,200 Km².

Table 2.3 Model Performance in Terms of R^2 for Different Models Obtained by Anmala *et al.*, (2000)

Catchment	Feedforward Network		Recurrent Network		Empirical Regression	
	Calibration	Validation	Calibration	Validation	Calibration	Validation
El Dorado	0.92	0.59	0.93	0.77	0.82	0.61
Marion	0.89	0.61	0.94	0.78	0.87	0.60
Council Grove	0.88	0.65	0.94	0.81	0.88	0.61

Zhang and Govindaraju (2000) demonstrated the applicability of a different type of network, namely, the modular neural network architecture to handle complex sets of rainfall-runoff data. They have utilized Bayesian concepts in deriving the training algorithm. A modular neural network (*MNN*) is a combination of different types of neural network with each network being designed for a specific task. This makes each module expert for a specific task and each module maps relationship in a subset of input space. A gating network receives the output from the expert modules. A weighted sum of the responses of experts forms the output of *MNN* with weights equal to outputs of gating network. The *MNN* was used for monthly runoff prediction based on monthly rainfall and temperature data. The data was partitioned into low, medium, and high flow events and was given to three expert network modules in the *MNN*. They observed improvement in the performance of *MNN* over the standard feedforward *ANN*.

In their discussion on the paper by Tokar and Johnson (1999), Kumar and Minocha (2001) have pointed out that the most significant input parameter to *ANN*, namely the rainfall, is subject to large errors and stated that the excess rainfall (*i.e.* Total rainfall – losses) instead of the total rainfall should be used as input to *ANN* or if total rainfall is to be used, then the connection weights relating total rainfall to runoff should vary with time so as to account for antecedent moisture conditions. The *ANNs*, which do not incorporate this, will yield poor results in validation stage. Kumar and Minocha suggested that the use of Kalman filter class of algorithm and the recursive least square algorithm may overcome

this difficulty. They have expected that the dynamic linear model might perform better than the *ANN* model used by Tokar and Johnson (1999).

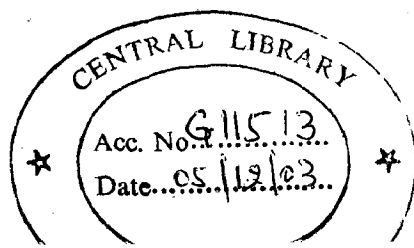
Hu *et al.* (2001) developed a new type of *ANN* namely Range Dependent Neural Network (*RDNN*) based on the clustering algorithm for obtaining better accuracy in prediction of hydrological time series. The performance of the *RDNN* was compared with the standard feedforward *BP ANN* for daily streamflow and annual reservoir inflow prediction using data from two catchments in China. They observed that the *RDNN* performed better than the *BP* network especially in reproducing the low flow events.

Wright and Dastorani (2001) applied *ANN* for river flood prediction from ungauged catchments using catchment descriptors. A multilayer feedforward *ANN* was applied for flood forecasting over a karstic catchment by Xiong *et al.* (2001) and it was observed that the *ANN* was very much successful in simulating the highly nonlinear relationship between rainfall and runoff over a Karstic catchment.

Birikundavyi *et al.* (2002) also investigated the feedforward *ANN* for forecasting daily streamflows for Mistassibi river located in northern Quebec, Canada. The results obtained by them show that the *ANN* outperformed the deterministic model used for the same up to 5-day ahead forecasts. The data for daily streamflow observed in the past, temperature, rainfall depths, and computed snowmelt were used for training the *ANN*.

Sivakumar *et al.* (2002) compared the performance of the phase-space reconstruction (*PSR*) and *ANN* approaches for forecasting the flows in the Chao Phraya river in Thailand (area = 1,10,569 Km²) for 1-day and 7-day ahead forecasts. They have noticed that the *MLP* used in the study was not suitable for runoff forecasting especially for longer lead times. For both the forecast lead-times, inputs to the *MLP* consisted of the daily observed streamflows values for past 7-days. The forecasts obtained by *PSR* approach were significantly better than the *ANN* approach for both the lead times because the *PSR* approach captures the important feature of the flow dynamics in a better way as it uses the local approximation against the global approximation being used in the *ANN*. The performance of the *MLP* was especially poor for 7-day lead-time.

The *ANN* was used for a different purpose by Shamseldin *et al.* (1997) who employed a neural network for combining the estimated outputs of five different rainfall-



runoff models to produce the combined estimated output. Such combined discharge was considered to be a better estimate of runoff than that obtained from individual models. Shamseldin and O'Connor (1999) extended this concept and developed a technique for real time combination of the outputs of different rainfall-runoff models called *RTMOCM*. Elshorbagy *et al.* (2000) developed a new statistical measure called pooled mean square error (*PMSE*) for comparing the performance of *ANN* with linear and nonlinear regression.

From the review above it can be inferred that the *ANN* methodology has been reported to provide reasonably good solutions for complex systems encountered in hydrology that may be poorly defined or understood using mathematical equations. It can be seen that the problem of rainfall-runoff modeling has perhaps received the maximum attention by the *ANN* modelers. The nonlinear nature of the relationship, availability of long historical records, and the complexity of physically based models in this regard are some of the factors that have caused researchers to look at alternative models, and the *ANNs* have been a logical choice (Hsu *et al.*, 1995). ASCE (2002 *b*) clubbed the studies involving use of *ANN* for rainfall-runoff modeling into two categories.

- (i) The first category includes studies where *ANNs* were trained and tested using the data similar to the existing models (*e.g.*, Smith and Eli, 1995; Shamseldin, 1997). After completion of the training process, the *ANNs* would provide much faster responses than the original model especially when the existing models have complex structure.
- (ii) The second category includes the studies, which have used observed rainfall-runoff data. Most of the *ANN* applications to rainfall-runoff modeling fall into this category. Frequently supplementary inputs such as temperature, snowmelt equivalent, and historical streamflows have been included and the performance of *ANN* is compared with other empirical or conceptual type models. Such studies provide a more comprehensive evaluation of *ANN* performance and are capable of establishing *ANNs* as viable tools for modeling rainfall-runoff process.

Alternatively, the studies pertaining to the streamflow forecasting and rainfall-runoff modeling reviewed in this chapter can be grouped into following two categories.

- (i) Studies in which *ANN* model uses only the discharges observed in the past as inputs and runoff in some future time is forecasted.
- (ii) Studies in which *ANN* model uses rainfall and other supplementary variables such as snowmelt, temperature *etc.* as inputs along with or without the discharges observed in the past.

Observed discharge of previous time period has been used as an input in *ANN* models in the previous studies on the premise that it indirectly represents the soil moisture state of the catchment (Gautam *et al.*, 2000). When the network inputs include the flows at previous time steps, the *ANN* could be considered to be modeling the change in flows rather than their absolute values (Minns and Hall, 1996). The use of runoff or river water level observed in the preceding time durations as one of the input to the *ANN* restricts such models from being applied to catchments which have scarce data on discharge and/or water level. Most of the studies involving use of the discharge values observed in the previous time period thus involved updating and are used in flow forecasting only. However, if a good estimates of the discharges, derived by using any auxiliary model, are instead used as input to the *ANN* then there is a strong possibility of enhancing the flow simulation efficiency of the *ANN* models in the non-updating case.

The only study of runoff analysis using *ANN* that stands apart from the rest is the study by Gautam *et al.* (2000), who attempted estimation of stream runoff from a very small sized area in Japan named Tono (area = 71.5 Ha), making use of soil moisture data. But such a study has inherent limitations of data availability. It is mentioned by Gautam *et al.* that their study area is one of the most extensively instrumented areas in the world and such data on spatial and temporal variation of soil moisture is mostly not available for rainfall-runoff modeling in a catchment.

2.13 CONCLUDING REMARKS

The review suggests that a wide variety of models ranging from simple black-box type to the complex physically based distributed ones are available in the literature for simulating the rainfall-runoff process and still the problem of runoff estimation on real time basis for forecasting and for synthesis of series of runoff in a variety of situations

continues to be an important topic of research. It is however desirable that the process of providing a satisfactory answer to these problems should involve as minimum cost as possible.

The physically based models for rainfall-runoff process have advantages over the other methods particularly when it is necessary to derive the spatially and temporally distributed information about runoff at the outlet and within various segments of the catchment area. But such models are found to have limitations related to data requirements, calibration, running cost *etc.*, because of which these models are still not adopted for day-to-day use in practice. The conceptual models have problems associated with the parameter calibration and model application. (Duan *et al.* 1992). The empiricism involved in determining the excess precipitation and separating the base flow for getting the *DRH* in case of the *UH* based models make their application subjective. A catchment is generally hydrologically nonlinear. Use of a linear model such as *UH* therefore often results in gross underestimation or overestimation of peak runoff (Rogers, 1982).

More recently the *ANN* based rainfall-runoff modeling has been practiced extensively due to the complexities involved in the conceptual modeling and physically based modeling of the rainfall-runoff process. From the studies involving use of *ANN* for modeling rainfall-runoff relationship reviewed above, it is evident that, inclusion of the runoff or the river stage observed in the past time periods as one of the input to the *ANN* is almost imperative for realistic simulation of the nonlinear rainfall-runoff relationship. The runoff or the river stage record observed in the past time period is considered to reflect the soil moisture state of the catchment. The soil moisture state of the catchment or the antecedent moisture condition (*AMC*) is the most important aspect that governs the generation of runoff from the rainfall over a catchment. It is however felt that the *SLM* can be considered as a convenient starting point in rainfall-runoff modeling using *ANN* and its output can be considered as an index for the state of the catchment. However, a major weakness of the lumped models is their inability to incorporate the spatial variation of rainfall and catchment heterogeneities especially in large sized catchments.

The present study attempts to fill the gaps identified through literature review on rainfall-runoff modeling. A linear/nonlinear system theoretic model is used as an auxiliary

model and is coupled with an *ANN* model for predicting runoff over a catchment without the use of runoff and/or the water level observed in previous time step as one of the input to the *ANN*. The weakness in catchment level lumping of parameters is partially compensated in the proposed study by dividing the large catchment into smaller sub-catchments having approximately uniform rainfall distribution and considering multiple input rainfall from these sub-catchments. In this modeling approach, the rainfall occurring in each hydrologically homogeneous sub-area of the catchment is treated as a separate input received in parallel by the overall catchment system.

The study presents the *ANN* as a flexible nonlinear rainfall-runoff black-box model, which is useful in sparse data scenario for non-updating simulation of discharges from rainfall, using daily data for the case of isolated events.

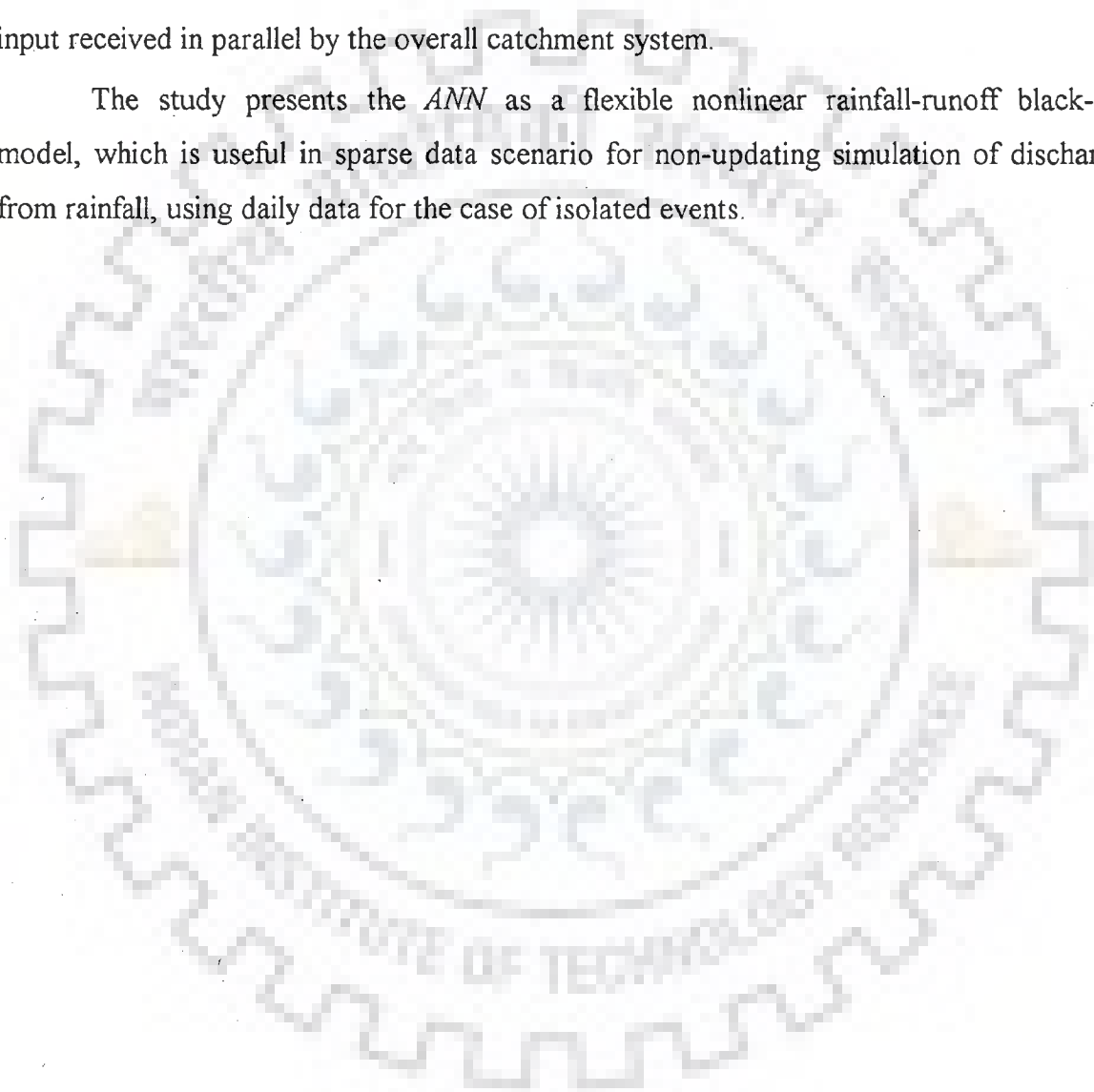


Table 2.4 Comparative Statement of the ANN Applications for Rainfall-Runoff Modeling

Sr. No.	Study By	Type of ANN Used	Input to the ANN	Output	Scale of Study/ Catchment Area
1	Half <i>et al.</i> (1993)	FF with BP	Observed Rainfall Hyetograph	Hydrograph	Storm Level, (Minutes)
2	Hjelmfelt and Wang (1993)	NN Based on UH Theory	Sequences of Rainfall	Rainfall Excess	Storm Level
3	Hjelmfelt and Wang (1996)	FF with BP	----- do -----	----- do -----	12.2 Km ²
4	Smith and Eli (1995)	FF with BP	Synthetic Rainfall Patterns	Runoff and Time to Peak	Synthetic Catchment
5	Hsu <i>et al.</i> (1995)	FF with BP	$P_t, P_{t-1}, P_{t-2}, P_{t-3}, P_{t-4},$ P_{t-5} , and $Q_t, Q_{t-1}, Q_{t-2},$ $Q_{t-3}, Q_{t-4}, Q_{t-5}$	Q_{t+1}	Daily 1949 Km ²
6	Lorrai and Sechi (1995)	FF with BP with 2 Hidden Layers	Point and Average Rainfall	Runoff	Monthly 121 Km ²
7	Hsu <i>et al.</i> (1997)	FF with BP and RNN	$P_t, P_{t-1}, P_{t-2}, P_{t-3}$, and $Q_t, Q_{t-1}, Q_{t-2}, Q_{t-3}$	Runoff	Daily 1949 Km ²
8	Carrier <i>et al.</i> (1996)	RNN	Lab. Experiment Data	Runoff Hydrograph	Minute Synthetic Catchment
9	Mason <i>et al.</i> (1996)	RBF and FF with BP	Time, Cumulative P , Intensity & Derivative of P	Q_t	
10	Minns and Hall (1996)	FF with BP with 1 and 2 Hidden Layers	Synthetic Storm Sequences with (14 P and 3 Q)	Runoff	Hourly Synthetic

NN – Neural Network, FF – Feedforward NN, BP – Backpropagation Algorithm, RNN – Recurrent NN, RBF – Radial Basis Function, P – Rainfall, Q – Runoff, T – Temperature, UH – Unit Hydrograph

Contd...

Table 2.4 Comparative Statement of the ANN Applications for Rainfall-Runoff Modeling

Sr. No.	Study By	Type of ANN Used	Input to the ANN	Output	Scale of Study/ Catchment Area
11	Shamseldin (1997)	FF with BP	Most Recent P_t , Seasonal Information of P and Q	Runoff	Daily (Continuous Data) 1207 – 18,000 Km ²
12	Dawson and Wilby (1998)	FF with BP	Various Parameters	15 min Flows with 6 Hr Lead Time	140 Km ²
13	Fernando and Jaywardena, (1998)	RBF with OLS and FF with BP	P_{t-1} , P_{t-2} , and Q_{t-1} , Q_{t-2}	Q_{t+1}	Hourly 3.12 Km ²
14	Hsu <i>et al.</i> (1998 a)	SOLO, RNN, TDNN	P_t , P_{t-1} , P_{t-2} , and Q_t , Q_{t-1} , Q_{t-2} , Q_{t-3}	Q_{t+1}	Daily 1949 Km ²
15	Campolo <i>et al.</i> (1999)	FF with BP	Station Rainfall and Q_{t-2} , Q_{t-4}	Q_{t+1}	Hourly, Event Based 1950 Km ²
16	Zealand <i>et al.</i> (1999)	FF with BP	Weekly P and T for past 7 weeks, Q for past 2 Weeks	1,2,3,4 Weeks Ahead Forecast	Weekly 19,270 Km ²
17	Sajikumar and Thandaveswara (1999)	TBP-NN	Only P	Q	Monthly 1030 and 1419 Km ²
18	Tokar and Johnson (1999)	FF with BP	P , T , SW	Q	Daily 98 Km ²
19	Tokar and Markus (2000)	FF with BP	Q_{t-1} , Q_{t-2} , SW_{t-1} , SW_{t-1} , T_{t-1}	Q_{t+1}	Monthly
20	Annala <i>et al.</i> (2000)	FF with BP and RNN	P , T	Q	Monthly 249, 200, and 246 mi ²

NN – Neural Network, FF – Feedforward NN, BP – Backpropagation Algorithm, RNN – Recurrent NN, RBF – Radial Basis Function, SOLO – Self Organizing Feature Map with Linear Output, TDNN – Time Delay NN, OLS – Ordinary Least Square Algorithm, TBP-NN – Temporal Backpropagation NN, P – Rainfall, Q – Runoff, T – Temperature

Contd...

Table 2.4 Comparative Statement of the ANN Applications for Rainfall-Runoff Modeling

Sr. No.	Study By	Type of ANN Used	Input to the ANN	Output	Scale of Study/ Catchment Area
21	Zhang and Govindaraju (2000)	MNN	Low, Medium, and High P	Q	Monthly 249, 200, and 246 mi ²
22	Tingsanchali and Gautam (2000)	FF with BP	Q_{t-1}, P_{t-1} and T_{t-1}	Q	Daily 6250 and 2200 Km ²
23	Birikundvvi <i>et al.</i> (2002)	FF with BP	$Q_t, Q_{t-1}, P_{t+1}, P_t, P_{t-1}, P_{t-2}, P_{t-3}, T_{t+1}, SW_{t-3}, SW_{t-2}, SW_{t-1}, SW_t, SW_{t+1}$	Q_{t+1}	Daily 932 Km ²
24	Sivakumar <i>et al.</i> (2002)	FF with BP	$Q_t, Q_{t-1}, \dots, Q_{t-6}$	1 and 7 Day Ahead Forecast	Daily 1,10,569 Km ²

NN – Neural Network, FF – Feedforward NN, BP – Backpropagation Algorithm, MNN – Modular NN, P – Rainfall, Q – Runoff, T – Temperature, SW – Snowmelt Equivalent

3.1 INTRODUCTION

The modeling of rainfall-runoff relationship on various time scales is reported in the literature. The time scale varied from hourly, daily, monthly, or even seasonal or annual scale. The selection of time scale mainly depends upon the purpose of analysis and the availability of the data required for it. The present study deals with modeling of the rainfall-runoff process on daily scale because simulation of the daily runoff is required for many purposes such as the formulation of long range forecast, computation of water availability in planning and operation of water resources development projects *etc.* A daily rainfall-runoff model is also required in order to get a long-term series of daily runoff. Normally, longer the time period, simpler is the model as the problem of relating long-term *i.e.* monthly or annual rainfall and runoff is easier due to the fact that over longer periods of time, the averaging of variety of storms tends to minimize the effects of rainfall intensity and antecedent moisture conditions on the volumetric relationship (Singh, 1982).

The hydrologic data used in the present study are from two large size catchments in India involving sub-divisions into smaller homogeneous areas and five other catchments from different parts of the world, which do not involve any sub-division. For the two Indian catchments (details given later) the daily rainfall data for individual raingauge stations was available, whereas for the other catchments the areal average rainfall data on daily scale were available. The data on pan evaporation or evapotranspiration on daily scale were also available for all the catchments. The daily runoff values at the outlet of each catchment were available. Runoff and the corresponding rainfall data of the runoff events that occurred during the flood period only are used in present study. As during flood period (monsoon season) high flows are experienced and modeling of which is important for flood forecasting, and design and operation of water resources structures *etc.* An event based analysis rather than the analysis of continuous hydrologic record is carried out in the present study because, in such an approach, when different models are compared the ability of the models to predict streamflow from rainfall events gets more importance,

and the lack of ability of the model in predicting antecedent moisture conditions, following long inter storm periods does not become a handicap in any way (Loague and Freeze, 1985).

3.2 EVENT IDENTIFICATION

The runoff events used in calibration and in validation of the model are identified from the daily rainfall and runoff data. A runoff event can be single peaked or may have multiple peaks. The sample event identification is shown in the definition diagram given in Fig. 3.1. There are three steps involved in the process of event identification. i) to decide about the starting point of the event, ii) to fix the end point of the event, and iii) to see if the event is single peaked or has multiple peaks.

The starting point: It is the time at which the observed runoff starts increasing and continues to rise with the passage of time to attain a significant peak daily runoff.

Consideration of multiple peaks: This is based on the study of the temporal pattern and duration of the complex storms.

The end point: This point is decided based on either of the following conditions.

- i) When the value of the observed runoff (Q_o) at that instance is less than that of the value of runoff at starting point (Q_s).
- ii) The event is terminated even if the value of observed runoff at a time $Q_o > Q_s$, but in such cases the subsequent rise in the hydrograph is due to a different storm.

The following paragraphs present the details about data availability and the preliminary analysis of the data carried out. First, the data used and description about the two large sized catchments from India is given, and this is followed by description of the other catchments.

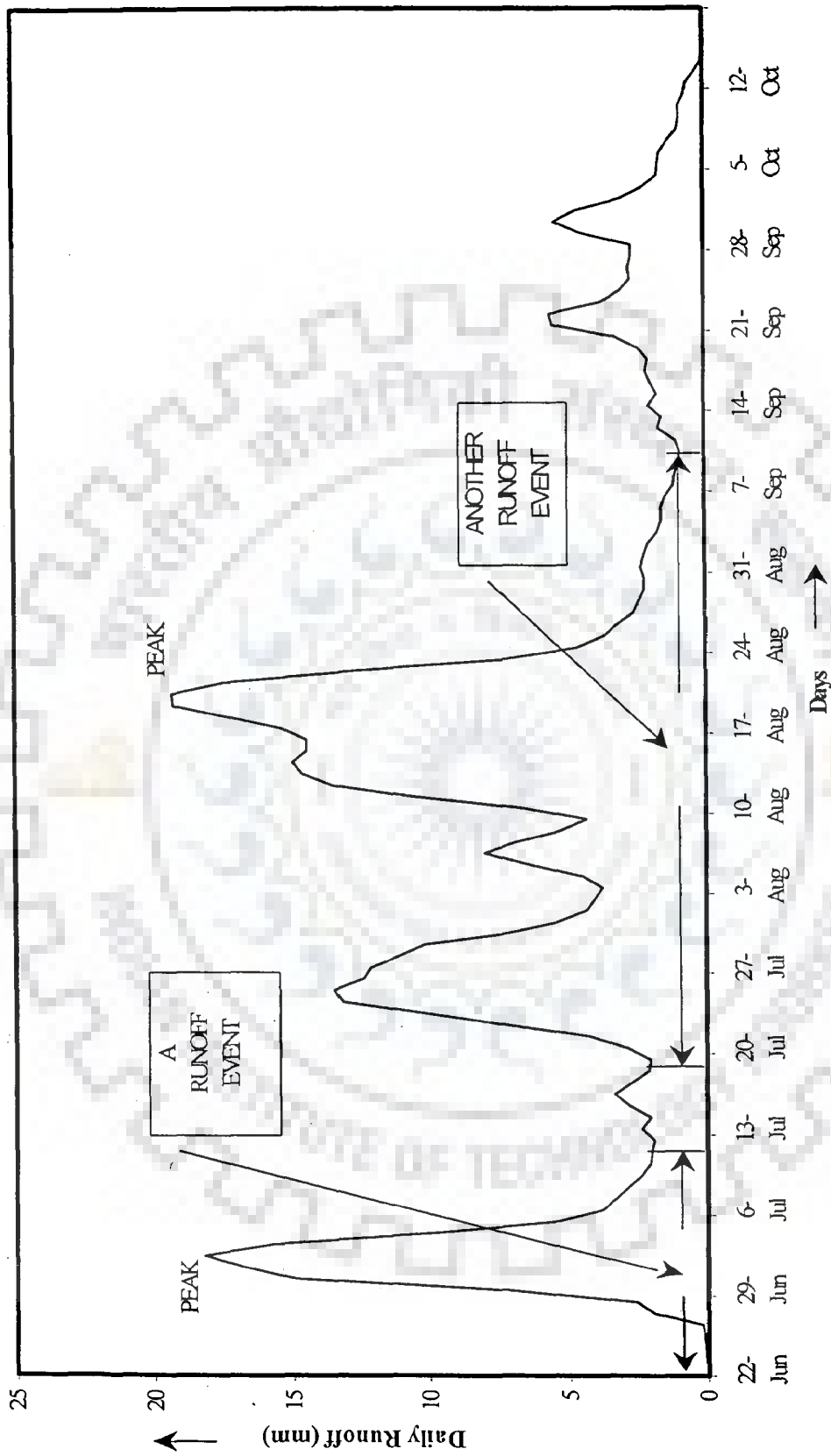


Fig. 3.1 Definition Diagram Showing Identification of The Runoff Event

3.3 THE NARMADA CATCHMENT

The data for upper part of Narmada river catchment up to Jamtara gauge and discharge (*G & D*) site covering an area of 17,157 km² are used. The river Narmada, the fifth largest basin of India, is a major river system in central India. It originates in the Maikala range near Amarkantak in Shahdol district of Madhya Pradesh State of India at an elevation of 1057 m above mean sea level (*m.s.l.*) and flows westwards over a length of 1312 km traversing through Madhya Pradesh, Gujrat, and Maharashtra States and finally meets the Arabian sea.

i) Location

The catchment area lies between north latitudes 21°40' to 23°20' and east longitudes 79°40' to 81°45'. Figure 3.2 shows the index map of the catchment along with the location of the raingauge stations in the catchment. Length of river up to Jamtara *G&D* site is 399 km. The elevation of Jamtara is 360 m above *m.s.l.*

ii) Climate

The climate in the catchment area is humid and tropical, very hot in summer and cold in winter. The area receives most of the rainfall from the Southwest monsoon during the months of June to October, of which, July and August are the wettest months. The average annual rainfall of the catchment is 1480 mm. Maximum temperature is around 42° to 43° C in the month of May whereas, the minimum is around 7°C in the month of December. The temperature during monsoon season ranges between 27.5° C to 30° C.

iii) Topography

The upper part of the Narmada catchment has a complex relief. The topography is hilly with forest cover having Sal and Teak wood trees. A large part of the catchment was under agriculture and forest during the period for which the data are available. The elevation in this area varies from 360m to 900m above *m.s.l.* There are number of falls in head reaches of the river, and the basin is heavily dissected by the stream network. Two major tributaries river Burhnar at 248 km (near Mannot) and river Banjar at 287 km (near Mandla) join the river Narmada from left. The average riverbed slope up to Jamtara is 1:740. The soil is loamy clay with 60% of area having red and yellow, 25% having deep

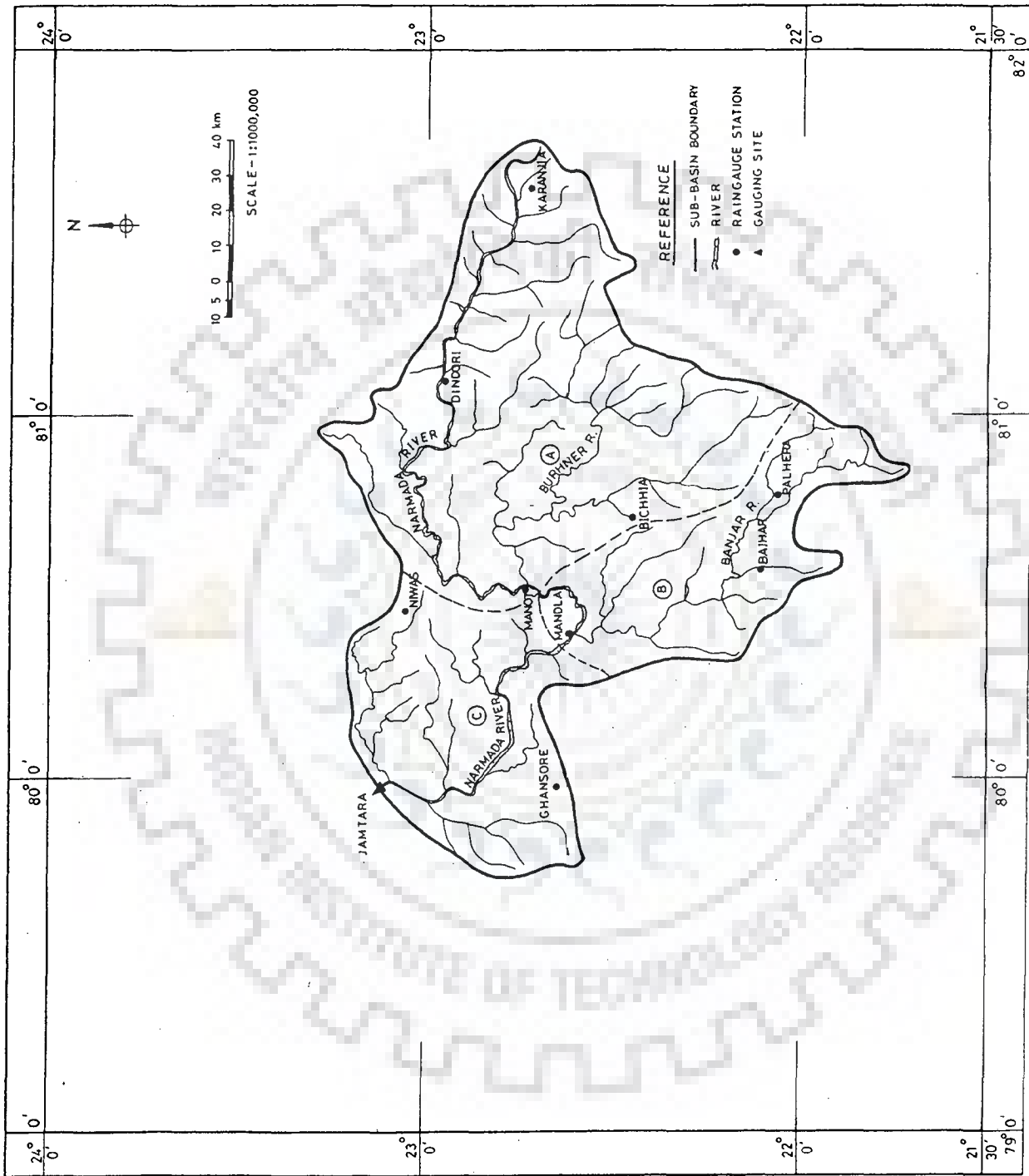


Fig. 3.2 Index Map of The Narmada Catchment up to Jamtara G&D Site

black, and the rest having medium black soil. The soil is derived from basalt and granite parent material with soil reaction being neutral to slightly alkaline. Vegetation observed in lower part includes a variety of crops. Scrub and bare soils are also observed.

iv) **Data Availability**

The daily rainfall data for the monsoon period (June to October) for the year 1981 to 1990 for nine raingauge stations as shown in Fig. 3.2 were procured from the India Meteorological Department, Pune (India). The daily discharge data for the same duration at Jamtara *G&D* site was collected from the Central Water Commission, New Delhi. The discharge is gauged by current meters up to three times a day during monsoon period and the mean daily values are worked out by arithmetic averaging. The stage is read at hourly interval. Float gauging is used when the stage of the river is too high for current metering. The available data was processed by filling up the missing records. Although the original units of these discharge data were cumecs, they were converted to equivalent depth in millimeter over the entire area of the catchment. The consistency of the daily rainfall and discharge data was checked and was found to be satisfactory.

v) **Analysis of Data**

The analysis of the available daily runoff data for monsoon period for ten years was carried out and finally ten runoff events were identified. The first six events were used for calibration or training of the model and remaining four events were used for validation or testing purpose. Table 3.1 gives details about these runoff events identified in the Narmada catchment. The average rainfall was worked out for each rainfall-runoff event using the Thiessen polygon method and used in further analysis.

3.3.1 **Catchment Representation**

The Narmada catchment has been represented in three different ways for the purpose of providing rainfall input to the models. First, the entire catchment was considered as a single unit then it was divided into two sub-areas. The catchment was further sub-divided into three sub areas (*A*), (*B*), and (*C*) as shown by dotted lines in Fig. 3.2. In the two input case one sub-division is as shown by (*A*) and the second sub-division comprises of the combined area of the sub-divisions (*B*) and (*C*) shown in

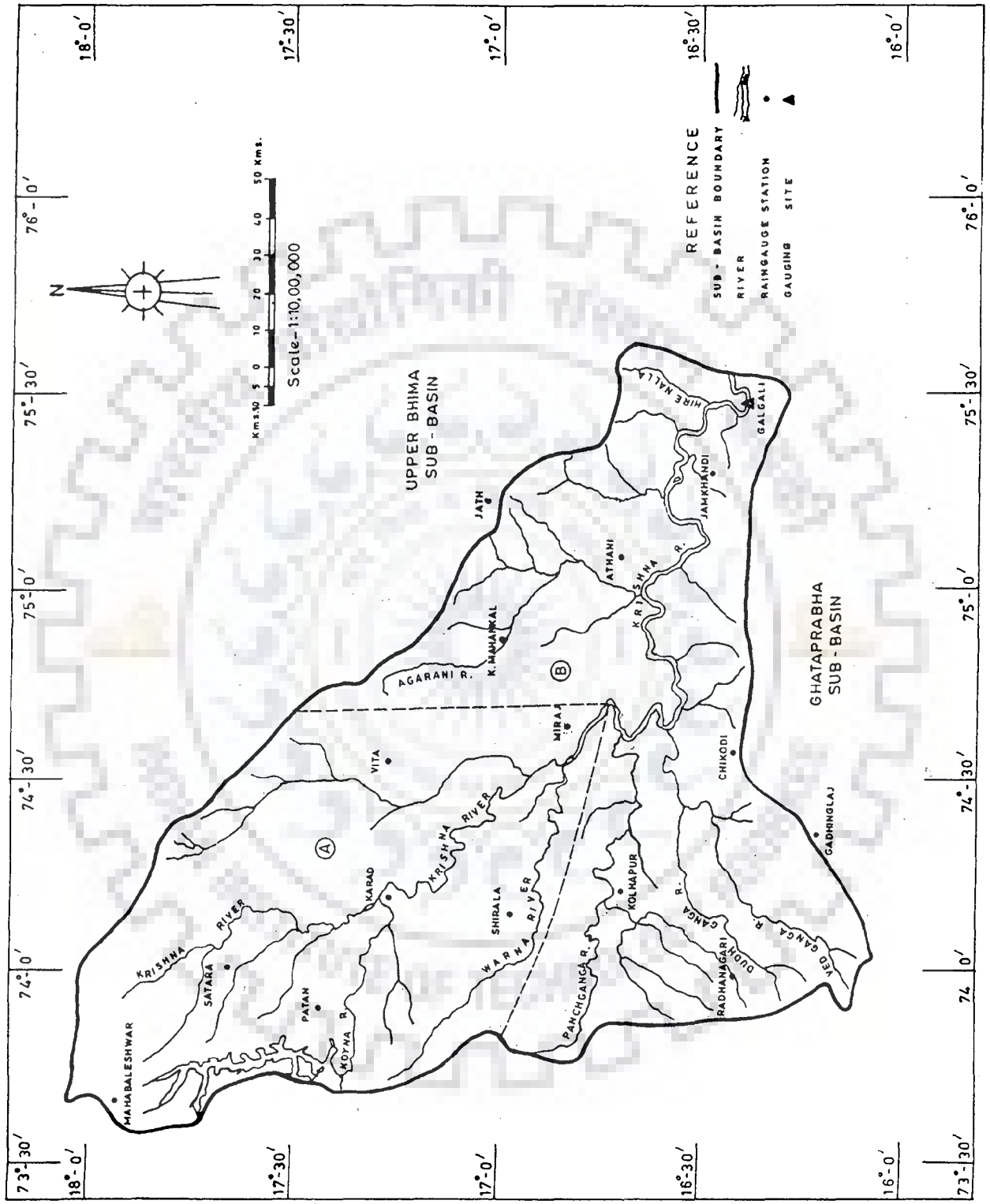


Fig. 3.3 Index Map of The Krishna Catchment up to Galgali G&D Site

Table 3.1 Runoff Events Selected For The Narmada Catchment

Catchment	Calibration Period	Duration (Days)	Verification Period	Duration (Days)
River Narmada at Jamtara, India	(1) July 19 – Aug. 14, 1981	27	(7) Sept. 08–Sept. 29, 1987	22
	(2) Aug. 8 – Sept 18, 1982	42	(8) July 20 – Aug. 19, 1988	31
	(3) Aug. 29 – Oct. 15, 1983	48	(9) July 12 – July 30, 1990	19
	(4) Aug. 7 – Sept. 18, 1984	43	(10) Aug. 27–Sept. 11, 1990	16
	(5) July 16 – Oct. 7, 1985	84		
	(6) July 6 – Sept. 9, 1986	66		

Table 3.2 Runoff Events Selected For The Krishna Catchment

Catchment	Calibration Period	Duration (Days)	Verification Period	Duration (Days)
River Krishna at Galgali, India	(1) June 22 – Sept. 22, 1980	93	(7) July 17 – Sept. 08, 1986	54
	(2) June 26 – July 21, 1981	26	(8) July 02 – Aug. 4, 1987	34
	(3) June 22– July 12, 1983	21	(9) June 25 – Aug. 21, 1988	58
	(4) July 19– Sept. 10, 1983	54	(10) Sept. 10– Oct. 17, 1988	38
	(5) June 29 –Sept. 25, 1984	89		
	(6) June 27 – Sept. 9, 1985	75		

Fig. 3.2. The sub-area demarcation exhibited in Fig. 3.2 was based on the hydro physiological homogeneities in the catchment as indicated by vegetation, slope, soil type and the long-term rainfall isohyetal maps for the catchment. The average rainfall for each sub area was computed separately using the Thiessen polygon method and this average rainfall in each sub-catchment is then considered as a parallel and separate lumped input to the models applied.

3.4 THE KRISHNA CATCHMENT

The upper and a part of middle sub-basin of Krishna river up to Galgali *G&D* site comprising of an area of 26,200 km² is considered for analysis. The river Krishna is the second largest river in peninsular India. The river rises in the Mahadev ranges of the Western Ghats near Mahabaleshwar in Maharashtra State at an altitude of about 1337 m above *m.s.l.* After traversing a distance of about 1400 km, the river joins the bay of Bengal covering the States of Maharashtra, Karnataka and Andhra Pradesh. Six major tributaries join river Krishna up to the Galgali *G&D* site. These are: i) river Koyna; ii) river Warna, iii) river Panchganga; iv) river Dudhganga; and v) river Vedganga joining the river from southwest direction and river Agarani joining from north side of the river Krishna near Athani.

i) Location

The catchment area under study is located between north latitudes 16° 05' to 18° 05' and east longitudes 73° 35' to 75° 40'. The catchment lies partly in Maharashtra and partly in the Karnataka State. Figure 3.3 shows the index map of the Krishna catchment with the locations of the raingauge stations marked on it.

ii) Climate

There are three seasons prevailing in the catchment viz. summer (March-May), monsoon (June-October), and winter (November-February). The monthly average maximum and minimum temperatures in the catchment are 31.2°C and 19.2°C respectively. The mean relative humidity is high, and the sky is heavily clouded during the southwest monsoon season. During the non-monsoon period the humidity is comparatively low and clear or lightly clouded sky prevails. The catchment lies in a low rainfall area; the

average annual rainfall is of the order of 600 mm. The climate of the catchment is generally dry except during the monsoon season.

iii) Topography

The major part of the catchment varies from altitude of 914 m to 1219 m above *m.s.l.* The catchment has flat to gently undulating terrain except for a few hillocks and valleys. The predominant rocks are limestones, shales, and quartzites. The alluvium is confined mainly to the deltaic regions of principal rivers.

iv) Data Availability

The daily discharge data at Galgali *G&D* site for monsoon season of the year 1981 to 1988 were procured from the Central Water Commission, New Delhi. The data was checked for consistency and found to be satisfactory. The catchment has a good network of raingauge stations. The daily rainfall data for corresponding periods (for which the daily runoff data were available) were procured from the India Meteorological Department, Pune. The daily rainfall data for many stations was available but finally fifteen stations, which were functioning during all the period of the runoff events, were selected. Figure 3.3 shows location of raingauges. As can be seen from this figure, the two raingauge stations, namely Jath and Gadhinglaj are adjacent but just outside the boundary of the catchment. The other thirteen raingauge stations are situated within the catchment.

vi) Analysis of Data

The similar exercise of runoff events identification from the daily runoff data as in the case of Narmada catchment was carried out and ten runoff events were identified. The first six runoff events were considered as calibration events and remaining four events were utilized for the purpose of validation or testing. The runoff events identified in Krishna catchment are given in Table 3.2. The average rainfall was worked out using the Thiessen polygon method.

3.4.1 Catchment Representation

The entire Krishna catchment was considered as a single unit initially. It was then divided into two sub catchments (*A*) and (*B*) as indicated by dotted lines in Fig. 3.3. This

Table 3.3 Runoff Events Selected For The Bird Creek Catchment

Catchment	Calibration Period	Duration (Days)	Verification Period	Duration (Days)
Bird Creek, (USA)	(1) April 17–May 08, 1957	22	(9) May 01 – May 17, 1961	17
	(2) May 08 – May 30, 1957	23	(10) July 11–July 28, 1961	18
	(3) June 09–July 08, 1957	30	(11) Aug. 12–Aug. 21, 1961	10
	(4) May 16–May 31, 1959	16	(12) Sept. 11–Sept. 20, 1961	10
	(5) Sept. 29–Oct. 12, 1959	14	(13) Sept. 13–Sept. 24, 1962	12
	(6) April 11–April 27, 1960	17		
	(7) May 04 – May 13, 1960	10		
	(8) May 27 – June 06, 1960	11		

Table 3.4 Runoff Events Selected For The Brosna Catchment

Catchment	Calibration Period	Duration (Days)	Verification Period	Duration (Days)
Brosna (Ireland)	(1) Jan. 06 – Feb. 20, 1969	46	(9) Nov. 22 – Dec. 20, 1975	29
	(2) Feb. 16 – Mar. 27, 1970	40	(10) Feb. 02–Mar. 30, 1977	57
	(3) April 11–May 29, 1970	49	(11) Jan. 26 – Feb. 20, 1978	26
	(4) N6v. 27–Dec. 27, 1973	31	(12) Nov. 30–Dec. 23, 1978	24
	(5) Jan. 01 – Jan. 25, 1974	24		
	(6) Jan. 25 – Mar. 12, 1974	47		
	(7) Sept. 01–Oct. 03, 1974	33		
	(8) Jan. 05 – Feb. 15, 1975	42		

sub-division of the catchment into smaller sub-areas was based on the drainage pattern and other characteristics of the catchment similar to that described in case of the Narmada catchment. The third sub-division of the Krishna catchment was also attempted however the same could not finally be used in the *ANN* based modeling for the reasons explained in chapter 5.

3.5 OTHER CATCHMENTS

In addition to the two catchments from India described above, the data from the five other catchments namely, Bird Creek (USA), Brosna (Ireland), Garrapatas (Colombia), Kizu (Japan), and Pampanganga (Philippines) are also utilized in the present study. For these catchments the average daily rainfall and the daily discharge data at the outlet of each of the catchment were available. The identification of runoff events from the daily runoff data was carried out in each of these catchments in a manner described earlier. These catchments are relatively small in size; hence sub-division of these catchments into smaller areas is not attempted. The catchments are located in various countries situated in different parts of the world and hence are having varying climatic conditions.

3.5.1 The Bird Creek Catchment

This catchment has an area of 2344 km², and is located near Sperry, Oklahoma in USA. The catchment has rolling topography and moderately humid climate. The land-use land-cover conditions were such that about 80% of the area was grassland and a small part of area is covered under forest for the period for which the data is available. From the analysis of the available daily discharge data for the duration 1957-1962, a total of thirteen runoff events were identified. The first eight events, which occurred during 1957-1960, were utilized for calibration and the later five events, which occurred between 1961-1962, were used for the purpose of validation or testing in the present study. The runoff events selected in this catchment are listed in Table 3.3.

3.5.2 The Brosna Catchment

The Brosna catchment is located in Ireland and has an area of 1207 km². The daily average rainfall and runoff data at Ferbane *G & D* site in this catchment for the duration

Table 3.5 Runoff Events Selected For The Garrapatas Catchment

Catchment	Calibration Period	Duration (Days)	Verification Period	Duration (Days)
Garrapatas (Colombia)	(1) Oct. 02 – Oct. 15, 1980	14	(11) Dec. 29, 83– Jan. 16, 84	19
	(2) Nov. 03–Nov. 23, 1980	21	(12) May 09 – May 23, 1984	15
	(3) April 15–May 09, 1981	25	(13) Sept. 16– Sept. 29, 1984	14
	(4) May 22–June 20, 1981	30	(14) Oct. 21– Dec. 06, 1984	47
	(5) Oct. 25 – Dec. 03, 1981	40		
	(6) Dec. 30, 81 – Jan. 22, 82	24		
	(7) Feb. 09 – Feb. 25, 1982	17		
	(8) April 10–April 25, 1982	16		
	(9) Nov. 03–Nov. 15, 1982	13		
	(10) Nov. 25–Dec. 25, 1983	31		

Table 3.6 Runoff Events Selected For The Kizu Catchment

Catchment	Calibration Period	Duration (Days)	Verification Period	Duration (Days)
Kizu (Japan)	(1) May 08–May 27, 1963	20	(11) May 31 – June 15, 1966	16
	(2) June 02 – June 27, 1963	26	(12) June 30 – July 24, 1966	25
	(3) June 24–July 06, 1964	13	(13) Aug. 12– Aug. 21, 1966	10
	(4) Sept. 20–Oct. 05, 1964	16	(14) Sept. 21– Oct. 06, 1966	16
	(5) Mar. 14 –Mar. 26, 1965	13	(15) July 06– July 17, 1966	12
	(6) April 29–May 14, 1965	16		
	(7) May 26 – June 11, 1965	17		
	(8) June 12 – July 17, 1965	36		
	(9) July 20 – July 30, 1965	11		
	(10) Sept. 07–Sept. 28, 1965	22		

1969 to 1978 were available. After analyzing this data, a total of twelve number of runoff events were identified and the model calibration or training was done with the first eight events whereas the validation or testing is carried out with the last four runoff events. These runoff events are given in Table 3.4.

3.5.3 The Garrapatas Catchment

The Garrapatas catchment, located in Colombia, has an area of 1490 km². The catchment is mountainous, forested, and has humid tropical climate. The average rainfall for the study period is 7.5 mm per day and the average discharge is about 3.83 mm per day. The daily discharge data at the La Union *G&D* site at the outlet of the Garrapatas catchment for duration 1980 to 1984 were available, from which fourteen runoff events were identified for use in the present study. The first ten events were used for calibration, whereas the remaining four events were employed for validation. The details of the runoff events used in this catchment are given in Table 3.5.

3.5.4 The Kizu Catchment

The Kizu catchment is located in Kinki region of Japan and is having an area of 1445 km². The terrain is hilly and forested and the climate is humid. The daily runoff data at the outlet of the catchment were available for the duration 1963 to 1966. Fifteen runoff events were identified from the analysis of this data. The first ten runoff events were used for calibration whereas the validation was carried out with the other five runoff events. Details of the runoff events identified in the Kizu catchment are given in Table 3.6.

3.5.5 The Pampanga Catchment

This catchment has an area of 5,273 km² and it is located in Philippines. It has recorded an average rainfall of 4.6 mm per day and average runoff of 2.6 mm per day during the period 1974 to 1978 for which the daily rainfall and daily runoff data were available. The catchment is having humid climate and the area is partly covered with grassland. From the daily discharge data at Arayat *G&D* site located at the outlet of the Pampanga catchment ten runoff events were identified. The calibration was performed with the first six events and the last four events were used for validation purpose. These runoff events identified are described in Table 3.7.

The summarized description of all the catchments, the number of runoff events identified and used for calibration and validation purpose and the range of events in days in each catchment are given in Table 3.8. The Table 3.9 shows the values for the average daily rainfall and average daily runoff worked out separately for the calibration and validation periods for each of the catchment being studied. The length of the data used for calibration and validation purpose along with the duration of total data (in days) in all the catchments is also given in this table. The available period of synchronous rainfall-runoff for each catchment was split into two samples, the first used for training and the second used for testing various models applied in the present study. This partitioning was carried in such a way that approximately seventy percent of data is used for calibration/training of the model and the remaining thirty percent of the data used for testing the models.

Table 3.7 Runoff Events Selected For The Pampanga Catchment

Catchment	Calibration Period	Duration (Days)	Verification Period	Duration (Days)
Pampanga (Philippines)	(1) June 09 – June 23, 1974	15	(7) July 30 – Aug. 20, 1976	22
	(2) July 12 – Aug. 08, 1974	28	(8) Sept. 29– Oct. 15, 1976	17
	(3) Aug. 13–Aug. 28, 1974	16	(9) Sept. 26– July 10, 1977	15
	(4) Oct. 10 – Oct. 28, 1974	19	(10) July 07– July 21, 1978	15
	(5) Oct. 18 – Nov. 18, 1975	32		
	(6) May 20 – June 10, 1976	22		

3.6 DETERMINATION OF EFFECTIVE RAINFALL

The consideration of losses due to evaporation and evapotranspiration is important in the present study as the rainfall-runoff modeling carried out is on daily scale and the rainfall-runoff events are spread over several days. The observed rainfall subtracted with the losses due to evaporation and evapotranspiration is called here as the *Effective Rainfall (EFR)*, which is the actual rainfall that is contributing to the process of runoff generation over any catchment. For the two catchments involving sub-divisions the values of potential evapotranspiration (*PET*) were taken from (Rao *et. al.*, 1976).

Table 3.8 Details of Runoff Events Selected in All The Catchments

Catchment	Country	Area (Km ²)	Runoff Events for Calibration			Runoff Events for Validation		
			Number	Period	Range of Runoff Events (Days)	Number	Period	Range of Runoff Events (Days)
Narmada	India	17,157	06	1981 - 86	27 - 84	04	1987 - 90	16 - 31
Krishna	India	26,200	06	1980 - 85	21 - 93	04	1986 - 88	34 - 58
Bird Creek	USA	2,344	08	1957 - 60	10 - 30	05	1961 - 62	10 - 18
Brosna	Ireland	1,207	08	1969 - 75	24 - 49	04	1975 - 78	24 - 57
Garrapatos	Colombia	1,490	10	1980 - 83	13 - 40	04	1983 - 84	14 - 47
Kizu	Japan	1,445	10	1963 - 65	11 - 36	05	1966 - 71	10 - 25
Pampanga	Philippines	5,273	06	1974 - 76	15 - 32	04	1976 - 78	15 - 22

The *PET* is defined as, “The amount of water transpired in unit time by a short green crop, completely shading the ground, of uniform height and never short of water”. The values of the *PET* as provided in (Rao *et. al.*, 1976) are computed for number of places in India by using the Modified Penman's Method on monthly time scale. These values were converted to daily scale by dividing it by number of days in respective months and used in this study.

The present study is limited to the monsoon period only, during which the climatic conditions are humid and the temperature variation during 24 hours is significantly less compared to hot and dry summer months. As the temperature and other climatological parameters in these months do not vary much during different years, the same value of *PETs* were utilized for obtaining the *EFR* values for all runoff events which occurred in different years. For Krishna catchment, the *PET* values at three locations in the catchment namely, Mahabaleshwar, Miraj and Kolhapur and one station just outside the catchment namely, Bijapur were available. The average daily values of *PET* for the catchment were worked out from these station *PET* values by taking the arithmetic average. The actual evapotranspiration taking place at any place is not at the *PET* rate but at a slightly lesser rate called the actual evapotranspiration (*AET*). The average *PET* values worked out above were then multiplied by a coefficient (*C*) < 1 so as to get the values of the *AET*. The coefficient *C* is different for every catchment studied. This *AET* values were then subtracted from the observed daily rainfall. (see Eq. 3.1 below) to get the required *EFR* values. The value of *EFR* is set to zero if the observed rainfall value is less than the *AET*.

$$\begin{aligned}
 AET &= \{ C * (Evaporation/Evapotranspiration) \} \\
 \text{Effective Rainfall (EFR)} &= \{ \text{Observed Rainfall} - AET \} \quad (3.1)
 \end{aligned}$$

For Narmada catchment the monthly *PET* values at two places namely, Mandla and Jabalpur were available. The daily *EFR* values were worked out in a similar fashion as described above using Eq. (3.1).

The daily average evaporation data were available for all the catchments without sub-divisions, except for the Kizu catchment, for which the daily evapotranspiration data were available. These data of evaporation or the evapotranspiration were used to derive the daily *EFR* values for the respective catchments. The value of *C* for all catchments was varied from 0.5 to 0.8 and the corresponding *EFR* values were worked out. Finally, the

value of C for which best results were obtained was selected and the corresponding EFR values are used in the analysis. Table 3.10 shows the values of the coefficient (C) adopted for all the catchments being studied. In case of the Bird Creek and Kizu catchments, the values of the coefficient derived were similar to that used by Kothyari *et al.* (1993).

Table 3.9 Brief Description of The Data Used

Catchment	Total Number of Daily Runoff Values Used			Average Rainfall (mm/day)		Average Runoff (mm/day)	
	Cal.*	Val.*	Total	Cal.	Val.	Cal.	Val.
Krishna	358	184	542	9.33	8.81	5.74	4.96
Narmada	310	88	398	10.36	12.93	4.92	6.99
Bird Creek	143	67	210	8.27	8.92	4.66	4.04
Brosna	312	136	448	3.25	3.25	2.32	2.34
Garrapatas	231	95	326	9.69	9.23	6.42	6.76
Kizu	190	79	270	8.63	8.27	6.38	6.46
Pampanga	132	69	201	15.48	10.80	12.18	8.19

*Cal. - Calibration; Val. - Validation

Table 3.10 The Value of The Coefficient (C)

Sr. No.	Catchment	The Value of Coefficient (C)
1	Narmada	0.80
2	Krishna	0.80
3	Bird Creek	0.60
4	Brosna	0.60
5	Garrapatas	0.60
6	Kizu	0.80
7	Pampanga	0.80

4.1 INTRODUCTION

As described earlier in detail, various approaches for modeling the rainfall-runoff relationship exist in literature. These range from simple black box type approach to the complex physically based distributed modeling approach. Each of these approaches has its advantages and limitations. The black box type of approach mostly considers a catchment as a lumped system that receives rainfall as the input and produces output in the form of runoff at the catchment outlet. Such an approach although has been useful in the past but now it is considered to be limited in scope of application due to the over simplified representation of the complex process of runoff generation over a catchment. The physically based distributed models on the other hand involve solving the mathematical formulations describing the component sub-processes involved in the transformation of rainfall into runoff. This makes such models data intensive and expensive to run in terms of time and cost. The application of conceptual models also requires significant amount of data and calls for expertise as well as experience with the model. As outlined earlier in chapter 2 such factors pose various difficulties in operation of these models.

In light of above, an approach is proposed in the present thesis for modeling the rainfall-runoff process that couples an auxiliary linear/nonlinear model with the *ANN*. It is a black box type of approach that requires minimum data and computational efforts. The proposed approach involves the application of *ANN* and is found to produce results with good accuracy. The studies reviewed in chapter 2 indicate that the *ANN* model fails to simulate the rainfall-runoff process satisfactorily in the absence of the information about the soil moisture state of catchment being given as one of the input. The runoff or the water level observed in the previous time period has been used in earlier studies for representation of the soil moisture state. This is termed as the updating flow simulation process. The disadvantages of using such inputs have been mentioned in chapter 2. The present study attempts to overcome the limitations of the existing *ANN* based rainfall-runoff modeling by exploring new inputs to the *ANN*. The proposed methodology is applied to the daily rainfall-runoff data from various catchments from different climates.

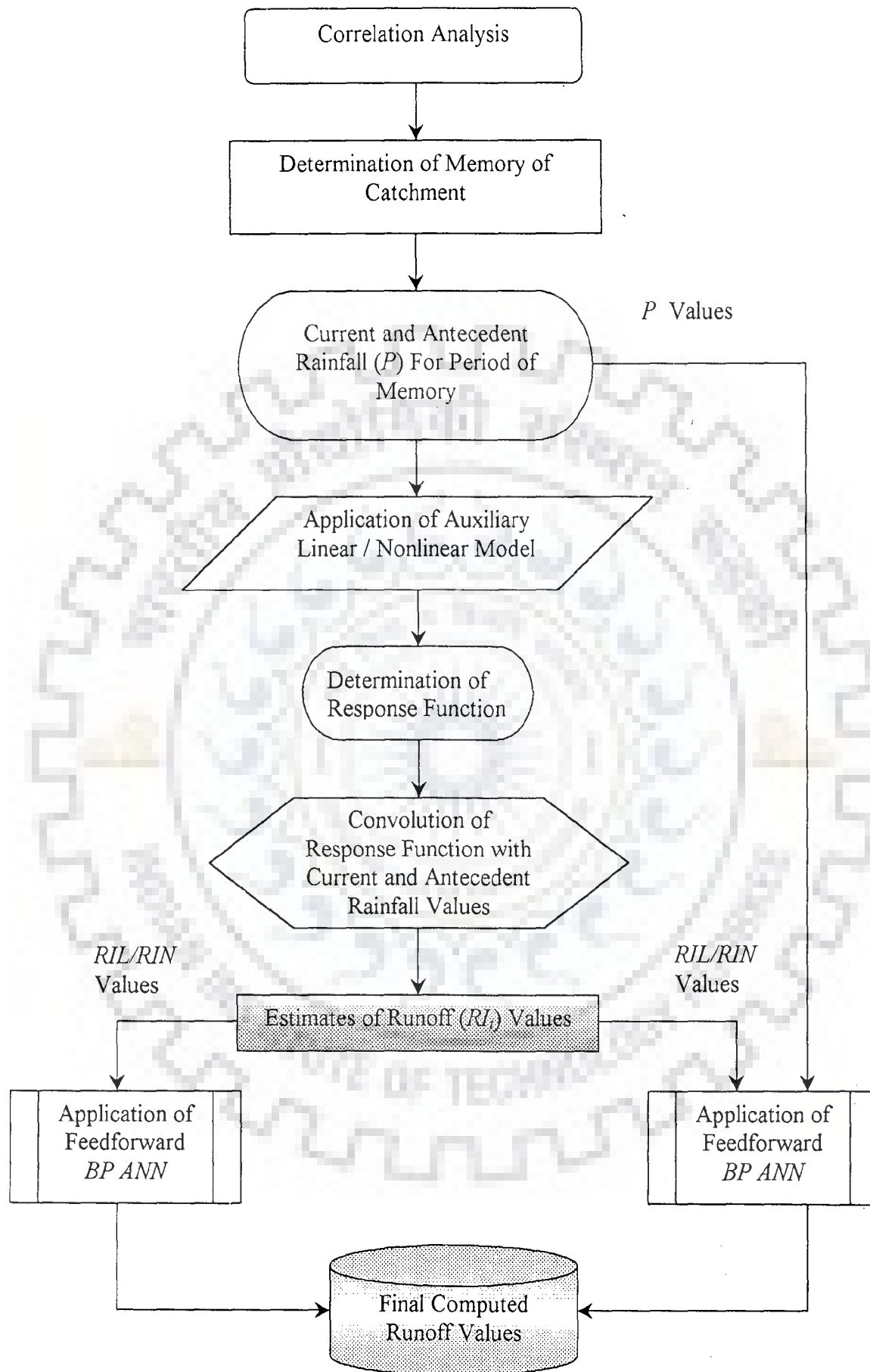


Fig. 4.1 Flowchart Depicting The Steps Involved in The Modeling Process

4.2 METHODOLOGY

The methodology to be used for application of proposed approach for modeling the daily rainfall-runoff relationship in non-updating mode is illustrated in the form of a flowchart in Fig. 4.1. This methodology is applied for daily rainfall-runoff modeling over seven catchments from different climatic regions. Out of these, two catchments being relatively large in size involve sub-divisions into smaller hydrologically homogeneous areas (see chapter 3) to account for the heterogeneity in the spatial distribution of rainfall. The overall procedure of modeling is similar in all the catchments in spite of their varying sizes, with the exception of the model to be used for determination of the response function of the catchment and the initial estimates of runoff. The selection of the model depends upon the size of the catchment. As can be seen from Fig. 4.1, the methodology involves various steps, the first of which is the correlation analysis between actual rainfall (Total rainfall – evapotranspiration) and total runoff values. From the correlation analysis, an approximate value of the memory of the catchment in units of days is arrived at. In the next step, which involves the selection of the model for determining the response function ordinates, the size of the catchment plays an important role as stated above. For relatively small sized catchments which do not involve any sub-division, the discrete form of *SLM* [Eq. (2.4)] and the nonlinear model expressed by Eq. (2.10) are used whereas, for the catchments having sub-divisions, a linear *MISO* and the nonlinear *MISO* given by Eqs. (2.7) and (2.11) respectively are employed.

The shape of the derived response function and the corresponding value of the Nash-Sutcliffe efficiency (E^2) (Nash and Sutcliffe, 1970) criterion were used to decide the final value of the catchment memory. The method of least squares (*MOLS*) or the smoothed least squares method is used for deriving the values of the vector of the response function ordinates. The next step in the modeling approach is the application of a three layer feedforward backpropagation *ANN*. The application of the three layer feedforward *ANN* is specifically made to account for the non-linearity present in the rainfall-runoff relationship. This feedforward *ANN* is known as a universal approximator, having the ability to learn the complex nonlinear relationship between any input and output. The *ANN* application involves two different input combinations as shown in Fig. 4.1. These are:

Case-I: Only the output of the auxiliary linear/nonlinear models computed through the convolution of the derived response function with the current and antecedent rainfalls is given as input to the *ANN*.

Case-II: The current and antecedent rainfall values for the length equal to memory of the catchment are also supplied as input to the *ANN* in addition to the input used in Case-I.

As outlined in chapter 2, the modeling with *ANN* involves various aspects. The data to be used needs to be normalized or rescaled before being fed as input to the *ANN*. The process of calibration of the hydrological model is called as training in case of an *ANN*. This is a trial and error procedure in which the optimum number of neurons in the hidden layer(s) is decided in such a way that the resulting *ANN* has minimum complexity and maximum performance. The *ANN* does not identify the form of model, such as nonlinear reservoir *etc.* in hydrological modeling terms. However, the form of the model is implicit in the *ANN* within the distribution of weights, which is obtained automatically. The *ANN* outputs are the final computed runoff values. Steps involved in the modeling process as enumerated above are described in detail in the following paragraphs.

4.3 DETERMINATION OF MEMORY OF THE CATCHMENT

The catchment is a variable, nonlinear, distributed system that operates on rainfall to transform it into runoff. For simplicity it has often been assumed to be time invariant, lumped system, which receives excess/effective rainfall instead of total rainfall as input and produces runoff as output. The influence of the rainfall on runoff lasts for only a finite duration of time which is called as the '*memory of the catchment*' or as '*precipitation influence history*' (Muftuoglu, 1991). The value of memory of catchment may vary from a few days to several months and it depends on the physical properties and the size of the catchment. When a system has finite memory, its behavior, its state, and its output depend on the history of the system for previous length of time equal to the memory (Dooge, 1973). Determination of the catchment memory length is the critical part of the system based rainfall-runoff modeling in which current and antecedent rainfall values are used as input. For determining the memory of a catchment a two-step procedure consisting of correlation analysis and determination of ordinates of response function of the catchment is adopted. These steps are discussed below.

4.3.1 Correlation Analysis

This is the first step in the identification of the memory of the catchment. The cross-correlation analysis between the runoff and the precipitation computed using Eq. (3.1) is carried out. The cross correlation coefficients between total runoff and rainfall lagged by one day at a time are worked out. These correlation coefficients are expected to increase initially with the lag between precipitation and runoff and then decrease after reaching maximum, first rapidly then more slowly. The plot of such cross correlation coefficients vs. time lag is called as 'Cross Correlogram'. The minimum positive or zero of this plot indicates the total memory length while the peak of correlogram indicates prediction lead-time. The secondary peaks, if any, do not have significance and they are supposed to occur due to periodicities of precipitation auto-correlation and its effect on runoff (Muftuoglu, 1991). Fig. 4.2 below illustrates a sample cross correlogram obtained for one of the event in the Krishna catchment.

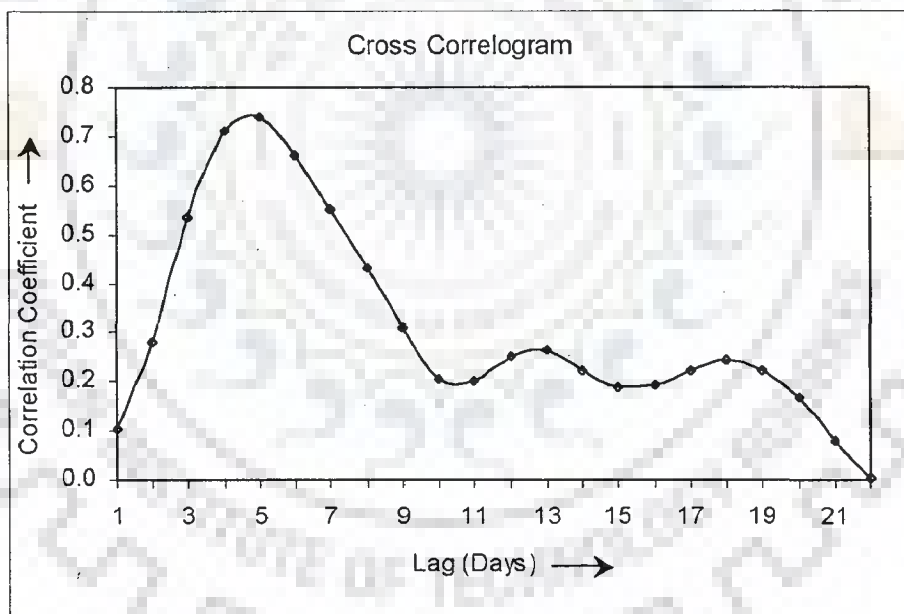


Fig. 4.2 A Sample Cross Correlogram

For each runoff event selected for analysis, the cross correlogram as shown in Fig. 4.2 is prepared from the correlation analysis between runoff and rainfall lagged by a day at a time resulting in a series of length of memory (m) values. These values are found to follow log-normal frequency distribution. The average of this frequency distribution is the

approximate value of m for that catchment. The value of m thus obtained is further refined considering the following criteria:

- a) The shape of the response function is physically realistic.
- b) The end ordinates of the response function are still much larger than the values of respective standard errors.
- c) Corresponding E^2 value of Nash-Sutcliffe efficiency should be maximum.

The procedure used for determining the response function is described below.

4.3.2 Determination of the Response Function

After deciding the approximate value of m , the next step in deciding upon its final value is determination of the response function for the catchment by making use of the appropriate linear/nonlinear model. As the present study involves modeling of daily rainfall-runoff relationship over small as well as large sized catchments, an appropriate auxiliary model depending upon the size of the catchment needs to be selected for determining the response function.

Linear Model:

For smaller sized catchments, which do not have any sub-divisions, the *SLM* is used for the reasons stated already in chapter 2. It is given by the Eq. (2.4) as

$$Q_t = \sum_{i=1}^m P_{t-i+1} U_i + e_t$$

where, U_i denotes the discrete series of pulse response ordinates, which sum up to yield the gain factor, t denotes the time of the sampling interval (day), and e_t designates the model output errors (*i.e.* the residuals).

Conventionally Eq. (2.4) is used without the inclusion of the error term and is written in matrix form as

$$[Q] = [P] [U] \tag{4.1}$$

Here Q is the column vector of runoff values (outputs), U is the column vector of response function ordinates, and P is the matrix of rainfall values (inputs) obtained using the approximate value of m derived above. As described in chapter 3 the set of runoff events

$$P = \begin{bmatrix}
P_m^1 & P_{m-1}^1 & P_{m-2}^1 & P_{m-3}^1 & \dots & P_1^1 & P_m^2 & P_{m-1}^2 & P_{m-2}^2 & P_{m-3}^2 & \dots & P_1^2 & P_m^3 & P_{m-1}^3 & P_{m-2}^3 & P_{m-3}^3 & \dots & P_1^3 \\
P_{m+1}^1 & P_m^1 & P_{m-1}^1 & P_{m-2}^1 & \dots & P_2^1 & P_{m+1}^2 & P_m^2 & P_{m-1}^2 & P_{m-2}^2 & \dots & P_2^2 & P_{m+2}^3 & P_{m+1}^3 & P_m^3 & P_{m-1}^3 & \dots & P_3^3 \\
P_{m+2}^1 & P_{m+1}^1 & P_m^1 & P_{m-1}^1 & \dots & P_3^1 & P_{m+2}^2 & P_{m+1}^2 & P_m^2 & P_{m-1}^2 & \dots & P_3^2 & P_{m+3}^3 & P_{m+2}^3 & P_{m+1}^3 & P_m^3 & \dots & P_3^3 \\
\dots & \dots & \dots & \dots & \dots & \dots & \dots & \dots & \dots & \dots & \dots & \dots & \dots & \dots & \dots & \dots & \dots & \dots \\
P_1^1 & P_{i-1}^1 & P_{i-2}^1 & P_{i-3}^1 & \dots & P_{i-m+1}^1 & P_i^2 & P_{i-1}^2 & P_{i-2}^2 & P_{i-3}^2 & \dots & P_{i-m+1}^2 & P_i^3 & P_{i-1}^3 & P_{i-2}^3 & P_{i-3}^3 & \dots & P_{i-m+1}^3 \\
\dots & \dots & \dots & \dots & \dots & \dots & \dots & \dots & \dots & \dots & \dots & \dots & \dots & \dots & \dots & \dots & \dots & \dots \\
P_N^1 & P_{N-1}^1 & P_{N-2}^1 & P_{N-3}^1 & \dots & P_{N-m+1}^1 & P_N^2 & P_{N-1}^2 & P_{N-2}^2 & P_{N-3}^2 & \dots & P_{N-m+1}^2 & P_N^3 & P_{N-1}^3 & P_{N-2}^3 & P_{N-3}^3 & \dots & P_{N-m+1}^3 \\
\leftarrow \text{Sub-Catchment-1} \rightarrow & \leftarrow \text{Sub-Catchment-2} \rightarrow & \leftarrow \text{Sub-Catchment-3} \rightarrow & \dots & \dots & \dots & \dots & \dots & \dots & \dots & \dots & \dots & \dots & \dots & \dots & \dots & \dots & \dots & \dots
\end{bmatrix}$$

Fig. 4.3 Structure of the Rainfall Matrix For Multiple (Three) Input Scenario (Linear Model)

$$P = \begin{bmatrix}
P_m^2 & P_m P_{m-1} & P_m P_{m-2} & \dots & P_m P_{m-(n-1)} & P_{m-1}^2 & P_{m-1} P_{m-2} & \dots & P_{m-1} P_{m-(n-1)} & P_{m-2}^2 & \dots & P_{m-2} P_{m-(n-1)} & P_{m-1}^2 & P_{m-1} P_{m-n} & \dots & P_{m-1} P_{m-(l+n)+1} \\
P_{m+1}^2 & P_{m+1} P_m & P_{m+1} P_{m-1} & \dots & P_{m+1} P_{m-n+2} & P_m^2 & P_m P_{m-1} & \dots & P_m P_{m-n+2} & P_{m-1}^2 & \dots & P_{m-1} P_{m-n+2} & P_{m-n+2}^2 & P_{m-n+1} P_{m-n} & \dots & P_{m-n+1} P_{m-(l+n)+2} \\
\dots & \dots & \dots & \dots & \dots & \dots & \dots & \dots & \dots & \dots & \dots & \dots & \dots & \dots & \dots & \dots & \dots & \dots \\
P_i^2 & P_i P_{i-1} & P_i P_{i-2} & \dots & P_i P_{i-(n-1)} & P_{i-1}^2 & P_{i-1} P_{i-2} & \dots & P_{i-1} P_{i-(n-1)} & P_{i-2}^2 & \dots & P_{i-2} P_{i-(n-1)} & P_{i-(n-1)}^2 & P_{i-n} P_{i-n-1} & \dots & P_{i-n} P_{i-(l+n)+1} \\
\dots & \dots & \dots & \dots & \dots & \dots & \dots & \dots & \dots & \dots & \dots & \dots & \dots & \dots & \dots & \dots & \dots & \dots \\
P_N^2 & P_N P_{N-1} & P_N P_{N-2} & \dots & P_N P_{N-(n-1)} & P_{N-1}^2 & P_{N-1} P_{N-2} & \dots & P_{N-1} P_{N-(n-1)} & P_{N-2}^2 & \dots & P_{N-2} P_{N-(n-1)} & P_{N-(n-1)}^2 & P_{N-n} P_{N-n-1} & \dots & P_{N-n} P_{N-(l+n)+1} \\
\leftarrow \text{Nonlinear Part } [n(n+1)/2 \text{ Columns}] \rightarrow & \dots & \dots & \dots & \dots & \dots & \dots & \dots & \dots & \dots & \dots & \dots & \dots & \dots & \dots & \dots & \dots & \dots \\
\leftarrow \text{Linear Part } [l \text{ Col.}] \rightarrow & \dots & \dots & \dots & \dots & \dots & \dots & \dots & \dots & \dots & \dots & \dots & \dots & \dots & \dots & \dots & \dots & \dots
\end{bmatrix}$$

Fig. 4.4 Structure of the Rainfall Matrix For Nonlinear Model (Eq. 2.10)

identified for every catchment are divided into two parts, the calibration set and the validation set. The matrices generated for individual events are stacked together vertically according to the number of events used for calibration and validation in order to make use of all the events which may have occurred at different times.

The above model [Eq. (2.4)] is sufficient for small catchments where the rainfall distribution can be assumed to be uniform. The larger the catchment is, the higher is the probability of the assumption of uniform rainfall being violated. So, the large catchments are considered as assemblies of sub-catchments, each assumed to have a uniform rainfall distribution. Equation (2.4) when generalized for the catchment divided into J sub-areas is termed as a linear *MISO* model and is expressed by the Eq. (2.7) as

$$Q_t = \sum_{j=1}^J \sum_{i=1}^m P_{t-i+1}^{(j)} U_i^{(j)} + e_t$$

where, $j = 1, 2, \dots, J$ designates the number of the sub-area.

For each sub-catchment in case of the large size catchments the rainfall input matrix $[P]$ involves vertical stacking for taking care of the different events as explained above and adjacent horizontal stacking of different sub-catchment averaged rainfall values is performed for obtaining the complete matrix. The structure of the matrix $[P]$ for the linear *MISO* model, for catchment divided into three sub areas is shown in Fig. 4.3. The superscript of P in this matrix denotes the sub-catchment number.

The outflow components Q_t from different sub-catchments are linearly additive (Liang and Nash, 1988) as given by the following equation

$$Q_t = Q_t^{(1)} + Q_t^{(2)} + \dots + Q_t^{(J)} \quad (4.2)$$

The solution of Eq. (2.7) for calibration series of N discharge values can be written in matrix form as

$$[Q] = [P^{(1)}] [U^{(1)}] + [P^{(2)}] [U^{(2)}] + \dots + [P^{(J)}] [U^{(J)}] \quad (4.3)$$

$U^{(j)}$ is $[m_{(j)} \times 1]$ column vector of pulse response ordinates for j^{th} input series and the entire vector of $[U]$ and $[P]$ are given by

$$\left. \begin{aligned} U &= [U^{(1)} \ U^{(2)} \ \dots \ U^{(J)}]^T \quad \text{and} \\ P &= [P^{(1)} \ P^{(2)} \ \dots \ P^{(J)}] \end{aligned} \right\} \quad (4.4)$$

In which case, writing $[Q] = [P] [U]$ results in Eq. (4.3).

The response function ordinates (column vector $[U]$) are determined by using the *MOLS* and the matrix inversion method (Singh, 1994) given by Eq. (2.6) as

$$[U] = [P^T P]^{-1} [P^T] [Q]$$

If some of the ordinates in the tail of the response function derived by using the *MOLS* are found to have negative values then the smoothed least squares method given by Eq. (4.5) (Bruen and Dooge, 1984) instead of the *MOLS* is used. This method, also known as ridge regression, involves a coefficient called the ridge parameter (R_p) and is given by the following equation.

$$[U] = [R_p \mathbf{I} + P^T P]^{-1} [P^T] [Q] \quad (4.5)$$

where \mathbf{I} is the identity matrix of the size $[P^T P]$ and value of the coefficient R_p is less than one. For $R_p = 1$ above equation reduces to the *MOLS*.

The adjustments in the approximate value of m decided earlier are done based on the shape of the derived response function of the catchment such that the criteria (a) to (c) discussed under section 4.3.1 are satisfied.

Nonlinear Model:

Alternatively, nonlinear model by Muftuoglu (1984) or by Kothiyari and Singh (1999) are also used for deriving the response function of the catchment depending upon its size. The objective behind replacing a *SLM* with a nonlinear model is to see whether there is any improvement in the final results obtained by coupling a nonlinear model with the *ANN*, as the nonlinear model is expected to produce a better estimate (than *SLM*) of the soil moisture state or the antecedent flow conditions in the catchment. The discrete form of the nonlinear model applied for the catchments which do not have any sub-divisions is given by the Eq. (2.10) as

$$Q_t = \sum_{i=1}^n \sum_{k=i}^n U_{i,k} P_{t-i+1} P_{t-k+1} + \sum_{l=1}^l U_{i+n} P_{t-(i+n)+1} + e_t$$

where, n denotes the nonlinear part of the memory, l is the linear part, and the total memory $m = (n + l)$.

Equation (2.10) can also be expressed in the form of Eq. (4.1) by appropriately modifying the structure of the matrix $[P]$. In case of the above nonlinear model, the immediate and moderately delayed flows are nonlinearly related to the corresponding rainfalls while the delayed flows are related linearly with the corresponding rainfalls. The linear part follows the nonlinear one. The corresponding response functions for the nonlinear and linear part of the memory are called as two dimensional unit hydrograph and a finite period UH respectively. This structure of $[P]$ matrix for the nonlinear model represented by Eq. (2.10) is shown in Fig. 4.4. The number of columns in such matrix are $[n(n+1)/2 + l] = NN$. For large size catchment divided into a number of sub-catchments, each of which having parallel rainfall input to the system, the Q values are related to the rainfalls by the Eq. (2.11) as

$$Q_t = \sum_{j=1}^J \sum_{i=1}^{n(j)} \sum_{k=i}^{n(j)} U_{i,k}^{(j)} P_{t-i+1}^{(j)} P_{t-k+1}^{(j)} + \sum_{j=1}^J \sum_{l=1}^{l(j)} U_{i+n}^{(j)} P_{t-(i+n)+1}^{(j)} + e_t$$

The notations in the above equation carry the same meaning as earlier.

Equation (2.11) is termed as nonlinear *MISO* model. The procedure of application of the nonlinear *MISO* model remains identical as described in case of the linear *MISO* with the only exception that here the column vector $[U^{(j)}]$ for j^{th} input series will be of the size $[NN_{(j)} \times 1]$. The entire vector of $[U]$ will be similar to that given by Eq. (4.4)

Memory length of the catchment is thus ascertained adopting the procedure described above. The main emphasis at this step is on the shape of the derived response functions such that it is physically realistic. The response functions having physically realizable shapes can be expressed in parametric form. Such parameter values are found to have a strong relationship with the catchment characteristics such as physiography, land use, and soil characteristics.

4.4 ASSESSMENT OF THE CATCHMENT NON-LINEARITY

The assessment of non-linearity of a catchment carries importance in the background that the *ANN* based rainfall-runoff modeling is being carried out in the present study. The *ANN*, a nonlinear model is being used on the premise that it is capable of taking care of the non-linearity existing in the process of rainfall-runoff transformation over a catchment.

Various measures of assessing the non-linearity of a catchment exist in literature as discussed under section 2.5 of chapter 2. Among these, the measure of non-linearity

introduced by Rogers (1980, 1982) known as the Standardized Peak Discharge Distribution (*SPDD*) is employed in the present study. Rogers (1980) proposed the relation between the peak discharge of the hydrograph and its volume given by Eq. (2.8) as

$$\log(Q_p) = B + M \log(V)$$

Here B is the intercept of the straight line relation between $\log(Q_p)$ and $\log(V)$ and M is the slope. The log inverse of B is the peak discharge when runoff volume is one unit. As per Rogers (1980), the slope of the line (M) that best fits the standardized peak discharge data is an indicator of the non-linearity of the runoff distribution. For a catchment to be linear the value of M should be equal to unity, while the catchment is said to be hydrologically nonlinear when the value of M is less than one. Mimikou (1983) pointed out that only *SPDD* measure is necessary and sufficient for checking the hydrologic linearity of a catchment, therefore the same is adopted in the present study.

For making use of the *SPDD* measure in identification of non-linearity of runoff distribution over a catchment, the runoff events should be single peaked. The earlier works related to identification of the catchment non-linearity utilized single peaked flood hydrographs in hourly scale whereas in the present study this concept is extended to daily scale for single peaked runoff events spread over days and the relationship of the type of Eq. (2.8) is studied between the total runoff and the peak discharge.

4.5 PROPOSED COUPLING OF AUXILIARY LINEAR/NONLINEAR MODELS AND THE ANN

The review of literature on application of the ANN to rainfall-runoff modeling (description summarized in Table 2.4 of chapter 2) revealed that

- i) Providing only rainfall information to the ANN is not sufficient in simulating the nonlinear process of runoff generation over a catchment.
- ii) The input variables used should represent the soil moisture state of the catchment for very accurate estimation of runoff by the ANN.
- iii) The ANN was used as an independent model and its performance compared with some of the existing conceptual or black box models.

The earlier applications, especially the studies that used the standard feedforward backpropagation ANN, involved the use of the observed values of runoff or river stage for the

previous time periods, as one of the input to the *ANN*. This type of modeling is the forecasting in updating mode. The variable 'runoff observed in the past time period (Q_{t-1})' used in these studies is representative of the soil moisture state of the catchment. The *ANN* based models, which use (Q_{t-1}) as input have drawbacks such as

- i) when the network inputs include the flows at previous time steps, the *ANN* could be considered to be modeling the change in flows rather than their absolute values (Minns and Hall, 1996).
- ii) it is difficult to use such models in scenarios having sparse data on runoff/ water level.

To overcome these drawbacks an *ANN* based modeling approach is proposed in this study such that the estimated values of runoff by a auxiliary linear/nonlinear model through the convolution of the response function with the current and antecedent rainfall values are used as input to the *ANN* to represent the soil moisture state of the catchment. The structure of the proposed linkage between the auxiliary system-based linear/nonlinear model and the *ANN* (substantive model) is shown in Fig. 4.5. Thus the *ANN*, instead of being used as an independent model, is coupled with an auxiliary linear/nonlinear model such that its output forms the input to the *ANN* used as a substantive model. Such modeling approach demonstrates the use of *ANN* in the non-updating flow simulation and is considered to be useful particularly in the scarce data scenarios.

A three layer feedforward *ANN* as shown in Fig. 1.2 (chapter 1) is used in the present study. It is known as the universal mathematical approximator as it can learn any kind of nonlinear relationship between input and the output. This *ANN* is trained with the backpropagation algorithm using the adaptive learning rate and the momentum factor. The training process was monitored using the mean square error (*mse*) criteria, and it was ensured that the *ANN* does not get overtrained.

The most commonly used transfer function for the neurons in the hidden layer(s) as well as the output layer is the logistic sigmoid which has a bounded range [0, 1]. The main reason for its use as a transfer function is that it is differentiable everywhere. Due to its bounded output range, the data used in *ANN* application needs to be rescaled to this range. This logistic sigmoid (shown in Fig. 2.2) is used as a transfer function in this study. The procedure adopted for data normalization is described in the following sub-section.

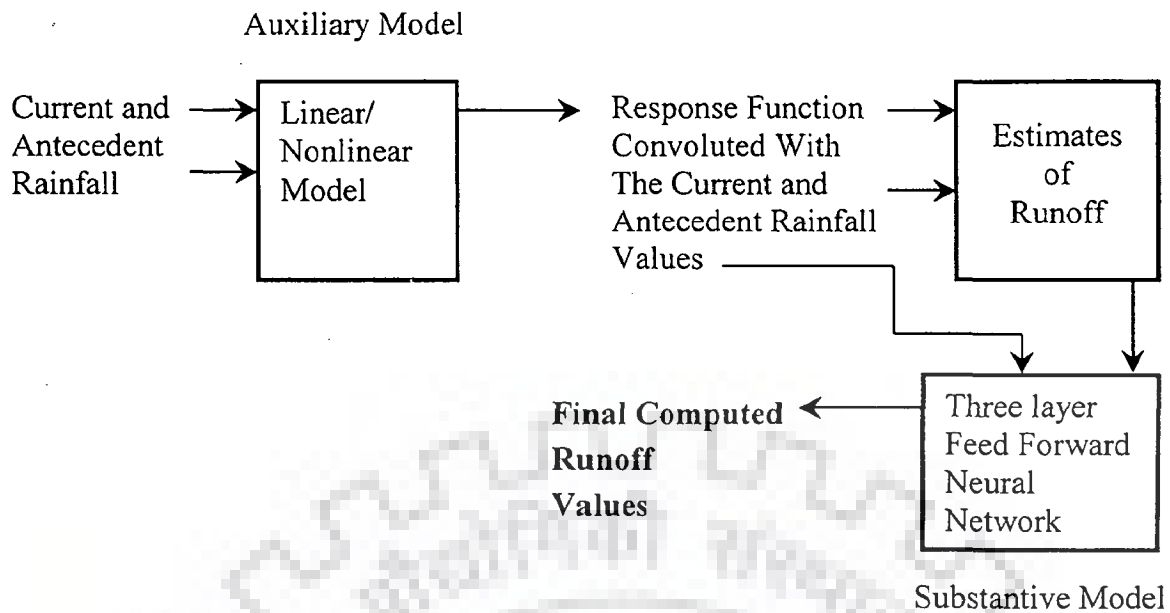


Fig. 4.5 Schematic Showing Linkages between the Auxiliary Model and the ANN

4.5.1 Normalization of Inputs for ANN

Before the data is presented to the ANN, it must be standardized in order to restrict its range to the interval [0, 1]. The actual observed outputs of the network being outside this bounded range of neuron transfer function, need to be normalized or rescaled such that they fall within the bounded output range. This facilitates proper comparison between network outputs and rescaled actual observed outputs. It is observed that training slows down making the learning ineffective and inefficient if the rescaled values are near to the bounds because the derivative of the sigmoid function approaches zero very fast when the target value is near to 0 or 1 (Ooyen and Nichhuis, 1992). The significance of the standardization should not be under estimated because the BP algorithm requires that the weighted sum at any computational neuron should not blow up to a very large value leading to numerical error in the computation of logistic nonlinear output function (Minns and Hall, 1996). Keeping this in mind the observed discharges and the rainfall values are normalized as per the following equation.

$$X_{norm} = 0.1 + 0.8 \times \left(\frac{X_i}{X_{max}} \right) \quad (4.6)$$

where X_{norm} is the normalized dimensionless variable, X_i is the observed value of the variable, and X_{max} is the maximum value in the data set. This linear transformation bounded the variables in the range [0.1, 0.9].

4.5.2 Proposed Inputs to the ANN

The review of literature showed that in the previous studies various types of inputs such as rainfall (P), temperature (T), runoff observed during previous days (Q_{t-1}), snowmelt equivalent (SW) (if applicable) are given as input to the ANN for predicting runoff over a catchment. An important aspect of the earlier studies as seen in Table 2.4 is that there exists subjectivity in selecting the type and the length of input variables. For example in one study $Q_{t-1}, Q_{t-2}, \dots, Q_{t-5}$ are used as input whereas in another study only Q_{t-1} and Q_{t-2} are given as input to the ANN. Similar subjectivity can also be observed in case of other input variables such as P and T . In actual sense the '*sensitivity analysis*' between the output and the input variables should guide this selection. However, the selection of the number of values for a variable used in many cases has been based on the discretion of the modeler, rather than based on the physical process of the rainfall-runoff being modeled. As per Dawson and Wilby, (1998) accurate flood forecasting using ANN requires input variables, which contain some memory of the antecedent catchment conditions.

As the present study deals with modeling the total runoff and the rainfall that actually contributes to the process of runoff generation over a catchment (Total rainfall – evapotranspiration), consideration of the memory of the catchment is important because the current time period runoff is the result of the rainfall that occurred in the past during the period equal to the memory of the catchment. Therefore, the rainfall values for the past time period equal to the length of memory of the catchment are given as one of the inputs to the ANN.

As discussed above the state of catchment or the antecedent moisture conditions play an important role in converting the rainfall occurring over a catchment into runoff. As per Ahsan and O'Connor, (1994) the output of a SLM can be considered to represent the soil moisture state of the catchment. More popular way of bringing the state of catchment into ANN based modeling is providing the runoff or the water level observed in the past time period as input to the ANN. This approach has some limitations as pointed out earlier.

It is well known that rainfall-runoff transformation cannot be adequately described by a simple linear system such as the one represented by Eq. (2.4) due to the constraints of proportionality and time invariance. The coefficients U_i of Eq. (2.4) are not found to be constant but varying as a function of current and antecedent rainfalls (Agorocho, 1973, Muftouglu, 1984, Kothari and Singh, 1999). This indicates that the relationship between rainfall and runoff is a nonlinear one (Agorocho and Orlob, 1961, Agorocho and Brandstetter, 1971). Therefore, the residuals *i.e.* differences between observed discharges and the discharges estimated by Eq. (2.4) do exhibit the evidence of persistence and seasonality *i.e.* time variance (Kachroo and Natale, 1992). Thus, Eq. (2.4) when used without inclusion of the error term shall compute the values, which are termed here as *RIL* given by Eq. (4.7) below. Similarly, the estimate of runoff obtained from Eq. (2.10) of the nonlinear model when used without the error term is called here as *RIN* (given by Eq. (4.8) below). These new type of inputs in the form of *RIL*, the output of the linear model or the *RIN* which is the estimate of runoff from nonlinear model, are given to the *ANN* for prediction of runoff over a catchment.

$$RIL = \sum_{i=1}^m P_{(t-i+1)} U_i \quad (4.7)$$

$$RIN = \sum_{i=1}^n \sum_{k=i}^n U_{i,k} P_{t-i+1} P_{t-k+1} + \sum_{i=1}^l U_{i+n} P_{t-(i+n)+1} \quad (4.8)$$

These *RIL* and *RIN* values are also considered to be related non-linearly to the corresponding observed values of runoff. The *ANN* technique has been found to be very successful in representing the complex nonlinear relationship; the same is therefore used for transforming the *RIL* and the *RIN* values obtained through use of Eq. (4.7) and (4.8) into the Q_t values as per Fig., 4.5. The following two cases of input combinations are considered.

Case 1: Only *RIL* or *RIN* values are given as input to the *ANN*

Case 2: Rainfall occurred during the catchment memory period is given as input to the *ANN* in addition to the *RIL* or *RIN* values.

By way of considering these inputs to the *ANN*, an attempt is made in the present study to bring some physical aspects into the *ANN* based rainfall-runoff modeling. Alternatively, the estimates of runoff from the other models such as linear *MISO* and the

nonlinear *MISO* (Eqs. 2.7 and 2.11 respectively) are also supplied as input to the *ANN* in a similar fashion as described in case 1 and case 2 above. These estimates of runoff generated through the use of linear or nonlinear models (*i.e.* *RIL* and *RIN* values) are considered to represent the soil moisture state of the catchment.

4.5.3 Training the Network

The purpose of training is to obtain a generalized network for application in the daily rainfall-runoff modeling. It is a trial and error procedure. The criterion used for training is mean square error (*mse*). The *ANN* objective function surface is typically highly non convex with extensive regions that are insensitive to variation in values of network weights. This surface contains numerous multi local optima (Hsu *et al.*, 1995). The error term is defined by

$$(mse)_A = \sum_{i=1}^N (Q_i - \hat{Q}_i)^2 \quad (4.9)$$

which is the error function (*mse*) for pattern *A*, \hat{Q}_i is the computed value of the runoff, and Q_i is its corresponding observed value. After each pattern is presented error on that pattern gets computed and each weight is moved down the error gradient towards its minimum for that pattern and the total error over entire input pattern is computed similarly.

During the training process the *mse* is minimized over number of epochs. The backpropagation algorithm used for the training involves a forward pass and a backward pass. In the forward pass the inputs pass through the hidden and output layer neurons, get multiplied with the connection weights and an output is produced at the output layer. This output is compared with the corresponding observed values and the error gets calculated. This error is then propagated backwards through modifications in the connection weights using the delta rule over number of epoch till the required *mse* is attained by the *ANN*. The *BP* algorithm uses derivatives of objective function with respect to weights in entire network to distribute the error among various neurons. Variation of the weight W_{ij} from node *i* to node *j* is calculated using the Eq. (2.14) as

$$\Delta w_{ij}(n) = -\varepsilon \times \frac{\partial E}{\partial w_{ij}} + \alpha \times \Delta w_{ij}(n-1)$$

the notations in the above equation are explained in chapter 2.

As mentioned earlier the total number of runoff events identified in a catchment are divided into two sets. A training set contains about 70% of the data and the other, is the testing set containing remaining values (approximately 30% of data). Ideally a training data set should contain all the information required to be given to the *ANN* so as to learn the relationship between input and output and finally when proper training is accomplished the network should be able to simulate the output as close to the observed as possible. However, due availability of limited number of high flow events in the daily runoff data for the catchments, validation of the *ANN* models with a third independent dataset could not be performed.

For ensuring proper training or in other words, to avoid any overtraining of the network, the help of the testing dataset is taken. First, a target *mse* for training is decided and the network is trained to this value of *mse*. Then with same configuration and weights the *mse* for the test dataset is computed. The output produced by network at testing is the scaled version of patterns stored during learning trials. In the next step the target *mse* during training is lowered and the training process is repeated. The test dataset is again given to this new *ANN*, which is having a set of weights that is different than that of the previous one and the corresponding *mse* is computed. If this *mse* during testing is reduced as compared to the earlier cycle, the above procedure of training and testing is repeated continuously reducing the target *mse* during training in small steps till it is observed that the *mse* during testing increases instead of reducing. This is an indication that the network is getting over trained, and if trained further with lower target *mse* it will perform very well during training but would fail to generalize when given an unknown input. This means that in trying to learn the relation between the data, the *ANN* has started to fit the noise (error), which may be present in the data.

In a three layer feedforward network the number of neurons in the input and output layers are fixed by the problem being studied. In the present case there is only one neuron in the output layer corresponding to the observed runoff at the catchment outlet. The neurons in the input layer depend upon the input scenario studied. Though training involves trial and error and consumes a lot of time, a proper planning and execution of the process adopting a systematized procedure helps in reducing both the number of trials and the time involved. In general the training process involves two components.

- i) Deciding upon the number of hidden layers
- ii) Deciding the number of neurons in the hidden layer(s)

In this study only one hidden layer is found to be sufficient in mapping the rainfall-runoff relationship. So the trials in training were reduced only to deciding the number of neurons in the hidden layer. This number should be optimal such that network remains simple and at the same time performs best in terms of the performance criteria. Too many hidden neurons will encourage each hidden neuron to memorize one of the input patterns and thereby diminish generalization capabilities of the *ANN* (Ranjithan *et al.*, 1993).

The process of arriving at optimal network configuration is started with selecting minimum number of neurons in hidden layer *i.e.* one. For this *ANN* configuration the entire training procedure is carried out as explained above and the performance of the network is noted. Then the number of hidden layer neuron is increased by one and the training cycle is repeated till the minimum possible *mse* in training is achieved without the network getting overtrained. If the performance of *ANN* improves then the process of adding neurons in the hidden layer is continued till no more improvement in the *ANNs* performance is noticed. Thus, the final *ANN* with optimal configuration having the best possible performance is derived. The finally selected *ANN* then becomes ready for prediction, as it has learned the input-output relationship. In case of *ANN*, the exact form of this relationship cannot be extracted from its structure, and also the fact that absolute value of individual weights cannot be interpreted to have any deeper physical meaning (Minns and Hall, 1996).

The output of the *ANN* being in the range $[0, 1]$ due to the use of the logistic sigmoid transfer function needs to be transformed back to the original domain. An inverse procedure of normalization is adopted for this. This facilitates proper comparison and presentation of results and also various performance assessing indices, or goodness of fit criteria could be computed based on these.

4.6 ALTERNATE INPUTS TO THE *ANN*

The methodology for the proposed modeling approach (shown in Fig. 4.1) considering two types of input cases is presented above. In addition to these the following other inputs to the *ANN* are also considered and the analysis is carried out for these. The performance of the *ANN* in these input scenarios is evaluated and compared with the other results obtained.

4.6.1 Only Rainfall (P)

In this case the *ANN* is provided with only the values of the rainfall, which occurred during the period equal to the catchment memory as input for prediction of runoff at the outlet of a catchment.

4.6.2 Q_{t-1} and Rainfall

Another combination of input to the *ANN* consisted of the runoff observed in the previous time period (Q_{t-1}) along with the rainfall that occurred during the length of the memory of a catchment. This has been the way of modeling the rainfall-runoff process using the *ANN* in updating mode.

4.6.3 RIL , $RIL_{(t-1)}$, and Rainfall

Alternatively, one more combination of inputs to the *ANN* selected in the present study is inclusion of the variable $RIL_{(t-1)}$ i.e. the output from a system theoretic model for previous time period. This was given as input to the *ANN* in addition to the RIL alone as well as along with RIL and rainfall values equal to the length of memory of the catchment.

The data used in training the *ANN* contains limited number of high flows due to which there could be a possibility that the *ANN* may not be able to learn the relation for high flows and it may result in underestimation of peak flows during testing. An attempt is also made to find out whether or not repeating the higher values in the training dataset (i.e. artificial generation of a new series for training) improves the performance of the *ANN* in matching the peaks during testing.

4.7 PARAMETERIZATION OF THE RESPONSE FUNCTIONS

The response functions derived using the *SLM* following the two-step procedure elaborated earlier can be expressed in parametric form by using the gamma function. The parameters of such a function can have relationship with the catchment characteristics. The continuous form of the gamma function is given by the following equation.

$$U(t) = \frac{1}{K \Gamma(N)} \left(\frac{t}{K} \right)^{N-1} e^{-t/K} \quad (4.11)$$

where, $U(t)$ = ordinates of the impulse response function

N = the shape parameter

K = the scale parameter

The above equation expresses the *IUH* of the Nash model (1957), which represents the catchment impulse response as the outflow obtained from routing volume of instantaneous excess rainfall input through a series of N successive linear reservoirs having equal delay time. The parameter N is a measure of catchment channel storage required to define shape of the *IUH*. Lower value of N tends to make peak higher *i.e.* less storage for attenuation of simulated peak flows. The scale parameter K reflects the dynamics of the rainfall-runoff process in a catchment. It is a function of velocity and varies from storm to storm and also in between storms. A smaller K value would indicate lower time to peak. Nash (1957) showed that the *IUH* has the form of the two parameter continuous gamma distribution given by Eq. (4.11).

The response functions determined in the present study are having discrete form. The discrete analogy to the equal reservoir cascade model was presented by O'Connor (1976). He used the approach of interpreting the impulse response of a discrete system (represented by a difference equation) as the sampled pulse response of the continuous system. As per him a convolution summation can also be used in place of the difference equation for the system representation. The impulse response of the discrete model can be represented by following equation as per O'Connor (1976).

$$U(m) = \frac{\Gamma(m+N)}{\Gamma(N) * \Gamma(m+1)} p^N q^m \quad \text{for } m \geq 0 \quad (4.12)$$

$$\text{where, } p = \frac{1}{1+K}; \quad q = \frac{K}{1+K} \text{ such that } p + q = 1$$

The discrete form of the gamma function distribution *i.e.* Eq. (4.12) was fitted to the response functions of various catchments obtained in the present study and the values of the parameters N and K for the response function of each catchment were determined. Next a relation between each of these parameters and the characteristics of the catchment (*e.g.* area) was studied. Such a relationship if derived could be used for arriving at the values of the parameters namely N and K for a given catchment.

4.8 PERFORMANCE EVALUATION CRITERIA

The performance of a model can be evaluated in terms of several criteria. Kachroo (1992) proposed three criteria for evaluation of a model.

- i) *Accuracy*: It is the ability of the model to reduce the calibration error
- ii) *Consistency*: Model consistency is checked by split sampling *i.e.* by breaking the record into two distinct periods, calibration and verification. The property of the model by which the level of accuracy and the estimates of parameter values persist through different samples of data is termed as consistency of the model. If calibration error is less than the verification error then there is lack of consistency in prediction.
- iii) *Versatility*: A versatile model is one, which is accurate and consistent when subject to diverse applications involving model evaluation criteria not directly based on the objective function used to calibrate the model.

WMO (1975) has proposed various graphical verification criteria, such as

- i) Linear scale plot of simulated and observed hydrographs during calibration and validation period.
- ii) Double mass curve of simulated versus observed runoff volumes for verification period.
- iii) Flow duration curve for both simulated and observed daily discharges for verification period only.
- iv) Scatter diagram of simulated versus observed flows for verification period.

There exist a wide array of numerical performance indicators used in hydrological studies. Aitken (1973) listed some of these statistical measures and tests to express the agreement or disagreement between computed and observed flows. The various criteria used in performance evaluation of the hydrological models are given below.

(1) Coefficient of Determination: It is used to measure degree of association between observed and estimated flows and is given by the equation

$$R^2 = \frac{\sum (Q_i - \bar{Q})^2 - \sum (Q_i - \hat{Q}_i)^2}{\sum (Q_i - \bar{Q})^2} \quad (4.13)$$

where R^2 is the coefficient of determination, Q_i are the observed discharge, \bar{Q} is the mean of the observed discharges, and \hat{Q} are the estimated discharges by the model. The first term in the numerator is called as the initial variation whereas the second term is called as the residual or unexplained variation (Aitken, 1973). High value of R^2 indicates good model result whereas a low value denotes otherwise but it does not indicate existence of systematic errors.

(2) **Coefficient of Efficiency (E^2):** This coefficient is originally proposed by Nash and Sutcliffe (1970). It is analogous to the coefficient of determination in linear regression but not identical. It gives the proportion of variance of the observation accounted for by the model (Kitanidis and Bras, 1980). It is given by

$$E^2 = \frac{F_0 - F}{F_0} \quad (4.14)$$

where,

$$F_0 = \sum (Q_i - \bar{Q})^2 \quad ; \quad \bar{Q} = \frac{1}{N} \sum_{i=1}^N Q_i \quad ; \quad N = \text{Number of data points}$$

and
$$F = \sum (Q_i - \hat{Q}_i)^2$$

F_0 = Measure of variability of observed and their mean *i.e.* the crudest possible prediction

F = Measure of association between predicted and observed flows or an index of residual error which reflects the extent to which a model is successful in reproducing the observed discharges.

In calibration the E^2 is identical to R^2 and varies between zero and one. In verification period the value of \bar{Q} used is still the mean of calibration period *i.e.* the initial variance is calculated as the sum of squares of deviations in validation period from the mean of calibration period, because the E^2 criterion expresses a comparison of model predictions with the no model situation. The only forecast which could be made for verification period is the mean value of discharges in calibration period. E^2 may take negative values in validation. This coefficient can be used for comparing the relative performances of different models, say model (1) and model (2) as

$$e^2 = \frac{F_1 - F_2}{F_1} \quad (4.15)$$

In this equation F_1 is the initial variance unaccounted for by model (1), which is subsequently accounted for by model (2), the initial variance of which is F_2 .

(3) Mean Square Error (*mse*): Measures the residual variance. The optimal value for this is zero. It is computed using following equation

$$mse = \frac{1}{N} \sum_{i=1}^N (Q_i - \hat{Q}_i)^2 \quad (4.16)$$

The notations carry the same meaning as stated earlier.

(4) Percentage of Volume Error (*VE*): It measures the percent error in volume under the observed and the simulated hydrographs, summed over the data period. Ideal value for this parameter is 0.0. A positive value indicates underestimation, and negative value indicates overestimation. The equation used for its computation is as follows

$$VE (\%) = \frac{(\sum Q_i - \sum \hat{Q}_i)}{\sum Q_i} \times 100 \quad (4.18)$$

(5) The Magnitude and Time to Peak: The magnitude and time of peak of the hydrograph are very important characteristics. The predicted values by a model are compared with that of observed and the error in time to peak and comparison of the predicted magnitude of peak compared with the observed.

The performance of the models applied in the present study (the system theoretic and the *ANN* models) is evaluated based on the various numerical criteria listed above which are indicative of the model performance. The E^2 being most widely used criterion for assessment of the model performance is also employed in the present study. *RMSE* is indicative of relative performance of different models for the same length of calibration and validation periods. If these periods are different then E^2 is a better choice (Liang *et al.*, 1994). The *mse* is used in assessing the performance of the *ANN* during training and testing. The %*VE* statistics and the error in magnitude and time to peak are also computed for calibration and validation events. Out of various graphical verification criteria stated above the scatter plots

for verification period are prepared and the coefficient of determination (R^2) determined from these plots is used for comparison. The linear scale plots of simulated and observed hydrographs during calibration and validation period are prepared for visual comparison of the overall output predications by various models.

4.9 CONCLUDING REMARKS

The modeling approach proposed for the study is described. An attempt is made to couple the system theoretic linear/nonlinear model with the *ANN* for representation of the process of transformation of rainfall into runoff over a catchment in the non-updating mode. An alternative way of estimating the soil moisture state of the catchment is suggested for use in prediction of runoff using *ANN*. This is achieved by way of coupling a system-based model with the *ANN* such that along with the other variables output from it becomes one of the inputs to the *ANN*. The proposed approach attempts to overcome the limitations of the existing *ANN* based rainfall-runoff models involving flow updating. Appropriate statistical and graphical criteria are chosen for evaluation of the performance of the models applied.

LINEAR AND NONLINEAR MODEL APPLICATION – RESULTS AND DISCUSSIONS

5.1 INTRODUCTION

The modeling approach proposed in the present study is applied for daily rainfall-runoff modeling over seven catchments, ranging in size from 1,207 Km² to 26, 200 Km². First the two types of system based models are employed in the study. The Simple Linear Model (*SLM*) and a Nonlinear Model are used in case of the smaller catchments, which do not involve any sub-divisions. For the two large sized catchments involving sub-divisions the Multiple Input Single Output (*MISO*) counterparts of the two models stated above are made use of. This chapter presents the results obtained for the linear/nonlinear models applied during the study. Results obtained through the coupling of these models as auxiliary models with the *ANN* model are discussed in the next chapter. The model performance is assessed on the basis of various criteria discussed in chapter 4. A comprehensive discussion on the results obtained in each case is provided and finally the conclusions drawn from the analysis of results are stated. In addition to this, the results of the analysis carried out for assessing the hydrologic non-linearity of the catchments being studied are enumerated. The present chapter also describes the results of the exercise on parameterization of the response functions derived by using the *SLM*.

The chapter is organized as follows: The results of the analysis for identification of hydrologic non-linearity of the catchment are presented first. This is followed by presentation of the results of the model application and discussion on these results. The presentation for, i) the catchments not involving sub-divisions; and ii) the catchments involving sub-divisions is made separately. Finally, the results obtained on the parameterization of the response function are provided.

5.2 IDENTIFICATION OF THE HYDROLOGIC NON-LINEARITY

As described in chapter 4, the exercise of assessing the hydrologic non-linearity of the different catchments studied is carried out by using the *SPDD* measure introduced by Rogers (1980). This relationship, given by Eq.(2.8), is between the peak discharge of a

hydrograph and its volume. The rainfall-runoff modeling using *ANN* carried out in the present study uses both isolated as well as multi-peaked storm events for the analysis. However, for the analysis of non-linearity only the single peaked runoff events are required to be used (Rogers, 1980). Such events are identified separately in each of the catchments and a relationship given by the Eq.(2.8) is determined in each case giving values of the slope of the best fit line M and the corresponding value of R^2 . The plots of $\log(Q_p)$ vs. $\log(V)$ for the different catchments are shown in Figs. 5.1 (a) – (c). The Table 5.1 gives the values of M and R^2 obtained through this analysis. It may be noted that mostly high R^2 value is obtained for relationship between $\log(Q_p)$ vs. $\log(V)$. It is observed that all the catchments are hydrologically nonlinear as the values of the slope parameter M are less than unity. The value of M is close to unity for the Pampanga catchment. The unit hydrograph approach of rainfall-runoff modeling would produce less accurate results when applied to the catchments having the value of $M < 1.0$. However, the coupling the linear model with the *ANN* is expected to produce better results for such hydrologically nonlinear catchments as discussed in the next chapter.

Table 5.1 Results of The Non-Linearity Analysis

Catchment	Area (Km²)	Slope Parameter (M)	Coefficient of Determination (R^2)
Bird Creek	2,344	0.879	0.755
Brosna	1,207	0.680	0.821
Garrapatos	1,409	0.515	0.527
Kizu	1,445	0.727	0.514
Pampanga	5,273	0.971	0.809
Krishna	26,200	0.626	0.832
Narmada	17,157	0.567	0.530

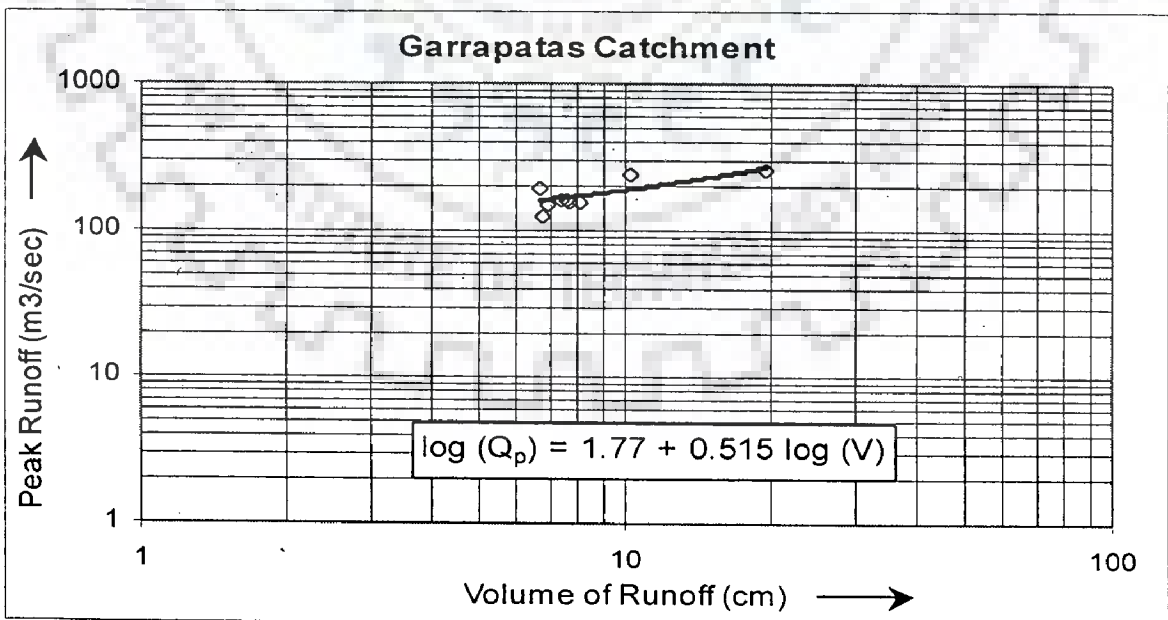
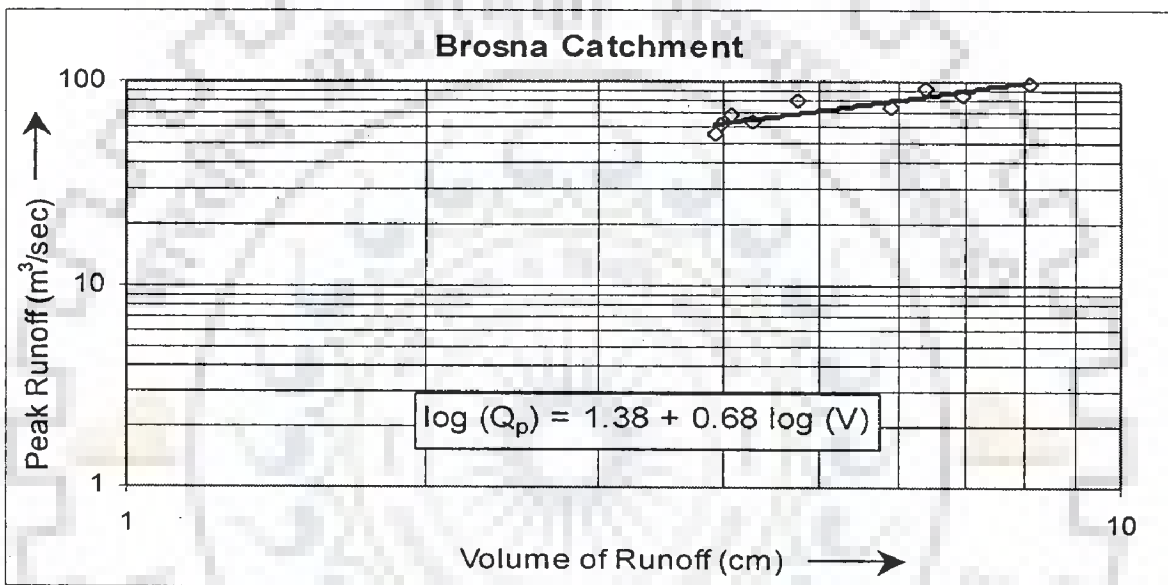
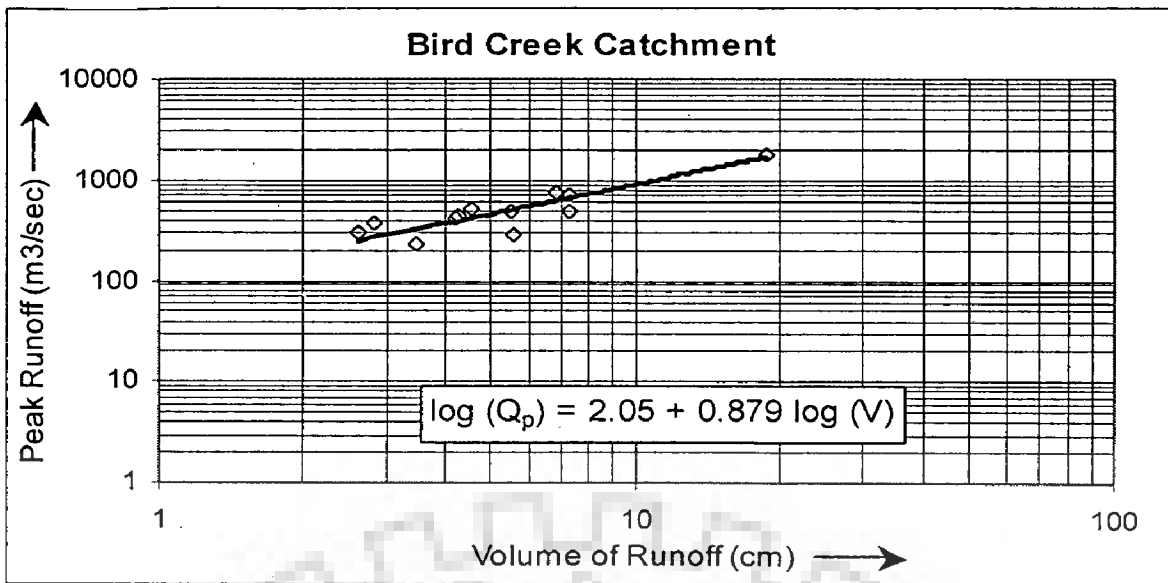


Fig. 5.1 (a) Plots between $\log(Q_p)$ and $\log(V)$ for Bird Creek, Brosna, and Garrapatos Catchments

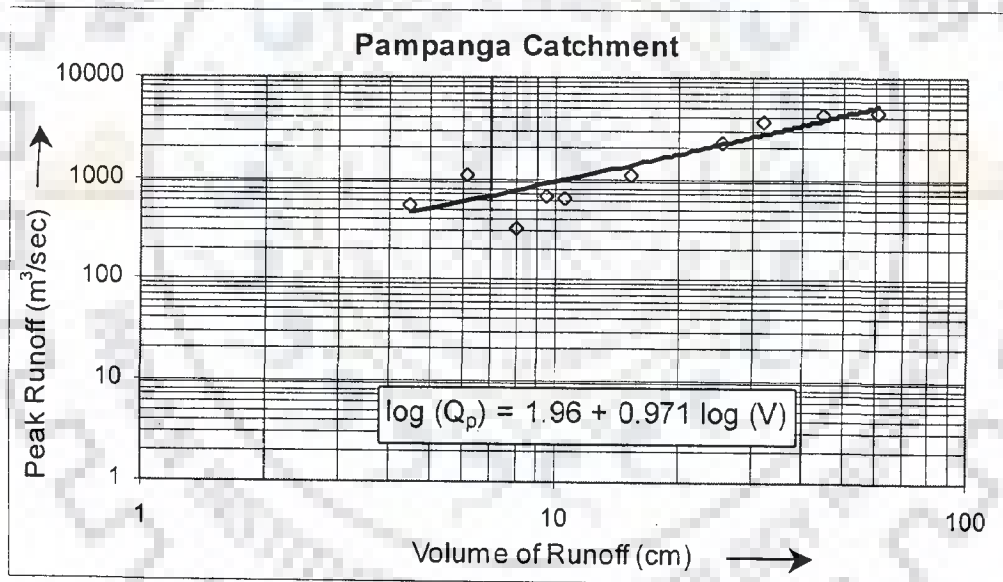
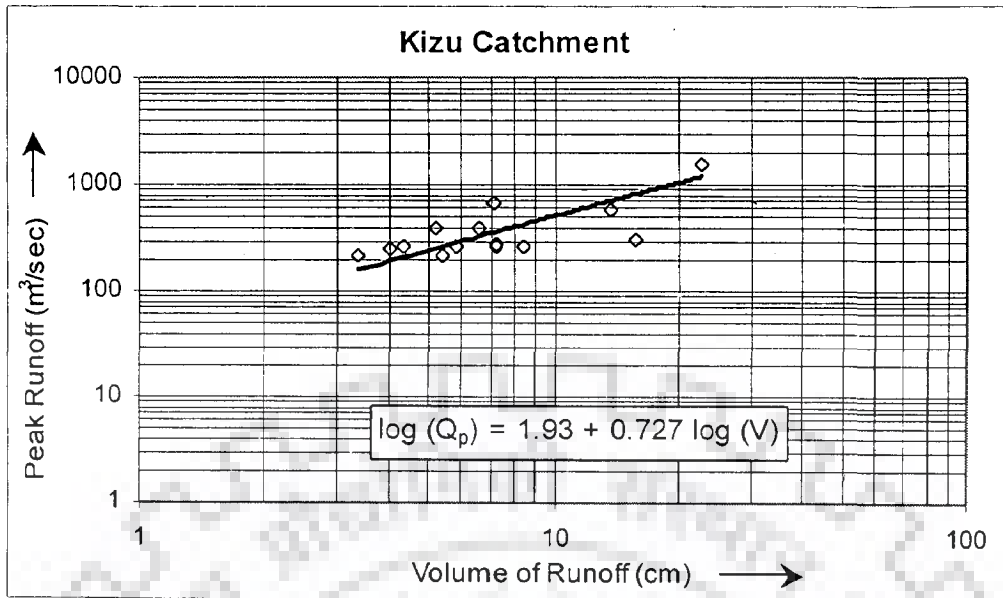


Fig. 5.1(b) Plots between $\log(Q_p)$ and $\log(V)$ for Kizu and Pampanga Catchments

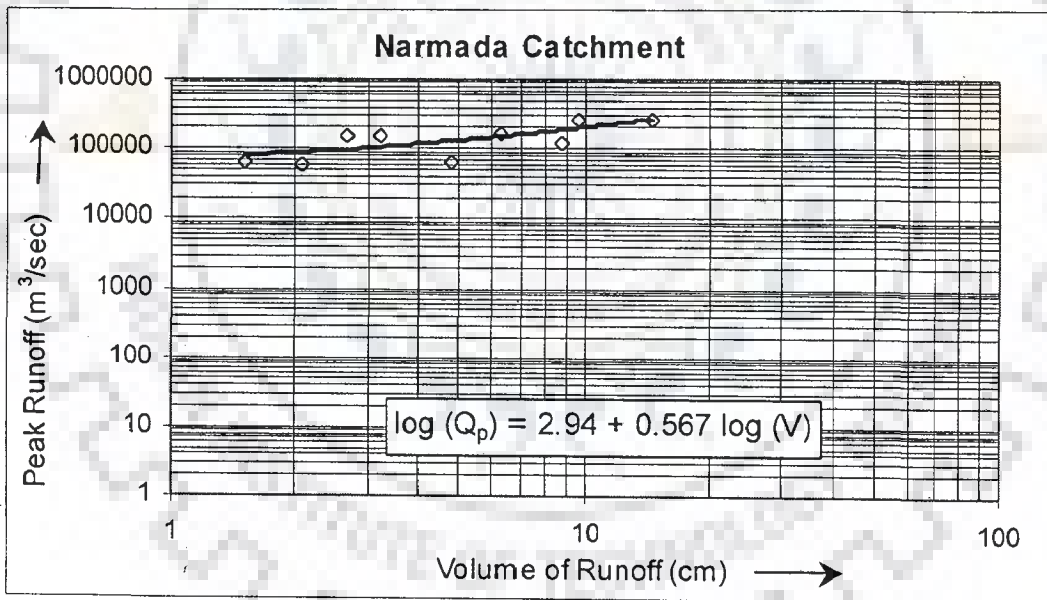
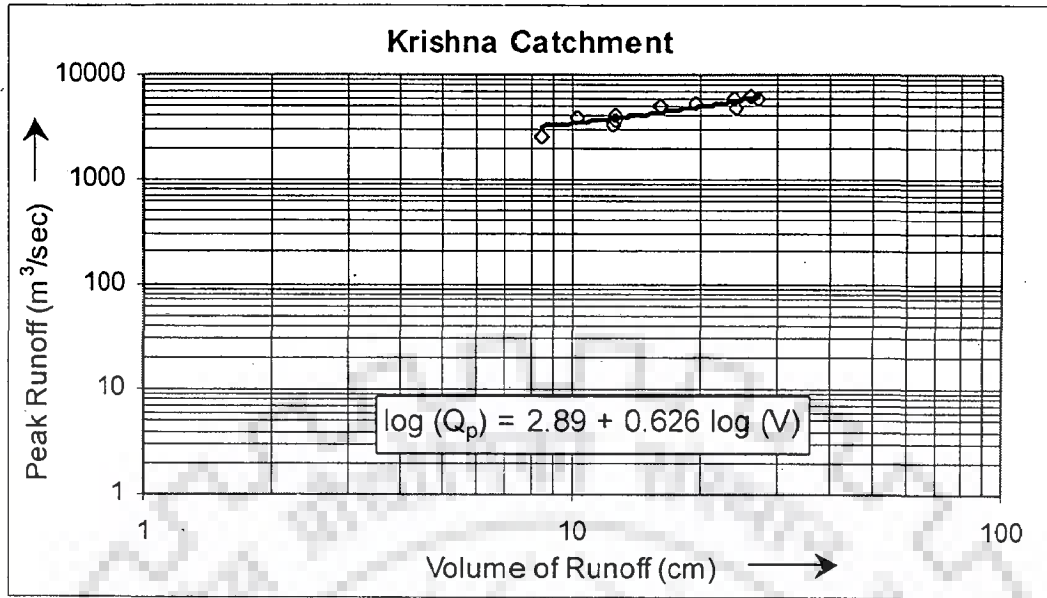


Fig. 5.1(c) Plots between $\log(Q_p)$ and $\log(V)$ for Krishna and Narmada Catchments

5.3 DETERMINATION OF THE RESPONSE FUNCTION

As outlined in the earlier chapter the memory length of a catchment is decided following a two-step procedure elaborated under section 4.3 (chapter 4). The shape of the response function derived along with other criteria mentioned in section 4.3.1 of chapter 4 guided the final decision about the value of the memory length of the catchments. The *SLM* and the linear Multiple Input Single Output (*MISO*) models are used first for deriving the response functions. The former model is used in case of the catchments which do not involve sub-divisions and the later is employed in case of the two large sized catchments which involve sub-divisions. Alternatively, the nonlinear model and its *MISO* counterpart are also used in a similar fashion for deriving the response functions of the various catchments studied.

5.3.1 Response Functions For Catchments Without Sub-Divisions

The *SLM* [Eq. (2.4)] is used for obtaining the values of the response function ordinates (*RFO*) for the relatively smaller sized catchments. As explained earlier the *MOLS* and the matrix inversion method are used to derive the column vector [U] in Eq. (4.1). If some of the ordinates in the response function derived using the Method of Least Squares (*MOLS*) are found to have negative values then the smoothed least squares method given by Eq. (4.5) (Bruen and Dooge, 1984) instead of *MOLS* is used. The values of the ridge parameter (R_p) for the catchments in which the ridge regression has to be used are given in Table 5.2. The problem of negative *RFOs* was encountered only in two of the five catchments involving no subdivisions. The response functions obtained for the finally selected memory lengths for all these catchments are plotted in Figs. 5.2 (a) - (e). The values of the memory lengths (in days) for these catchments are also given in Table 5.2. Relatively large values of memory length m are obtained for Brosna, Garrapatas, and Pampanga catchments. Similar results for these catchments were obtained by O'Connor and Ahsan (1991), in a study, which made use of the perturbation models. These catchments have geological formations with characteristics of holding the rainwater for long time and then release it slowly. The physically realistic shapes (*i.e.* monotonically increasing or decreasing values) of the response function shown in Figs. 5.2 (a) - (e) may

be noted. Such shapes can also be parameterized by making use of the gamma function as shown in the later part of this chapter.

The application of the nonlinear model [Eq. (2.10)] was also carried out in all the catchments by using different values for the nonlinear part of the memory n and the linear part of memory l . The derived values of the $RFOs$ for these by the application of the nonlinear model with $n = 1$ are presented in Table 5.3.

Table 5.2 Memory Length and Ridge Parameter For Catchments Without Sub-Divisions (Linear Model)

Name of The Catchment	Length of Memory (m) (Days)	Ridge Parameter (R_p)
Bird Creek	07	0.0875
Brosna	38	--
Garrapatas	20	--
Kizu	07	--
Pampanga	17	0.89

5.3.2 Response Functions For Catchments Involving Sub-Divisions

The two large sized catchments namely, the Krishna and the Narmada involve sub-divisions into smaller areas. The reasons stating the need for such sub-divisions are already given in chapter 3. For these catchments the linear *MISO* model is employed for deriving the response functions. The values of the memory lengths finally chosen for the different sub-division scenarios in both the catchments are given in Table 5.4. Some of these scenarios involved use of the smoothed least squares method; the value of ridge parameter R_p for the same is also given in this table. The map of the catchments showing different sub-divisions for the Narmada and the Krishna catchments are shown in Fig. 3.2 and Fig. 3.3 respectively. The response functions as obtained for the finally selected memory lengths in case of Krishna catchment are shown in Figs. 5.3 (a) and (b) for one and two sub-division scenarios respectively. Whereas, Figs. 5.3 (c) - (e) illustrate the shapes of the response functions obtained for all the three sub-division scenarios in the

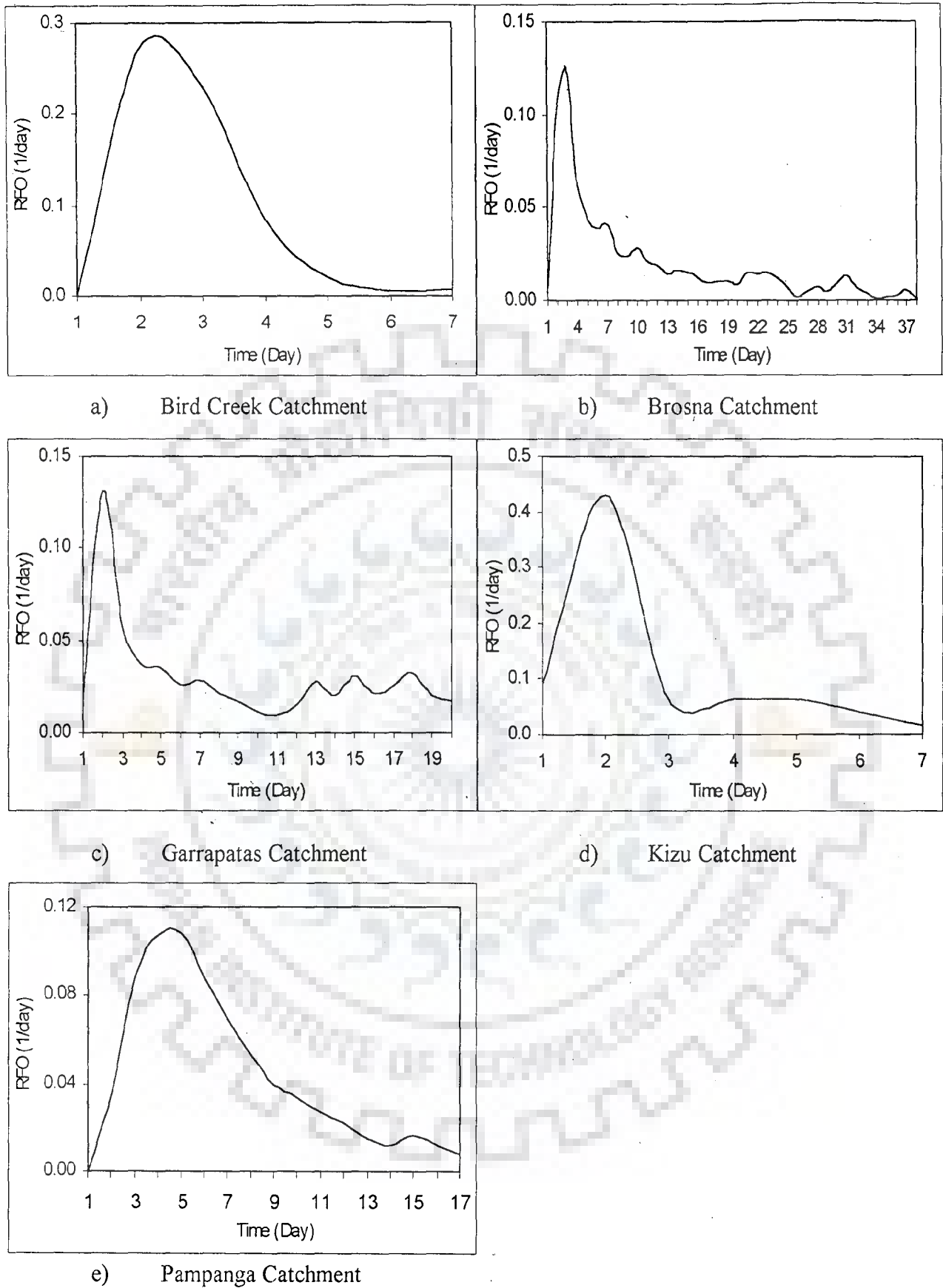


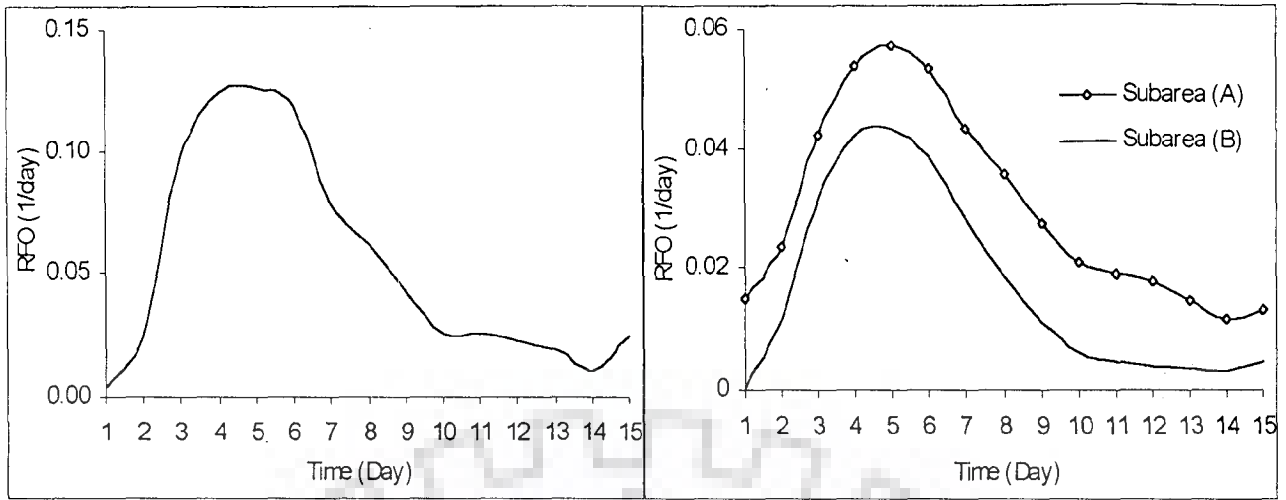
Fig. 5.2 Response Functions For the Catchments Without Sub-Divisions (Linear Model)

Narmada catchment. It can be seen from these Figs. 5.3(a) and (b) that the memory of 15 days provided realistic shape for both the sub-division cases in the Krishna catchment. In case of the Narmada catchment for one sub-division scenario, memory of 6 days provided realistic shape of the response functions and also satisfied the other criteria used in selection of the memory lengths. When the catchment was divided into two sub-areas a value of 6 and 5 days for the sub-areas A and B (see Fig. 3.2, chapter 3) respectively was optimal. For the three sub-division scenario, combination of 6, 5, and 5 days of memory length for sub-areas A, B, and C (shown in Fig. 3.2) gave realistic shape and also satisfied the other criteria. The physically realistic shapes of these response functions may also be noted. Similar to the application of the nonlinear model in case of the catchments without any sub-divisions the *RFOs* for these two catchments were obtained by using the nonlinear *MISO* model [Eq. (2.11)] also. The values of the *RFO* obtained for the nonlinear *MISO* model ($n = 1$) are also presented in Table 5.3.

Further sub-division of the Narmada catchment *i.e.* more than three sub-divisions was not attempted because of the paucity of the well-distributed raingauge stations. An attempt of dividing the Krishna catchment in to three sub-catchments as represented by *A*, *B*, and *C* in Fig. 5.4 was made but could not be adopted finally for the further analysis. The reasons for this would be clear from Fig. 5.5, which shows the response functions obtained for the three sub-catchments into which the Krishna catchment was divided. It can be observed from this figure that the magnitude of the response function ordinates is very small and the response function for the third sub-catchment *B* has negative values. The presence of high correlation amongst the average rainfall values for the different sub-catchments is considered to be the reason for the same.

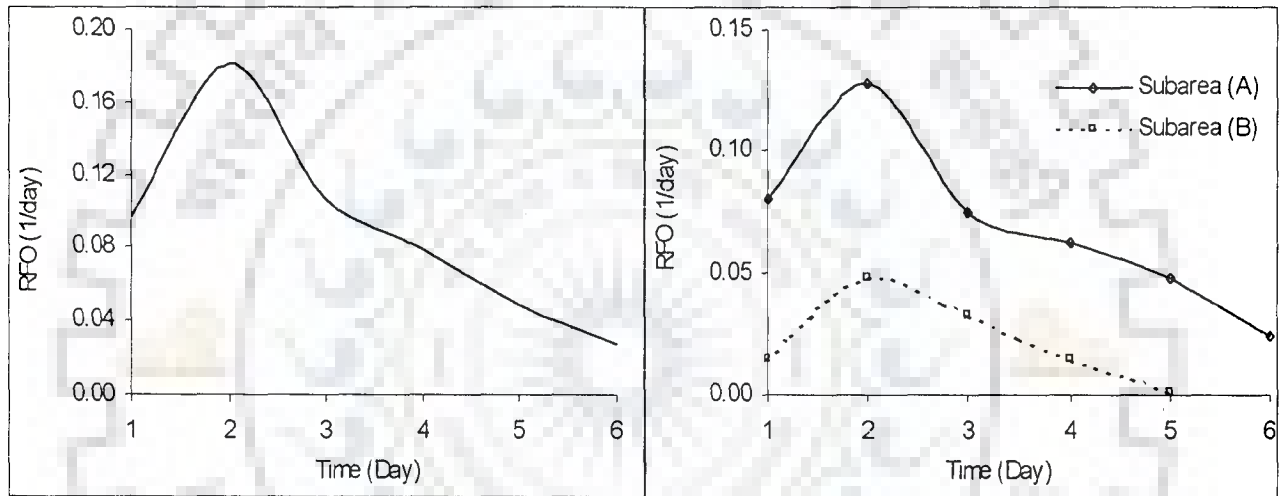
5.4 APPLICATION OF THE LINEAR AND NONLINEAR MODELS

The linear and the nonlinear models are applied to all the catchments studied in their appropriate form depending upon whether the catchment involves sub-division or not. In the following sections, the results of application of these models to all the catchments in terms of statistical as well as the graphical performance indicators are presented and discussed. The statistical criteria used include E^2 and R^2 for data used for



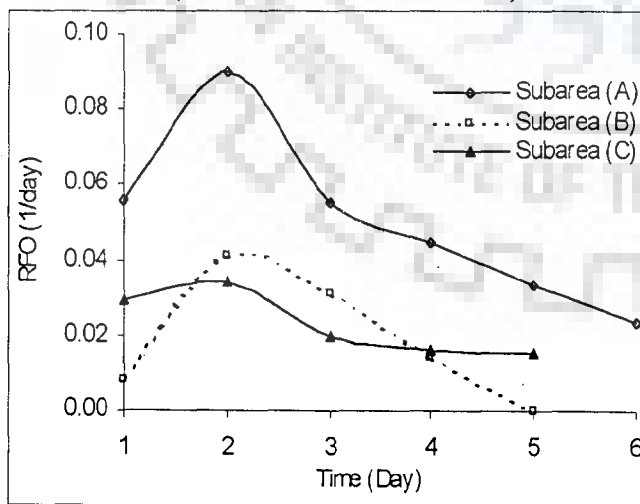
a) Krishna Catchment
(No Sub-Division Scenario)

b) Krishna Catchment
(Two Sub-Division Scenario)



c) Narmada Catchment
(No Sub-Division Scenario)

d) Narmada Catchment
(Two Sub-Division Scenario)



e) Narmada Catchment (Three Sub-Division Scenario)

Fig. 5.3 Response Function For Catchments With Sub-Divisions (Linear Model)

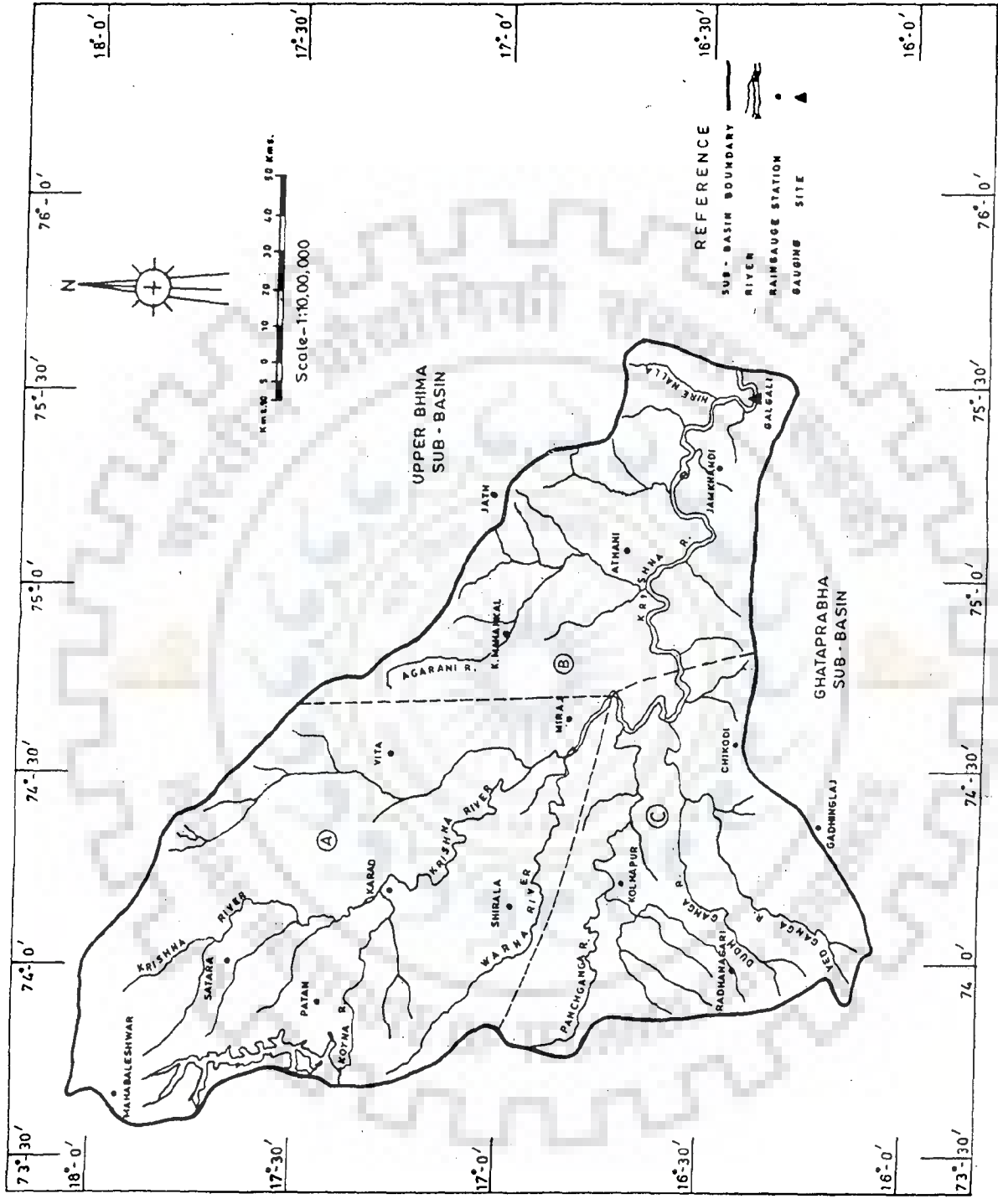


Fig. 5.4 Map of Krishna Catchment Showing Three Sub-Divisions (A), (B), and (C)

Table 5.3 Response Function Ordinates For The Nonlinear Model ($n = 1$)

Response Function Ordinate	Catchments With Sub-Divisions				Catchments Without Sub-Divisions						
	Krishna		Narmada		Bird Creek	Garrapatas	Kizu	Pampang	Brosna		
	One	Two	One	Two					Three	U ₂₅	U ₂₆
U _{1,1}	0.0000	0.0002	0.0014	0.0008	0.0008	0.0	0.0012	0.000	0.0	U ₂₅	0.0061
U ₂	0.0290	0.0308	0.1957	0.1478	0.1375	0.2415	0.4430	0.014	0.1075	U ₂₆	0.0028
U ₃	0.0960	0.0382	0.1093	0.0782	0.0801	0.2064	0.0623	0.146	0.1271	U ₂₇	0.0049
U ₄	0.1252	0.0526	0.0763	0.0608	0.0628	0.0833	0.0568	0.150	0.0642	U ₂₈	0.0083
U ₅	0.1261	0.0619	0.0558	0.0563	0.0560	0.0239	0.0576	0.148	0.0433	U ₂₉	0.0047
U ₆	0.1196	0.0642	0.0407	0.0354	0.0348	0.0071	0.0255	0.102	0.0396	U ₃₀	0.0090
U ₇	0.0771	0.0452				0.0095	0.0291	0.081	0.0418	U ₃₁	0.0135
U ₈	0.0629	0.0531	U _{1,1}	0.0007	0.0000		0.0214	0.038	0.0252	U ₃₂	0.0068
U ₉	0.0422	0.0354	U ₂	0.0382	0.0206		0.0185	0.037	0.0245	U ₃₃	0.0033
U ₁₀	0.0260	0.0237	U ₃	0.0329	0.0261		0.0124	0.031	0.0291	U ₃₄	0.0025
U ₁₁	0.0253	0.0165	U ₄	0.0128	0.0050		0.0099	0.024	0.0212	U ₃₅	0.0032
U ₁₂	0.0233	0.0428					0.0147	0.022	0.0187	U ₃₆	0.0055
U ₁₃	0.0192			U _{1,1}	0.0007		0.0282	0.026	0.0140	U ₃₇	0.0013
U ₁₄	0.0113			U ₂	0.0220		0.0204		0.0173		
U ₁₅	0.0249			U ₃	0.0085		0.0305		0.0153		
U ₁₆				U ₄	0.0058		0.0208		0.0122		
U ₁₇	U _{1,1}	0.0000					0.0274		0.0097		
U ₁₈	U ₂	0.0041					0.0328		0.0093		
U ₁₉	U ₃	0.0549					0.0192		0.0107		
U ₂₀	U ₄	0.0711					0.0186		0.0100		
U ₂₁	U ₅	0.0631							0.0151		
U ₂₂	U ₆	0.0583							0.0138		
U ₂₃	U ₇	0.0281							0.0148		
U ₂₄	U ₈	0.0046							0.0132		

Table 5.4 Memory Length and Ridge Parameter For Catchments With Sub-Divisions (Linear Model)

Name of The Catchment	No. of Sub-Divisions	Length of Memory (m) (Days)	Ridge Parameter (R_p)
Krishna	One	15	--
	Two	15, 15	0.68
Narmada	One	06	--
	Two	06, 05	0.0175
	Three	06, 05, 05	0.0125

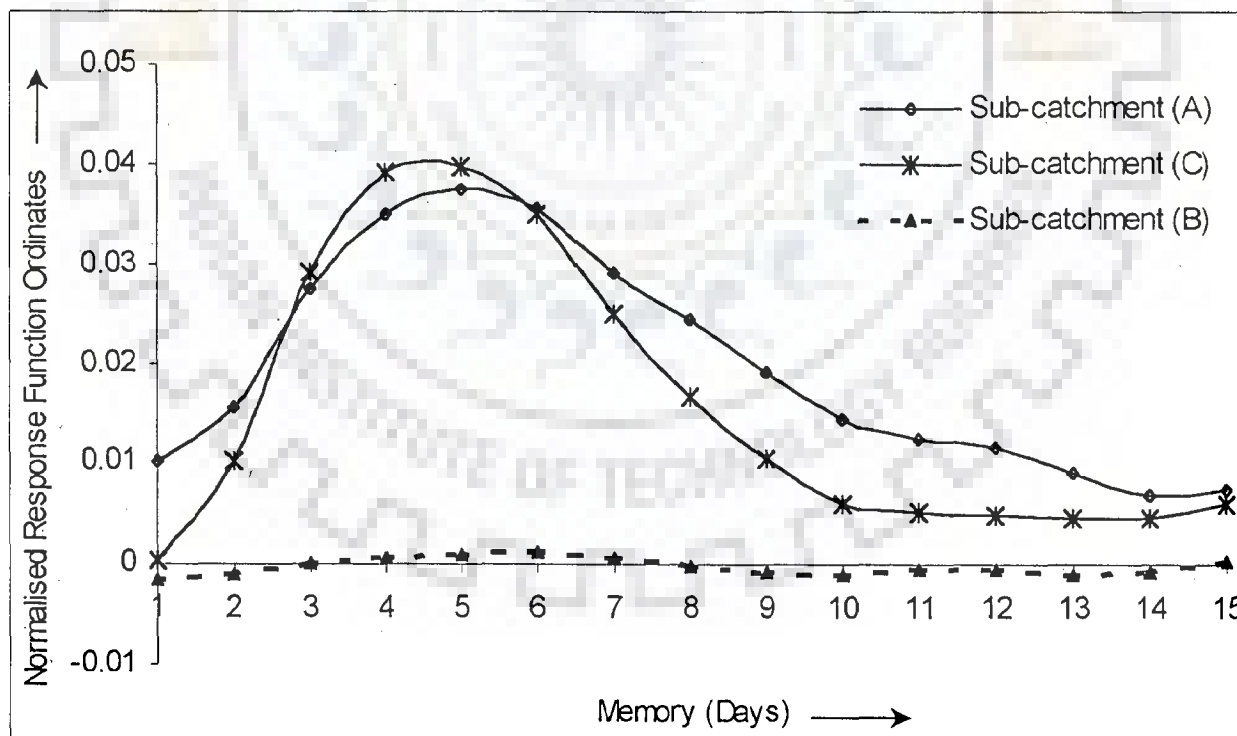


Fig. 5.5 The Response Functions for Three Sub-Divisions Scenario in Krishna Catchment

the calibration and verification periods whereas the graphical presentation include linear scale plots of simulated vs. observed runoff. These plots are prepared for all the events used for calibration and for validation but only the figures of those events that contain the highest of the daily peak discharges amongst all the storm events are presented as illustration. The scatter diagrams are prepared for the entire data used in the calibration and validation period.

5.4.1 Linear and Nonlinear Model Application to Catchments Without Sub-Divisions

Linear Model:

The performance of the *SLM* applied to the relatively small sized catchments in terms of E^2 and R^2 criteria is presented in Table 5.5. The *SLM* performed poorly in most of the cases except for the calibration data in Bird Creek, Kizu, and Pampanga catchments and for validation data in the Brosna catchment in terms of the Nash-Sutcliffe (E^2) criterion. A similar trend in the performance of the *SLM* in terms of R^2 criterion can be noted from this table. More discussion on the application of linear model results is presented at the end of the following section.

Nonlinear Model:

The nonlinear model application involved two different cases. First, the value of n was taken equal to unity and the results in each catchment are obtained. Then the value of n was increased to two. The nonlinear model with $n = 2$ was not applicable to two catchments namely Brosna and Pampanga as the *RFO* obtained for these with $n = 2$ had negative values. Value of n more than two was also used, but in that case the *RFO* obtained for all the catchments were found to have negative values.

Table 5.6 presents the results of the nonlinear model for $n = 1$ and 2 in terms of E^2 , R^2 . For $n = 1$ the E^2 values of the nonlinear model are almost similar to those obtained for the linear model with the exception of the Pampanga and Kizu catchments where some improvement in E^2 values for the calibration and the validation data can be noted. A

significant increase in R^2 value for nonlinear model over that for the linear model in case of Kizu catchment only could be observed.

The Table 5.7 gives the details of the results obtained for the individual events used for calibration in each of the five catchments when the *SLM* and the nonlinear models are applied. The information about computed and observed volume of runoff (mm), the observed and predicted peak of daily discharges, and time to peak is provided in this table. It can be seen that the time to peak matched very well in most of the cases but in some events (event 5 in Pampanga catchment) the error in time to peak is more. The prediction of the peak daily discharges matched in a very few cases (event 3, 9, 10 in Garrapatas catchment; event 3 in Brosna catchment for example) but in other cases the *SLM* and the nonlinear model has either under predicted or over predicted the peak runoff values.

Similar kind of presentation of the results for individual events used for validation purpose is provided in Table 5.8. As can be seen from this table that a maximum error in prediction of time to peak is one day only. The peak of runoff value is well predicted only for two events in Brosna catchment but in other events either under prediction or the over prediction of the peak daily discharges can be seen. It is however noticed from Table 5.7 and 5.8 that the relatively larger peaks are mostly under estimated by the *SLM* and the nonlinear models. This reveals the persistence present in the model residuals, which could not be accounted for by the nonlinear model used. The computed runoff volume is better only for a few events as the *VE* values were less than $\pm 10\%$. Larger error in volume prediction however can be noticed in some other events. The absolute *VE* values are smaller than 20% for many runoff events of calibration and validation. However, in a few cases the *VE* values are greater than 20%.

Graphical Presentation:

The performance of linear model in all the catchments without any sub-divisions is presented in the form of scatter diagrams for the validation period in Figs. 5.6 (a) – (e) and similar plots for the nonlinear model ($n = 1$) are shown in Figs. 5.7 (a) – (e). These plots are given for the entire data selected for validation in each of the catchment. It may be noted that the events used for validation are not used earlier for the purpose of calibration.

For the data used for calibration, relatively better results are generally obtained and hence these scatter plots are not shown here. The scatter plots shown in Figs. 5.6 and 5.7 clearly indicate that except for Brosna catchment the scatter is large and the points are shifted towards one side of the ideal line. This is an indication of the poor performance of the models indicating existence of persistence and time variance in error values and presence of the systematic errors.

Figures 5.8(a) – (c) show as illustration the linear scale plots of the computed and observed runoff for calibration events containing the highest of the peak flows as illustration in each of the catchments studied. From the analysis of Figs. 5.8(a) – (c) and Table 5.7 it can be said that there is significant difference in the magnitude of peaks predicted by the linear model indicating its poor performance. These values are predicted with relatively greater degree of accuracy by the nonlinear model in Bird Creek, Kizu, and Pampanga catchments whereas in case of Brosna and Garrapatas the performance of linear and the nonlinear model in predicting magnitude of peak is almost the same. The analysis of the similar plots prepared for other events used for calibration (not shown) reveals that both the models have over predicted the low flows in almost all the cases.

The linear scale plots of the observed and the computed runoff for one validation event containing the highest of the peak flows are shown as illustration in Figs. 5.9(a) – (c) for each of the catchment. The performance of both the linear and the nonlinear model with $n = 1$ and $n = 2$ (wherever applicable) is shown in these figures. Such linear scale plots (not shown here) prepared for all the other events used for validation indicate similar kind of results

Table 5.5 Results of the Linear Model Application to Catchments Without Sub-Divisions

Catchment	E^2 (%)		R^2	
	Cal.*	Val.*	Cal.	Val.
Bird Creek	87.50	62.71	0.875	0.754
Brosna	63.26	86.62	0.633	0.867
Garrapatas	45.92	59.19	0.459	0.693
Kizu	85.16	69.96	0.852	0.816
Pampanga	80.30	66.58	0.803	0.813

* Cal. -Calibration; Val. -Validation;

Table 5.6 Results of the Nonlinear Model Application to Catchments Without Sub-Divisions

Catchment	Nonlinear Model ($n = 1$)				Nonlinear Model ($n = 2$)			
	E^2 (%)		R^2		E^2 (%)		R^2	
	Cal.*	Val.*	Cal.	Val.	Cal.	Val.	Cal.	Val.
Bird Creek	86.13	68.67	0.861	0.754	83.93	74.49	0.839	0.753
Brosna	63.22	86.78	0.632	0.868	← N.A. →			
Garrapatas	46.43	58.19	0.464	0.685	38.82	55.34	0.388	0.667
Kizu	88.60	71.10	0.886	0.831	86.87	69.19	0.869	0.747
Pampanga	85.76	77.1	0.858	0.816	← N.A. →			

* Cal. -Calibration; Val. -Validation;

Table 5.7 Performance of Linear and Nonlinear Models For Catchments Without Sub-Divisions (Calibration Events)

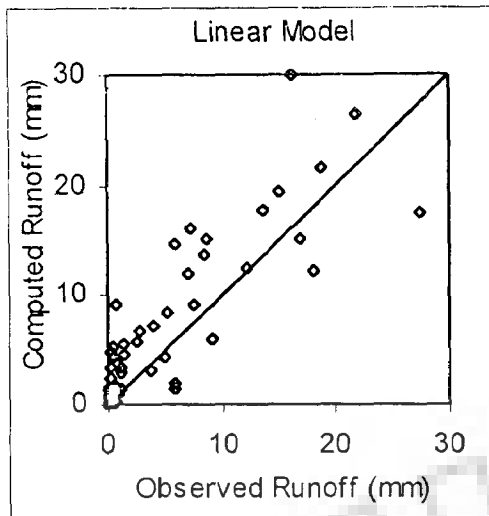
Runoff Event No.	Runoff Volume (mm)				Peak of Daily Discharges (mm)				Time to Peak (Day)			
	Obs.	Computed			Obs.	Computed			Obs.	Computed		
		SLM	Nonlinear			SLM	Nonlinear			SLM	Nonlinear	
			n=1	n=2			n=1	n=2			n=1	n=2
Bird Creek Catchment												
1	70.9	107	97.0	66.8	10.7	16.3	14.6	9.18	6	5	5	5
2	153.7	134	122	92.0	22.6	15.0	13.7	10.0	19	18	18	19
3	152.1	136	124	96.2	26.9	20.1	18.1	13.2	5	5	5	5
4	34.5	60.2	55.0	37.5	8.3	8.7	7.7	5.7	12	12	12	13
5	188.6	174	158	174	64.1	46.7	41.9	67.8	5	5	5	5
6	20.2	25.9	23.5	16.3	6.4	9.5	8.5	5.4	4	5	5	5
7	26.1	41.1	37.4	29.9	11.2	17.2	15.3	9.9	3	3	3	4
8	20.2	33.6	30.6	21.2	9.2	11.2	10.0	6.5	4	3	3	4
Brosna Catchment												
1	141.8	95.5	95.7	N.A.	6.9	4.6	4.7	N.A.	16	17	17	N.A.
2	67.5	76.6	76.9		4.9	4.6	4.7		7	7	7	
3	71.7	81.9	82.2		4.4	4.3	4.3		16	16	16	
4	70.6	78.1	78.3		4.6	5.1	5.1		5	5	5	
5	72.2	63.0	63.2		5.3	3.9	4.0		8	7	7	
6	112.8	98.6	98.9		5.9	4.3	4.4		7	7	7	
7	60.0	98.4	98.8		4.1	5.3	5.4		8	8	8	
8	126.0	115	115		6.1	5.3	5.4		19	19	19	
Garrapatos Catchment												
1	76.4	70.4	69.7	66.8	9.1	7.6	7.7	7.1	5	6	6	6
2	131.2	105	105	106	10.7	8.0	8.0	7.4	6	5	8	8
3	165.8	176	177	179	11.1	10.8	10.8	12.9	5	5	5	5
4	206.2	176	176	174	17.5	10.5	10.5	11.2	6	6	6	6
5	316.8	333	333	332	14.1	11.9	11.9	12.3	6	8	8	8
6	138.1	100	100	98.0	11.3	7.6	7.7	6.9	11	11	11	11
7	99.2	73.5	72.7	69.6	9.7	6.4	6.4	5.3	4	4	4	4
8	96.7	136	136	137	8.9	11.4	11.4	11.1	8	10	10	10
9	76.4	86.5	86.7	87.9	9.2	9.7	9.8	9.9	4	2	2	2
10	177.2	173	172	168	8.6	8.1	8.2	7.5	13	13	13	13
Kizu Catchment												
1	165.6	160	150	105	18.1	20.0	19.1	15.6	11	10	10	10
2	158.1	101	95.7	70.0	18.5	19.5	19.1	12.4	3	3	3	3
3	33.7	53.0	51.5	34.9	13.0	22.1	22.4	8.7	5	5	5	5
4	53.9	78.3	73.2	51.0	13.4	17.7	16.5	11.7	6	6	6	6
5	71.3	100	98.6	91.2	39.9	35.8	35.4	38.0	4	4	4	4
6	72.6	61.7	57.6	42.2	16.9	16.5	17.0	11.2	6	6	6	5
7	85.6	86.0	83.3	60.4	23.4	27.9	27.9	16.1	2	2	2	2
8	204.6	195	183	126	15.8	18.8	18.2	12.2	10	10	10	9
9	43.1	41.8	39.6	28.2	15.9	17.7	17.2	8.6	3	3	3	3
10	328.9	320	331	354	95.2	79.3	80.2	101	12	12	12	12
Pampanga Catchment												
1	61.7	174	214	N.A.	17.9	22.8	30.7	N.A.	4	6	6	N.A.
2	152.2	197	234		17.3	18.9	25.5		10	12	11	
3	449.5	328	407		72.0	42.0	58.1		7	7	7	
4	255.9	196	239		36.7	21.0	28.6		11	11	10	
5	79.9	93.5	111		5.25	9.2	12.1		9	6	5	
6	609.2	508	608		72.7	56.5	74.6		8	8	8	

* Obs. – Observed; N.A. – Not Applicable

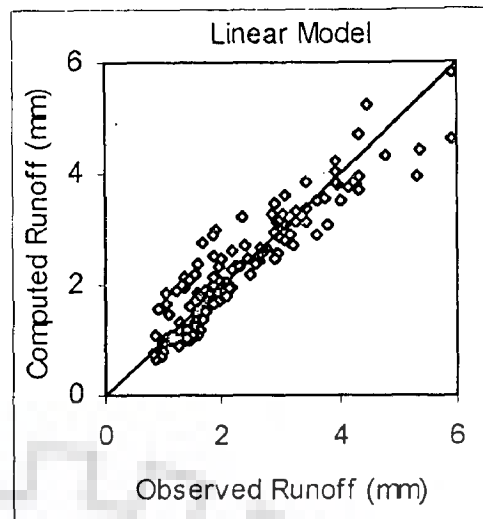
Table 5.8 Performance of Linear and Nonlinear Models For Catchments Without Sub-Divisions (Validation Events)

Runoff Event No.	Runoff Volume (mm)				Peak of Daily Discharges (mm)				Time to Peak (Day)			
	Obs.*	Computed			Obs.	Computed			Obs.	Computed		
		SLM	Nonlinear			SLM	Nonlinear			SLM	Nonlinear	
			n=1	n=2			n=1	n=2			n=1	n=2
Bird Creek Catchment												
9	73.0	75.7	68.9	51.9	18.1	15.0	13.3	9.9	10	9	9	10
10	58.3	98.0	89.2	66.8	18.6	21.7	19.6	13.9	6	6	6	6
11	42.8	78.0	71.0	62.7	16.3	29.9	26.7	20.9	4	4	4	4
12	68.3	64.5	58.7	51.0	27.4	26.4	23.5	17.8	5	4	4	4
13	28.1	57.8	52.7	43.9	13.6	17.8	15.8	11.4	4	4	4	4
Brosna Catchment												
9	39.2	43.0	43.2	N.A.	4.0	3.8	3.8	N.A.	11	11	11	N.A.
10	155.1	145	146		6.6	5.3	5.3		22	22	22	
11	62.2	54.5	54.7		5.3	4.3	4.4		10	11	11	
12	62.4	74.7	74.9		5.9	5.8	5.9		16	16	16	
Garrapatos Catchment												
11	110.5	76.1	75.5	72.8	8.1	5.6	5.5	4.4	6	5	5	5
12	74.3	81.7	81.0	79.2	9.2	8.2	8.3	7.6	5	5	5	5
13	67.8	59.2	59.0	59.1	7.1	6.7	6.7	5.9	4	4	4	4
14	389.4	347	346	348	15.1	10.4	10.4	10.1	12	13	13	13
Kizu Catchment												
11	87.5	96.8	91.1	63.7	15.1	19.6	20.1	6.7	11	11	11	12
12	208.4	156	158	135	35.2	41.0	41.3	32.7	10	10	10	10
13	52.0	65.5	65.6	47.2	23.2	32.5	33.4	16.1	5	5	5	5
14	71.8	69.6	66.6	51.9	15.6	20.1	19.0	15.2	5	4	4	4
15	90.8	123	119	92.3	20.2	28.0	27.9	14.9	7	7	7	7
Pampanga Catchment												
7	105.7	135	163	N.A.	10.3	12.1	17.1	N.A.	14	14	14	N.A.
8	94.8	87.3	100		11.1	11.2	15.3		3	4	4	
9	44.6	70.5	87.1		8.8	7.8	10.2		7	8	8	
10	319.6	193	242		60.6	25.6	35.9		6	7	6	

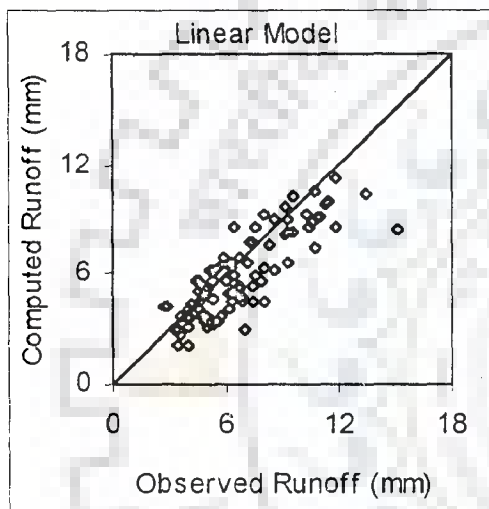
* Obs. – Observed; N.A. – Not Applicable



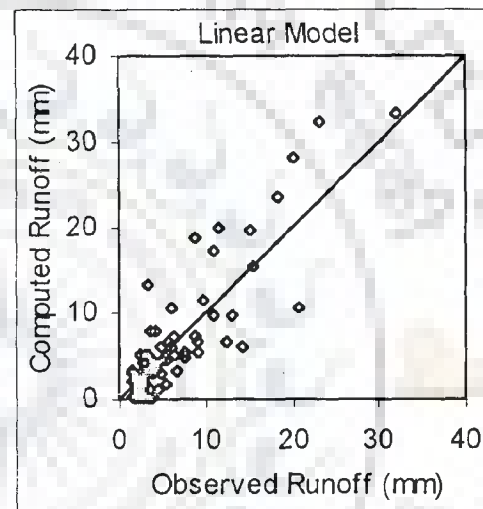
a) Bird Creek Catchment



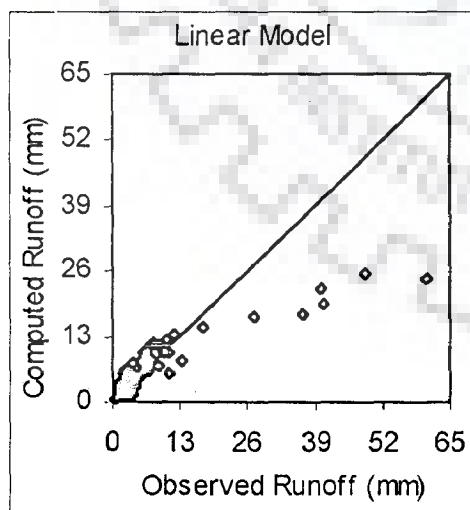
b) Brosna Catchment



c) Garrapatas Catchment

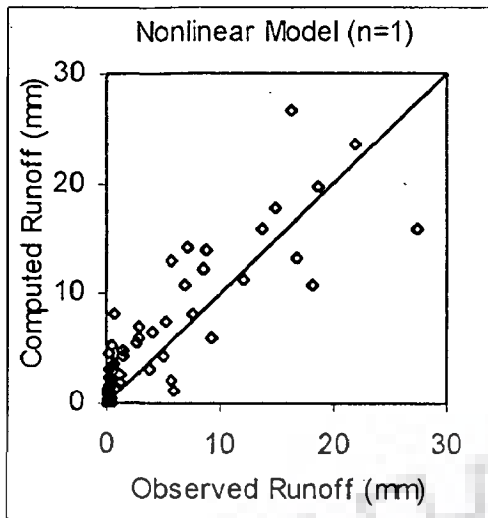


d) Kizu Catchment

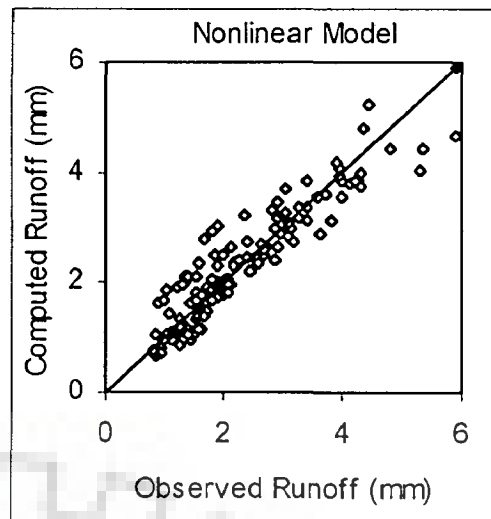


e) Pampanga Catchment

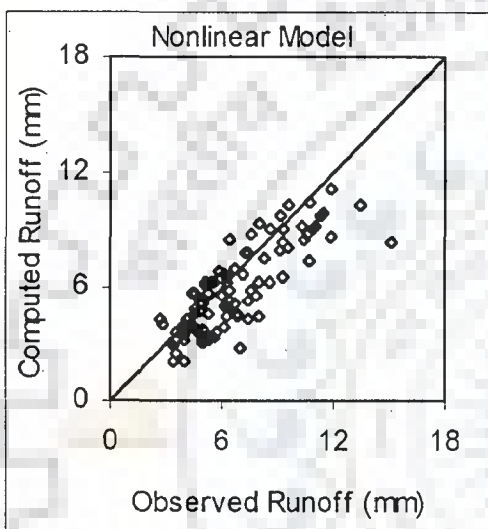
Fig. 5.6 Scatter Plots For the Catchments With No Sub-Divisions (Linear Model - Validation)



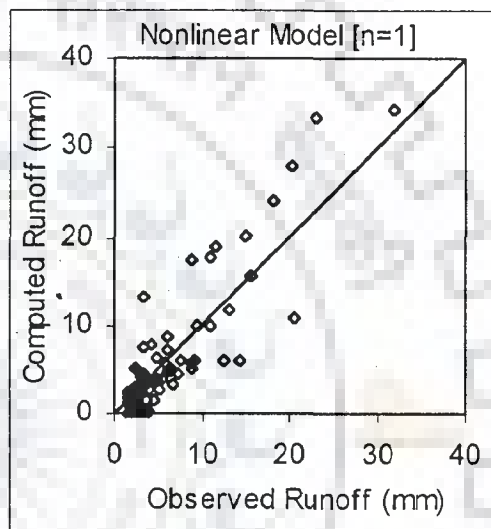
a) Bird Creek Catchment



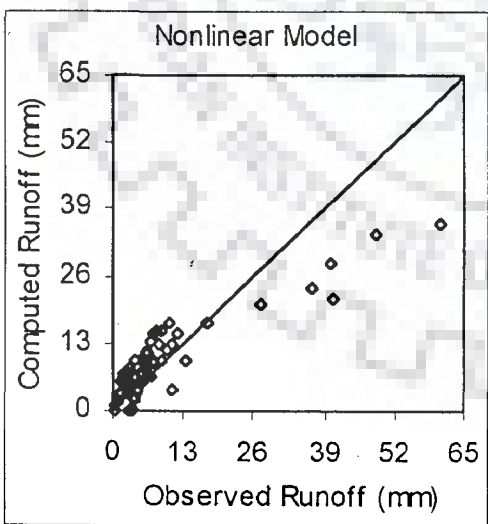
b) Brosna Catchment



c) Garrapatas Catchment

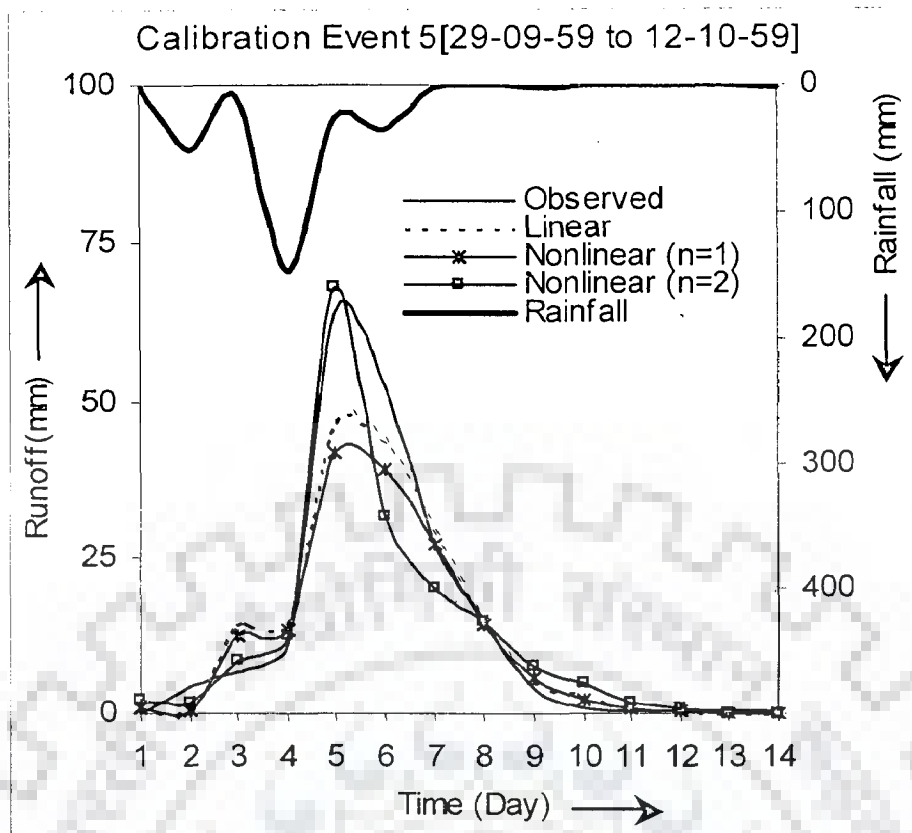


d) Kizu Catchment

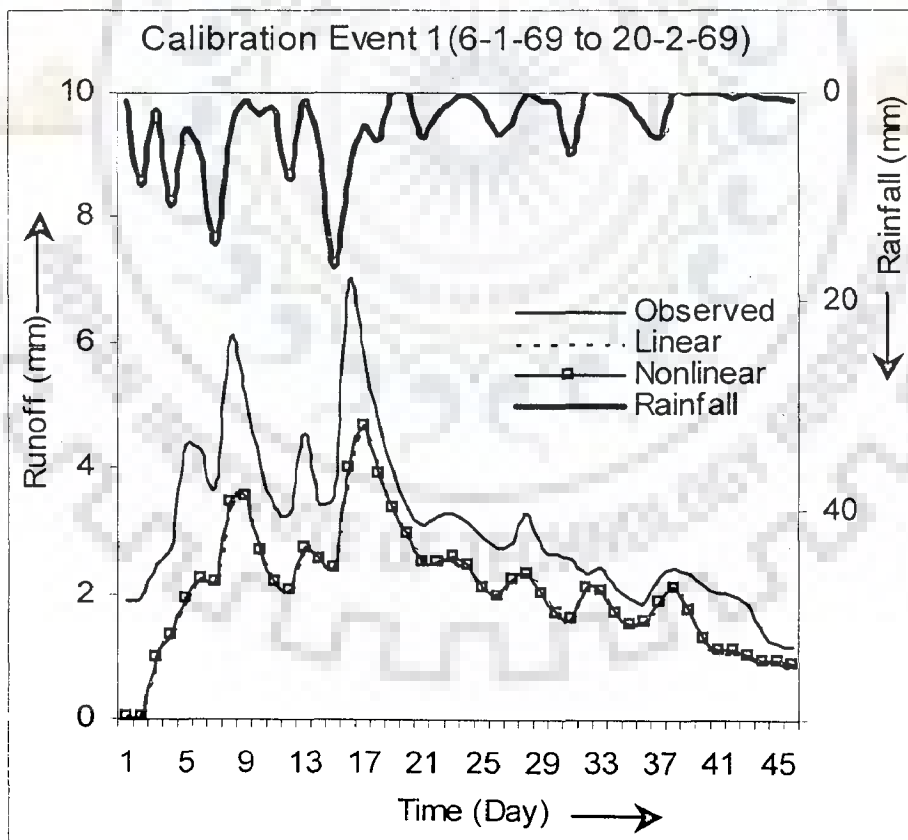


e) Pampanga Catchment

**Fig. 5.7 Scatter Plots For the Catchments With No Sub-Divisions
(Nonlinear Model - Validation)**

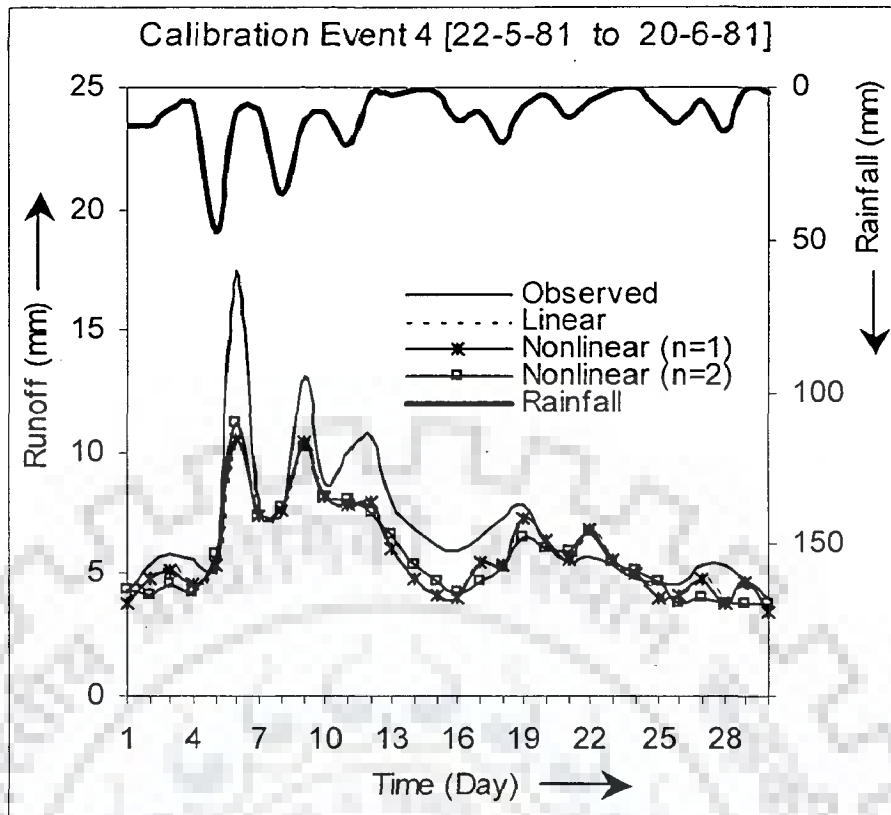


i) Bird Creek Catchment

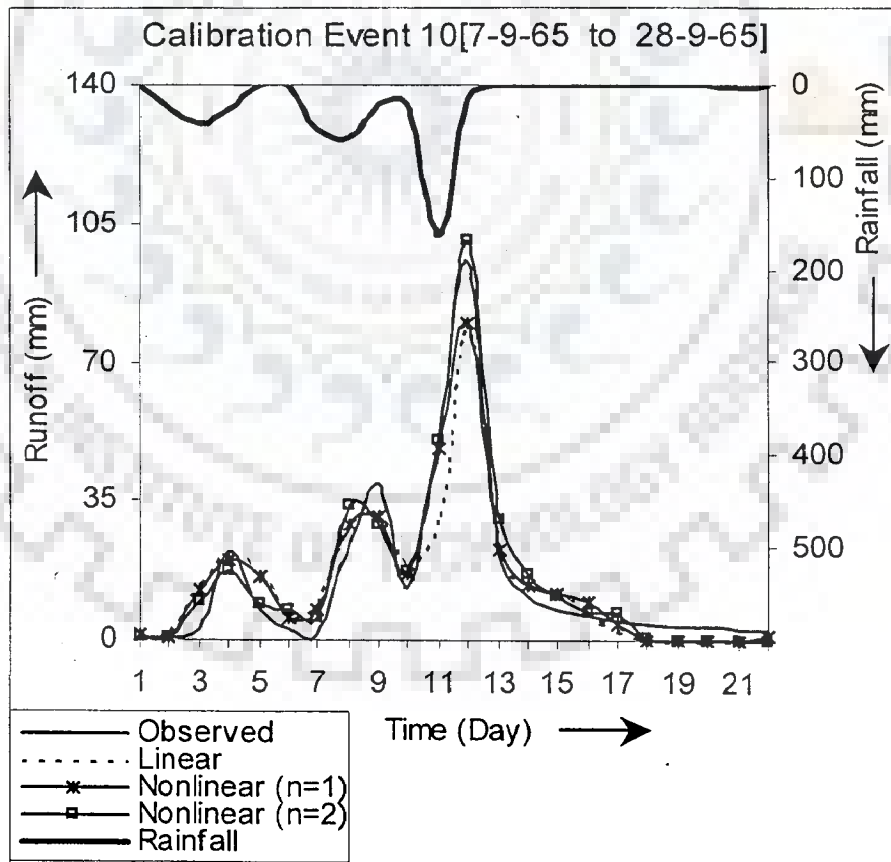


ii) Brosna Catchment

Fig. 5.8(a) Linear Scale Plots For Linear and Nonlinear Models For Catchments With No Sub-Divisions (Calibration Events)

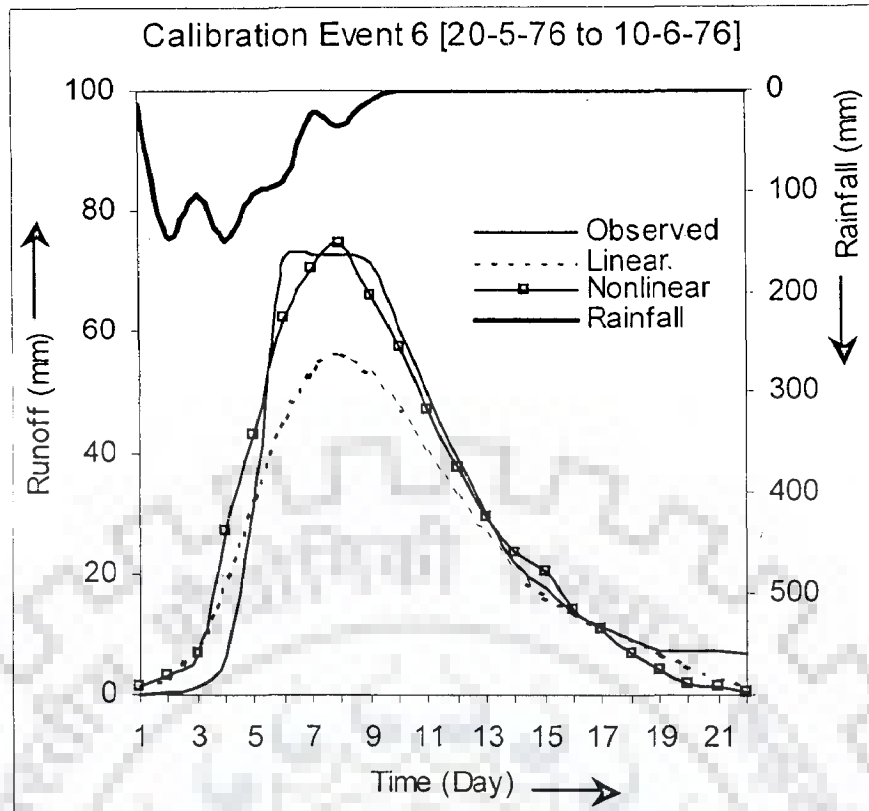


iii) Garrapatas Catchment



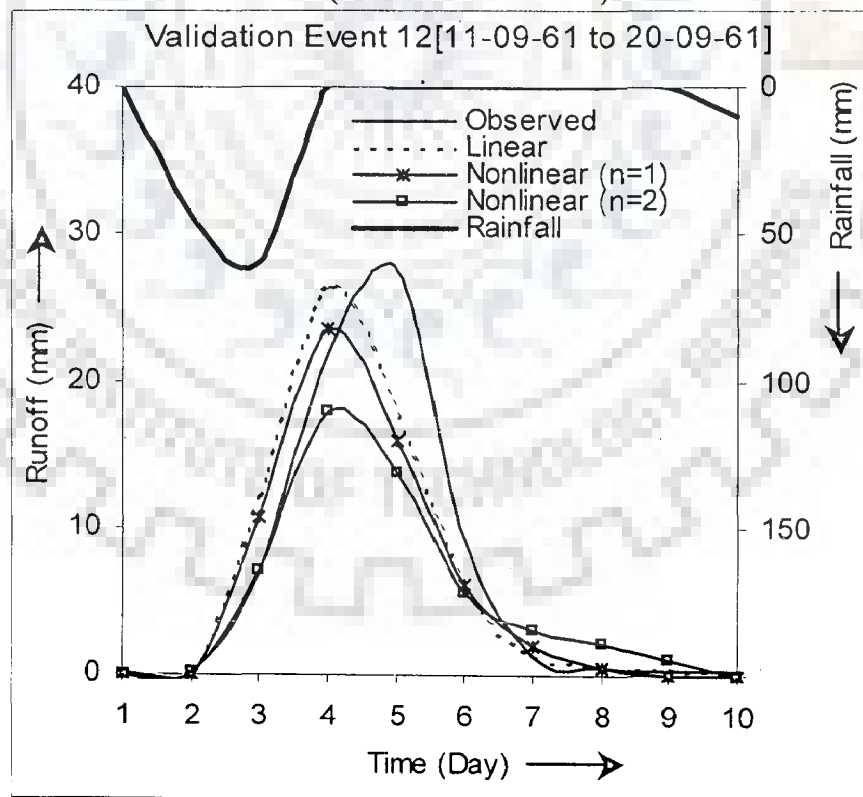
iv) Kizu Catchment

Fig 5.8(b) Linear Scale Plots For Linear and Nonlinear Models For Catchments With No Sub-Divisions (Calibration Events)



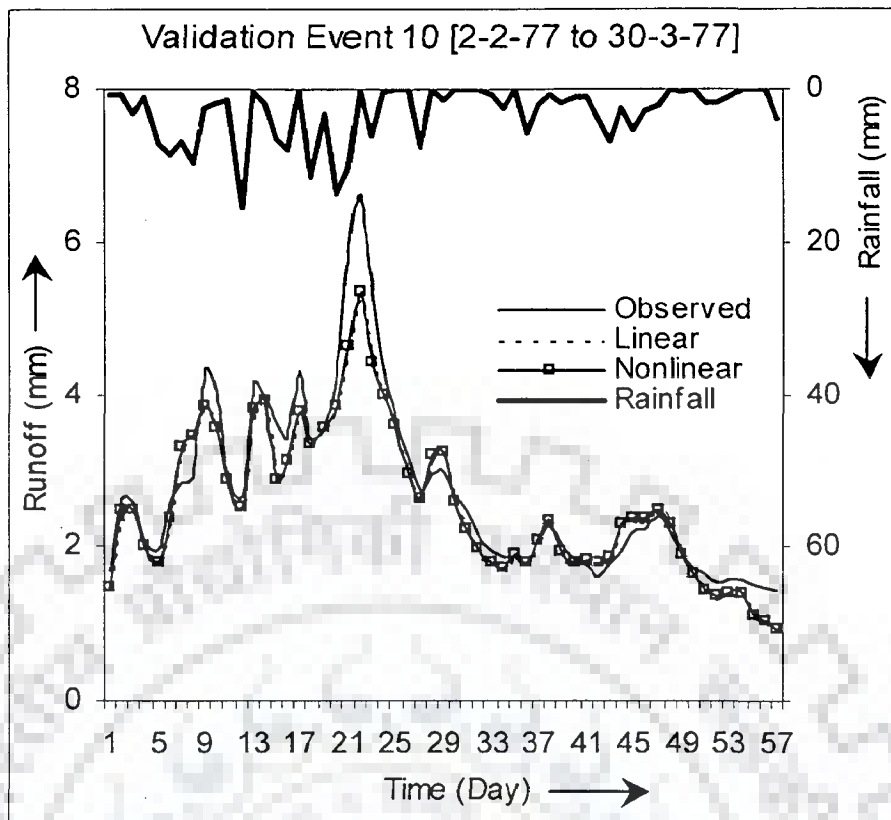
v) Pampanga Catchment

Fig 5.8(c) Linear Scale Plots For Linear and Nonlinear Models For Catchments With No Sub-Divisions (Calibration Events)

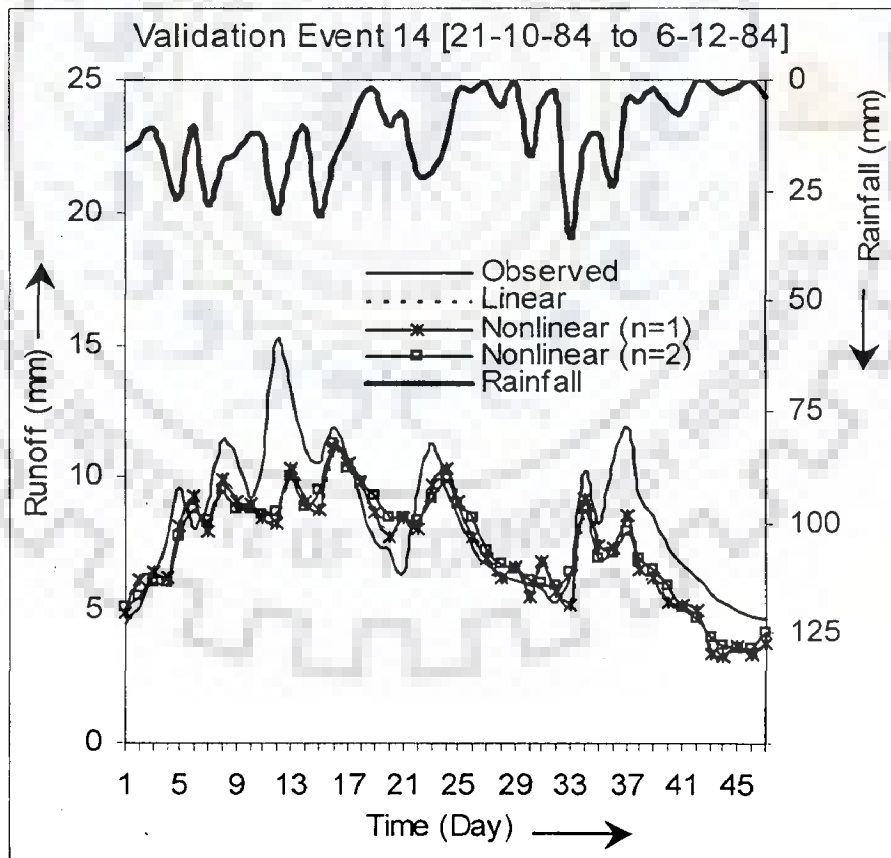


i) Bird Creek Catchment

Fig. 5.9(a) Linear Scale Plots For Linear and Nonlinear Models For Catchments With No Sub-Divisions (Validation Events)

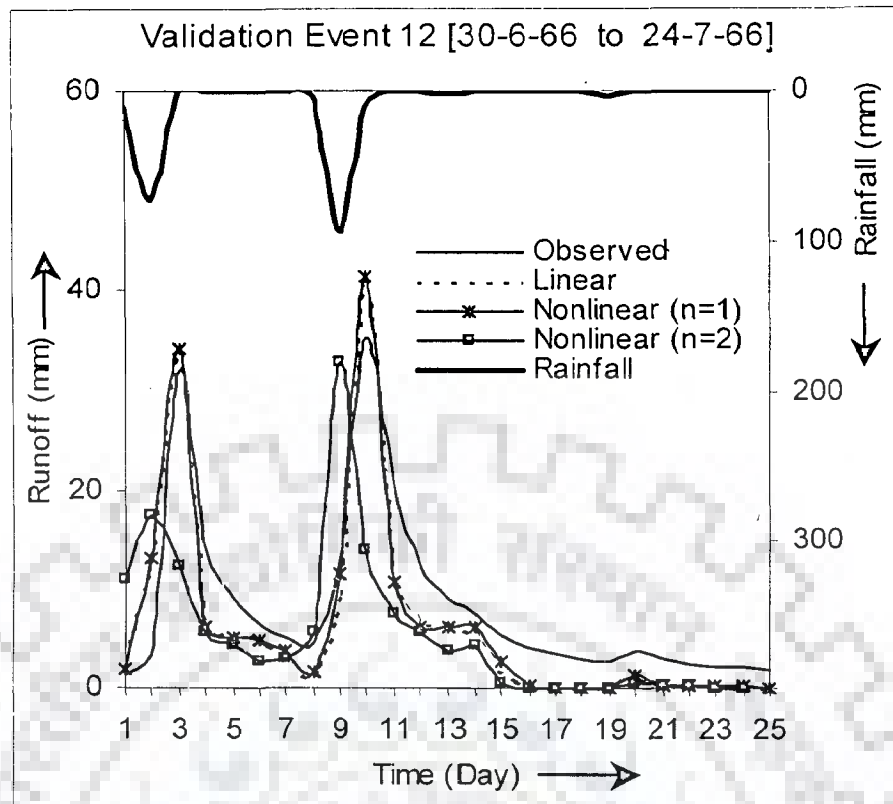


ii) Brosna Catchment

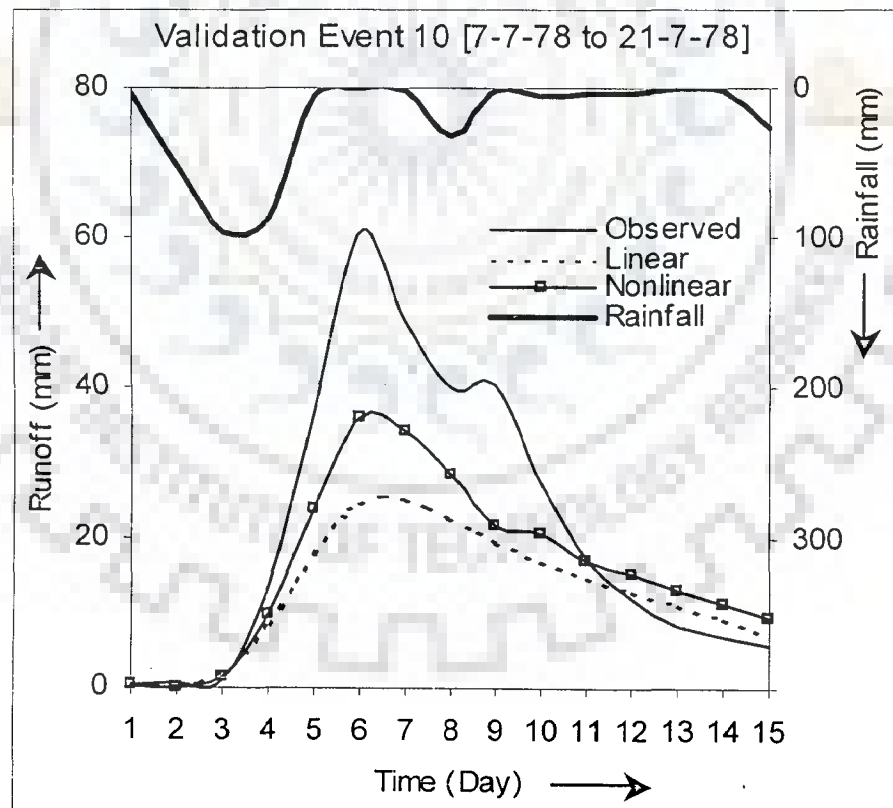


iii) Garrapatas Catchment

Fig. 5.9(b) Linear Scale Plots For Linear and Nonlinear Models For Catchments With No Sub-Division (Validation Events)



iii) Kizu Catchment



v) Pampanga Catchment

Fig. 5.9(c) Linear Scale Plots For Linear and Nonlinear Models For Catchments With No Sub-Division (Validation Events)

5.4.2 Application of Linear and Nonlinear Models to Catchments With Sub-Divisions

Linear Model:

In case of the two large size catchments, which involve division of the catchment into small sub-areas, the linear *MISO* model given by Eq. (2.7) is employed first. The rainfall matrix **[P]** in the multiple input case has a typical structure as shown in Fig. 4.2, which involves vertical stacking of the data from different runoff events for a sub-catchment and the horizontally adjacent stacking of such values for each sub-catchment. The matrix **[P]** was generated using a program developed using *FORTRAN - 77* for the same. The results obtained in terms of E^2 and R^2 criteria by application of the linear *MISO* model to Krishna and Narmada catchments are given in Table 5.9. The E^2 values for the validation data have shown an improvement for two sub-division scenario as compared to one sub-division scenario in the Krishna catchment. The linear *MISO* model performance in Narmada catchment shows that the value of E^2 for both the calibration and the validation data have increased for two sub-division scenario than the one sub-division case but a slight decrease is observed for three sub-division scenario. The increase in the R^2 values for the validation has been consistent with the increase in the number of sub-divisions studied. More results obtained through application of the linear *MISO* model are described later.

Nonlinear Model:

The nonlinear *MISO* model is applied in the Krishna and the Narmada catchments. The input rainfall matrix **[P]** having the structure as shown in Fig. 4.3 was generated by a program developed in *FORTRAN - 77* for various values of n selected in the study. The results of the nonlinear *MISO* model in terms of E^2 and R^2 criteria application to Krishna and Narmada catchments are given in Table 5.10. The nonlinear *MISO* model with $n = 2$ was inapplicable in case of two and three sub-division scenarios in the Narmada catchment owing to the negative values in the *RFOs* obtained. So a comparison of the performance of nonlinear *MISO* model with two different values of n is given for the Krishna catchment only.

As can be seen from Table 5.10 that the performance of nonlinear *MISO* model (with $n = 1$ and 2) during calibration in the Krishna catchment improved with respect to both E^2 and R^2 values with an increase in the number of sub-divisions.

In the Narmada catchment the nonlinear *MISO* model performance improved with number of sub-divisions for the calibration data in terms of E^2 and R^2 statistics but for the data used for validation the performance has not similar consistency. The E^2 value is higher for two sub-division scenario than for the one sub-division case but did not show such improvement for the three sub-division scenario.

The Table 5.11 provides the results obtained through application of linear and nonlinear models for the individual events used for calibration and for validation in the Krishna catchment. The parameters used for assessing the performance of predicted runoff are the same as given in Table 5.7 and 5.8 in case of catchments without any sub-divisions. In case of the Krishna catchment the predicted peak matched relatively closely with the observed in events 2, 5, and 6. The error in volume prediction indicated by the VE values varied from -0.7% to 14.4% for all but one event (no. 3) used for calibration, indicating relatively satisfactory performance of these models. But during validation period the error in volume prediction is large and gross over prediction of the runoff volume can be observed except for event 7 for which the runoff volume is over predicted. For the Narmada catchment results for individual events are similarly presented in Table 5.12. It can be seen from Tables 5.11 and 5.12 that the time to peak runoff has perfectly matched for most of the events in all the sub-division scenarios studied with some exceptions (for example event 10 in Krishna catchment and events 2, 6, 8 in Narmada catchment). In case of the Narmada catchment (see Table 5.12) the values of the peak of daily discharges is under predicted by both the models in all the sub-division cases particularly for the validation events. Also the predicted volume of runoff is less than the observed for the validation events except for the event number 10.

Graphical Presentation:

The scatter plots are prepared by using all the data of the validation events for the Krishna and Narmada catchments for the different sub-division scenarios studied. These are illustrated in Figs. 5.10 and 5.11 respectively for the Krishna and the Narmada catchments. The Figs. 5.10 (a) and (b) show that the scatter is almost similar for the one and two sub-divisions scenario for the linear *MISO* and the nonlinear *MISO* models. The

R^2 values for validation in Table 5.9 and 5.10 for the two sub-divisions scenario are slightly less than for the one sub-division case. The observation of Fig. 5.11(a) for the linear *MISO* model in case of the Narmada catchment reveals that the scatter has progressively reduced with the number of sub-divisions and the corresponding R^2 values are improved (see Table 5.9) but the same is not true for the scatter for nonlinear *MISO* model ($n = 1$) shown in Fig. 5.11 (b).

The linear scale plots for one calibration and one validation event that contained the highest of the peak daily flows in the Krishna catchment are shown in Figs. 5.12 and 5.13 respectively. A close study of Fig. 5.12 for one and two sub-division scenarios, and Table 5.11 indicate that the peak of the event is better predicted for the two sub-divisions by all the models than for the one sub-division scenario. The plots for the validation event 9, given as illustration, in Fig. 5.13 also indicate similar model performance. In case of the Narmada catchment the plots for one validation event containing the peak flow is given as illustration in Figs. 5.14 (a) – (c). The performance in matching the peak has improved for the two sub-divisions scenario over the one sub-division scenario but it has not improved further for the three sub-divisions case. The *VE* statistic was also computed for all scenarios of the model applications in both the Krishna and the Narmada catchments. For Krishna catchment the absolute of *VE* values was less than 20% except for one runoff event both in calibration and validation. Likewise, the absolute of *VE* values was less than 20% for most of the runoff events of the Narmada catchment.

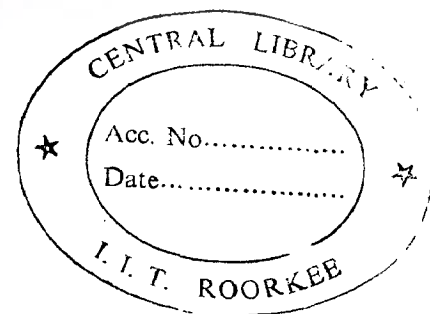


Table 5.9 Results of the Linear Model Application to Catchments With Sub-Divisions

Catchment	No. of Sub-Divisions	E^2 (%)		R^2	
		Cal.*	Val.*	Cal.	Val.
Krishna	One	86.77	85.92	0.875	0.877
	Two	85.26	87.00	0.871	0.869
Narmada	One	74.09	75.49	0.747	0.791
	Two	74.27	80.11	0.747	0.794
	Three	73.53	76.17	0.740	0.806

* Cal. -Calibration; Val. -Validation

Table 5.10 Results of the Nonlinear Model Application to Catchments With Sub-Divisions

Catchment	No. of Sub-Divisions	Nonlinear Model ($n = 1$)				Nonlinear Model ($n = 2$)			
		E^2 (%)		R^2		E^2 (%)		R^2	
		Cal.*	Val.*	Cal.	Val.	Cal.	Val.	Cal.	Val.
Krishna	One	86.77	85.91	0.876	0.877	86.55	84.78	0.874	0.872
	Two	87.17	84.98	0.883	0.872	87.22	77.35	0.883	0.867
Narmada	One	76.44	76.53	0.779	0.807	81.09	74.04	0.828	0.774
	Two	77.04	80.03	0.782	0.791	← N.A. →			
	Three	77.68	79.21	0.788	0.803	← N.A. →			

* Cal. -Calibration; Val. -Validation; N.A. - Not Applicable

Table 5.11 Results of Linear and Nonlinear Model Application to The Krishna Catchment

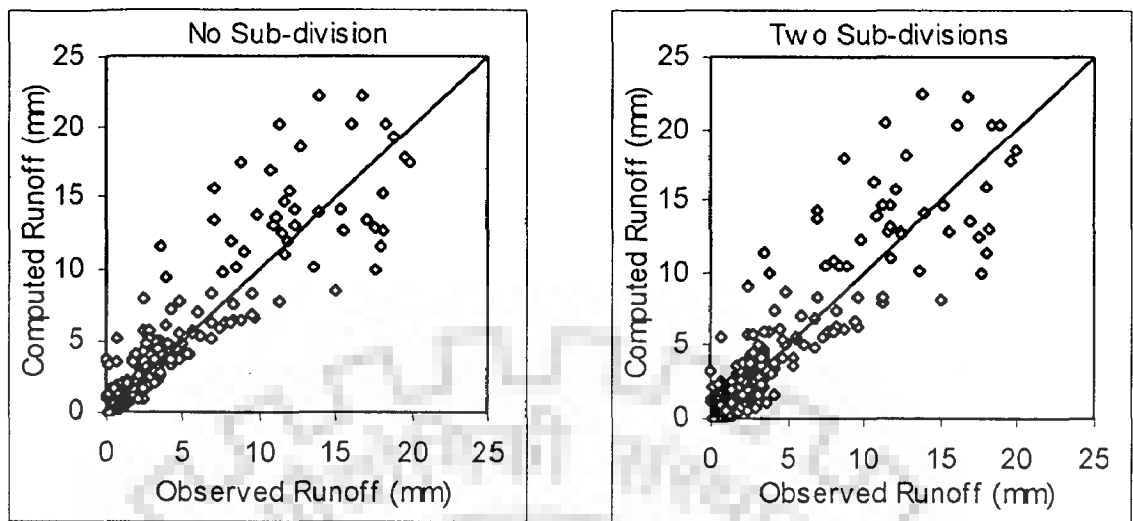
Runoff Event No.	Runoff Volume (mm)						Peak of Daily Discharges (mm)						Time to Peak (Day)						
	Linear		n = 1		n = 2		Linear		n = 1		n = 2		Linear		n = 1		n = 2		
	SD*-1	SD*-2	SD-1	SD-2	SD-1	SD-2	SD-1	SD-2	SD-1	SD-2	SD-1	SD-2	SD-1	SD-2	SD-1	SD-2	SD-1	SD-2	
Calibration Events																			
1	640.4	569.8	548.4	568.9	585.2	573.4	596.2	20.1	23.8	21.4	23.9	23.5	23.9	23.9	24.0	16	16	16	16
2	160.0	175.1	151.8	175.1	165.5	176.5	167.0	17.0	17.5	13.9	17.6	17.0	17.6	17.6	17.1	17	17	17	17
3	111.2	152.3	126.4	152.3	136.9	154.4	141.7	18.2	17.2	13.1	17.3	17.2	17.4	17.5	17.5	11	11	11	11
4	394.3	341.9	327.8	341.9	348.7	343.9	355.0	19.3	18.9	16.5	18.9	18.7	19.2	18.9	33	31	31	31	31
5	409.4	387.4	372.8	387.4	395.7	389.7	404.7	16.3	16.4	14.0	16.4	16.0	16.5	15.8	24	24	24	24	24
6	340.3	329.7	318.9	329.8	337.6	330.1	342.8	15.8	15.6	13.6	15.7	15.7	15.7	15.6	40	40	40	40	40
Validation Events																			
7	278.6	223.9	211.6	224.0	225.6	223.9	228.1	17.9	14.1	12.3	14.1	14.7	14.2	14.6	30	28	28	28	28
8	124.9	178.5	170.0	178.5	179.1	180.2	183.0	12.0	16.9	14.1	17.0	16.3	17.0	16.4	10	10	10	10	10
9	387.2	446.9	416.6	446.9	447.5	454.4	459.9	19.9	20.1	17.6	20.1	20.3	20.0	19.8	44	43	43	44	43
10	122.7	144.7	130.0	144.8	136.9	144.5	139.6	11.2	8.3	7.5	8.2	8.4	8.4	8.6	18	17	17	16	17

* - SD-1: One Sub-Division; SD-2: Two Sub-Divisions; ** Obs. - Observed

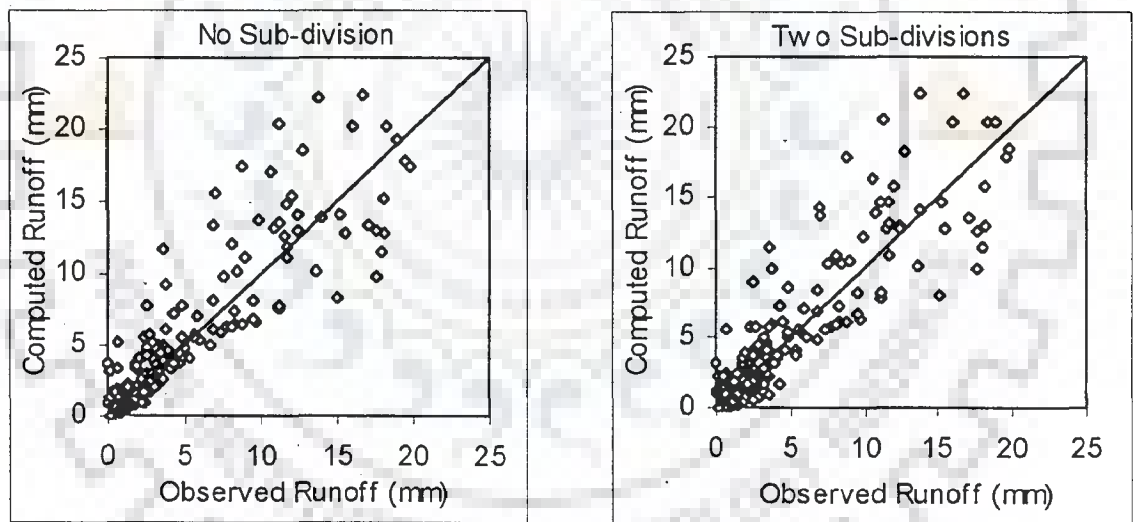
Table 5.12 Results of Linear and Nonlinear Model Application to Narmada Catchment

Runoff Event No.	Runoff Volume (mm)						Peak of Daily Discharges (mm)						Time to Peak (Day)							
	Linear MISO			Nonlinear MISO			Linear MISO			Nonlinear MISO			Linear MISO			Nonlinear MISO				
	SD*-1		SD*-2	SD*-3	SD-1		SD-2	SD-3	SD-1		SD-2	SD-3	SD-1		SD-2	SD-3	SD-1		SD-2	SD-3
	Obs.**		Obs.**		Obs.**		Obs.**		Obs.**		Obs.**		Obs.**		Obs.**		Obs.**		Obs.**	
Calibration Events																				
1	103.1	117.4	110.3	112.2	110.7	105.6	105.0	9.2	10.8	9.7	10.5	10.6	9.7	9.8	11	11	11	11	11	11
2	224.6	247.8	234.0	234.7	234.1	222.0	223.5	16.6	11.7	11.5	11.8	10.9	10.5	11.0	10	9	9	9	10	10
3	214.2	184.2	184.6	176.9	174.4	175.8	176.3	24.1	17.8	17.1	16.7	17.3	17.1	17.6	12	12	12	12	12	12
4	370.0	319.9	315.3	305.3	331.9	329.9	330.7	38.3	31.6	32.1	30.4	35.2	35.0	34.7	13	13	13	12	12	12
5	351.9	351.6	348.2	339.7	336.6	335.2	336.2	23.9	20.7	19.5	19.1	20.7	19.5	19.1	25	25	25	25	25	25
6	261.6	222.7	257.4	256.5	205.6	240.1	239.6	10.9	9.4	10.0	10.4	9.2	9.8	10.1	19	20	20	20	20	20
Validation Events																				
7	131.3	74.9	103.5	97.4	73.9	105.8	107.7	25.5	15.4	19.1	18.1	14.9	19.8	20.4	9	9	9	9	10	9
8	311.2	240.6	286.3	231.5	237.8	297.1	246.0	37.7	25.5	28.8	23.7	26.2	33.7	30.1	16	17	16	17	17	16
9	96.8	91.0	70.5	81.6	85.3	66.8	67.2	20.7	10.9	8.6	9.9	10.8	7.8	8.0	11	11	11	11	11	11
10	75.5	95.1	102.4	94.9	89.8	97.6	97.3	24.5	14.4	15.7	14.4	14.1	15.6	16.1	11	11	10	11	11	11

* - SD-1: One Sub-Division; SD-2: Two Sub-Divisions; SD-3: Three Sub-Divisions; ** Obs. - Observed

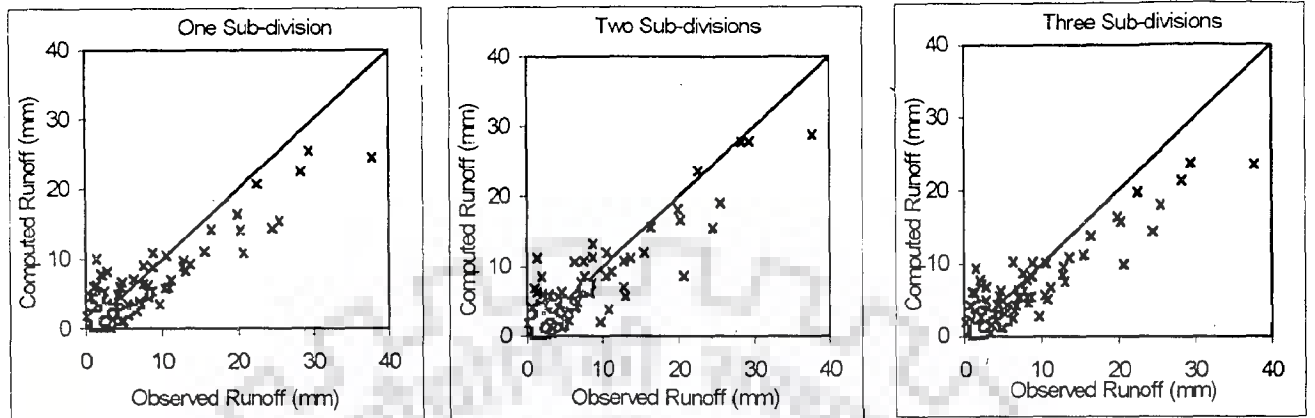


a) Linear *MISO* Model

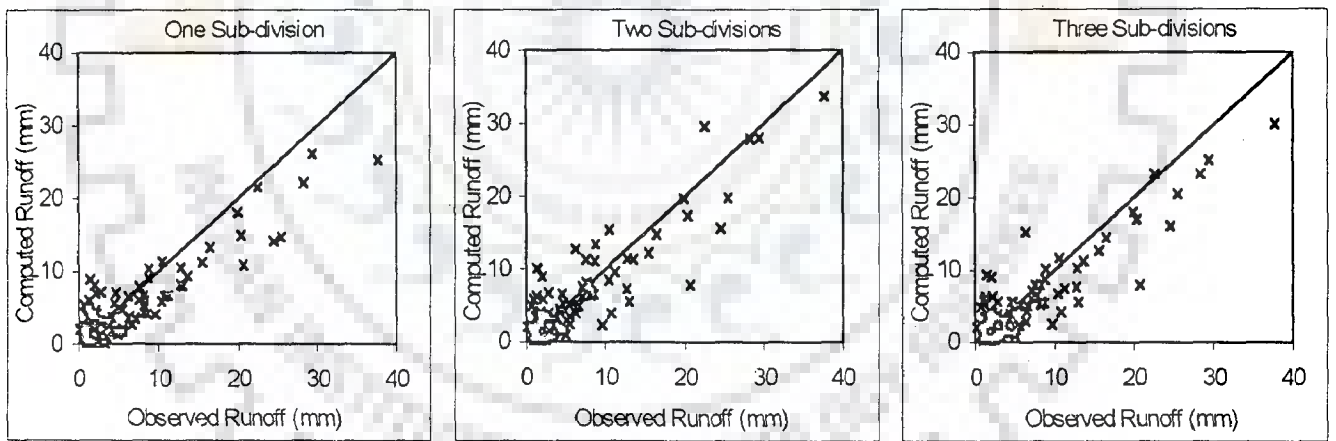


b) Nonlinear *MISO* Model ($n = 1$)

Fig. 5.10 Scatter Plots For Validation in The Krishna Catchment

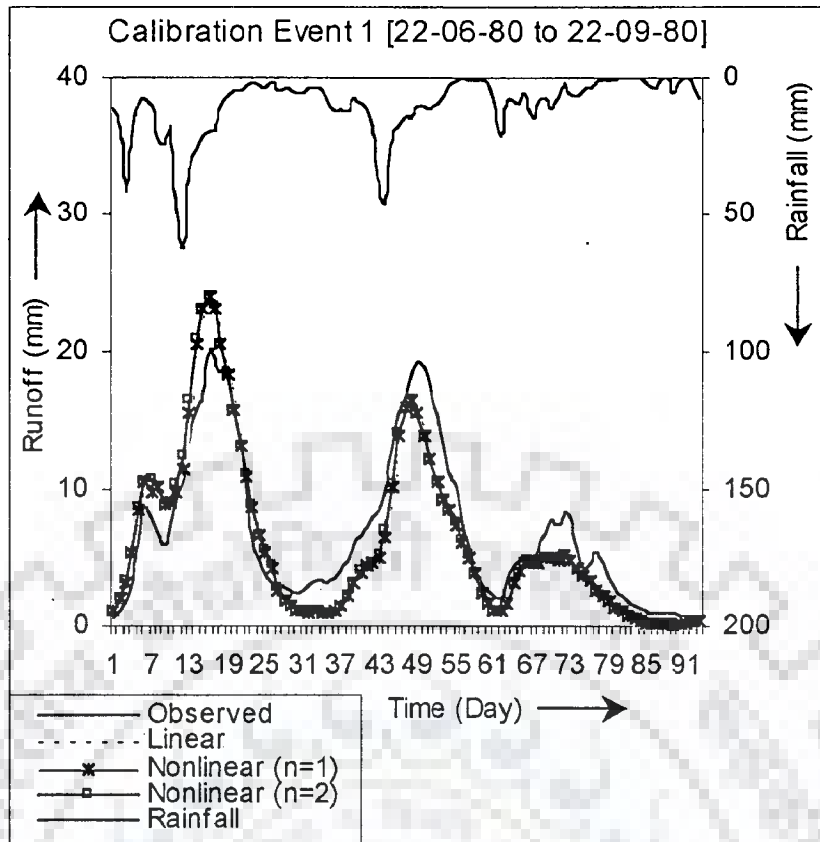


a) Linear *MISO* Model

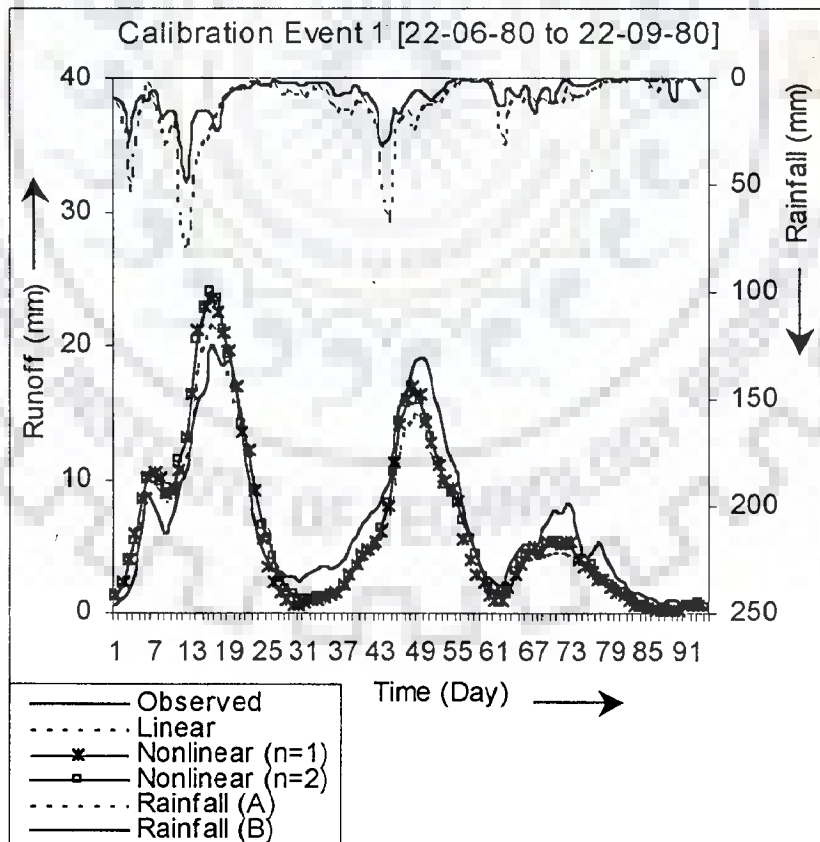


b) Nonlinear *MISO* Model ($n = 1$)

Fig. 5.11 Scatter Plots For Validation in The Narmada Catchment

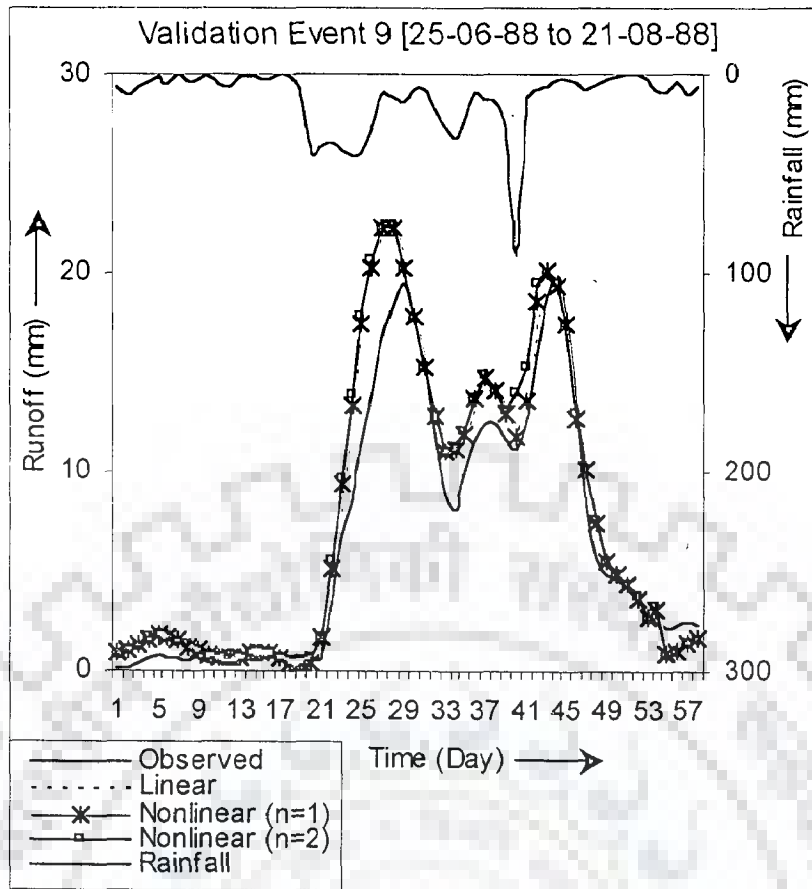


i) One Sub-Division Scenario

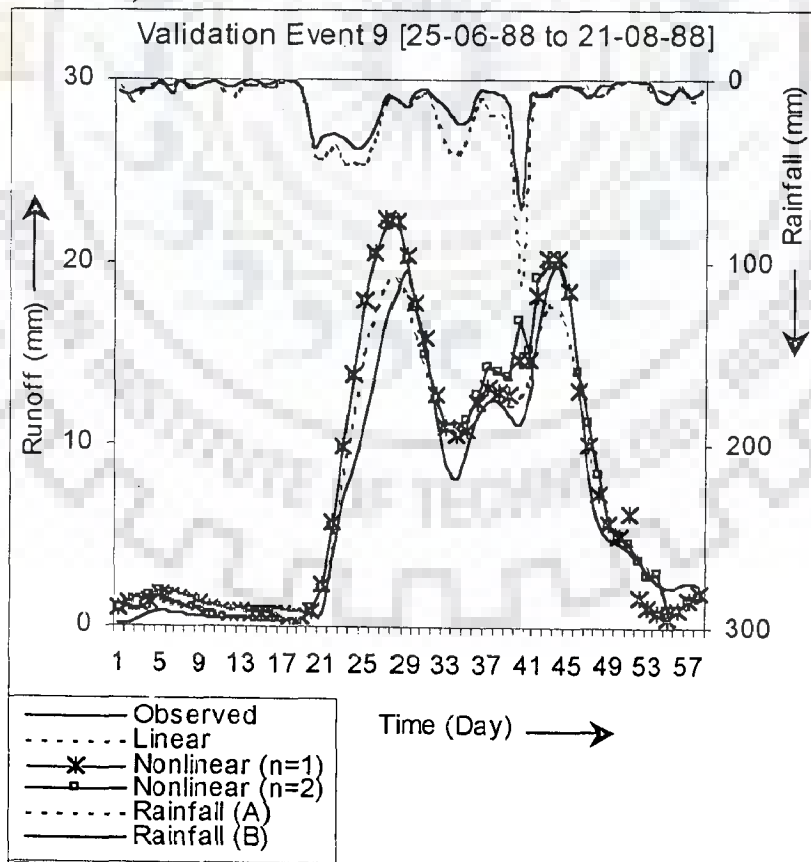


ii) Two Sub-Division Scenario

Fig. 5.12 Linear Scale Plots For Calibration Event in Krishna Catchment (Linear/Nonlinear Model)

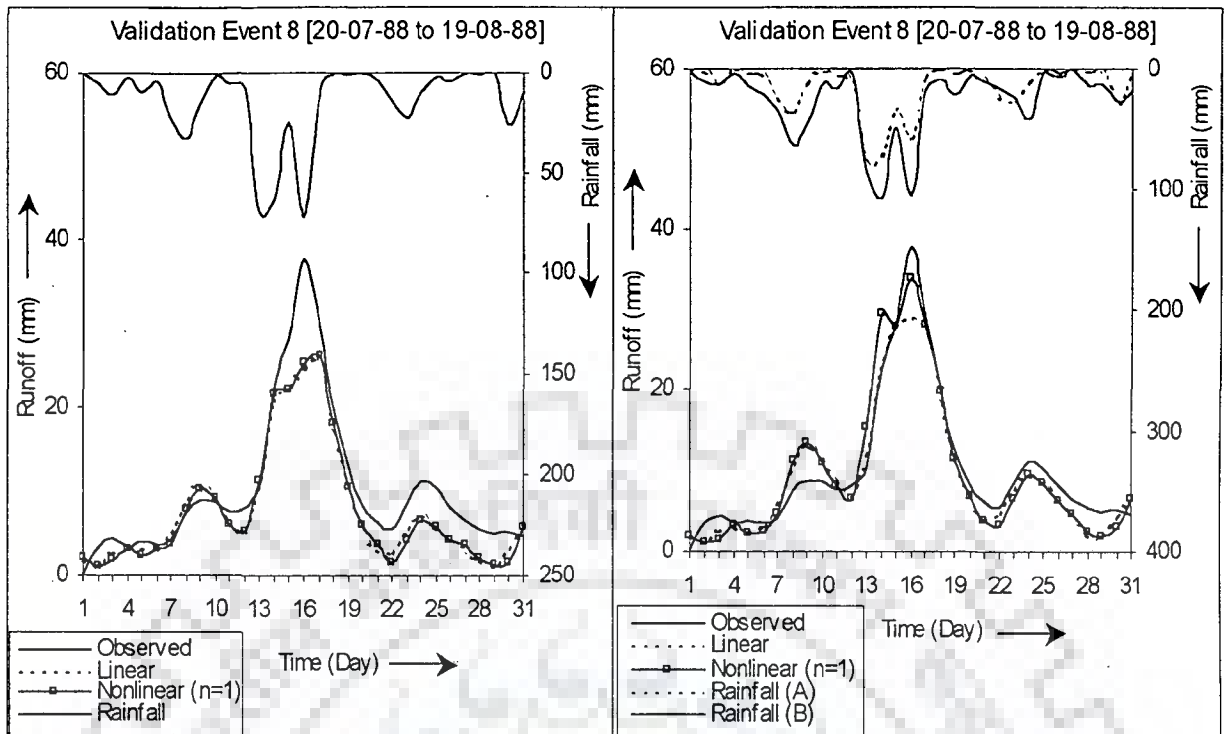


i) No Sub-Division Scenario



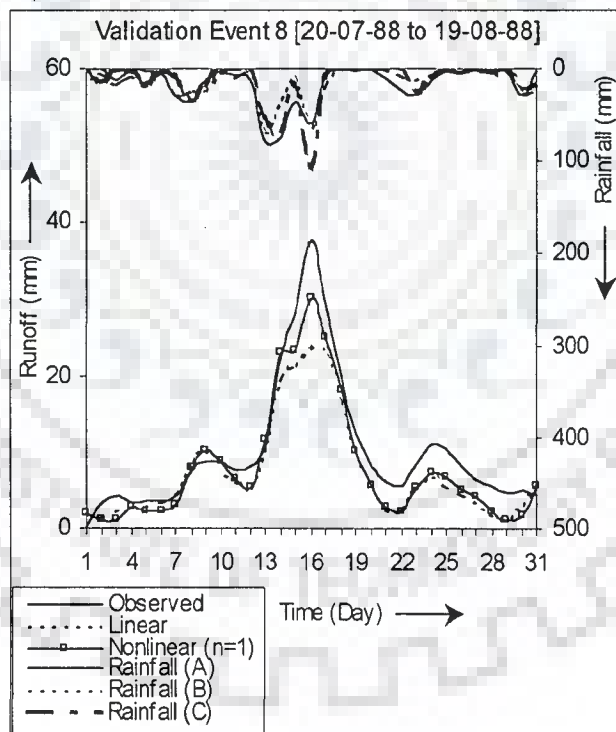
ii) Two Sub-Division Scenario

Fig. 5.13 Linear Scale Plots For Validation Event in Krishna Catchment (Linear/Nonlinear Model)



a) One Sub-Division Scenario

b) Two Sub-Division Scenario



c) Three Sub-Division Scenario

Fig. 5.14 Linear Scale Plots For Validation Event in Narmada Catchment (Linear/Nonlinear Model)

5.5 PARAMETERIZATION OF THE RESPONSE FUNCTIONS

The response functions obtained by using the *SLM* in case of all the catchments studied are expressed in the parametric form. As the response functions determined in the present study are having discrete form, the discrete form of the gamma function given by O'Connor (1976) is used. The values of the parameters N and K in the Eq. (4.12) were determined for each of the response function such that the parameterized shape matches as closely as possible with the derived response function. The peak and time to peak are the two important features to be matched. The values of the shape parameter (N) and the scale parameter (K) for the best possible match between the reproduced and the originally derived response function in each of the catchment are given in Table 5.13.

The shapes of the derived response functions along with the fitted discrete gamma function, N and K values for which are given in Table 5.13, are plotted in Figs. 5.15 (a) – (c). It can be observed from these figures that a close match between the derived and fitted shapes is attained in case of Pampanga and Krishna catchments, whereas for other catchments the match is relatively less accurate.

As the parameters N and K are known to have relationship with the catchment characteristics, the relation of these parameters with the area of the catchment, which is the only characteristic available for most of the catchments studied, is investigated. It is noticed from Table 5.13 that the N values seem to vary directly with the size of the catchment. However, the K values are not related explicitly with the catchment area. Quantitative relationships for N and K are however not attempted because limited data on catchment characteristics was available for the catchment studied.

Table 5.13 Parameter Values For The Discrete Gamma Function

Catchment	Area (Km ²)	Values of The Parameters	
		N	K
Krishna	26,200	7.25	0.75
Narmada	17,157	4.50	0.80
Bird Creek	2,344	3.00	0.70
Brosna	1,207	2.45	2.00
Garrapatas	1,490	2.40	2.00
Kizu	1,445	5.00	0.27
Pampanga	5,273	4.55	1.40

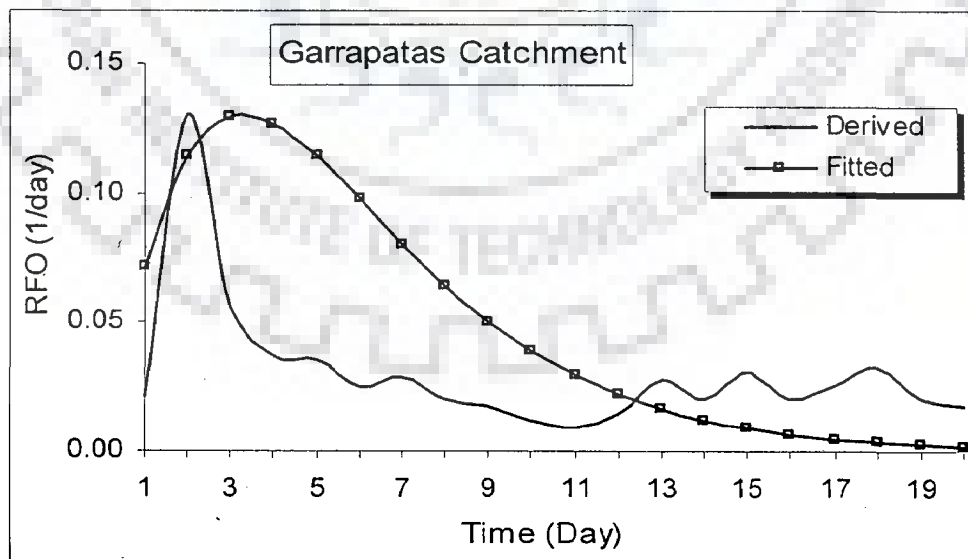
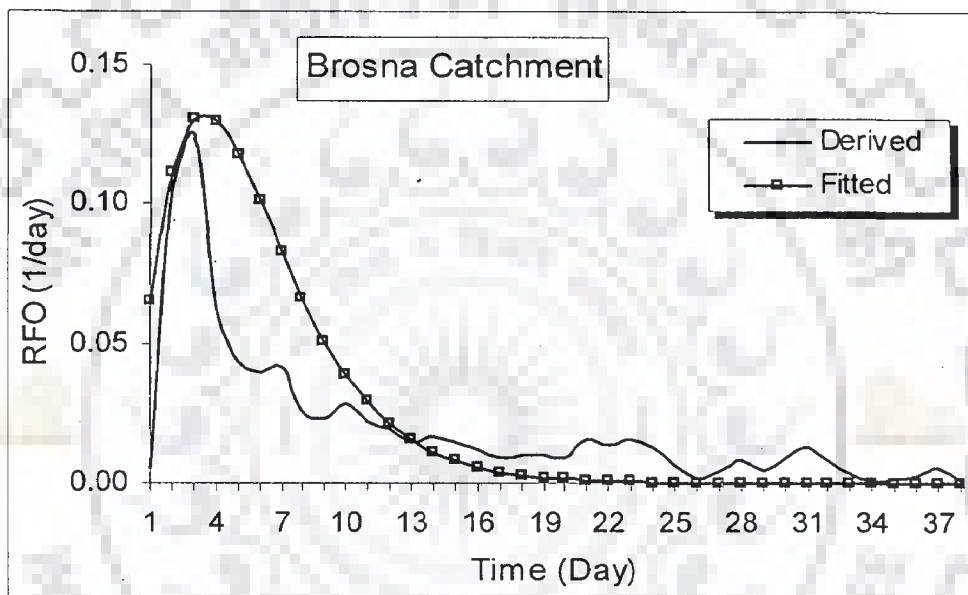
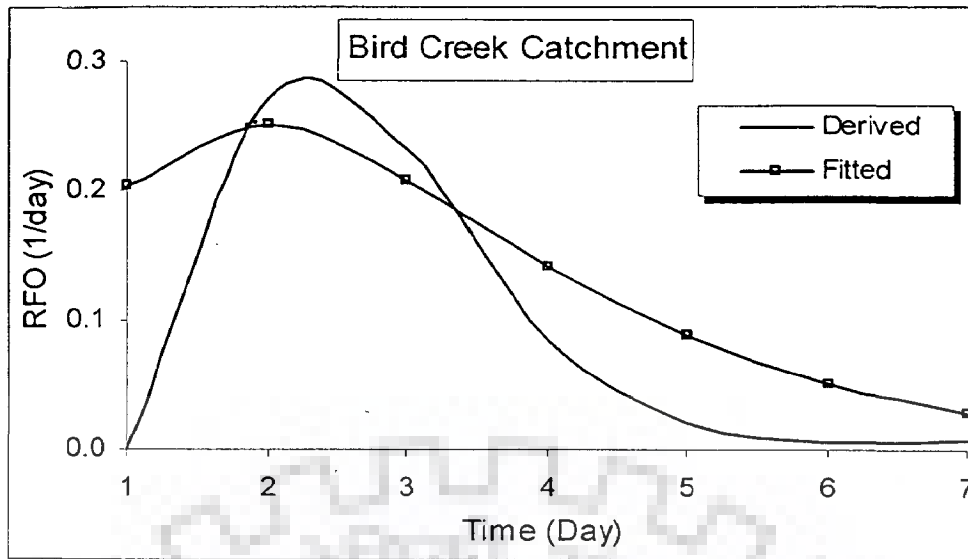


Fig. 5.15(a) Match between the Derived and the Fitted Response Function for Bird Creek, Brosna, and Garrapatas Catchments

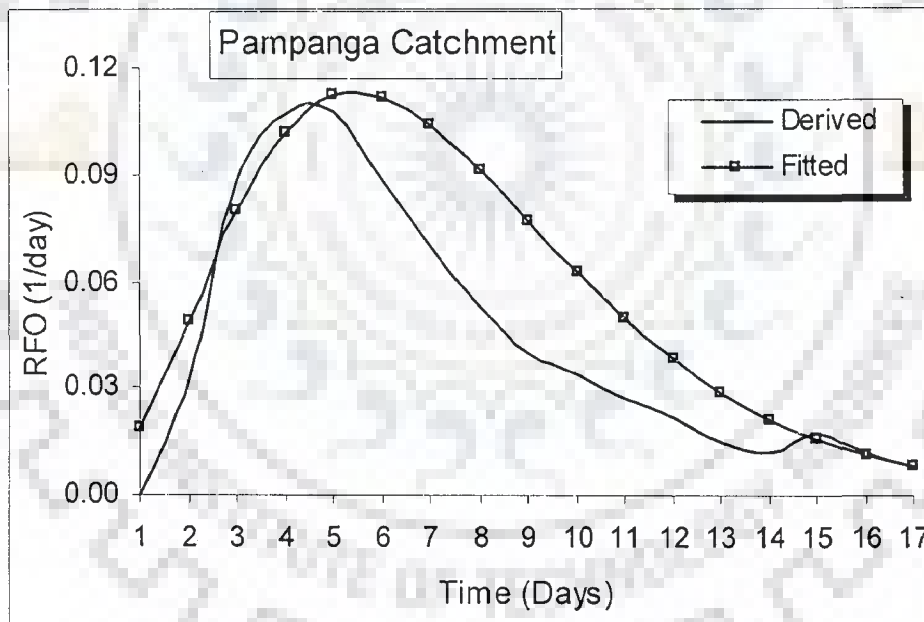
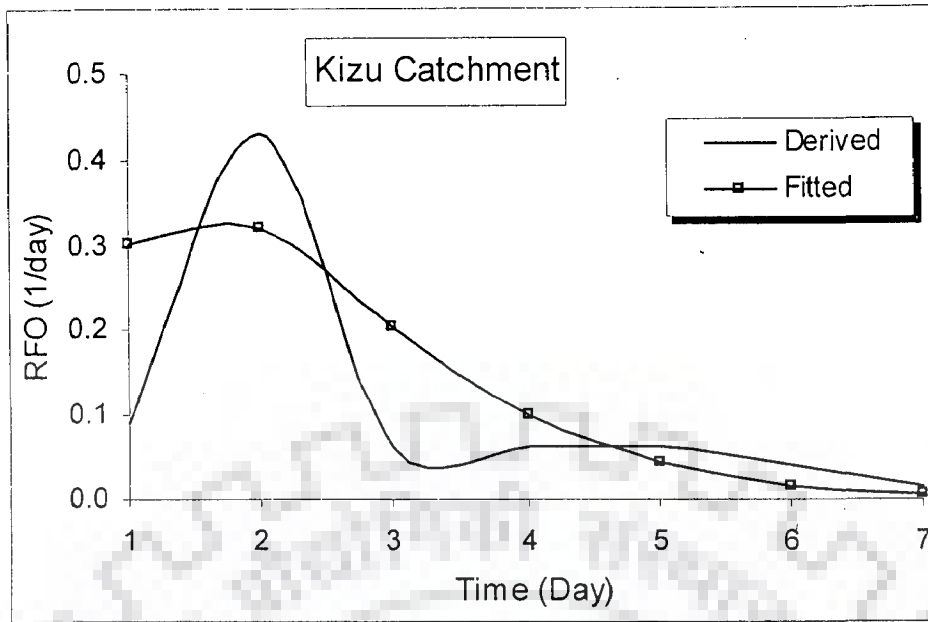


Fig. 5.15(b) Match between the Derived and the Fitted Response Function for Kizu and Pampanga Catchments

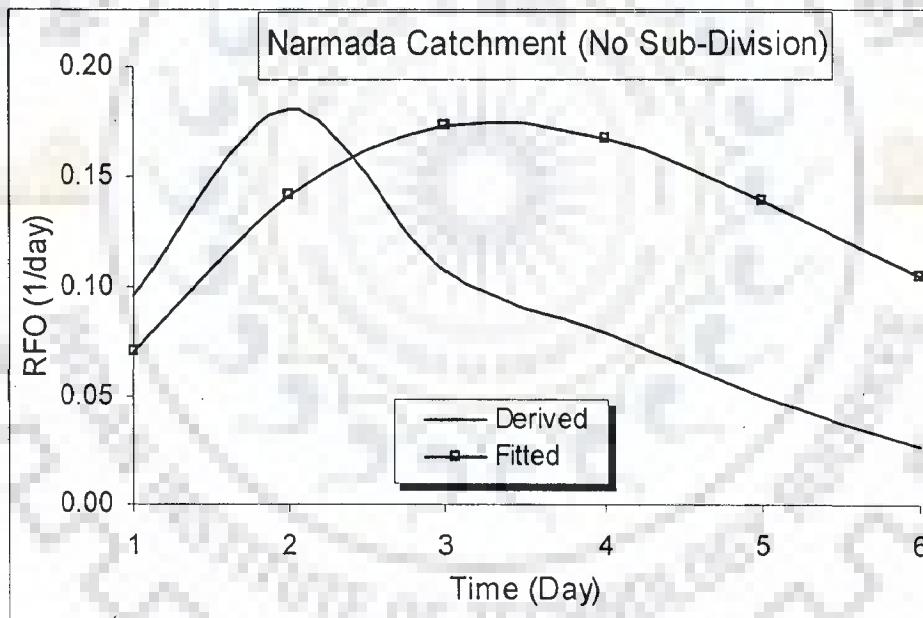
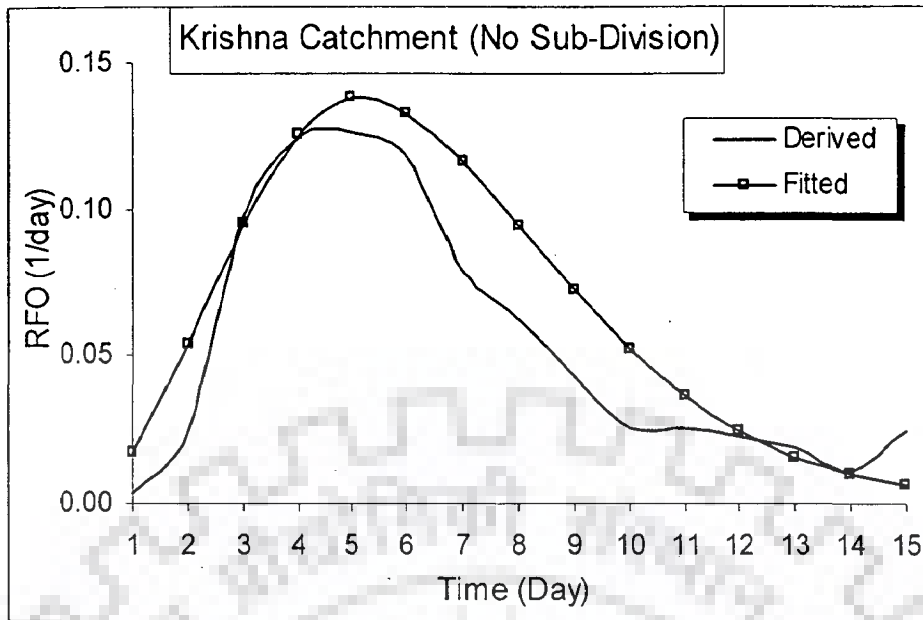


Fig. 5.15(c) Match between the Derived and the Fitted Response Function for Krishna and Narmada Catchments

5.6 CONCLUDING REMARKS

The response functions obtained are physically realistic in all the catchments studied. The non-linearity analysis reveals that all the catchments are hydrologically nonlinear. The results for the linear/nonlinear models applied to the catchments without sub-divisions indicate that the model performance (E^2 values) are better for three catchments in calibration (Bird Creek, Kizu, and Pampang) but during validation period these models did not perform as satisfactorily with an exception for the Brosna catchment. The peak of the daily flows is either under predicted or over predicted by these models, but the time to peak has matched in most of the cases. The absolute error in runoff volume prediction in most of the events is less than 20%.

For the catchments involving sub-divisions the performance of the model applied has been mostly consistent with respect to the increase in the number of sub-divisions. The results of the exercise on parameterization of the derived response functions indicate that the match is reasonable mostly, and very good in three of the catchments studied.

The results presented in this chapter have indicated the presence of significant hydrologic non-linearity in the rainfall-runoff data used in the study. The form of the nonlinear model used is found not to fully describe the non-linearity present in the data. The *ANN* models are considered to describe the nonlinear process in a better way. Therefore, the linear and nonlinear models used above are only considered as an auxiliary model (see Fig. 4.5).

The output from such an auxiliary model is given as one of the inputs to the *ANN* model as next step in modeling approach. Estimates of the runoff by the auxiliary model are considered to be representative of the soil moisture state of the catchment. The runoff observed in the previous time periods was used for this purpose in the earlier studies involving the application of the *ANN* model. The use of the runoff observed in the previous time period is considered to be an updating process in the flow simulation and such models that use the past observations of runoff values as input to the *ANN* are considered to be modeling the change in flow rather than their absolute values.

The performance of the *ANN* model, which is eventually used as the substantive model, with these and other input combinations applied to all the catchments is presented in the next chapter.

ANN MODEL APPLICATION – RESULTS AND DISCUSSIONS

6.1 INTRODUCTION

As stated in the earlier chapters a system based linear/nonlinear model is used as an auxiliary model in the proposed approach and is coupled with a three layer feedforward *ANN*, that acts as the substantive model. Thus proposed linkage is depicted in Fig. 4.5 (chapter 4). The application of the Simple Linear Model (*SLM*) and the Nonlinear Model in case of the catchments not involving any sub-divisions and the Multiple Input Single Output (*MISO*) counterparts of these two models for the two large sized catchments involving sub-divisions are already discussed in chapter 5. The employment of these models is followed by the application of a three layer feedforward backpropagation *ANN* such that the output of any of these auxiliary models is supplied as one of the inputs to the *ANN*. By providing such an input to the *ANN* the current soil moisture state of the catchment is utilized into the *ANN* based rainfall-runoff modeling. As already mentioned, the updating flow simulation carried out in the earlier studies involved use of the Q_{t-1} (*i.e.* the observed runoff in the previous time period) as one of the input to the *ANN*, which also describes the soil moisture state of the catchment.

This chapter presents the results obtained for non-updating flow simulation using the *ANN* model applied for rainfall-runoff modeling over catchments with varying sizes and other characteristics. The *ANN* is being supplied with various alternative input combinations for predicting runoff at the outlet of the catchment as explained in detail in chapter 4. The discussions on the results obtained in the individual catchments are provided in this chapter and finally the conclusions drawn from the analysis of results are stated. The results of the *ANN* model application and discussions on these results are provided separately for, i) the catchments involving no sub-divisions; and ii) the catchments involving sub-divisions.

6.2 APPLICATION OF THE ANN MODEL

As per the flowchart illustrated in Fig. 4.1 (chapter 4) after the application of the linear/nonlinear models, the next step in the proposed approach is the application of a

three layer feedforward backpropagation *ANN* for realistic estimation of runoff. This *ANN* is provided with the output of the linear/nonlinear models, which in other words is an estimate of the runoff for the current time period and it is assumed to represent the soil moisture state of the catchment. This is a new type of input to the *ANN* proposed in this study as an alternative to the observed discharges or water level in the previous time period being given as one of the input to the *ANN* by the earlier researchers. Almost all the *ANN* based rainfall-runoff modeling studies in general and those involving the application of the three layer feedforward *ANN* in particular invariably involved the use of Q_{t-1} as one of the input to the *ANN*. The limitations of using such input are outlined earlier.

The output of the linear model given by Eq. (4.7) is denoted by *RIL* and that of the nonlinear model as per Eq. (4.8) is denoted by *RIN*. The overall procedure of the *ANN* model application to various catchments is similar irrespective of their sizes. A three layer feedforward *ANN* is used. It is trained with the backpropagation algorithm using the gradient descent method along with adaptive learning rate (ε) and momentum factor (α). The addition of these two parameters improves the speed of convergence of the algorithm and also ensures that the algorithm does not get trapped in the local minima but attains the global minima (see Fig. 2.3).

The reasons for using a feedforward *ANN* are already stated in the previous chapters. The logistic sigmoid [Eq. (2.13)] is used as the transfer function for neurons in the hidden and the output layers. The input data to the *ANN* is normalized in the range [0.1, 0.9] by using Eq. (4.6).

The training of the *ANN* is carried out using the *TRAINGD* function in *MATLAB* routines. It works on the gradient descent method and uses an adaptive learning rate and the momentum factor. The *ANN* implementation is carried out using *MATLAB* 5.1 version. The various input combinations to the *ANN* as described in chapter 4 consisted of the following (i) Only rainfall (*P*); (ii) *RIL*; (iii) *RIN*; (iv) *RIL+P*; (v) *RIN+P*; and (vi) $Q_{t-1}+P$.

The *ANN* with these different inputs is applied to each of the catchments. Every time in training the *ANN* it was ensured that the *ANN* does not get overtrained by using the data for training and testing. However, due availability of limited number of high flow events in the daily runoff data for the catchments, validation of the *ANN* models with a third independent dataset could not be performed. The *mse* criterion is used in training the network. Initially minimum number of nodes in the hidden layer (*i.e.* one) was selected

and this number was increased gradually till this trial and error process of training lead to an optimal network configuration having the best possible performance.

In the following sections the results of the best performing *ANNs* with various input combinations as applied to the seven catchments studied are presented in tabular and graphical form and discussions on the results obtained is provided. First, the discussion on the performance of *ANN* model in each of the catchment in terms of the statistical indicators is provided. This is followed by the graphical presentations separately for i) The catchments without sub-divisions, and ii) The Krishna and the Narmada catchments, which involved sub-divisions.

6.2.1 The Bird Creek Catchment

The normalized data files for each of the input combinations supplied to the *ANN* have been prepared by adopting the procedure already explained. The memory of the Bird Creek catchment is 7 days (see Fig.5.2 (a)), so when only rainfall is given as input to the *ANN*, the input layer consisted of 7 neurons corresponding to $P_t, P_{t-1}, P_{t-2}, \dots, P_{t-6}$. As described earlier, the training procedure is started with minimum (one) number of hidden nodes and this number is increased gradually. The three layer feedforward *ANN* with this input was found to have the best possible performance *i.e.* minimum *mse* in training and testing and correspondingly maximum value of E^2 for four number of nodes in the hidden layer. Further addition of neurons in the hidden layer did not result in any improvement in the performance of the *ANN* model. When *RIL* or *RIN* *i.e.* the output of a linear or a nonlinear model respectively, was given as input to the *ANN*, the input layer consisted of only one neuron. Similarly, when $RIL + P$ or $RIN + P$ were the inputs to the *ANN*, the input layer had 8 neurons *i.e.* 7 for the rainfall values and one additional for the *RIL* or *RIN* values.

The best performing *ANN* configurations for different input combinations applied to the Bird Creek catchment and their results are presented in Table 6.1. These results indicate that the *ANN* with $RIL+P$ as input has the best performance amongst all in terms of E^2 and R^2 criteria both in training and testing. As expected, the *ANN* with only P as input performs poorly as compared with the other *ANN* models. Not much improvement is seen in the performance of the *ANN* when a nonlinear model instead of the linear model is coupled with the *ANN*. The *RIN* ($n = 2$) input resulted in even lower values of E^2 in training and testing compared to the case when *RIN* ($n = 1$) was used as the input. Similar

comments can be made by the comparison of performance of *ANN* with *RIL + P*, *RIN + P* ($n = 1, 2$), *i.e.* the performance for the *ANN* with *RIL + P* is the best in terms of the E^2 values.

The reason for results of *ANN* model with *RIN* as input being not better than the *ANN* with *RIL* as input is that the *ANN* being a nonlinear model in itself accounts for the non-linearity involved in the rainfall-runoff process. One important thing can be noted in the Bird Creek catchment that the *ANN* with $Q_{t-1} + P$ as input has lower performance than that with *RIL + P* as input. The results obtained through the *ANN* application are also presented in graphical form and discussed later in this chapter.

Table 6.1 Results of ANN Applications for The Bird Creek Catchment

Input Combination for ANN	ANN Structure (i-H-o)	E^2 (%)		R^2	
		Training	Testing	Training	Testing
Only <i>P</i>	7-4-1	78.63	65.35	0.786	0.728
<i>RIL</i>	1-3-1	89.25	74.46	0.893	0.748
<i>RIN</i> ($n = 1$)	1-3-1	87.17	77.53	0.872	0.781
<i>RIN</i> ($n = 2$)	1-3-1	87.47	33.35	0.876	0.670
<i>RIL + P</i>	8-3-1	92.70	80.22	0.927	0.809
<i>RIN + P</i> ($n = 1$)	8-3-1	90.05	73.65	0.902	0.748
<i>RIN + P</i> ($n = 2$)	8-3-1	84.62	51.53	0.846	0.689
$Q_{(t-1)} + P$	8-3-1	87.11	72.69	0.871	0.748

* I - Number of neurons in input layer, H - Number of neurons in hidden layer, O - Number of neurons in output layer

6.2.2 The Brosna Catchment

In this catchment nonlinear model with $n = 2$ was inapplicable. So only the discussion about the performance of *ANN* model with the other input combinations is presented. The Brosna catchment has a large memory value *i.e.* 38 days (see Fig. 5.2 (b)),

the highest amongst all the catchments studied. Such observation on memory of the Brosna catchment is also made by O'Connor and Ahsan (1991). Difficulty was experienced when only P and RIL or RIN values with P was given as input in determination of the optimal performing network configuration because initially all the 38 values of P were given as input to the ANN . Due to this the ANN structure became complicated and the learning rate slowed down greatly posing difficulties in training. To overcome this problem an alternative procedure of trial and error was chosen in which, the first 10 P values in backward time steps were given to ANN initially and the best performing network was derived. As next step, one more P value from the rest of the backward time step was added to the input and the procedure of training was repeated. This step was continued till such addition of P values resulted in further improvement in the ANN s performance. This procedure for only P as input has resulted in an ANN structure 25-5-1 as the best performing network. For $RIL + P$ as input, a similar procedure was repeated and finally it was found that RIL along with 20 P values *i.e.* the ANN configuration 21-7-1 performed the best. So, for $RIN + P$ and $Q_{t-1} + P$ the same 20 values of P were given as input to the ANN along with RIN and Q_{t-1} values.

Table 6.2 presents the results of the best performing ANN s obtained for the Brosna catchment. The performance of ANN with RIL and RIN as input is very much similar in terms of E^2 and R^2 criteria both in training and testing. The E^2 values for ANN with $RIL + P$ or $RIN + P$ are less as compared to that in the Bird Creek catchment. Nevertheless, the E^2 values for ANN with $RIL + P$ as input are improved over RIL as input. The relatively less satisfactory performance of the ANN models in the Brosna catchment may be due to the large memory length, which made the ANN structure complex and posed problems in identification of the best performing ANN . This case owing to its large memory may be looked upon as one of the limitation of the feedforward ANN used in the proposed approach in which the rainfall values for the duration equal to the memory of the catchment are given as input to the ANN for predicting the runoff. Even though the Brosna catchment is 1,207 km² in areal extent, it has such large memory length because it is located in humid climatic conditions. The runoff events (see Table 3.4) identified also show that these events are having very long durations, ≥ 40 days. This is due to the prevalent rainfall patterns and the humid climatic conditions in which the base flow contribution continues for a very long time (O'Connor and Ahsan, 1991).

6.2.3 The Garrapatas Catchment

The results of the best performing *ANNs* with different input combinations applied to the Garrapatas catchment are presented in Table 6.3. The memory of this catchment is 20 days so, when only P was given as input, the input layer of the three layer feedforward *ANN* consisted of 20 neurons as can be seen from the structures of the *ANNs* presented in Table 6.3. It can be noted from this table that all *ANN* models including the one with $Q_{t-1}+P$ as input applied to the Garrapatas catchment performed less satisfactorily in testing as well as in training in terms of the E^2 and R^2 criteria.

6.2.4 The Kizu Catchment

As the memory for this catchment is 7 days when only P was the input to *ANN* the input layer had 7 neurons and the *ANN* with configuration 7-4-1 performed the best among all tried. The best performing *ANN* configurations for the different input combination applied to the Kizu catchment and the corresponding results obtained are presented in Table 6.4. A significant improvement when the *ANN* was supplied $RIL + P$ as input over the *ANN* with RIL as input in terms of E^2 and R^2 values can be observed. The *ANN* with the input $RIN + P$ ($n = 1$) performed better than $RIL + P$ as input during testing. This result indicates that in the Kizu catchment the RIN values are better representative of the soil moisture state compared to the RIL values. When RIL and RIN are given as input to the *ANN* the E^2 and R^2 values are improved over those obtained for the *ANN* with only P as input, both during testing and training.

6.2.5 The Pampanga Catchment

The *ANN* with various input combinations was also applied in the Pampanga catchment. The nonlinear model with $n = 2$ was not applicable in this catchment due to the reasons already stated. The best performing *ANN* configurations and the results obtained for these are given in Table 6.5. The E^2 values during testing for *ANN* with $RIL+P$ and $RIN + P$ as input are very much improved over those for *ANN* with RIL and RIN alone as input respectively. In training however the increase in the E^2 values for the same is relatively less. The performance of *ANN* with RIL and RIN as input is better than that with only P as input in terms of E^2 and R^2 criteria both in training and testing.

Table 6.2 Results of ANN Applications for The Brosna Catchment

Input Combination for ANN	ANN Structure (I-H-O)	E^2 (%)		R^2	
		Training	Testing	Training	Testing
Only P	25-5-1	76.91	53.14	0.767	0.806
RIL	1-2-1	65.22	79.03	0.652	0.885
RIN ($n=1$)	1-2-1	65.06	79.10	0.651	0.882
RIN ($n=2$)	← N.A. →				
$RIL + P$	21-7-1	74.06	79.06	0.741	0.880
$RIN + P$ ($n=1$)	21-7-1	79.09	74.03	0.791	0.866
$RIN + P$ ($n=2$)	← N.A. →				
$Q_{(t-1)} + P$	21-7-1	93.75	91.03	0.938	0.917

*I-Number of neurons in input layer, H-Number of neurons in hidden layer, O-Number of neurons in output layer, N.A.-Not Applicable

Table 6.3 Results of ANN Applications for The Garrapatas Catchment

Input Combination for ANN	ANN Structure (I-H-O)	E^2 (%)		R^2	
		Training	Testing	Training	Testing
Only P	20-4-1	63.56	65.58	0.636	0.660
RIL	1-2-1	60.32	67.43	0.603	0.707
RIN ($n=1$)	1-3-1	56.93	59.10	0.569	0.691
RIN ($n=2$)	1-3-1	53.07	56.05	0.531	0.665
$RIL + P$	21-7-1	57.26	73.00	0.573	0.681
$RIN + P$ ($n=1$)	21-7-1	62.46	73.16	0.625	0.675
$RIN + P$ ($n=2$)	21-4-1	62.46	72.25	0.625	0.663
$Q_{(t-1)} + P$	21-3-1	77.03	82.32	0.770	0.784

* I - Number of neurons in input layer, H - Number of neurons in hidden layer, O - Number of neurons in output layer

Table 6.4 Results of ANN Applications for The Kizu Catchment

Input Combination for ANN	ANN Structure (I-H-O)	E^2 (%)		R^2	
		Training	Testing	Training	Testing
Only P	7-4-1	83.92	67.45	0.839	0.682
RIL	1-3-1	88.25	72.72	0.882	0.764
RIN ($n=1$)	1-3-1	87.31	81.36	0.873	0.830
RIN ($n=2$)	1-3-1	89.39	73.07	0.894	0.736
$RIL + P$	8-4-1	94.15	77.39	0.941	0.822
$RIN + P$ ($n=1$)	8-3-1	94.37	80.00	0.944	0.851
$RIN + P$ ($n=2$)	8-3-1	91.65	77.17	0.916	0.799
$Q_{(t-1)} + P$	8-3-1	90.35	71.81	0.903	0.812

* I - Number of neurons in input layer, H - Number of neurons in hidden layer, O - Number of neurons in output layer

Table 6.5 Results of ANN Applications for The Pampanga Catchment

Input Combination for ANN	ANN Structure (I-H-O)	E^2 (%)		R^2	
		Training	Testing	Training	Testing
Only P	17-4-1	86.96	70.20	0.870	0.859
RIL	1-3-1	89.88	70.28	0.899	0.923
RIN ($n=1$)	1-3-1	89.23	74.25	0.892	0.909
RIN ($n=2$)	← N.A. →				
$RIL + P$	18-3-1	91.07	77.53	0.911	0.894
$RIN + P$ ($n=1$)	18-5-1	91.60	71.51	0.916	0.910
$RIN + P$ ($n=2$)	← N.A. →				
$Q_{(t-1)} + P$	18-6-1	99.08	95.15	0.991	0.953

*I-Number of neurons in input layer, H-Number of neurons in hidden layer, O-Number of neurons in output layer;
N.A.-Not Applicable

6.2.6 Results For The Individual Runoff Events

In the above sub-sections the results of the *ANN* with different input combinations applied to each of the catchments were presented that represented the entire dataset used for calibration/training and validation/testing. In this section the results obtained for the individual runoff events used in training and testing are presented. Details regarding the individual runoff events are presented in chapter 3. Table 6.6 provides the results obtained during training when the *ANN* was supplied *RIL* only and *RIL + P* values as inputs. The observed and computed values for the volume of runoff, the peak daily discharge, and time to peak for each event used in training is given in this table. It can be observed that the time to peak has matched almost perfectly for all the events in three catchments viz. Brosna, Garrapatas, and Kizu. In the Bird Creek and the Pampanga catchments also the time to peak is well matched by the *ANN* models except for 2 events in each of these catchments wherein the time to peak is simulated less accurately. The runoff volume predicted by the *ANN* model with *RIL* as input are more closer to the observed values than the corresponding values for the *SLM* given in Table 5.7 in particular for Garrapatas, Kizu, and Pampanga catchments. The absolute values of *VE* statistic for most of the runoff events (except those in the Bird Creek and the Pampanga catchment) were found to be smaller than 15%. The prediction of the peak daily runoff values has improved for events in Brosna, Kizu, and Pampanga catchments when *RIL+P* was supplied as input to the *ANN* as compared to the *ANN* with input only *RIL*.

The results obtained for the runoff events used in testing the *ANN* models with the same inputs as described in Table 6.6 (*i.e.* *RIL* alone and *RIL + P*) are provided in Table 6.7. It can be seen that the time to peak is predicted with a maximum error of only one day by the two *ANN* models for all the events except for two events in the Pampanga catchment. The runoff volume prediction by the *ANN* model with *RIL* as input has improved over those by the *SLM* model (see Table 5.8) for most of the events listed in Table 6.7. In Bird Creek, Kizu, and Pampanga catchments the predicted peak by the *ANN* with the input *RIL + P* is more close to the observed values as compared to the results obtained by the *ANN* with *RIL* as input.

A similar kind of results for the *ANN* with *RIN* alone and *RIN + P* as input ($n = 1$ only) are presented in Tables 6.8 for the events used in training and in Table 6.9 for the events used in testing the *ANN*. As can be observed from the comparison of corresponding values of the parameters given in Tables 6.6 and 6.7 for *ANN* with *RIL* alone and *RIL + P*

Table 6.6 Linear Model + ANN Results For Catchments Without Sub-Divisions (Calibration Events)

Runoff Event No.	Runoff Volume (mm)			Peak of Daily Discharges (mm)			Time to Peak (Day)		
	Obs.	Computed		Obs.	Computed		Obs.	Computed	
		RIL	RIL + P		RIL	RIL + P		RIL	RIL + P
Bird Creek Catchment									
1	70.9	88.9	88.9	10.7	16.5	18.1	6	5	5
2	153.7	108.8	116.2	22.6	14.5	13.4	19	18	18
3	152.1	130.0	123.6	26.9	26.7	23.3	5	5	5
4	34.5	48.8	41.3	8.3	5.7	5.8	12	12	12
5	188.6	197.5	196.7	64.1	60.0	55.9	5	5	5
6	20.2	29.8	20.5	6.4	6.2	8.1	4	5	5
7	26.1	41.9	38.5	11.2	19.0	16.6	3	3	3
8	20.2	29.5	25.7	9.2	7.6	9.2	4	3	4
Brosna Catchment									
1	141.8	93.7	104.3	6.9	4.3	5.5	16	17	17
2	67.5	75.8	80.2	4.9	4.3	4.6	7	7	7
3	71.7	86.8	89.3	4.4	4.1	4.2	16	16	16
4	70.6	73.7	74.4	4.6	4.5	4.9	5	5	5
5	72.2	60.5	67.7	5.3	3.8	4.3	8	7	7
6	112.8	96.5	102.6	5.9	4.1	4.6	7	7	7
7	60.0	92.9	85.6	4.1	4.6	4.0	8	8	9
8	126.0	109.5	116.7	6.1	4.6	5.7	19	19	19
Garrapatas Catchment									
1	76.4	81.8	78.7	9.1	8.1	7.2	5	5	6
2	131.2	117.9	118.7	10.7	8.0	7.4	6	5	5
3	165.8	176.5	175.2	11.1	10.2	9.9	5	5	5
4	206.2	187.6	187.0	17.5	10.4	9.7	6	6	6
5	316.8	305.9	317.3	14.1	10.3	10.4	6	6	8
6	138.1	124.9	117.6	11.3	7.3	7.2	11	11	11
7	99.2	91.5	86.4	9.7	6.8	6.5	4	4	4
8	96.7	123.4	127.9	8.9	10.4	10.2	8	10	10
9	76.4	88.7	87.4	9.2	9.7	9.0	4	2	2
10	177.2	185.1	187.2	8.6	7.9	7.6	13	13	13
Kizu Catchment									
1	165.6	141	135	18.1	19.8	18.1	11	10	10
2	158.1	113	112	18.5	19.1	16.7	3	3	3
3	33.7	58.6	58.5	13.0	22.2	17.0	5	5	5
4	53.9	78.7	75.9	13.4	16.9	12.5	6	6	6
5	71.3	93.1	104.1	39.9	30.4	39.9	4	4	4
6	72.6	69.0	67.4	16.9	15.2	13.0	6	6	6
7	85.6	86.2	89.9	23.4	27.3	25.1	2	2	2
8	204.6	186	185.6	15.8	18.2	15.2	10	10	10
9	43.1	47.2	46.7	15.9	16.9	12.4	3	3	3
10	328.9	329	340.4	95.2	97.0	95.0	12	12	12
Pampanga Catchment									
1	61.7	156	160.4	17.9	24.6	24.1	4	6	6
2	152.2	165	151.9	17.3	17.9	16.0	10	12	11
3	449.5	390	379.7	72.0	61.9	63.8	7	7	7
4	255.9	164	176.5	36.7	21.3	28.5	11	11	10
5	79.9	98.5	70.5	5.25	6.7	5.8	9	6	6
6	609.2	636	643.8	72.7	73.1	72.5	8	8	8

* Obs. – Observed

Table 6.7 Linear Model + ANN Results For Catchments Without Sub-Divisions (Validation Events)

Runoff Event No.	Runoff Volume (mm)			Peak of Daily Discharges (mm)			Time to Peak (Day)		
	Obs.*	Computed		Obs.	Computed		Obs.	Computed	
		RIL	RIL + P		RIL	RIL + P		RIL	RIL + P
Bird Creek Catchment									
9	73.0	56.7	57.5	18.1	13.8	13.1	10	9	9
10	58.3	66.6	78.8	18.6	15.7	19.7	6	6	6
11	42.8	63.0	66.5	16.3	25.7	22.3	4	4	5
12	68.3	49.9	55.5	27.4	19.0	20.7	5	4	5
13	28.1	42.1	38.0	13.6	15.0	12.3	4	4	4
Brosna Catchment									
9	39.2	43.4	41.5	4.00	3.4	3.5	11	11	11
10	155.1	127.5	124.6	6.6	4.4	4.8	22	22	22
11	62.2	49.6	50.4	5.3	3.9	4.1	10	11	11
12	62.4	63.8	61.5	5.9	4.6	5.2	16	16	16
Garrapatos Catchment									
11	110.5	100.6	83.2	8.1	6.9	5.5	6	5	5
12	74.3	90.0	81.3	9.2	8.8	7.2	5	5	5
13	67.8	71.3	64.1	7.1	7.0	6.0	4	4	4
14	389.4	347.5	313.7	15.1	10.1	8.8	12	13	13
Kizu Catchment									
11	87.5	90.5	89.3	15.1	19.2	14.7	11	11	11
12	208.4	147.9	173.6	35.2	30.7	49.1	10	10	10
13	52.0	61.6	67.7	23.2	29.6	31.5	5	5	5
14	71.8	74.6	77.1	15.6	19.7	15.9	5	4	4
15	90.8	113.5	104.3	20.2	27.5	20.2	7	7	7
Pampanga Catchment									
7	105.7	106.5	98.1	10.3	9.3	10.8	14	14	14
8	94.8	74.1	65.6	11.1	8.5	11.6	3	4	6
9	44.6	58.8	55.5	8.8	5.7	6.2	7	8	10
10	319.6	186.7	207.2	60.6	29.7	38.9	6	6	6

*Obs. – Observed

Table 6.8 Nonlinear Model + ANN Results For Catchments Without Sub-Divisions (Calibration Events)

Runoff Event No.	Runoff Volume (mm)			Peak of Daily Discharges (mm)			Time to Peak (Day)		
	Obs.	Computed		Obs.	Computed		Obs.	Computed	
		R/N	R/N + P		R/N	R/N + P		R/N	R/N + P
Bird Creek Catchment									
1	70.9	89.5	85.1	10.7	14.4	16.5	6	5	5
2	153.7	114	105	22.6	13.4	11.7	19	18	19
3	152.1	125	137	26.9	20.8	23.0	5	5	5
4	34.5	48.7	46.0	8.3	8.1	6.4	12	12	13
5	188.6	197	199	64.1	50.0	56.1	5	6	5
6	20.2	21.4	30.5	6.4	8.7	7.2	4	5	5
7	26.1	36.0	43.5	11.2	15.0	16.0	3	3	3
8	20.2	25.0	28.2	9.2	10.0	7.9	4	3	4
Brosna Catchment									
1	141.8	98.4	109	6.9	4.5	5.7	16	17	17
2	67.5	79.2	77.9	4.9	4.5	4.9	7	7	7
3	71.7	90.6	89.8	4.4	4.2	4.2	16	16	16
4	70.6	77.5	76.6	4.6	5.0	4.6	5	5	5
5	72.2	63.1	69.8	5.3	3.9	5.0	8	7	7
6	112.8	101	101	5.9	4.2	4.9	7	7	7
7	60.0	97.8	75.9	4.1	5.4	3.9	8	8	8
8	126.0	114	121.1	6.1	5.4	5.7	19	19	19
Garrapatos Catchment									
1	76.4	77.9	81.0	9.1	7.5	8.3	5	6	5
2	131.2	117	120.5	10.7	8.0	8.4	6	8	5
3	165.8	174	178.0	11.1	9.6	11.3	5	5	5
4	206.2	185	187.3	17.5	9.6	11.0	6	6	6
5	316.8	318	303.5	14.1	10.2	11.1	6	8	6
6	138.1	122	128.5	11.3	7.5	7.9	11	11	11
7	99.2	86.9	91.1	9.7	6.5	7.4	4	4	4
8	96.7	129	122.4	8.9	9.9	9.9	8	10	10
9	76.4	87.9	86.9	9.2	9.0	10.1	4	2	2
10	177.2	184	184.7	8.6	7.8	7.8	13	13	13
Kizu Catchment									
1	165.6	156	133	18.1	15.1	16.4	11	10	10
2	158.1	102	113	18.5	15.2	16.6	3	3	3
3	33.7	54.7	58.5	13.0	16.4	18.2	5	5	5
4	53.9	79.6	77.4	13.4	14.2	12.3	6	6	6
5	71.3	97.7	100	39.9	28.4	37.4	4	4	4
6	72.6	64.5	68.4	16.9	14.3	14.4	6	6	6
7	85.6	88.4	89.3	23.4	20.1	25.8	2	2	2
8	204.6	201	185	15.8	14.8	15.1	10	10	10
9	43.1	43.5	46.8	15.9	14.4	13.0	3	3	3
10	328.9	312	345	95.2	78.2	95.2	12	12	12
Pampanganga Catchment									
1	61.7	161	160	17.9	27.0	22.2	4	6	6
2	152.2	173	161	17.3	19.5	23.2	10	11	11
3	449.5	379	405	72.0	66.1	71.1	7	7	7
4	255.9	169	150	36.7	23.7	17.6	11	10	9
5	79.9	117	94	5.25	7.4	6.4	9	5	5
6	609.2	610	630	72.7	73.5	76.4	8	8	8

* Obs. – Observed

Table 6.9 Nonlinear Model + ANN Results For Catchments Without Sub-Divisions (Validation Events)

Runoff Event No.	Runoff Volume (mm)			Peak of Daily Discharges (mm)			Time to Peak (Day)		
	Obs.*	Computed		Obs.	Computed		Obs.	Computed	
		RIN	RIN + P		RIN	RIN + P		RIN	RIN + P
Bird Creek Catchment									
9	73.0	49.8	54.4	18.1	11.4	11.7	10	9	10
10	58.3	69.0	67.1	18.6	20.8	22.5	6	6	6
11	42.8	62.9	67.5	16.3	21.2	25.4	4	4	4
12	68.3	53.6	58.6	27.4	21.4	24.6	5	4	4
13	28.1	44.4	46.4	13.6	17.2	14.6	4	4	4
Brosna Catchment									
9	39.2	43.1	41.3	4.00	3.4	2.9	11	11	11
10	155.1	127.1	122.1	6.6	4.5	4.9	22	22	22
11	62.2	49.5	47.2	5.3	3.8	4.2	10	11	11
12	62.4	64.2	59.6	5.9	5.2	5.3	16	16	16
Garrapatos Catchment									
11	110.5	86.0	102.7	8.1	5.4	7.9	6	5	5
12	74.3	81.1	96.7	9.2	7.6	10.3	5	5	5
13	67.8	64.8	76.0	7.1	6.3	8.7	4	4	4
14	389.4	320.2	373.5	15.1	8.7	10.6	12	13	13
Kizu Catchment									
11	87.5	96.9	88.4	15.1	15.5	16.1	11	11	11
12	208.4	163.9	174.0	35.2	40.4	46.3	10	10	10
13	52.0	65.8	67.6	23.2	26.0	32.4	5	5	5
14	71.8	70.8	74.2	15.6	15.1	15.3	5	4	4
15	90.8	111.2	103.5	20.2	19.5	22.9	7	7	7
Pampanganga Catchment									
7	105.7	116.2	97.8	10.3	10.9	8.9	14	14	14
8	94.8	80.9	75.9	11.1	9.5	9.2	3	4	3
9	44.6	67.3	52.5	8.8	6.4	5.5	7	8	7
10	319.6	194.5	186.8	60.6	35.9	36.0	6	6	6

* Obs. - Observed

as input that the nonlinear – *ANN* coupled model performance is not much different than the *SLM* - *ANN* coupled model. Nevertheless, as improvement in the peak values predicted by the nonlinear - *ANN* coupled model over that predicted by the nonlinear model ($n = 1$) (see Tables 5.7 and 5.8) can be observed in training in general, and for Brosna and Garrapatas catchments, in particular. The performance of the *ANN* with *RIL* and *RIN* as input is almost same during testing in the Brosna catchment in terms of runoff volume and peak discharge prediction as can be noted from values given in Table 6.7 and 6.9. The *ANN* with *RIL* + *P* as input has performed better for the Bird creek and Pampanga catchments in terms of matching the peak than the *ANN* with *RIN* + *P* as input. The absolute values of *VE* statistic were however smaller than 20% in most of the results obtained through the *ANN* application.

6.2.7 The Krishna Catchment

The Krishna catchment involves sub-divisions. In the no sub-division scenario, the entire catchment is considered as a single unit and in the two sub-divisions scenario the catchment is divided into two sub-areas. The *ANN* application is carried out separately for both these scenarios. The best performing *ANN* configurations and the results obtained for this catchment are presented in Table 6.10.

In case of the two sub-divisions scenario the output of the linear *MISO* or the nonlinear *MISO* is given as input to the *ANN*, because of which, the input layer in these cases consisted of two neurons as against one for the no sub-division scenario. The structure of the *ANN* for the other input combinations also changed in a similar fashion. The E^2 values for two sub-divisions scenario are improved over the corresponding values for the no sub-division scenario both during training and testing with the exception of *ANN* with *RIN* ($n = 2$) as input. The performance of all the *ANN* models in terms of E^2 and R^2 criteria is very good in this catchment.

Similar to the observation made in case of other catchments, the E^2 and R^2 values for Krishna catchment during training and testing for *ANN* with *RIL* + *P* as input are larger than that for *RIL* alone as input. Similarly, the performance of *ANN* with *RIN* + *P* ($n = 1$,

2) is improved as compared to *ANN* with *RIN* ($n = 1, 2$) as input in both the sub-division scenarios studied.

The comparison of E^2 values given in Table 6.10 indicates that the performance of *ANN* with *RIL* and *RIN* ($n = 1, 2$) as input is almost similar for the one sub-division scenario, whereas in the two sub-divisions scenario the E^2 values for *ANN* with *RIN* ($n = 1, 2$) as input are less than those for *ANN* with *RIL* as input. This is indicative of the fact that there is no any definite advantage of coupling a nonlinear model with the *ANN* in place of a linear model. As already stated, the *ANN* based models account for the non-linearity involved in the rainfall-runoff process and this task is better performed if the linear model is coupled with the *ANN*, *i.e.* when the *RIL* is supplied as input to the *ANN*.

The results obtained for the individual runoff events used in calibration/training and validation/testing are also presented in tabular form for the Krishna catchment. The Table 6.11 presents the event wise results for the *ANN* with *RIL* and *RIN* ($n = 1, 2$) as input and the results from the *ANN* models with inputs *RIL+P* and *RIN+P* ($n = 1, 2$) are presented in Table 6.12 for the different sub-division scenarios.

With the *RIL* as input the volume of predicted runoff by the *ANN* matched more closely for the two sub-division scenario than in no sub-division scenario in 8 of the 10 events listed in Table 6.11 whereas, this number for *ANN* with *RIN* ($n = 1$) as input is only 5. For $n = 2$ the *RIN* input resulted in larger deviation in runoff volume prediction. Table 6.11 shows that the time to peak is matched for five events in training and one event in testing by the *ANN* with *RIL* only as the input, whereas, for the *ANN* with *RIN* as input this number of events in calibration is 4 only. The similar kind of analysis of Table 6.12 reveals that the *ANN* with *RIL + P* has predicted the time to peak accurately for more number of events than mentioned as above.

The peak discharges predicted by the *ANN* with *RIL + P* as input are better than that predicted by the *ANN* with *RIL* as input for all events in training and for one event in testing as can be seen from corresponding values for both sub-division scenarios in Tables 6.11 and 6.12. Comparison of the performance of the linear model (see Table 5.8) with the corresponding *ANN* coupled model in terms of matching peak daily discharges has improved for three events in validation/testing. There is however a marginal difference in the results obtained through *ANN* with *RIL* and *RIN* and between the results obtained by the *ANN* with *RIL + P* and *RIN + P* as inputs. In general, satisfactory results are obtained for most of the runoff events as can be seen from Tables 6.11 and 6.12.

Table 6.10 ANN Model Application Results for The Krishna Catchment

Input Combination For ANN	ONE SUB-DIVISION						TWO SUB-DIVISION					
	ANN Structure (I-H-O)	E ² (%)		R ²		ANN Structure (I-H-O)	E ² (%)		R ²			
		Trg.	Test.	Trg.	Test.		Trg.	Test.	Trg.	Test.		
Only P	15-4-1	91.03	80.44	0.910	0.876	30-6-1	92.61	86.17	0.926	0.897		
R/L	1-2-1	88.69	83.72	0.887	0.878	2-4-1	89.70	85.84	0.897	0.864		
R/N (n=1)	1-3-1	88.78	83.00	0.888	0.880	2-4-1	89.44	80.35	0.894	0.879		
R/N (n=2)	1-3-1	88.70	82.67	0.887	0.866	2-4-1	84.17	77.35	0.841	0.850		
R/L + P	16-4-1	92.34	88.19	0.923	0.902	32-12-1	94.06	89.75	0.941	0.900		
R/N + P (n=1)	16-4-1	90.52	89.00	0.905	0.897	32-12-1	93.00	90.00	0.930	0.903		
R/N + P (n=2)	16-4-1	91.03	87.62	0.910	0.881	32-12-1	93.40	88.03	0.934	0.893		
Q _(n-1) + P	16-4-1	97.63	96.59	0.976	0.966	31-8-1	98.71	98.02	0.987	0.980		

* I - Number of neurons in input layer, H - Number of neurons in hidden layer, O - Number of neurons in output layer, Trg. - Training, Test. - Testing

Table 6.11 ANN Models Application to Krishna Catchment (RIL, RIN (n = 1, 2))

Runoff Event No.	Runoff Volume (mm)						Peak of Daily Discharges (mm)						Time to Peak (Day)									
	Obs.**	RIL		RIN (n=1)		RIN (n=2)		Obs.	RIL		RIN (n=1)		RIN (n=2)		Obs.	RIL		RIN (n=1)		RIN (n=2)		
		SD-1	SD-2	SD-1	SD-2	SD-1	SD-2		SD-1	SD-2	SD-1	SD-2	SD-1	SD-2		SD-1	SD-2	SD-1	SD-2	SD-1	SD-2	SD-1
Calibration Events																						
1	640.4	590.4	601.2	590.3	604.5	583.4	601.0	20.1	19.0	18.8	19.5	20.0	18.7	17.2	16	16	16	16	16	16	16	15
2	160.0	178.0	171.6	178.1	166.7	181.8	153.7	17.0	17.1	17.4	17.2	16.1	16.9	12.6	17	17	17	17	17	17	17	17
3	111.2	153.5	143.7	153.7	140.3	157.0	123.9	18.2	17.0	17.4	17.0	16.4	16.9	13.6	11	11	11	11	11	11	11	11
4	394.3	358.6	368.4	358.6	367.4	355.9	369.2	19.3	17.7	18.0	17.8	18.7	17.2	16.8	33	31	32	31	32	31	32	32
5	409.4	418.8	419.4	419.0	424.9	424.4	440.2	16.3	16.5	16.3	16.5	16.6	16.7	15.6	24	24	24	24	24	24	24	24
6	340.3	357.2	352.7	357.4	360.3	352.7	379.7	15.8	16.0	15.8	16.0	16.3	16.4	15.5	40	40	40	40	40	40	40	40
Validation Events																						
7	278.6	265.3	232.4	265.5	278.6	260.9	293.8	17.9	15.5	14.4	15.4	16.7	15.9	15.7	30	28	28	28	28	28	28	28
8	124.9	195.1	181.5	195.6	209.1	197.1	222.9	12.0	17.2	15.9	17.3	18.1	16.9	17.1	10	10	10	10	10	10	10	10
9	387.2	478.8	450.5	480.0	493.7	475.0	473.8	19.9	18.3	17.9	18.5	19.7	17.5	17.4	44	43	43	43	43	43	43	43
10	122.7	160.3	119.5	161.1	162.8	158.9	189.3	11.2	8.9	7.3	8.9	9.7	8.3	11.0	18	17	17	17	17	17	16	17

* - SD-1: One Sub-Division; SD-2: Two Sub-Divisions; ** Obs. - Observed

Table 6.12 ANN Models Application to Krishna Catchment (RIL + P, RIN + P (n = 1, 2))

Runoff Event No.	Runoff Volume (mm)						Peak of Daily Discharges (mm)						Time to Peak (Day)									
	Obs. **	RIL + P		RIN + P (n=1)		RIN + P (n=2)		Obs.	RIL + P		RIN + P (n=1)		RIN + P (n=2)		Obs.	RIL + P		RIN + P (n=1)		RIN + P (n=2)		
		SD -1	SD -2	SD -1	SD -2	SD -1	SD -2		SD -1	SD -2	SD -1	SD -2	SD -1	SD -2		SD -1	SD -2	SD -1	SD -2	SD -1	SD -2	SD -1
Calibration Events																						
1	640.4	606.4	611.7	600.4	608.9	594.0	601.9	20.1	20.4	20.2	20.2	20.2	19.6	19.8	19.8	16	18	18	17	18	17	16
2	160.0	172.2	158.0	177.7	158.2	174.1	161.9	17.0	17.1	16.7	16.2	16.8	16.8	17.9	16.7	17	17	17	17	17	17	17
3	111.2	146.2	133.7	148.4	132.6	147.8	134.0	18.2	18.2	19.0	16.6	17.5	17.9	17.8	11	11	11	11	11	11	11	11
4	394.3	376.1	382.3	363.2	375.1	367.2	378.8	19.3	20.2	19.6	18.4	19.2	18.8	19.3	33	33	33	33	32	33	33	33
5	409.4	395.1	401.7	410.0	408.3	409.9	405.1	16.3	16.6	15.9	17.6	16.0	15.7	15.2	24	24	24	24	24	24	24	25
6	340.3	361.4	369.3	355.5	371.0	365.5	373.0	15.8	15.7	16.0	15.8	16.1	16.1	16.0	40	40	40	40	41	41	40	41
Validation Events																						
7	278.6	215.4	244.5	241.5	239.9	223.1	248.1	17.9	12.1	14.4	13.8	13.8	13.8	11.9	14.2	30	30	28	28	28	30	28
8	124.9	146.2	171.9	169.6	172.1	160.7	180.6	12.0	13.1	14.9	15.1	15.1	15.3	15.8	10	10	10	10	10	10	10	10
9	387.2	384.9	407.1	424.7	416.7	411.5	439.4	19.9	17.8	17.8	16.7	18.2	17.7	19.5	44	44	44	43	44	44	44	44
10	122.7	135.0	147.4	150.6	139.2	137.0	151.6	11.2	7.3	8.9	8.5	8.3	7.7	9.7	18	18	18	18	18	18	18	18

* - SD-1: One Sub-Division; SD-2: Two Sub-Divisions; ** Obs. - Observed

6.2.8 The Narmada Catchment

The Narmada catchment also involves sub-divisions. There are three different sub-division scenarios studied in this catchment. First, the entire catchment was considered as one unit, called as no sub-division scenario, then the two sub-divisions scenario when the catchment was divided into two sub areas and the three sub-divisions scenario when it was further divided to three sub-areas. The catchment memory for all these cases is different (see Table 5.4) and accordingly the numbers of nodes in the input layer varied for the three scenarios. The structures of the best performing *ANNs* and their performance in this catchment are presented in Table 6.13. The nonlinear *MISO* model with $n = 2$ is not applicable in the two and three sub-division scenarios in this catchment.

The performance of the *ANN* with different inputs for two sub-divisions scenario is improved than the no sub-division case and it further improves for the three sub-divisions scenario as can be seen from the E^2 and R^2 values given in Table 6.13 with a few exceptions. This improvement with the increase in the number of sub-divisions vindicates the division of larger catchments into smaller homogeneous areas and the results reflect that the *ANN* is able to capture this type of disaggregated input and produce more satisfactory results.

Another aspect of the results obtained which can be noticed from this table is that the *ANNs* performance with $RIL + P$ as input in terms of E^2 and R^2 criteria is improved over the performance of *ANN* with RIL alone as input and the same is true for $RIN + P$ and RIN alone input cases.

Another feature that is revealed by analysis of the results is that the E^2 and R^2 values obtained for the *ANN* with RIN and $RIN + P$ inputs are almost similar or less than the corresponding values for *ANN* with RIL only and $RIL + P$ as input. This strengthens the statement made earlier that there are no definite advantages of coupling a nonlinear model instead of a linear model with the *ANN* as the *ANN* itself, being a nonlinear model, is capable of accounting for the non-linearity present in the rainfall-runoff relationship.

Table 6.14 presents the event wise results for the coupled linear-*ANN* model applied to all the sub-division scenarios in the Narmada catchment. As can be seen from this table that observed and predicted values for the time to peak are well matched. The

values of the predicted volume of runoff improved with the number of sub-divisions for the *ANN* with *RIL* as input in most of the events. Whereas, for the *ANN* with *RIL + P* as input this matching improved for more number of events. In general the peak values are better predicted by the *ANN* models.

A similar kind of results for the case of nonlinear model outputs given as input to the *ANN* are presented, for all the events used in training and testing, in Table 6.15. The results of such *ANN* model shows a similar trend as discussed above for the linear-*ANN* coupled model, with some minor changes of values for some of the events.

Based on the analysis of the results in Tables 6.14 and 6.15 presented above it can be stated that the coupled linear-*ANN* model performance is quite satisfactory considering the information supplied to the *ANN* model for prediction of the daily runoff. Secondly, an improvement in the results with the increase in the number of sub-divisions can be observed in most of the events.

The graphical results in terms of the scatter diagrams prepared with the entire set of data used in model testing and the linear scale plots for the training and testing events that contained the highest of the peak flows of the data used are presented in the remaining part of this chapter.

Table 6.13 ANN Model Application Results for The Narmada Catchment

Inputs For ANN	ONE SUB-DIVISION						TWO SUB-DIVISIONS						THREE SUB-DIVISIONS					
	ANN Struct. (I-H-O)		E^2 (%)		R^2		ANN Struct. (I-H-O)		E^2 (%)		R^2		ANN Struct. (I-H-O)		E^2 (%)		R^2	
	Trg	Test	Trg	Test	Trg	Test	Trg	Test	Trg	Test	Trg	Test	Trg	Test	Trg	Test	Trg	Test
Only P	6-2-1	80.35	78.33	0.80	0.81	80.36	77.44	0.80	0.77	16-4-1	82.30	79.45	0.82	0.79				
RIL	1-2-1	82.29	78.92	0.82	0.81	82.53	79.83	0.82	0.80	3-1-1	83.03	80.42	0.83	0.80				
RIN (n=1)	1-3-1	78.84	77.78	0.79	0.78	80.32	79.35	0.80	0.78	3-2-1	82.88	80.19	0.83	0.79				
RIN (n=2)	1-3-1	83.76	76.21	0.84	0.77													
RIL + P	7-3-1	83.27	80.30	0.83	0.80	84.47	81.90	0.84	0.81	13-4-1	87.01	82.28	0.87	0.82				
RIN + P (n=1)	7-4-1	82.29	79.66	0.82	0.80	83.66	81.22	0.84	0.81	13-5-1	87.21	82.23	0.87	0.82				
RIN + P (n=2)	7-4-1	83.18	77.96	0.83	0.81													
$Q_{(t-1)} + P$	7-3-1	91.14	84.01	0.91	0.83	93.60	84.34	0.94	0.84	13-4-1	94.09	85.78	0.94	0.85				

* I - Number of neurons in input layer, H - Number of neurons in hidden layer, O - Number of neurons in output layer; Trg. - Training, Test. - Testing; Struct. - Structure

Table 6.14 ANN Models Application to Narmada Catchment (Linear Model + ANN)

Runoff Event No.	Runoff Volume (mm)						Peak of Daily Discharges (mm)						Time to Peak (Day)										
	Obs.**	RIL			RIL + P			Obs.	RIL			RIL + P			Obs.	RIL			RIL + P				
		SD-1	SD-2	SD-3	SD-1	SD-2	SD-3		SD-1	SD-2	SD-3	SD-1	SD-2	SD-3		SD-1	SD-2	SD-3	SD-1	SD-2	SD-3		
Calibration Events																							
1	103.1	115.4	107.7	106.4	114.7	110.6	109.5	9.2	9.8	8.4	7.7	8.9	8.2	8.2	8.2	11	11	11	10	11	11	11	11
2	224.6	228.1	210.7	212.3	227.9	216.5	213.7	16.6	10.9	10.4	9.3	10.1	11.1	10.9	11.1	10	9	9	9	9	9	10	10
3	214.2	206.0	205.0	205.9	205.6	201.6	207.3	24.1	19.8	20.5	21.2	20.0	21.9	22.7	21.9	12	12	12	12	12	12	12	12
4	370.0	349.4	352.8	355.9	354.7	351.5	361.8	38.3	38.8	38.1	37.6	36.7	37.6	38.9	37.6	13	13	13	13	13	13	13	13
5	351.9	382.8	377.4	378.1	380.0	378.1	374.3	23.9	25.1	22.6	23.5	24.6	23.6	23.9	23.6	25	25	25	25	25	25	25	25
6	261.6	244.7	268.4	264.3	239.9	265.9	258.3	10.9	8.1	8.6	8.3	7.5	8.2	7.7	8.2	19	20	20	20	20	19	20	20
Validation Events																							
7	131.3	113	122.5	123.6	107.2	121.2	129.1	25.5	22.1	24.2	24.7	21.5	24.7	23.8	24.7	9	9	9	9	9	9	9	9
8	299.6	311.8	283.6	260.9	267.6	288.9	251.3	37.7	38.8	33.2	33.8	36.8	39.8	42.1	39.8	16	17	16	16	16	16	16	16
9	96.75	107.4	71.04	68.71	92.89	72.66	71.87	20.7	13.3	7.5	6.2	10.2	7.2	8.0	7.2	11	11	11	11	11	11	11	11
10	75.52	118.7	109.5	102.1	115.2	106.6	91.49	24.5	20.0	19.8	16.8	22.2	19.4	15.2	19.4	11	11	10	10	10	10	10	11

* - SD-1: One Sub-Division; SD-2: Two Sub-Divisions; SD-3: Three Sub-Divisions; ** Obs. - Observed

Table 6.15 ANN Models Application to Narmada Catchment (Nonlinear Model + ANN)

Runoff Event No.	Runoff Volume (mm)						Peak of Daily Discharges (mm)						Time to Peak (Day)							
	Obs.**	R/N			Obs.	R/N + P			Obs.	R/N			Obs.	R/N						
		SD-1	SD-2	SD-3		SD-1	SD-2	SD-3		SD-1	SD-2	SD-3		SD-1	SD-2	SD-3				
Calibration Events:																				
1	103.1	114.7	110.6	109.5	119.6	105.3	106.6	9.2	8.4	6.7	7.5	9.0	9.4	8.6	11	11	11	11	11	11
2	224.6	227.9	216.5	213.7	226.1	200.7	209.1	16.6	8.7	9.6	9.3	10.0	11.4	9.9	10	10	9	10	10	10
3	214.2	205.6	201.6	207.3	206.7	210.8	206.7	24.1	20.0	20.9	20.0	20.3	20.3	22.3	12	12	12	12	12	12
4	370.0	354.7	351.5	361.8	345.3	362.7	361.8	38.3	36.7	34.9	36.6	34.6	38.3	38.2	13	13	13	13	13	12
5	351.9	380	378.1	374.3	381.9	383.5	379.9	23.9	24.6	23.0	21.8	24.7	22.4	22.5	25	25	25	25	25	25
6	261.6	239.9	265.9	258.3	244.4	263.7	261.4	10.9	8.2	7.7	8.2	7.4	8.3	9.6	19	20	20	20	20	20
Validation Events																				
7	131.3	91.25	129.2	129.9	95.38	122.6	122.4	25.5	15.3	23.6	24.3	15.4	23.5	27.8	9	10	9	9	9	9
8	299.6	250.5	259.7	257.1	249.2	304.1	258.1	37.7	29.5	31.9	33.8	31.6	38.5	34.0	16	17	17	16	17	16
9	96.75	87.51	62.38	67.08	85.29	71.82	69.54	20.7	8.6	4.9	5.8	9.0	7.1	7.4	11	11	11	11	11	12
10	75.52	90.05	113	101.5	93.14	101.8	96.57	24.5	13.5	20.2	17.2	14.7	18.0	17.3	11	11	11	11	11	11

* - SD-1: One Sub-Division; SD 2: Two Sub-Divisions; SD-3: Three Sub-Divisions; ** Obs. - Observed

6.3 GRAPHICAL PRESENTATION OF THE RESULTS OF ANN APPLICATIONS

In the above section the results of the ANN application with various input combinations are presented in tabular form in terms of the statistical indicators of model performance for each catchment separately. In this section the results from the ANN application are presented in the graphical form and these are analyzed and discussed. The ANN application involved eight different input combinations in a catchment. The graphical presentation for all these results is not given, as that would make the presentation very lengthy and complex. So for clarity in understanding, only the results of the best performing ANNs supplied with the input combinations identified in this study are presented here.

The presentation is divided in two sub-sections. First, the results obtained by the ANN application in the catchments not having any sub-divisions are presented and this is followed by the presentation of results for different sub-division scenarios involved in the Krishna and the Narmada catchments.

6.3.1 Results Obtained in Catchments Without Sub-Divisions

Linear Model + ANN:

Figures 6.1(a) - (c) present, as illustration, the linear scale plots of the observed and simulated runoff for one calibration event (containing the highest of the peak flow) in each of the five catchments studied. These figures show the results of ANN models with two separate input combinations; i) only *RIL*, and ii) *RIL + P* i.e. when the rainfall values over the memory length are also given as input to the ANN in addition to *RIL* values. It was observed from Figs. 6.1(a) - (c) and other such plots (not shown here) that the results of ANN with *RIL + P* as input are better than that with *RIL* only as input as the simulated hydrographs match more closely with the observed especially in terms of the magnitude and time to peak in most of the events. For the Garrapatas catchment the output of the ANN with *RIL* as input is marginally better than with *RIL + P* but it can be noted that both the models performed less satisfactorily in this catchment.

A comparison of corresponding Figs. 6.1(a)-(c) with Figs. 5.8(a)-(c) in which the results of the system based linear model during calibration for the same events are presented shows that results of ANN models are much more improved over the results

obtained from the linear model. The comparison of the predicted values of peak discharges given in tables earlier also revealed similar results.

The performance of the *ANN* with same inputs as above (*RIL* only and *RIL + P*) during testing is depicted as illustration, in the forms of linear scale plots of simulated and observed runoff vs. time in Figs. 6.2 (a) - (c) for the runoff events that contained the highest peak. These and other such figures (not shown here) showed that *ANN* with *RIL + P* as input mostly performed better than *RIL* only as input in predicting the magnitude of the peak flow. Similar figures showing the performance of the linear model in all these catchments for the same validation events are given in earlier chapter vide Figs. 5.9(a) - (c). It can be noted that whereas the *SLM* in particular failed to predict the time to peak in Bird Creek and Pampanga catchments and also underestimated the peak flow in all cases (except in the Kizu catchment), both of these parameters are matched with more accuracy by the *ANN* with *RIL* only and *RIL + P* as inputs. The scatter diagrams prepared using the entire data for testing or validation period showing the performance of the *ANN* with *RIL* only and *RIL + P* as inputs are given in Figs. 6.3 (a) and (b) for all the catchments. It can be seen that the scatter for *ANN* with *RIL + P* as input is less in case of Bird Creek and Kizu catchments. This is also reflected from comparison of the R^2 values given in Tables 6.1 and 6.4 respectively. But in other three cases the scatter for the *ANN* with *RIL + P* as input is almost same or marginally more than with *RIL* only as input. When these plots are compared with Fig. 5.6, which shows similar plots for the linear model a definite shifting of the points closer to the ideal line by the application of the *ANN* models can be noticed.

Nonlinear Model + ANN:

The Figs. 6.4 (a) - (c) show the linear scale plots for the results obtained in training the *ANN* when the *ANN* is given *RIN* alone and *RIN + P* values as input *i.e.* when a nonlinear model is coupled with the *ANN*. When these plots are compared with the corresponding output of the nonlinear model shown in Fig. 5.8(a) - (c) a definite improvement in the results can be noticed, as the plots for the simulated runoff in case of *ANN* are closer to the observed one. The careful observation of Figs. 6.4(a) - (c) and Figs. 6.1 (a) - (c) reveals that there is not much discernable difference between the simulated outputs for *ANN* with *RIN+P* and *RIL + P* as inputs whereas, the performance of *ANN* with *RIN* as input is less satisfactory than with *RIL* as input in case of Bird Creek, Kizu, and Pampanga catchments.

The comparison of outputs of the *ANN* with *RIN* only and *RIN + P* as inputs for validation dataset is presented by way of illustration in Figs. 6.5 (a) - (c) in the form of linear scale plots. It was noticed from these and other such plots that *ANN* with *RIN + P* as input performed better in matching the peak than the *ANN* with *RIN* as input in most of the cases.

When Figs. 6.5 (a) - (c) are compared with Figs. 6.3 (a) - (c), which show the results of coupling a linear model with the *ANN* it was noticed that the output predicted by both the input combinations are more or less similar. In case of the Garrapatas and the Kizu catchments the *ANN* performance with *RIN + P* is better than *RIL + P* as input in predicting the peak flow. Whereas, in Bird Creek, Brosna, and Pampang catchments the performance of *ANN* with *RIL + P* is better as compared to that with *RIN + P* as input. A similar comment for the comparative performance of *ANN* with *RIL* and *RIN* as inputs can also be made.

Figures 6.6 (a) and (b) illustrate the scatter plots showing the performance of *ANN* with *RIN* only and *RIN + P* as inputs for the entire dataset used for validation in the five catchments. There is very marginal difference between these plots and corresponding plots shown in Figs. 6.3 (a) and (b). This again validates the statement that coupling a nonlinear model with *ANN* in place of the linear model could not attain much improvement in the final results.

Data for the catchments described above have previously been used by many investigators for simulation of the continuous records of daily runoff (O'Connor and Ahsan, 1991, Ahsan and O'Connor, 1994, Shamseldin, 1997 and others). A direct comparison of the results obtained in the present study with those of the other investigators is not appropriate as only the isolated runoff events are utilized in this study. Nevertheless, it may be noted that higher E^2 values are obtained for the flow simulation carried out in the present study than those obtained by other investigators.

6.3.2 Results Obtained For The Krishna Catchment

Linear Model + *ANN*:

The *ANN* application in this catchment also involved similar kind of input combinations as discussed above. First the results of the *ANN* coupled with a linear *MISO* model applied to both the sub-division scenarios in Krishna catchment are presented.

Figure 6.7(a) shows by way of illustration the plots for runoff simulated by the *ANN* with *RIL* and *RIL + P* as input and the observed runoff vs. time for one event used in calibration/training that contains the highest of the peak flow for no sub-division and two sub-divisions scenarios. A comparative analysis of these two and other such plots (not shown here) for one sub-division and two sub-division scenarios shown in Fig. 6.7(a) indicated that the performance of the *ANN* with *RIL + P* as input is better in two sub-divisions scenario as compared to that with the no sub-division scenario and in both the scenarios the output of *ANN* with *RIL + P* as input has matched more closely with the observed values than with *RIL* alone as the input.

Similar kind of plots for one validation event that contained the highest of the peak flows are given in Fig. 6.7(b) as illustration. An improvement in the performance of *ANN* with *RIL + P* as input over *RIL* as stated above was observed in this and other such figures too. The performance of the *ANN* has also improved with the number of sub-divisions.

The scatter diagrams, prepared using the entire data used for validation purpose in the Krishna catchment, exhibiting the performance of the *ANN* model with *RIL* alone and *RIL + P* as inputs are given for no sub-division and two sub-division scenarios in Fig. 6.8 (a) and (b) respectively. A noticeable change in the scatter, becoming progressively more symmetric around the ideal line can be observed when it is compared with the Fig. 5.10(a) for the linear *MISO* model. When corresponding plots for other models given in Figs. 6.8 (a) and (b) are compared, it was noticed that the scatter in case of Fig. 6.8 (b) *i.e.* for two sub-divisions scenario is more symmetric around the ideal line as compared with the corresponding case in no sub-division scenario.

Nonlinear Model + *ANN*:

In addition to the linear *MISO*, a nonlinear *MISO* was also coupled with the *ANN* and the results thus obtained are presented here. The outcome of this linkage is illustrated in the form of linear scale plots in Figs. 6.9 (a) and (b) respectively, for the same events as given above containing the highest of the peak flow.

The close observation of these plots lead to the conclusion that the *ANN* coupled with a nonlinear *MISO* model performed almost equally well as that coupled with a linear *MISO* model. The scatter plots for the *ANN* with *RIL* and with *RIL + P* as inputs for no

sub-division and two sub-division scenarios are represented in Figs. 6.10 (a) and (b) so as to have a comparison of the two different model linkages proposed in the study. It can be seen that the corresponding plots shown in Figs. 6.10 (a) - (b) and Figs. 6.8 (a) and (b) are almost similar and without much noticeable difference between them.

6.3.3 Results Obtained For The Narmada Catchment

Similar to the Krishna catchment the *ANN* application in this catchment also involved the *RIL*, *RIL + P*; and *RIN*, *RIN + P* input combinations with the difference that the Narmada catchment involved an additional sub-division referred to as the three sub-divisions scenario.

Linear Model + *ANN*:

The performance of *ANN* during training is better as can be seen from the figures earlier for the other catchments. So in case of the Narmada catchment only the results of the *ANN* model application for validation/testing events are presented.

The Figs. 6.11(a) - (c) represent the linear scale plots of model simulated and observed runoff for *ANN* with *RIL* only and *RIL + P* as inputs in all the sub-division scenarios, as illustration, for the validation event containing the highest of the peak values. A progressive improvement in the match of the simulated runoff with the observed values can be noted from the comparison of plots for none, two, and three sub-division scenarios. The scatter diagrams for the *ANN* with *RIL* only and *RIL + P* as inputs for all the sub-division scenarios are depicted in Fig. 6.12. The scatter for the linear *MISO* model for the same period is shown in the Fig. 5.11 (a). It can be observed that the scatter in this figure is more and a shift from the ideal line can be noted. This is an indication of persistence present in the error values of the model, which is supposed to be overcome by the *ANN* model as indicated by a more symmetrical scatter in Fig. 6.12 for *ANN* with *RIL* only and *RIL + P* as inputs for corresponding scenarios. It can also be noted that the scatter for three sub-divisions scenario in all the cases is minimum, which justifies the division of larger catchments into smaller areas to account for heterogeneity in the spatial distribution of rainfall over the large sized catchment.

Nonlinear Model + ANN:

Similar to the plots shown in Figs. 6.11(a) - (c) for the best performing ANN models coupled to the linear MISO model, the plots for the linkage of the nonlinear MISO model with the ANN, showing the final outputs of best performing ANNs are shown in Figs. 6.13 (a) - (c). A similar kind of trend can be analyzed as in case of Figs. 6.11 (a) - (c). It can also be observed from comparison of the Figs. 6.13 (a) - (c) and 6.11(a) - (c) that these figures are almost similar indicating that the final outcome of the ANN either coupled to the linear or nonlinear model is not much different.

Figure 6.14 shows the scatter plots for the ANN with RIN only and RIN + P as inputs. This figure is found to be similar to Fig. 6.12 obtained in case of linear MISO model coupled with ANN the similar trend in the results obtained can be noted.

6.4 PERFORMANCE OF ANN WITH OTHER INPUTS

In addition to the new inputs proposed in the present study *i.e.* the output of the linear and the nonlinear models, the ANN was also applied with other input combinations, mentioned in section 4.6, in all the seven catchments. The results obtained for ANN with only P and $Q_{t-1} + P$ as inputs applied to each of the catchment are already presented in tables for the respective catchment along with the other results.

It can be seen from these tables that the performance of the ANN with only P (*i.e.* rainfall values equal to the memory of the catchment) as input in terms of F^2 values in training and testing is inferior compared to all other ANN model results in case of Bird Creek, Kizu, Pampanga, and two and three sub-divisions scenario in the Narmada catchment. For other catchments the E^2 values for only P as input lie between those obtained for RIL and RIL + P or between RIN and RIN + P as inputs.

The ANN when given the previous day's runoff as input along with the rainfall values equal to the memory of the catchment, performed excellently as expected, with the E^2 and R^2 values in training and testing being the highest among all the other input combinations for all the catchment except for the Bird Creek and Kizu catchments in which the ANNs with other inputs perform better.

Alternatively, some experiments were conducted to evaluate performance of the ANN with following input combinations.

- i) When RIL, RIL_{t-1} , and P is given as input to the ANN

- ii) Repetition of higher values in the dataset for RIL , $RIL + P$ as inputs.

The results obtained for these were not much different *i.e.* no improvement in the ANN results on account of some additional information being provided in the form of above two input combination was noticed. Hence these results are not reported.

6.5 STUDY ON POSSIBLE USE OF THE ANN BASED MODELING IN THE UNGAUGED CATCHMENTS

The results of the best performing ANN configurations for the various input combinations are provided in the above sections for the catchments with different sizes studied. The ANN configurations used for obtaining the reported results consisted of i) one number of hidden layer, ii) different number of neurons in the hidden layer, iii) weights of the connections links between input layer – hidden layer and between the hidden layer – output layer along with the bias values for each of the node in the hidden and output layer. The information about the first two parameters for each of the ANN configuration that had the best possible performance for each input combination is provided earlier along with the results. In this section the information about the remaining parameters listed above is provided. The connection weights can have positive as well as negative values and so is the case with the bias values. The positive weights are called excitory connections whereas the negative weights are termed as inhibitory connections. The bias or the threshold value associated with node must be exceeded before the node can be activated. These values for the best performing ANN s when the RIL values are used as inputs are given in Figs. 6.15 (a) - (e) by way of illustration for the five catchments not having any sub-divisions and for the two different sub-division scenarios in the Krishna catchment and for the three different sub-division scenarios in the Narmada catchment. When the rainfall values equal to the memory of the catchment are supplied as input to the ANN in addition to the above input the ANN structure became much more complicated owing to the long memory in some of the catchments and due to the sub-divisions involved in the two catchments. Therefore the ANN structures for these cases involve a large number of values for the connection weights making the presentation complex and hence these are not provided.

As was seen in section 5.5 (chapter 5) the parameters of the gamma function could be related with the catchment characteristics. If such empirical regression relations are available then the RIL values can be determined by using the catchment characteristics and rainfall data. Thus obtained RIL values can be used as inputs to the ANN in a catchment

that is ungauged for discharges provided that somehow a trained *ANN* model is available for the ungauged catchment. For this purpose a qualitative study was made for identification of the relationship, if any, between the *ANN* weights and bias values shown in Figs. 6.15 (a) - (c) and the corresponding catchment areas. However, because of the wide variation, as can be seen from the Figs. 6.15 (a) - (c), in the values of weights and other parameters, the identification of such a relation was not possible. It is however hypothesized that if a trained *ANN* is available from a gauged and hydrologically similar catchment, that could possibly be used for generation of discharges from the empirically computed *RIL* values for the ungauged catchments. Data available in the present study was not found to be sufficient enough for investigating the hypothesis suggested above.

6.6 CONCLUDING REMARKS

An approach is presented for modeling the daily rainfall-runoff relationship by way of coupling a linear/nonlinear model as an auxiliary model with the *ANN*. The *ANN* is envisaged to account for non-linearity inherent in the process of rainfall-runoff transformation. The catchments studied are grouped into two categories based on their sizes, i) Those not involving any sub-divisions, ii) Those with sub-divisions. The sub-division of larger catchments into smaller areas is carried out to account for the heterogeneity in the spatial distribution of the rainfall.

These estimates of runoff by the auxiliary models are considered to represent the soil moisture state of the catchment. The earlier *ANN* based rainfall-runoff modeling has established the fact that the *ANN* fails to produce satisfactory results without the information about the soil moisture state of the catchment being given as one of the input, as the runoff generation over a catchment is controlled by the prevailing soil moisture status.

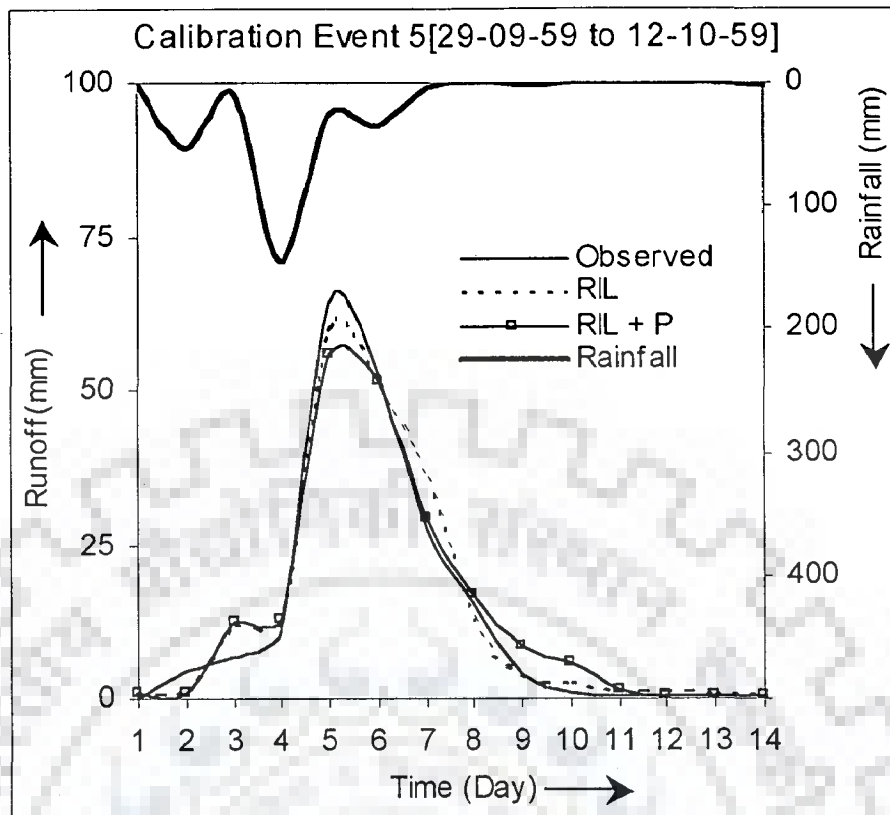
By way of coupling the linear/nonlinear model with the *ANN* an alternative way of providing the information about the soil moisture state of the catchment is proposed. In the earlier studies involving use of the *ANN* for rainfall-runoff modeling, runoff or river water level observed in the previous time were used for representing the soil moisture state which then becomes the updating flow simulation process. The inputs proposed in the present study overcome the drawbacks associated with existing *ANN* based rainfall-runoff modeling and the application of the *ANN* for non-updating flow simulation is demonstrated. Such a linkage is found to provide a better system theoretical representation

of the rainfall-runoff relationship on catchments from varying climates investigated in the present study as demonstrated by the results presented.

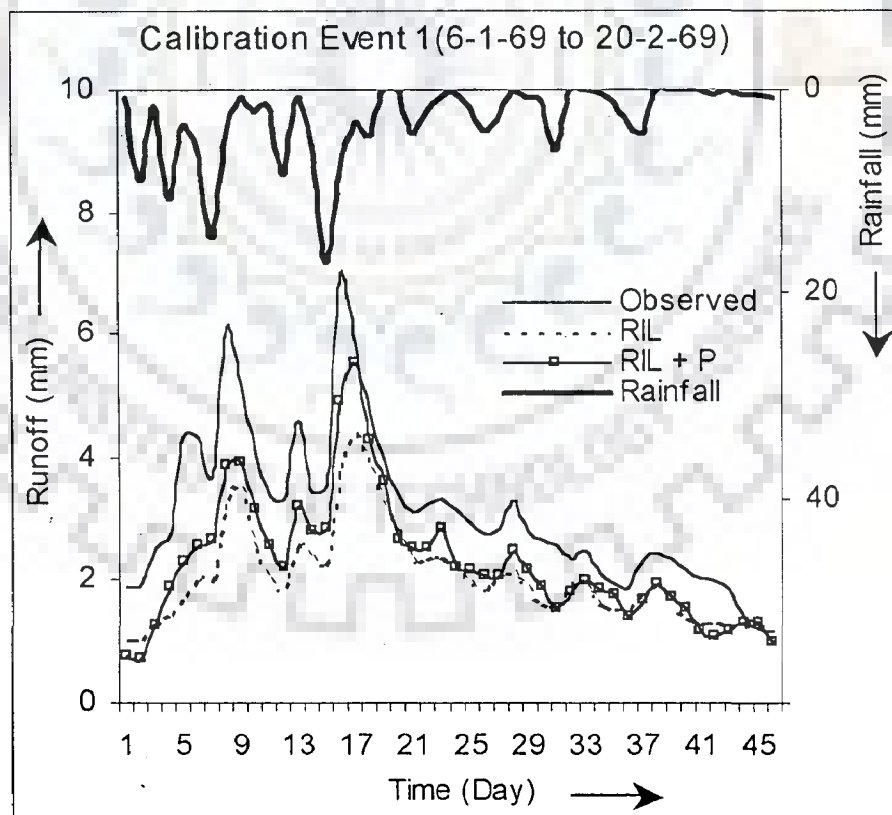
The alternative coupling of a nonlinear model with *ANN* in place of the linear model attempted in the present study did not result in much improvement in the final results obtained. This suggests that the assumption made in the study '*ANN being a nonlinear model takes care of the non-linearity present in the rainfall-runoff process*' to be proper and the results obtained also validate this.

The results obtained in case of the large sized catchments divided into smaller sub-areas demonstrate that performance of the *ANN* models, in terms of E^2 values and other parameters improve with the number of sub-divisions thus, justifying the division of larger catchments into smaller homogeneous areas for consideration of the inputs. This also demonstrates the ability of the *ANN* in understanding the change in the inputs with the increase in the number of sub-divisions.

The linear response functions derived from the data are having physically realizable shapes. These shapes are parameterized using the discrete gamma functions, the parameters of which have relationship, albeit qualitative, with the catchment characteristics. Nevertheless, the present approach cannot be extended to the catchments that are ungauged for discharges because of non-availability of a trained *ANN* for such catchments.

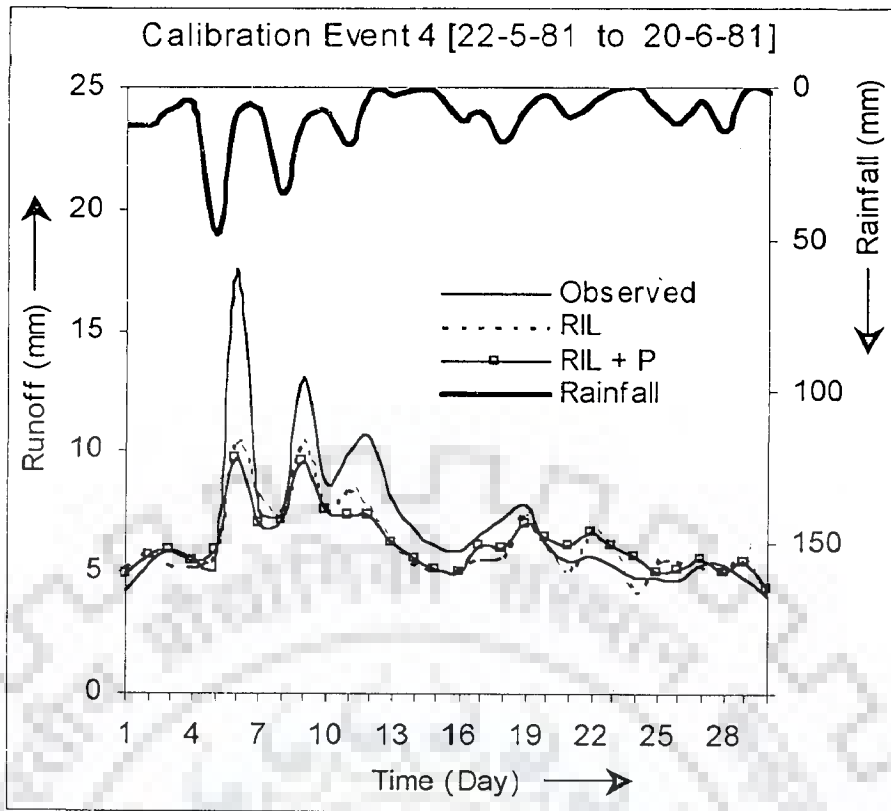


i) Bird Creek Catchment

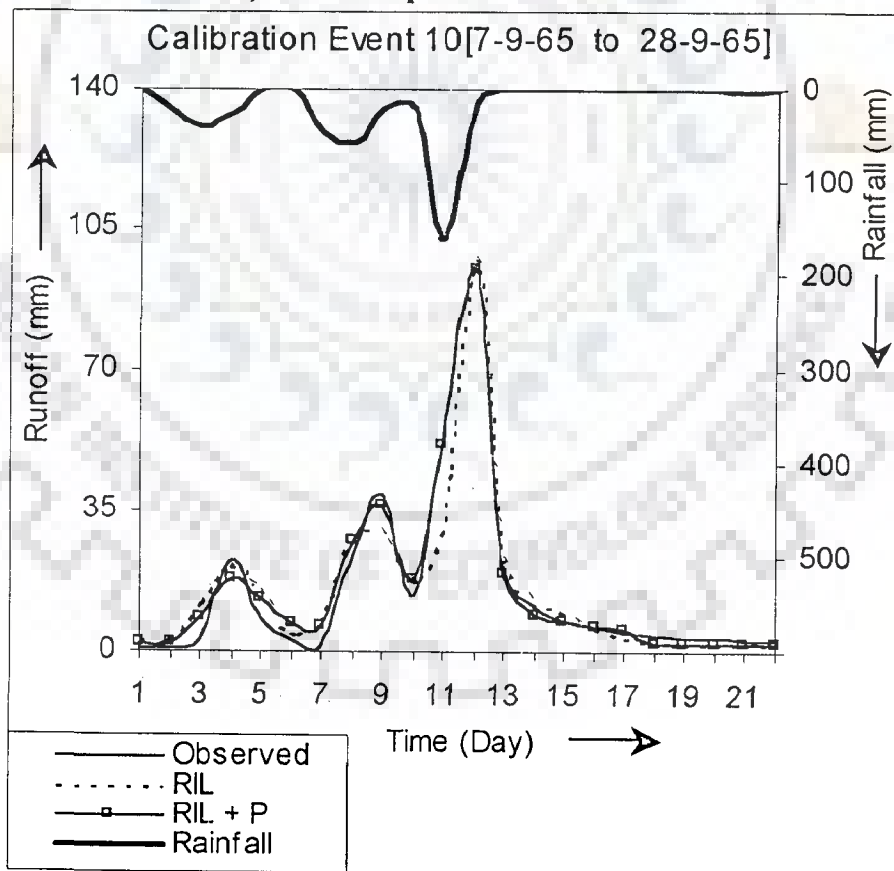


ii) Brosna Catchment

Fig.6.1(a) Linear Scale Plots For Calibration Event For Catchment Without Sub-Divisions (Linear Model + ANN)

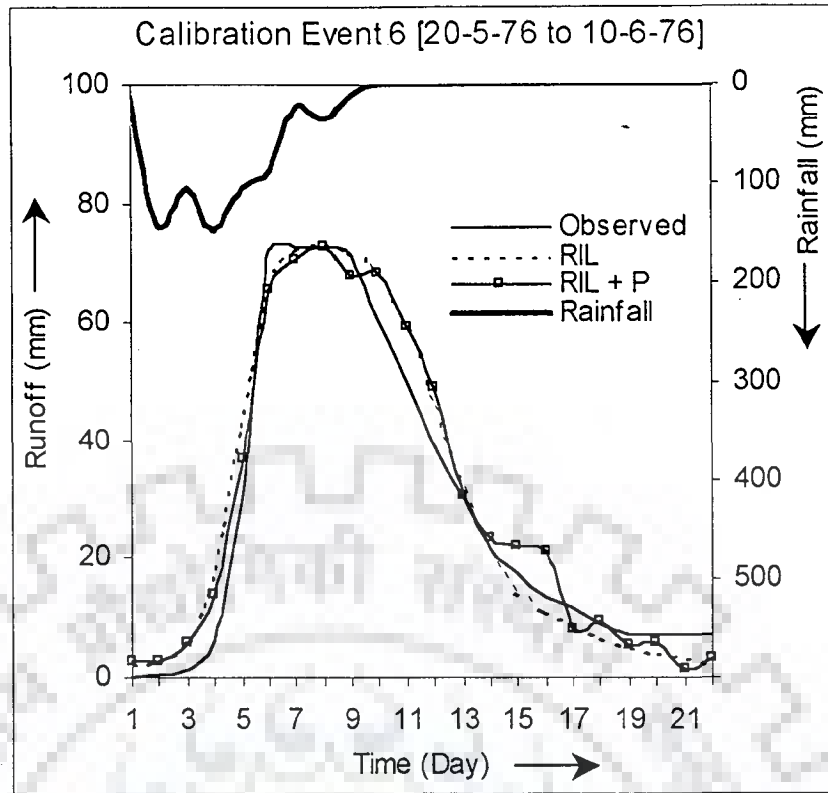


iii) Garrapatas Catchment



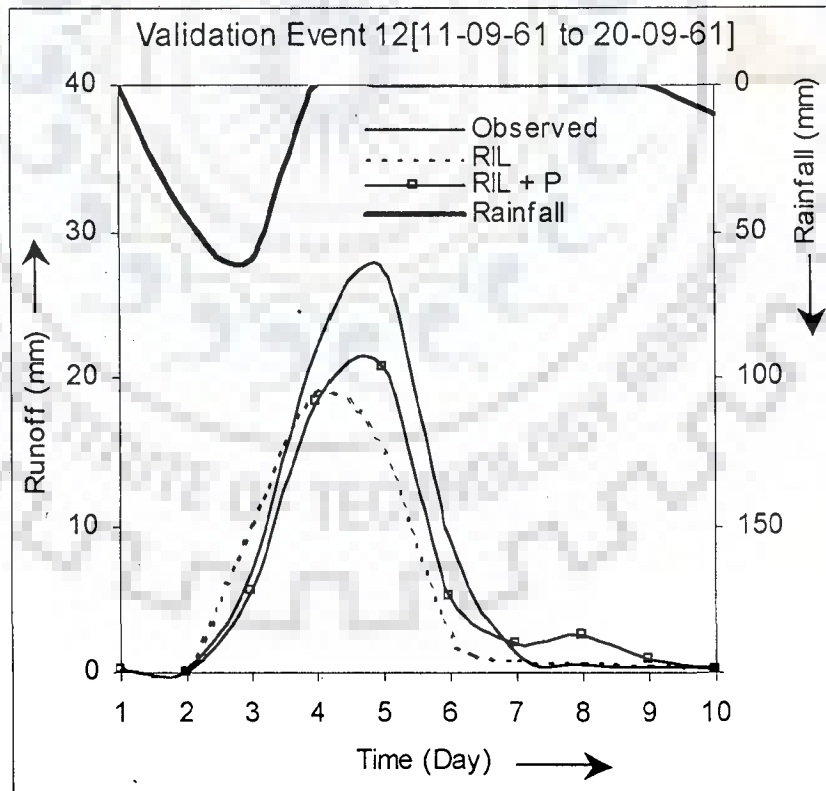
iv) Kizu Catchment

Fig. 6.1(b) Linear Scale Plots For Calibration Event For Catchment Without Sub-Divisions (Linear Model + ANN)



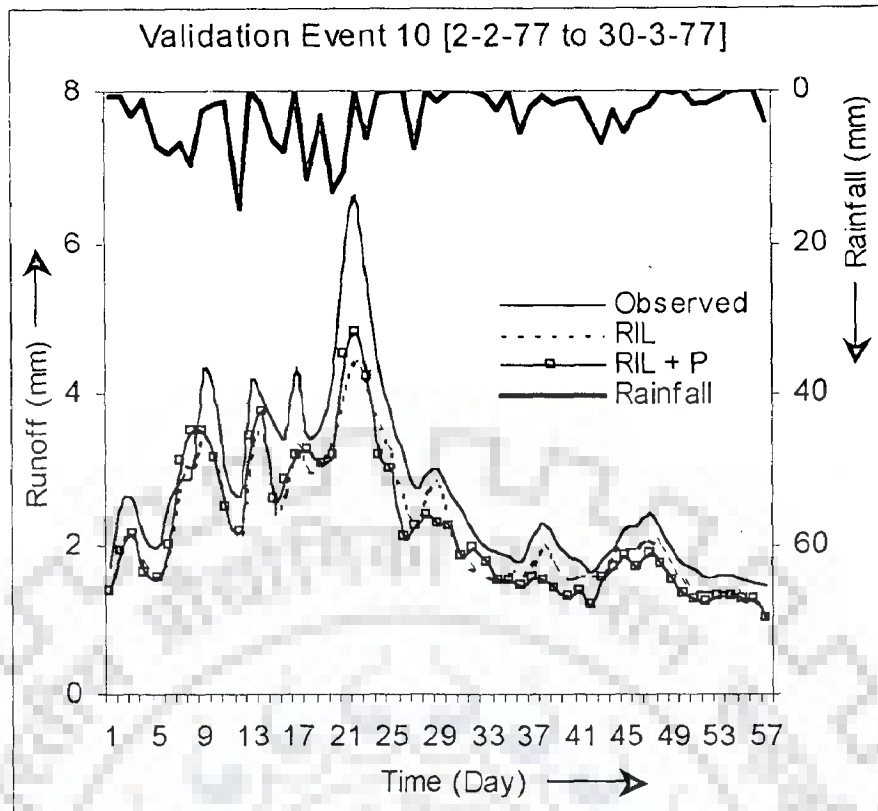
v) Pampanga Catchment

Fig. 6.1(c) Linear Scale Plots For Calibration Event For Catchment Without Sub-Divisions (Linear Model + ANN)

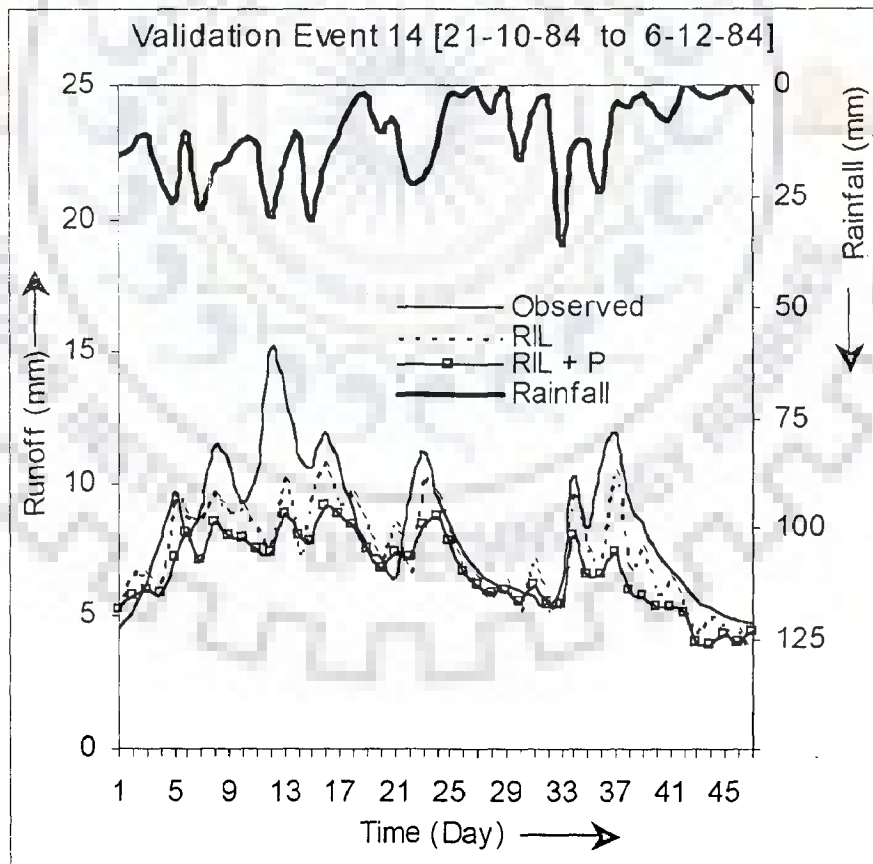


i) Bird Creek Catchment

Fig. 6.2(a) Linear Scale Plots For Validation Event For Catchment Without Sub-Divisions (Linear Model + ANN)

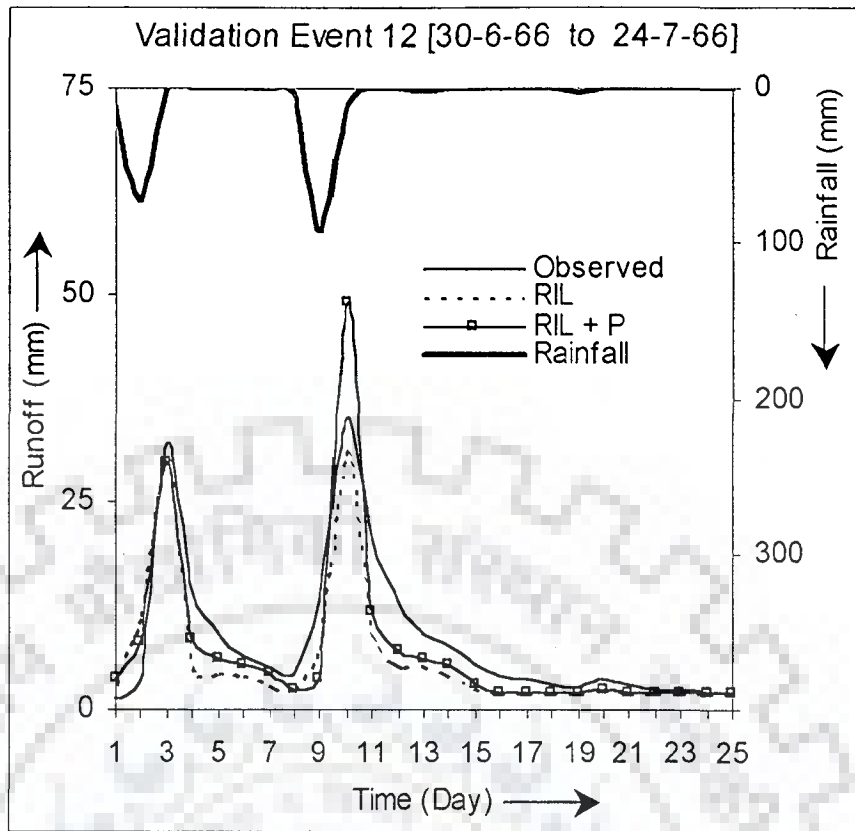


ii) Brosna Catchment

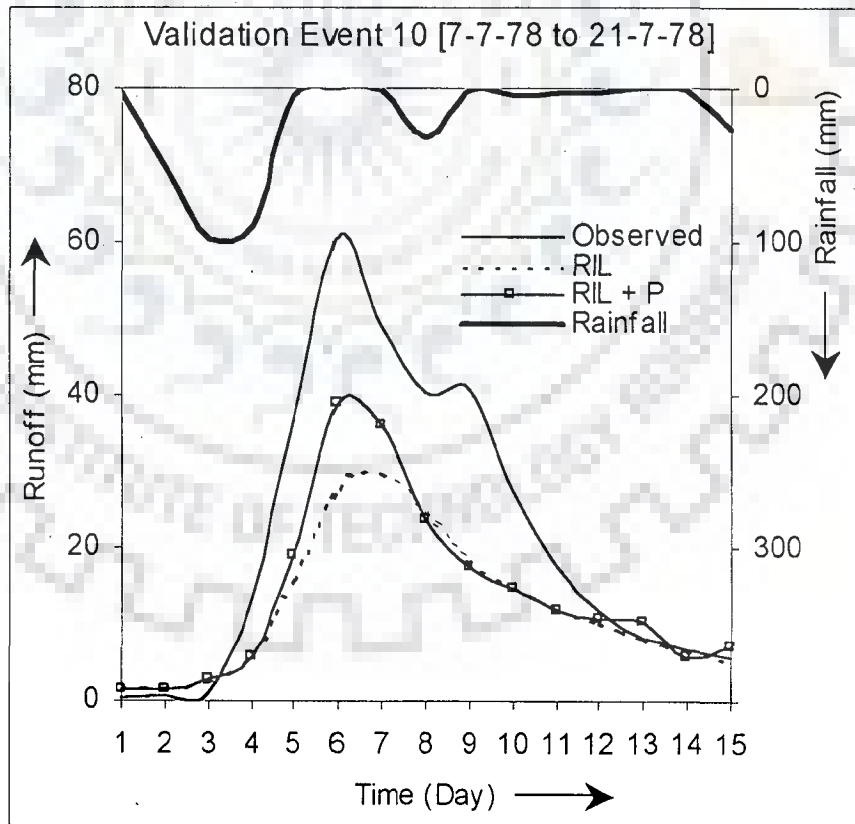


iii) Garrapatos Catchment

Fig.6.2(b) Linear Scale Plots For Validation Event For Catchment Without Sub-Divisions (Linear Model + ANN)

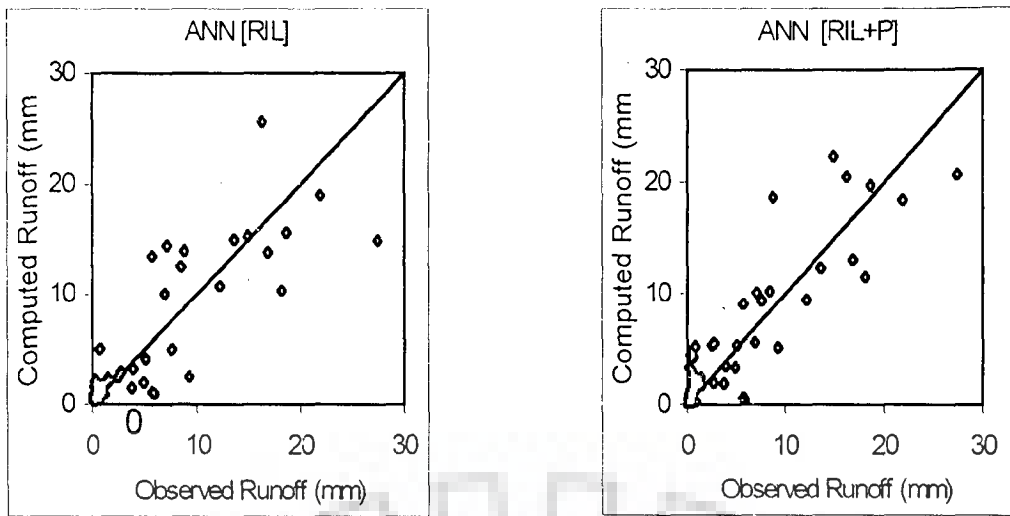


iv) Kizu Catchment

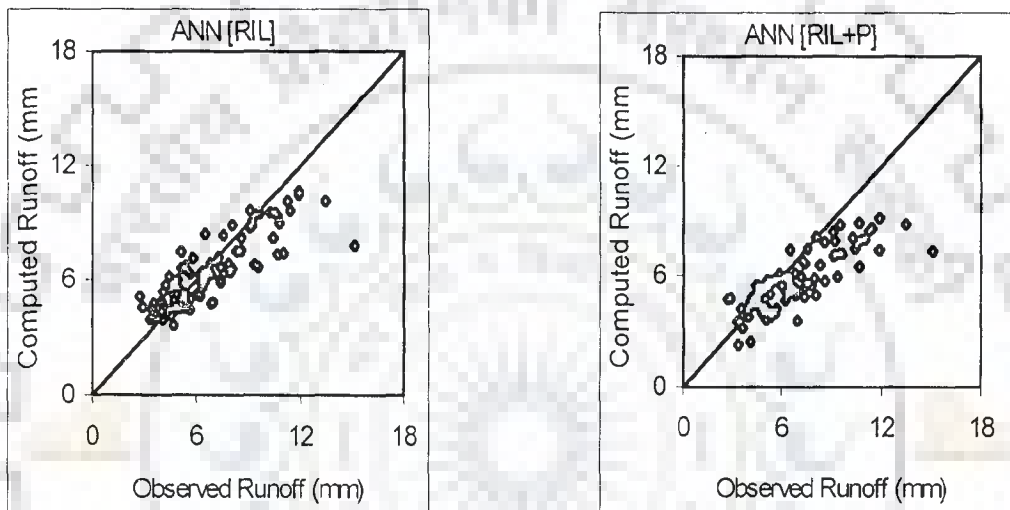


v) Pampanga Catchment

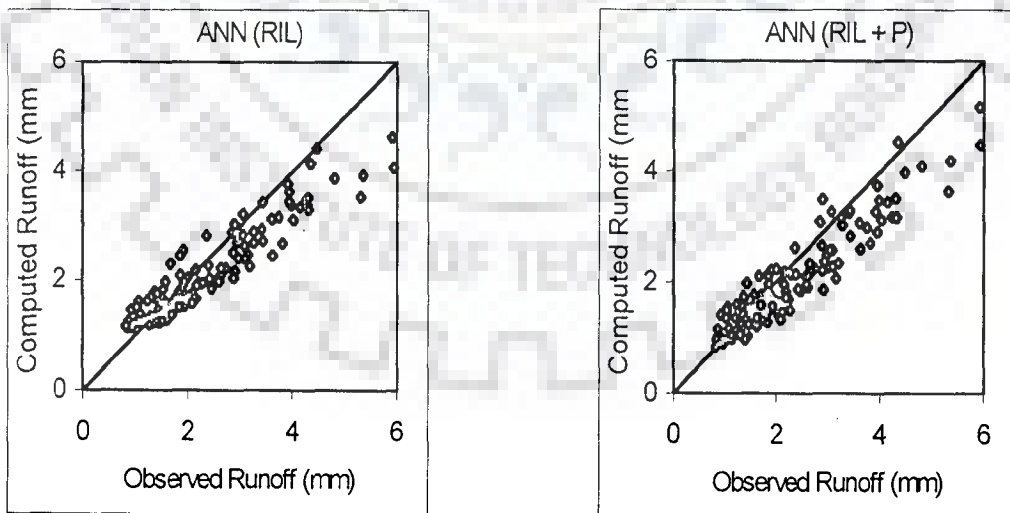
Fig. 6.2(c) Linear Scale Plots For Validation Event For Catchment Without Sub-Divisions (Linear Model + ANN)



i) Bird Creek Catchment

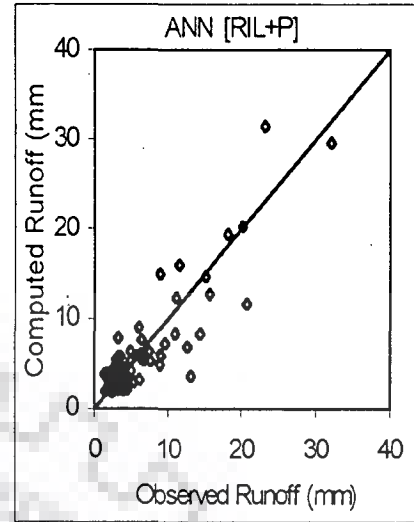
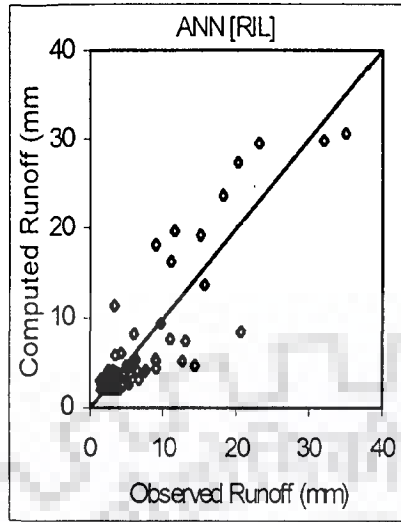


ii) Brosna Catchment

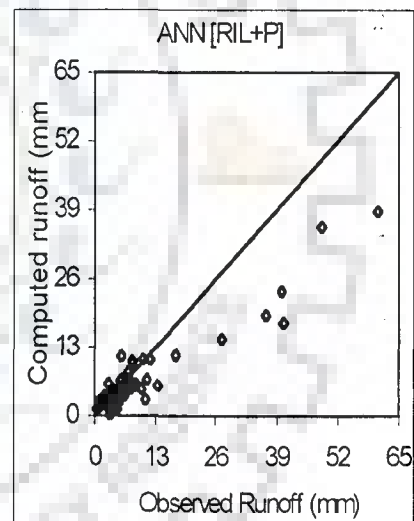
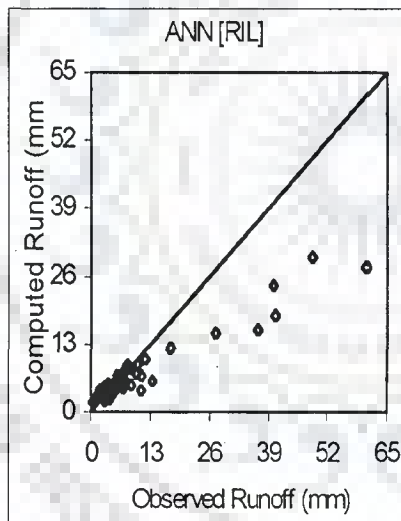


iii) Garrapatas Catchment

Fig. 6.3(a) Scatter Plots For Catchments Without Sub-Divisions (Validation – Linear Model + ANN)

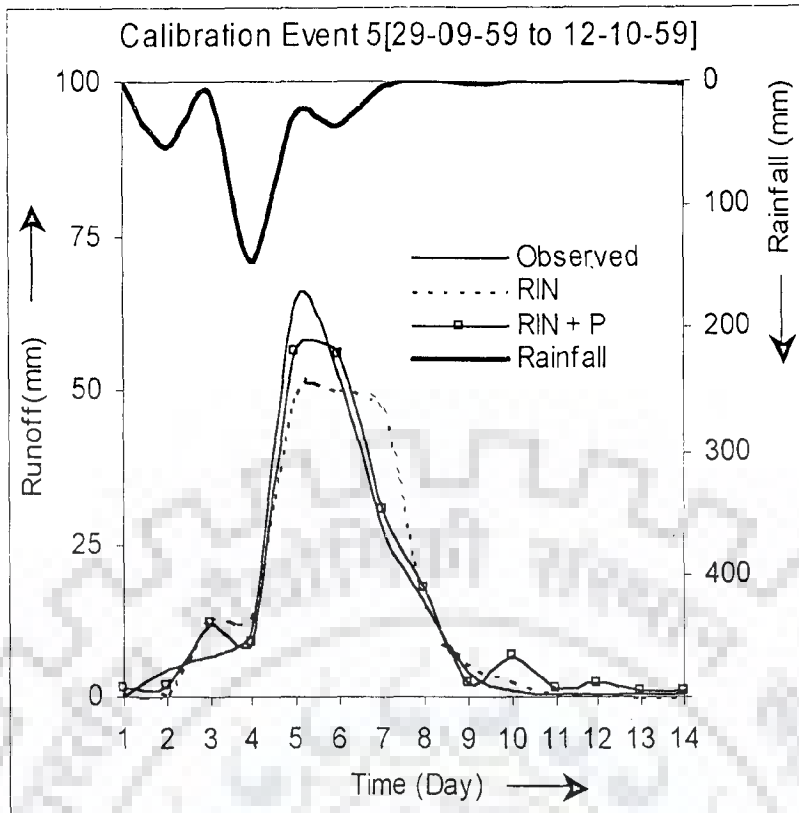


iv) Kizu Catchment

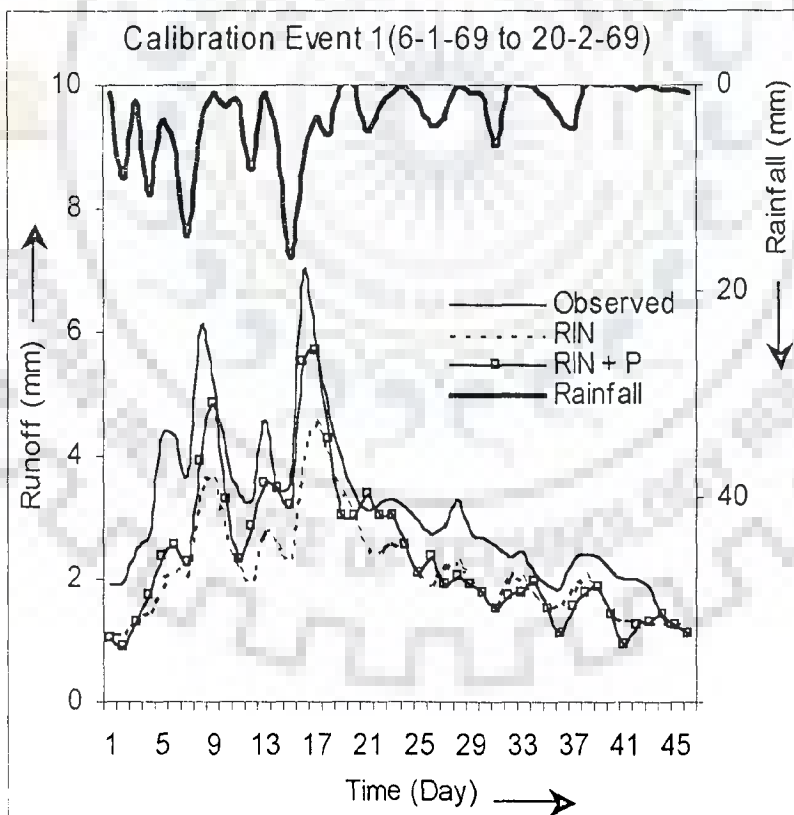


v) Pampanga Catchment

Fig. 6.3(b) Scatter Plots For Catchments Without Sub-Divisions (Validation – Linear Model + ANN)

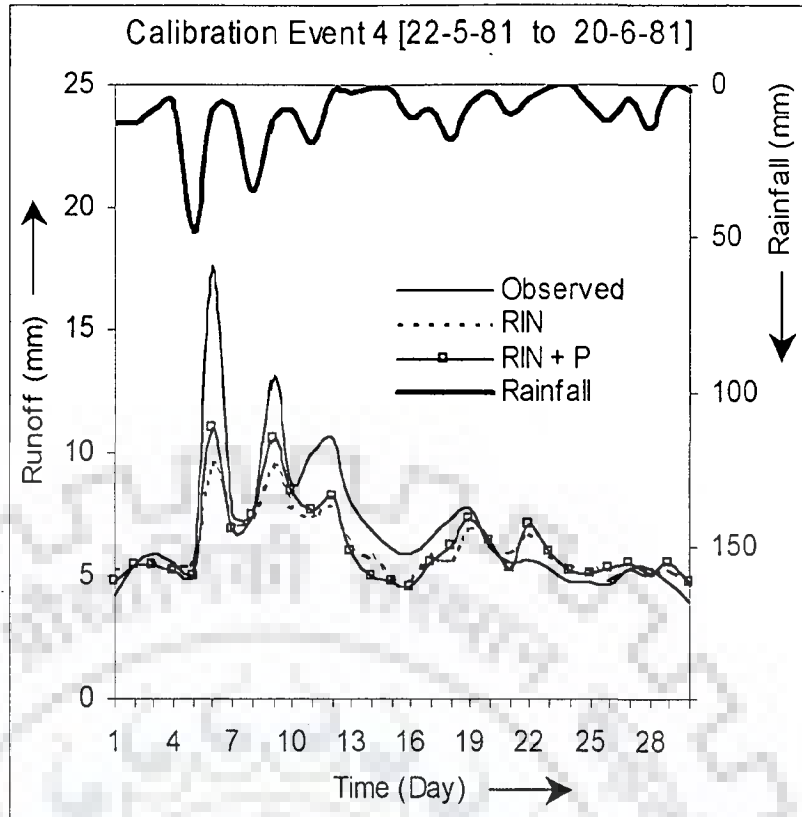


i) Bird Creek Catchment

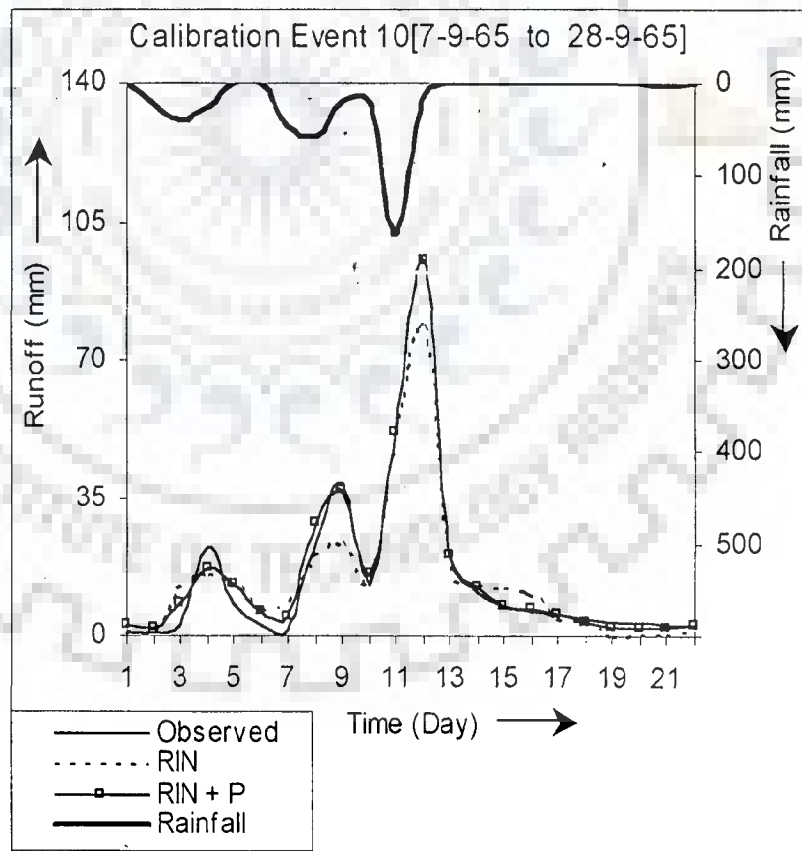


ii) Brosna Catchment

Fig. 6.4(a) Linear Scale Plots For Calibration Event For Catchment Without Sub-Divisions (Nonlinear Model + ANN)

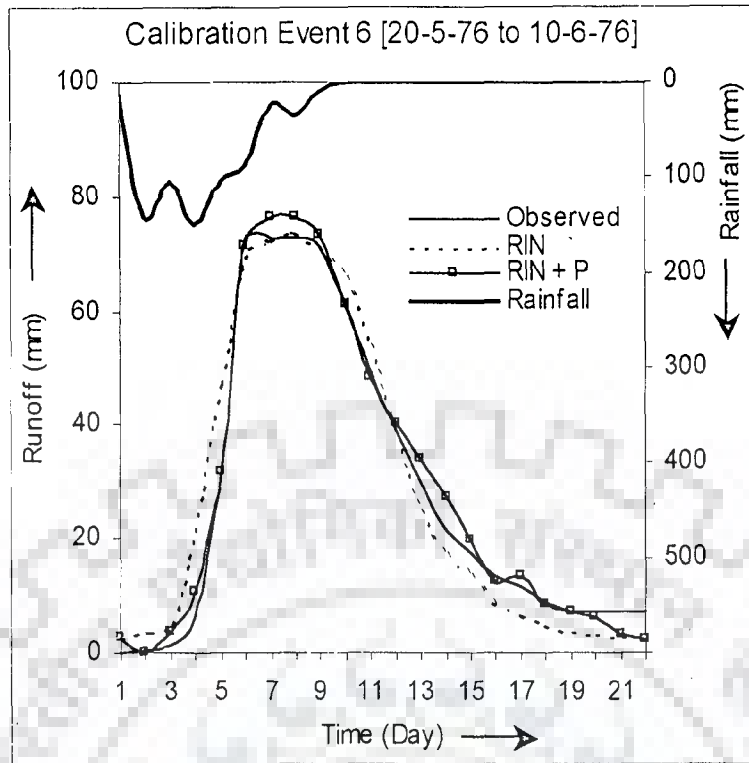


iii) Garrapatas Catchment



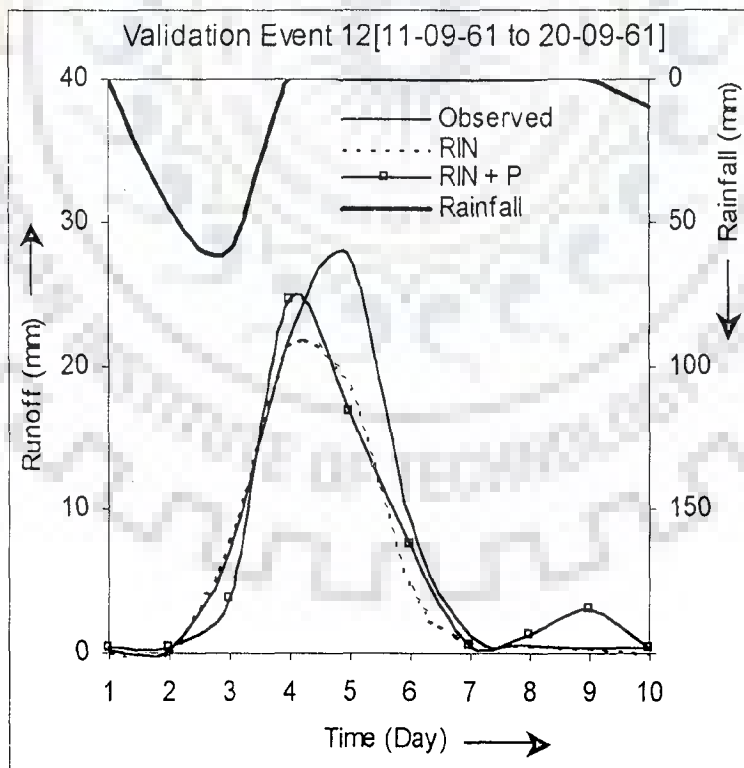
iv) Kizu Catchment

Fig. 6.4(b) Linear Scale Plots For Calibration Event For Catchment Without Sub-Divisions (Nonlinear Model + ANN)



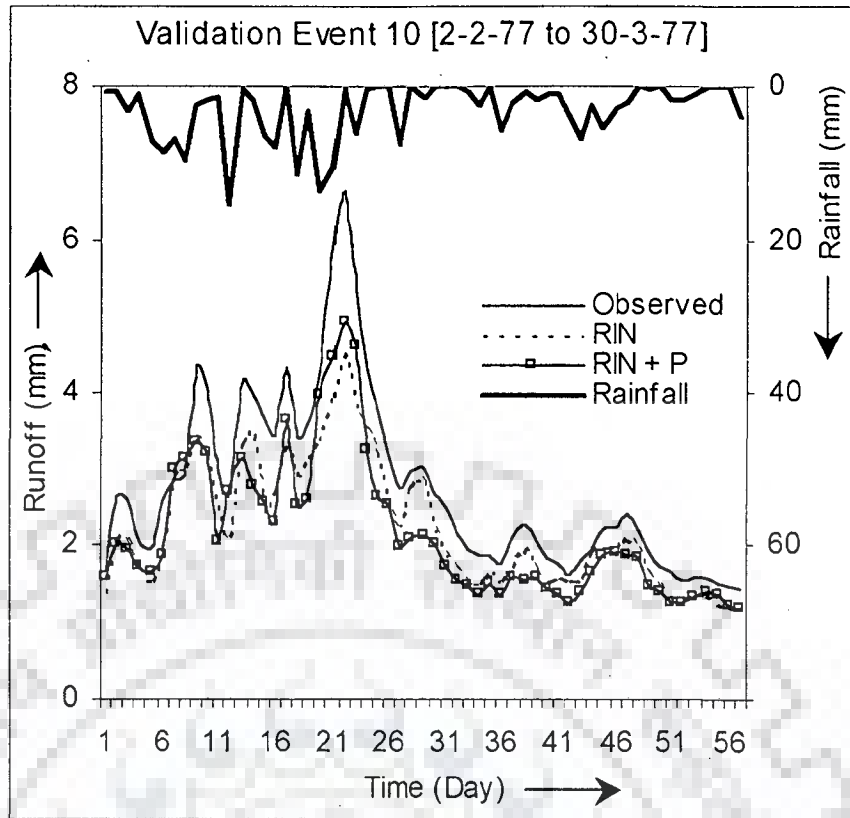
v) Pampanga Catchment

Fig. 6.4(c) Linear Scale Plots For Calibration Event For Catchment Without Sub-Divisions (Nonlinear Model + ANN)

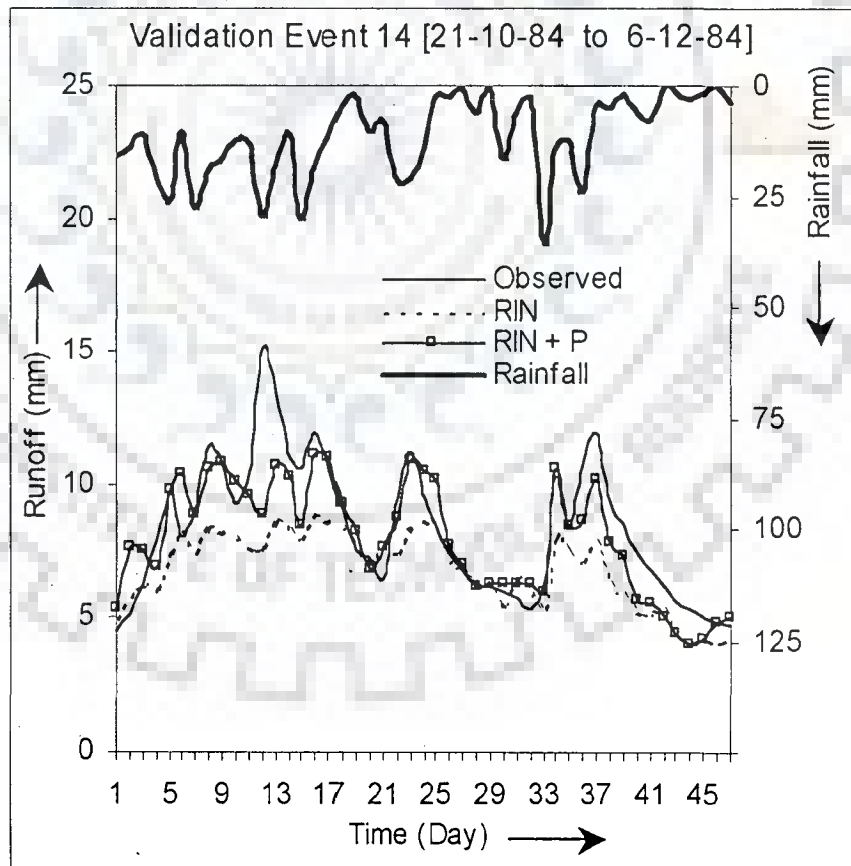


i) Bird Creek Catchment

Fig. 6.5(a) Linear Scale Plots For Validation Event For Catchment Without Sub-Divisions (Nonlinear Model + ANN)

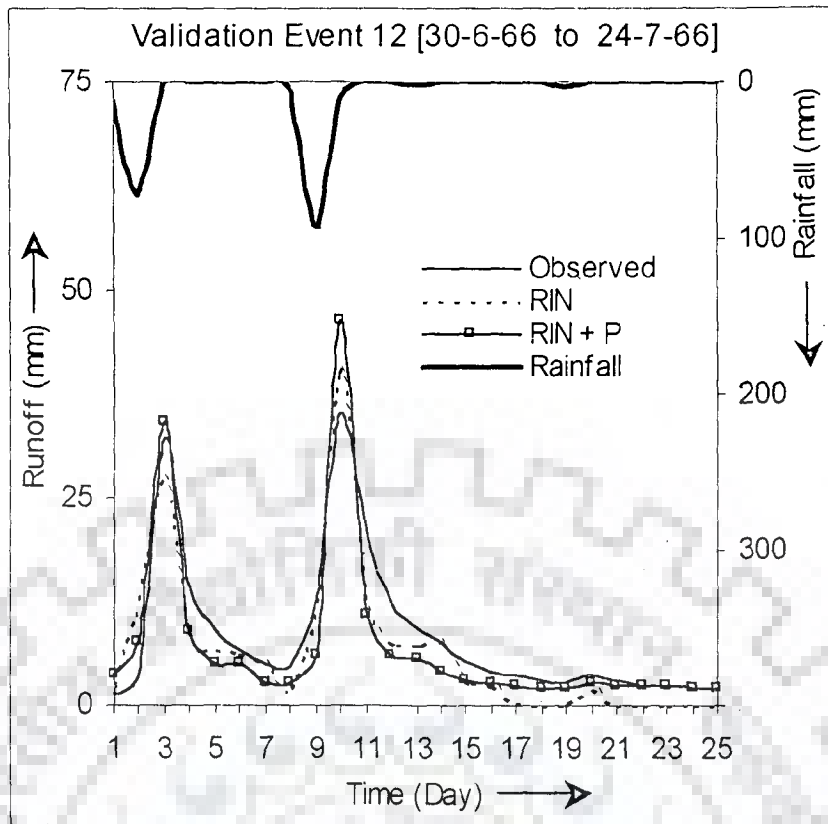


ii) Brosna Catchment

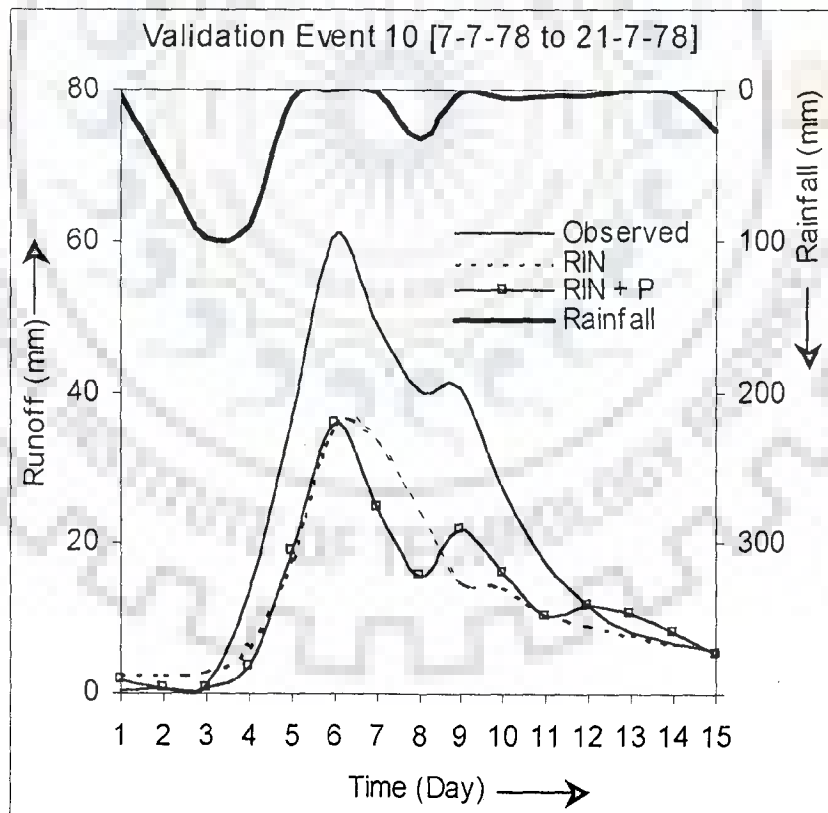


iii) Garrapatas Catchment

Fig. 6.5(b) Linear Scale Plots For Validation Event For Catchment Without Sub-Divisions (Nonlinear Model + ANN)

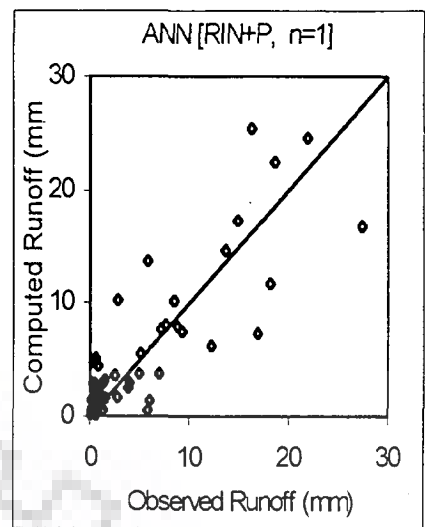
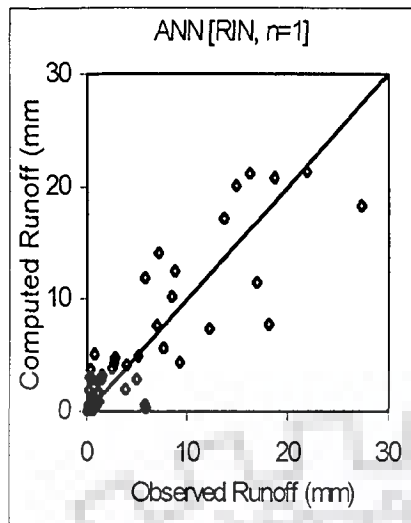


iv) Kizu Catchment

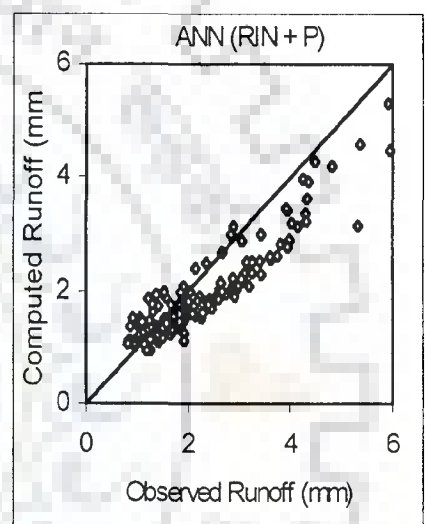
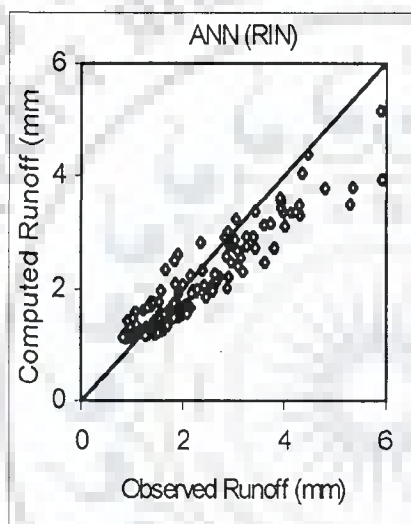


v) Pampanga Catchment

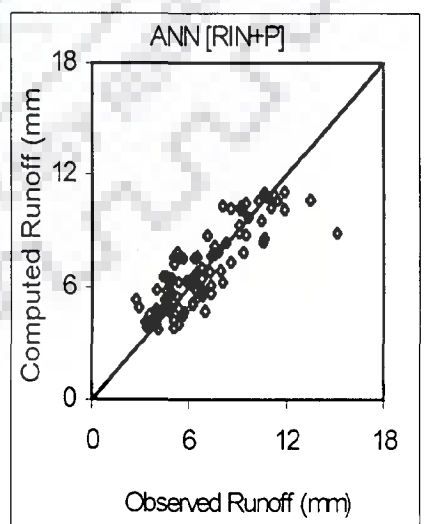
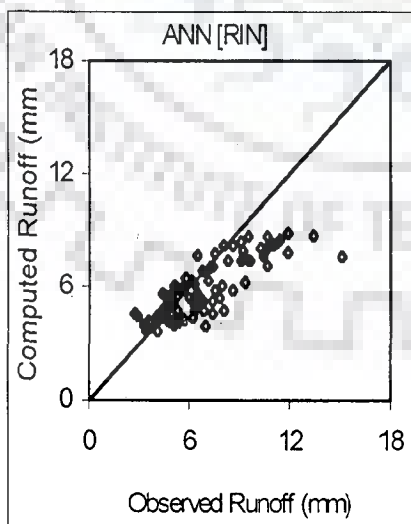
Fig. 6.5(c) Linear Scale Plots For Validation Event For Catchment Without Sub-Divisions (Nonlinear Model + ANN)



i) Bird Creek Catchment

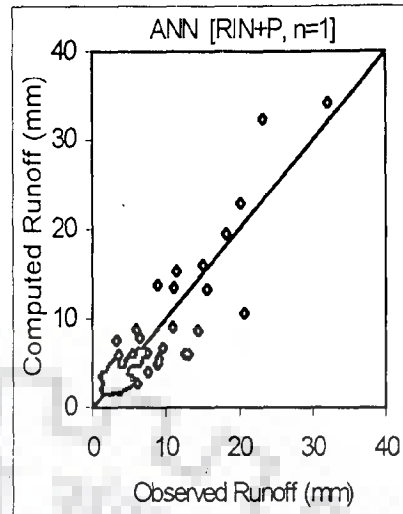
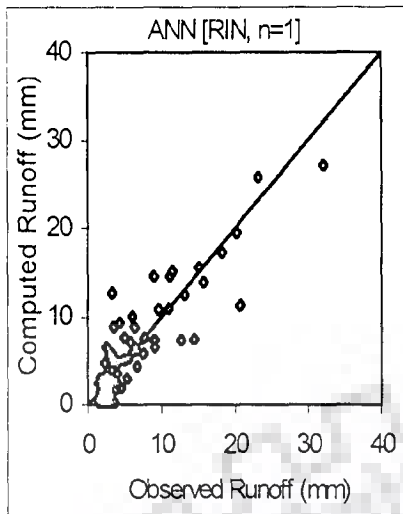


ii) Brosna Catchment

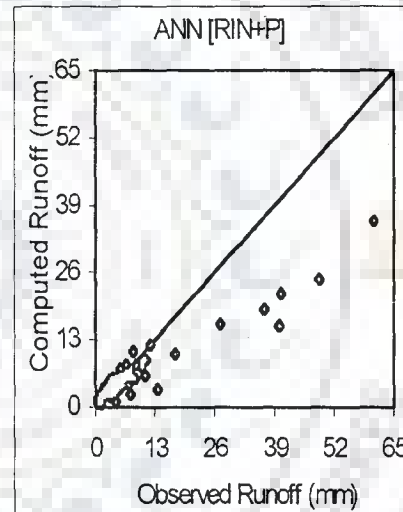
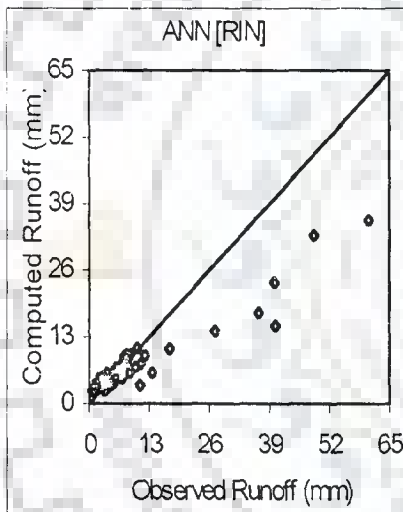


iii) Garrapatas Catchment

Fig. 6.6(a) Scatter Plots For Catchments Without Sub-Divisions (Validation – Nonlinear Model + ANN)

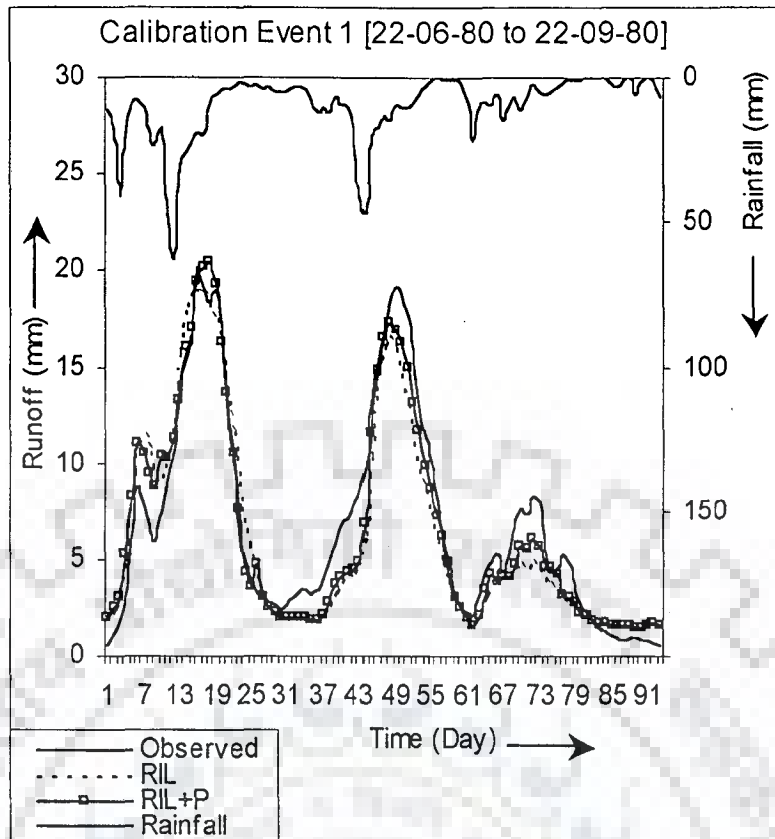


iv) Kizu Catchment

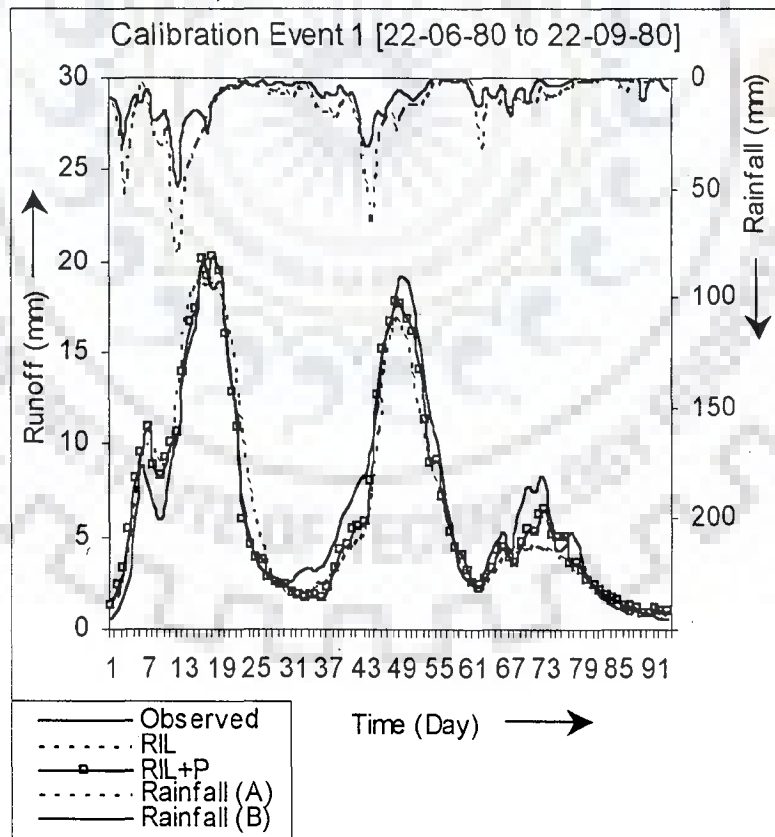


v) Pampanga Catchment

Fig. 6.6(b) Scatter Plots For Catchments Without Sub-Divisions
(Validation – Nonlinear Model + ANN)

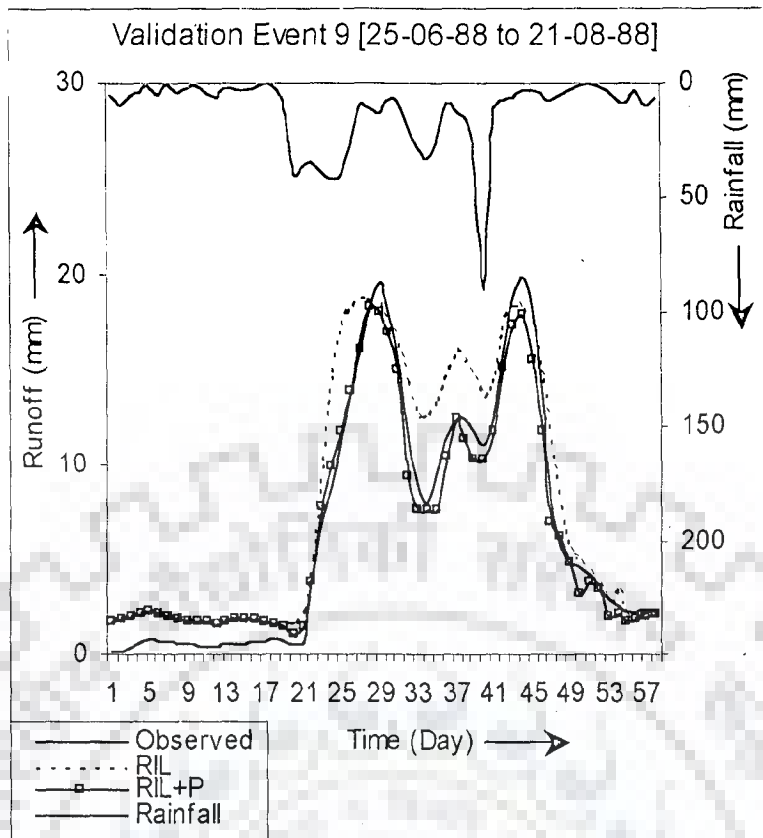


i) No Sub-Division Scenario

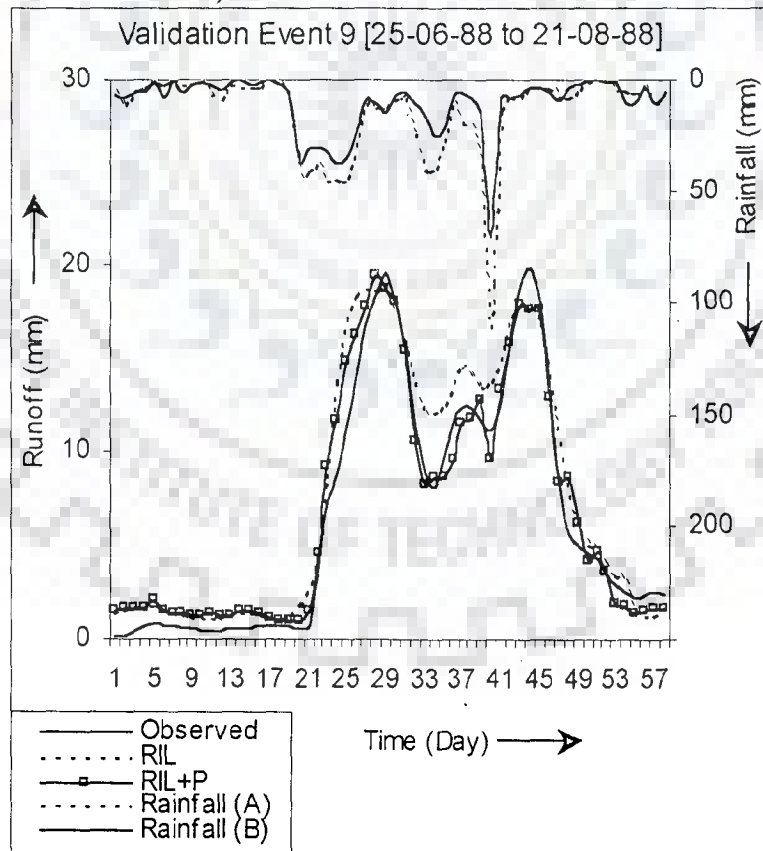


ii) Two Sub-Divisions Scenario

Fig. 6.7(a) Linear Scale Plots For Calibration Event in Krishna Catchment (Linear Model + ANN)

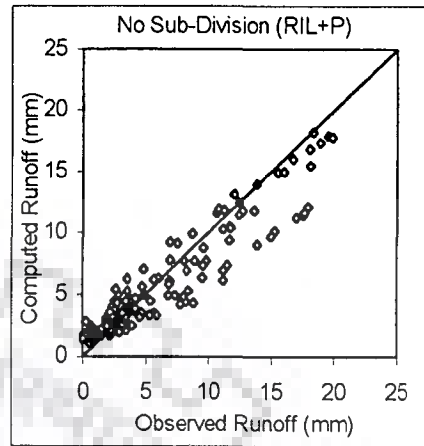
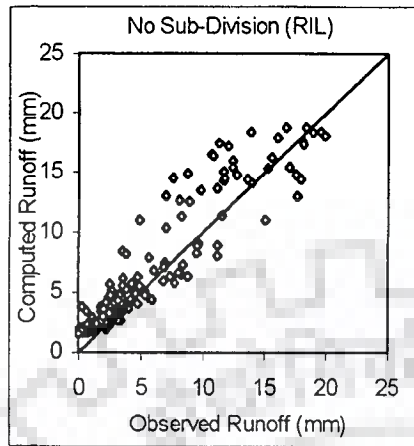


i) No Sub-Division Scenario



ii) Two Sub-Divisions Scenario

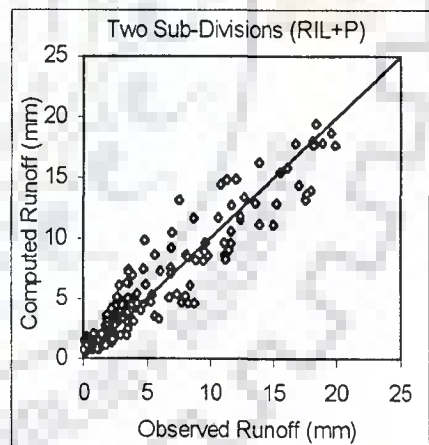
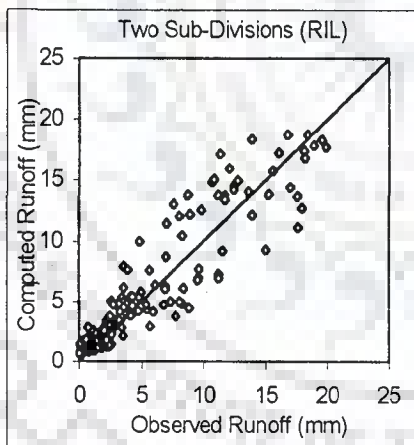
Fig. 6.7(b) Linear Scale Plots For Validation Event in Krishna Catchment (Linear Model + ANN)



i) ANN (RIL)

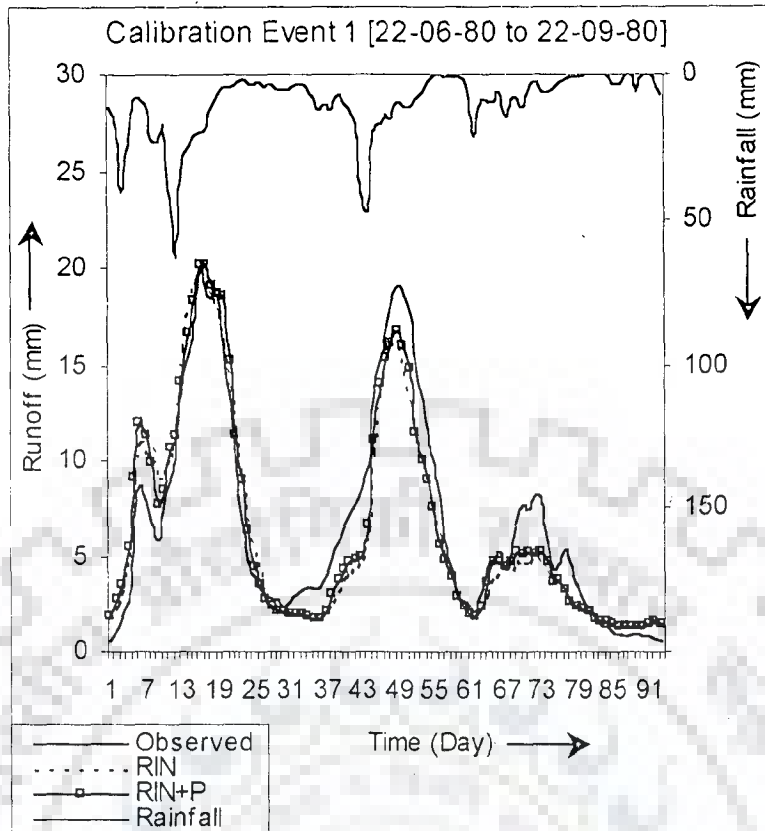
ii) ANN (RIL+P)

a) No Sub-Division Scenario

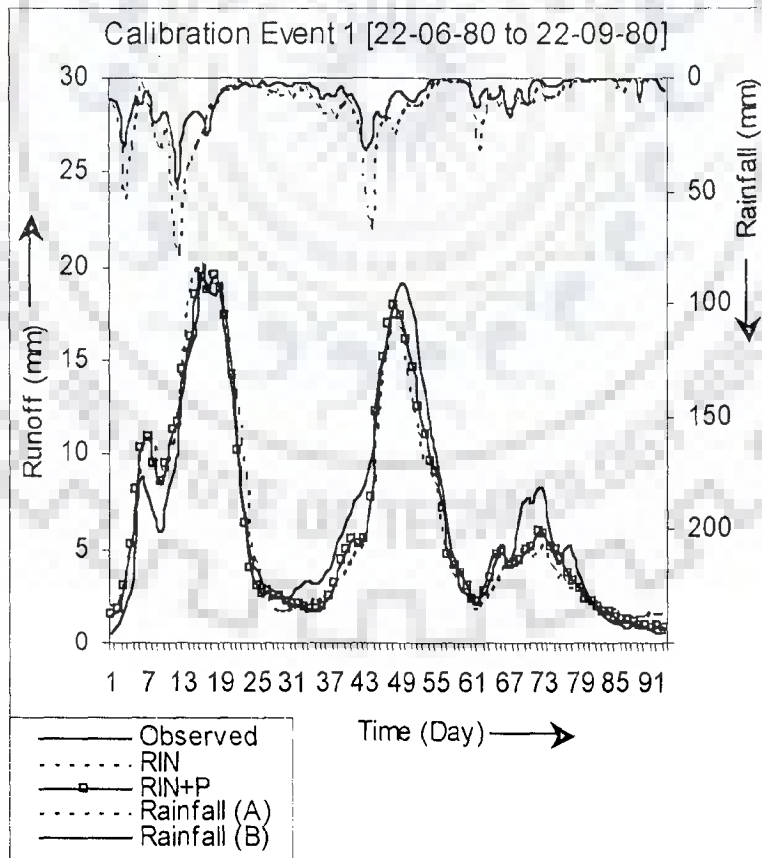


b) Two Sub-Divisions Scenario

Fig. 6.8 Scatter Plots For Validation in Krishna Catchment (Linear Model + ANN)

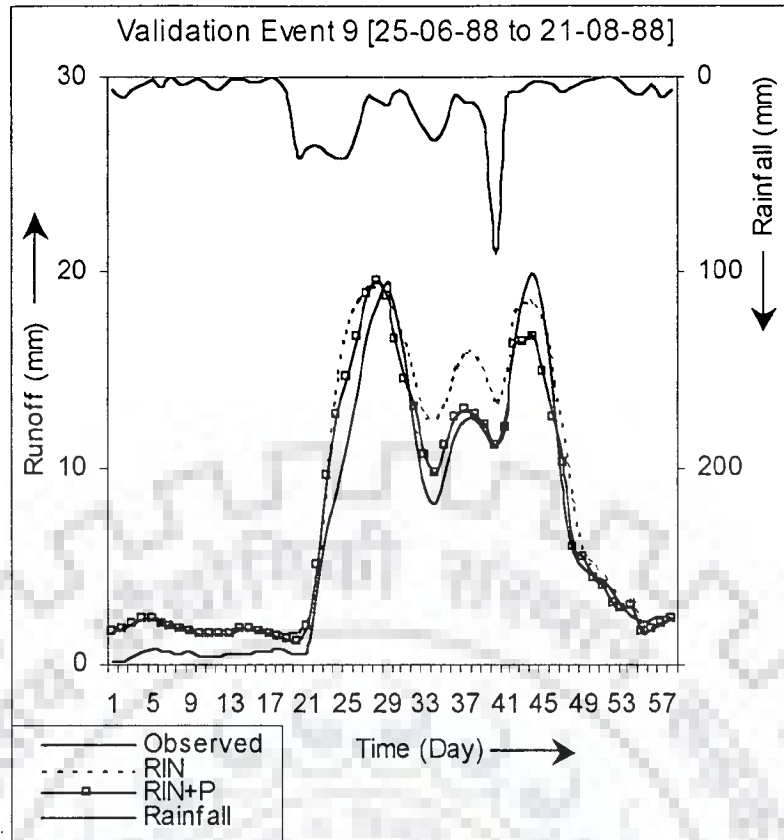


i) No Sub-Division Scenario

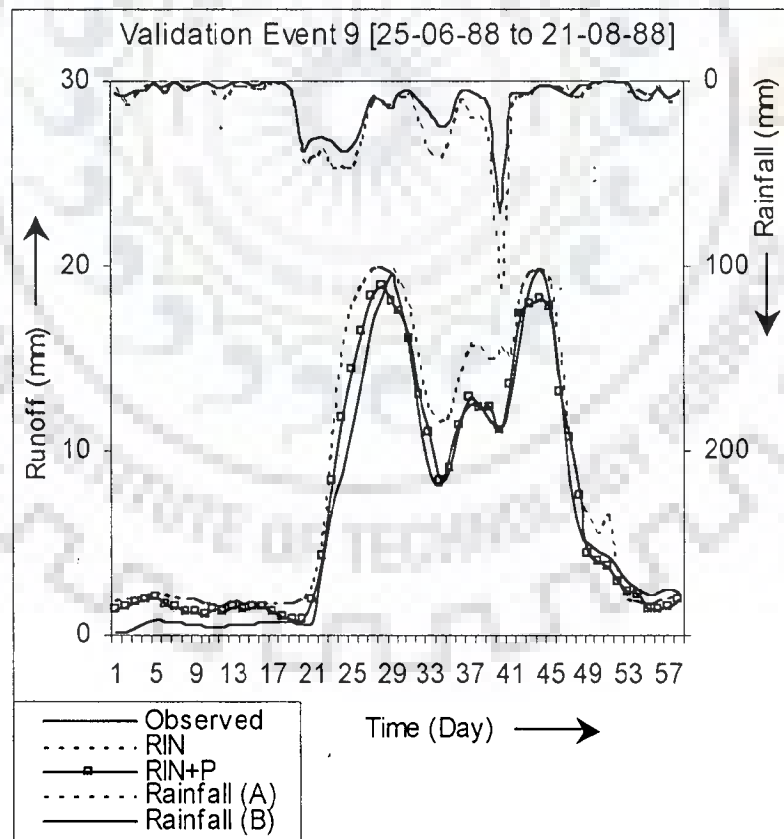


ii) Two Sub-Divisions Scenario

Fig. 6.9(a) Linear Scale Plots For Calibration Event in Krishna Catchment (Nonlinear Model + ANN)

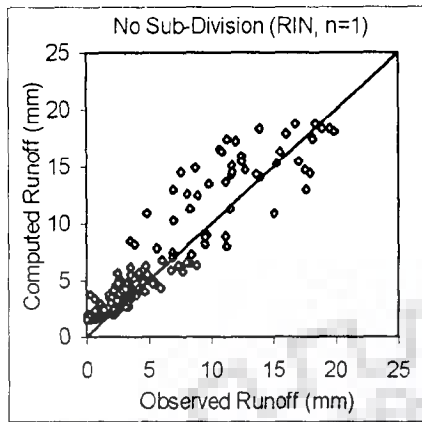


i) No Sub-Division Scenario

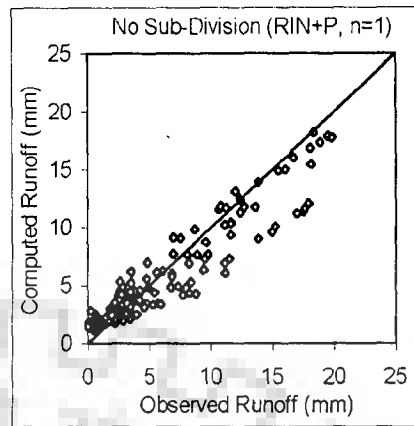


ii) Two Sub-Divisions Scenario

Fig. 6.9(b) Linear Scale Plots For Validation Event in Krishna Catchment (Nonlinear Model + ANN)

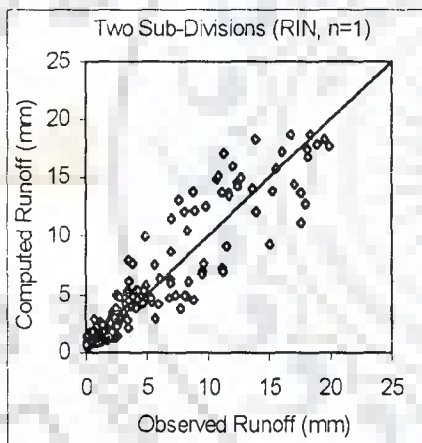


i) ANN (RIN)

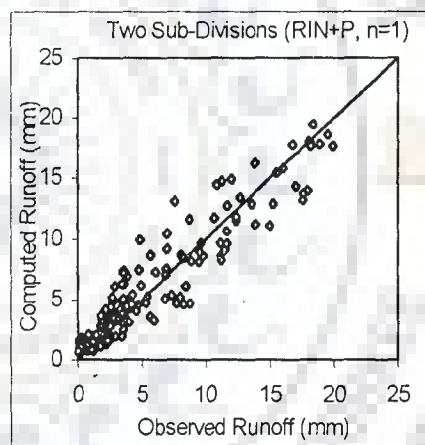


iii) ANN (RIN+P)

a) No Sub-Division Scenario



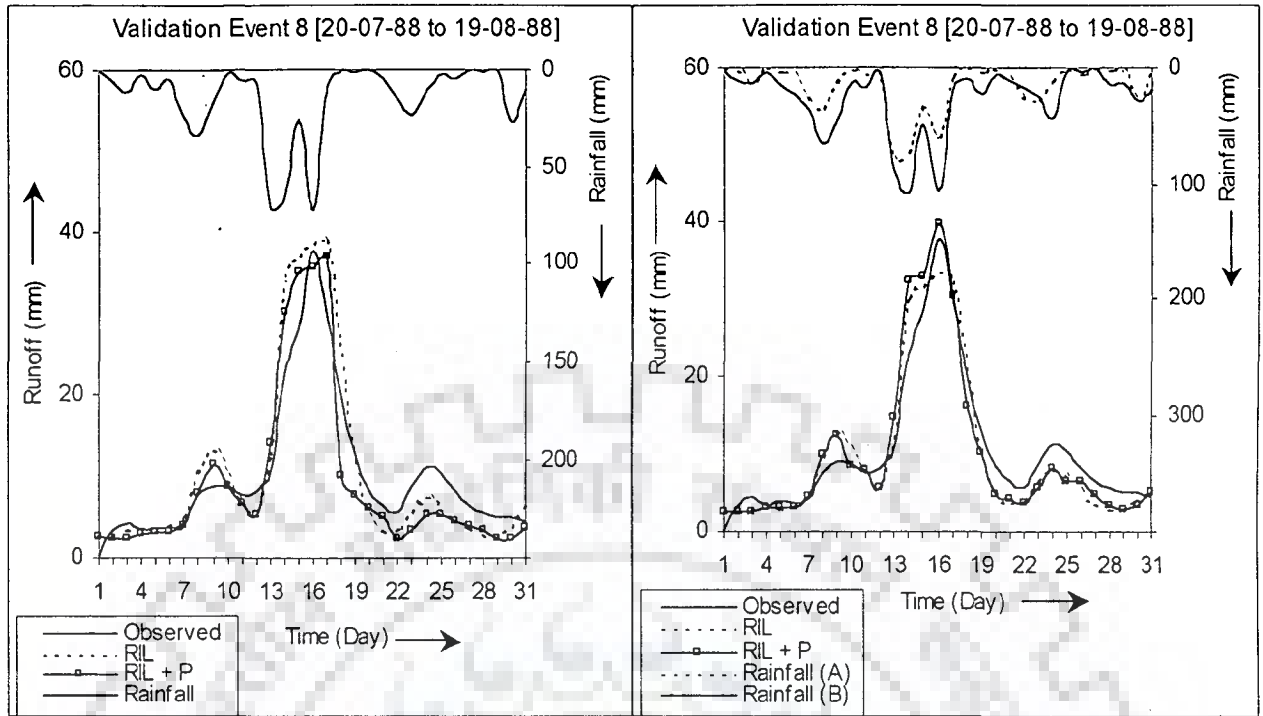
i) ANN (RIN)



ii) ANN (RIN+P)

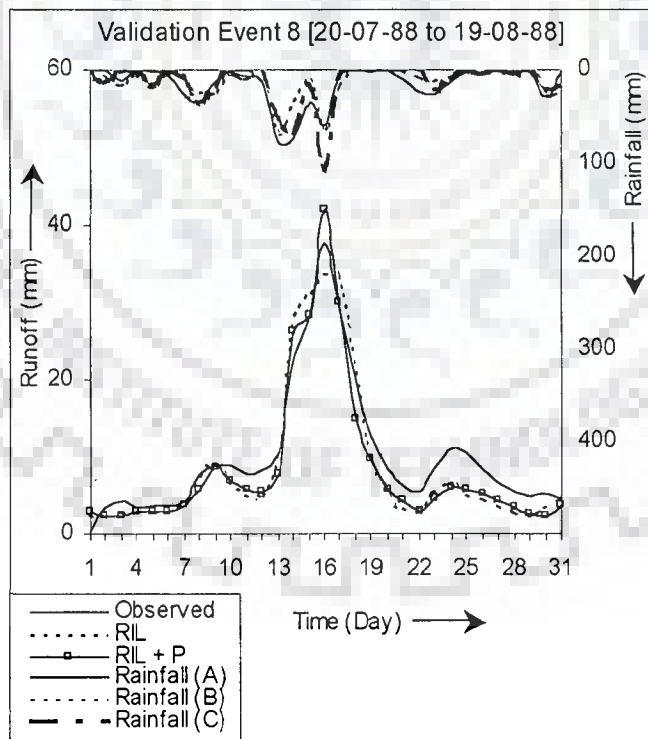
b) Two Sub-Divisions Scenario

Fig. 6.10 Scatter Plots For Validation in Krishna Catchment (Nonlinear Model + ANN)



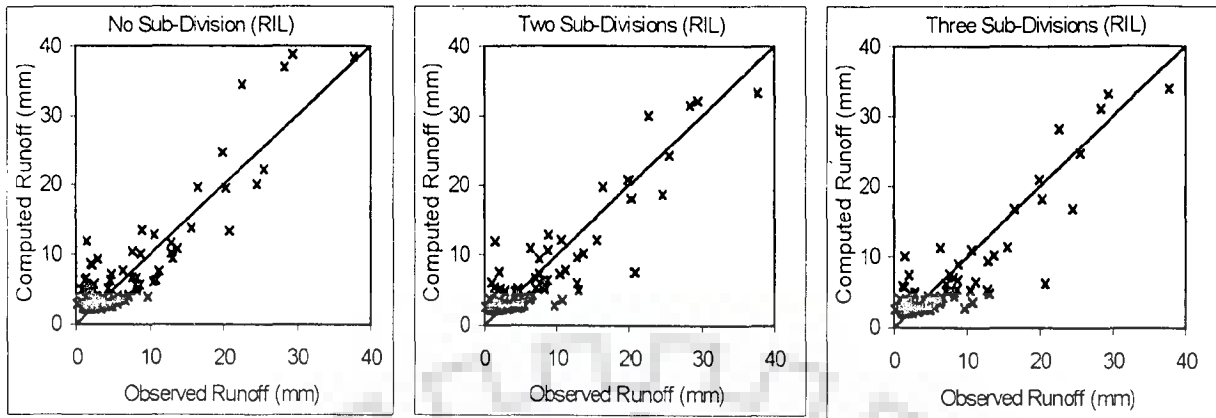
a) No Sub-Division Scenario

b) Two Sub-Divisions Scenario

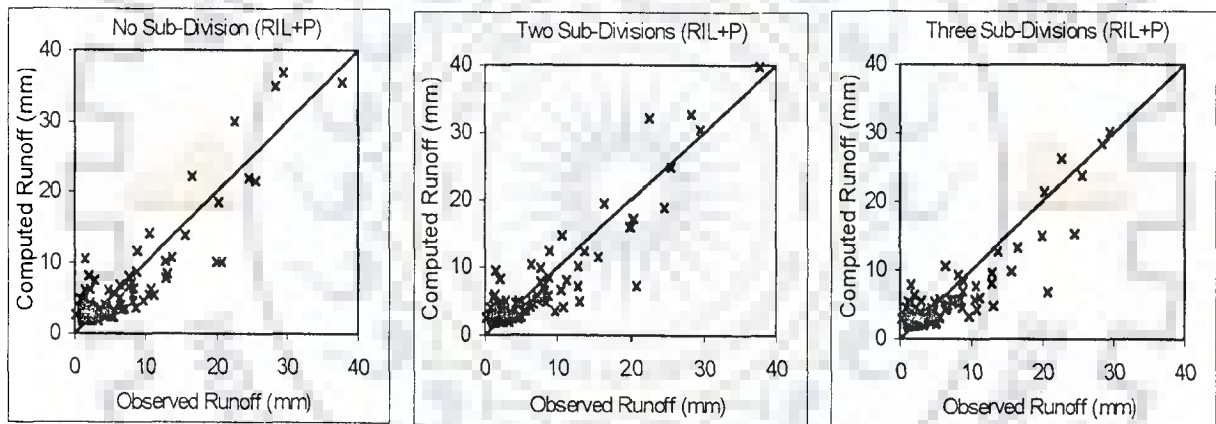


c) Three Sub-Divisions Scenario

Fig. 6.11 Linear Scale Plots For Validation Event in Narmada Catchment (Linear Model + ANN)

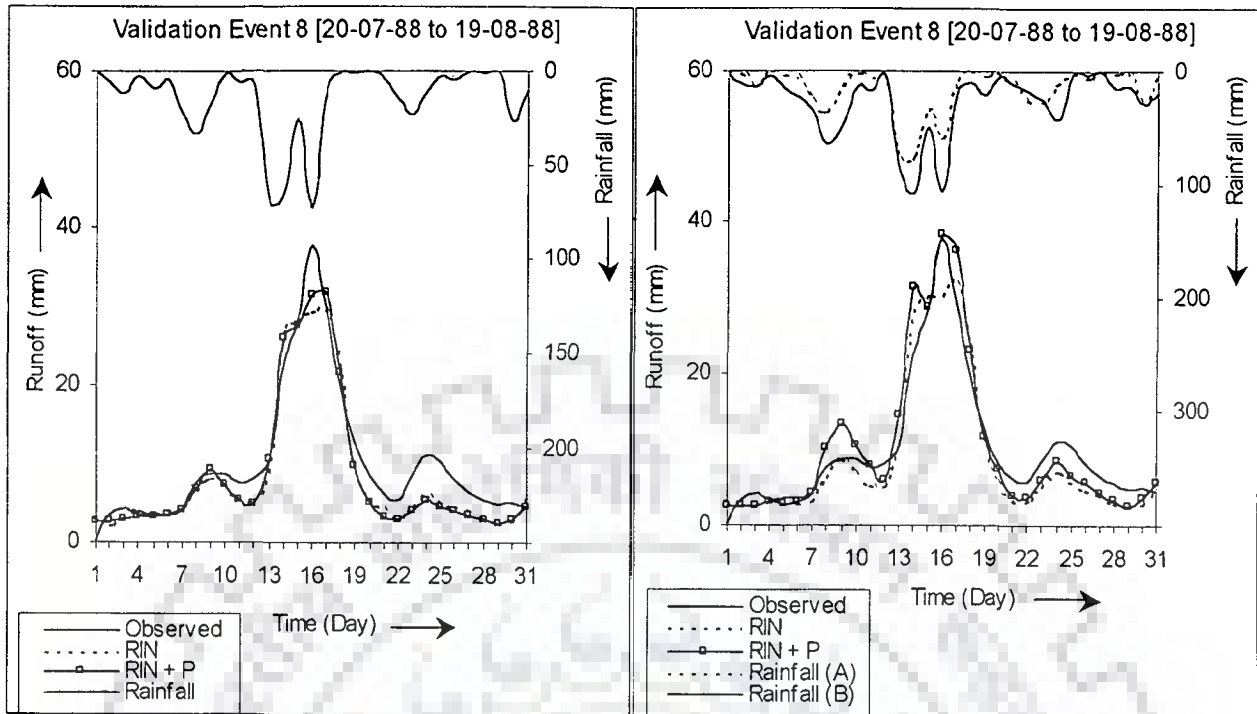


i) ANN (RIL)



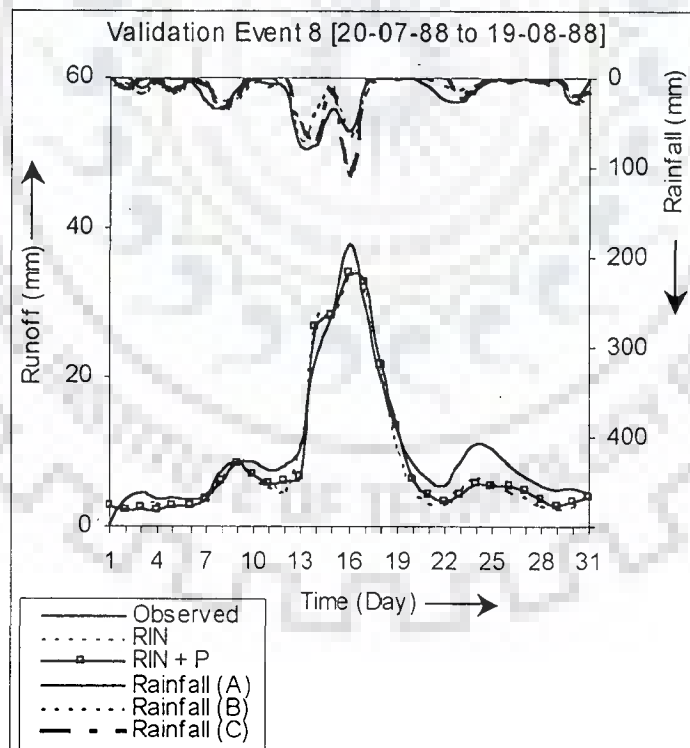
ii) ANN (RIL+P)

Fig. 6.12 Scatter Plots For Validation in Narmada Catchment (Linear Model + ANN)



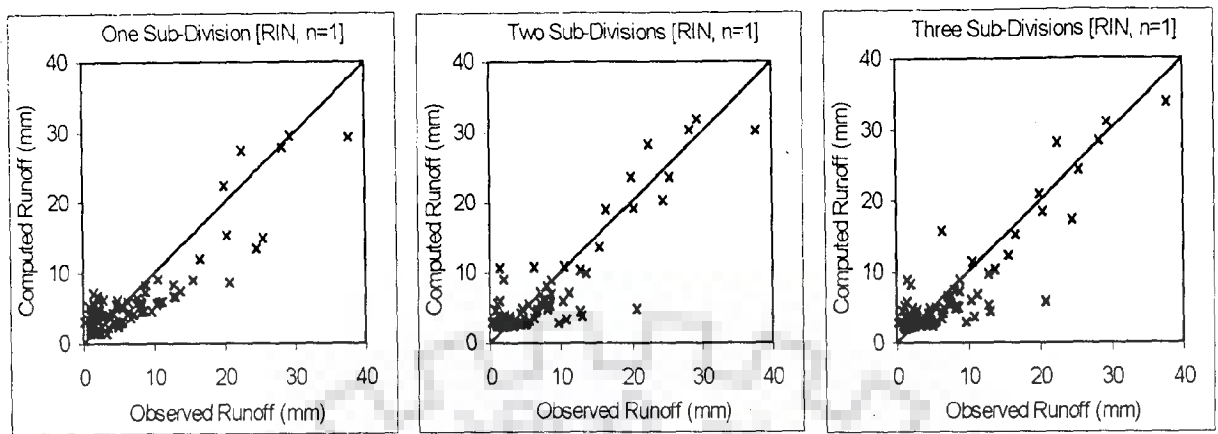
a) No Sub-Division Scenario

b) Two Sub-Divisions Scenario

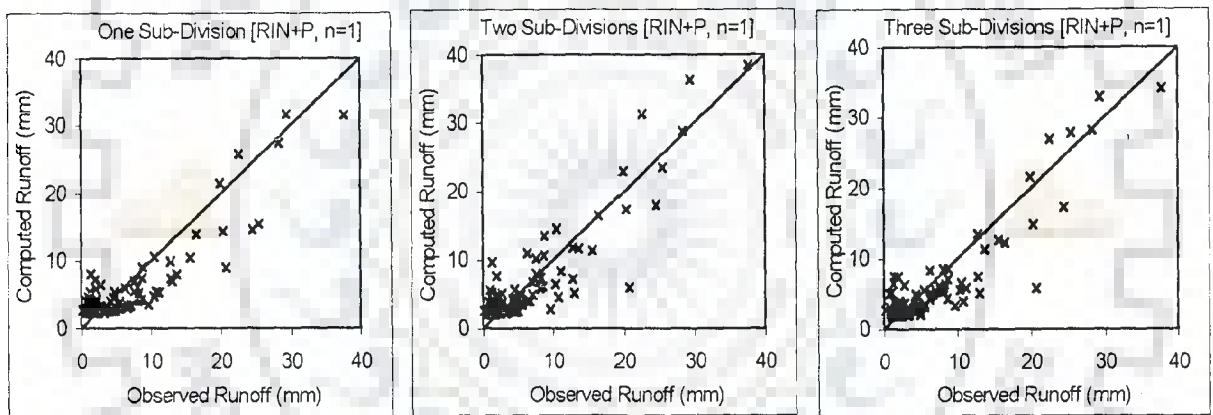


c) Three Sub-Divisions Scenario

Fig. 6.13 Linear Scale Plots For Validation Event in Narmada Catchment (Nonlinear Model + ANN)

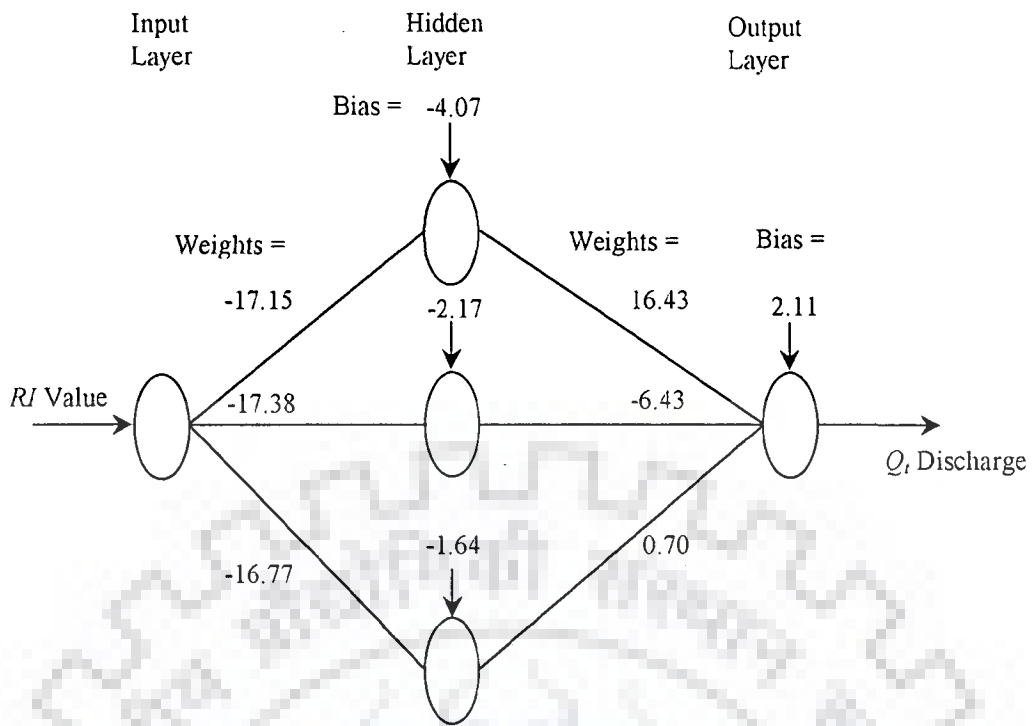


i) ANN (RIN)

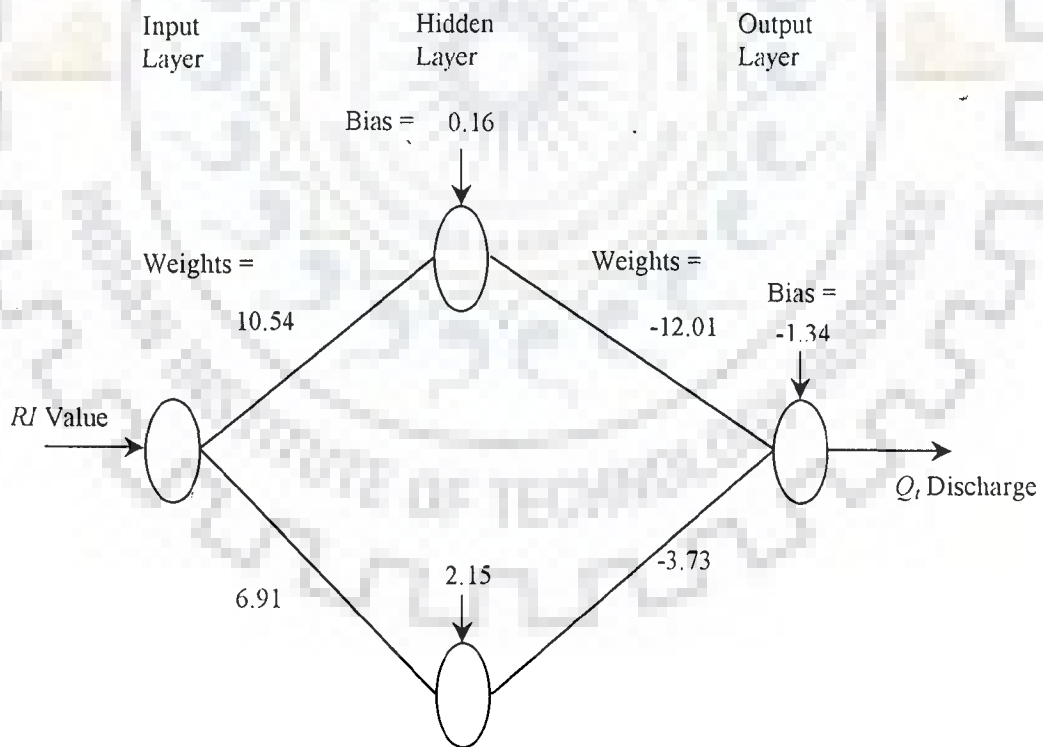


ii) ANN (RIN+P)

Fig. 6.14 Scatter Plots For Validation in Narmada Catchment (Nonlinear Model + ANN)

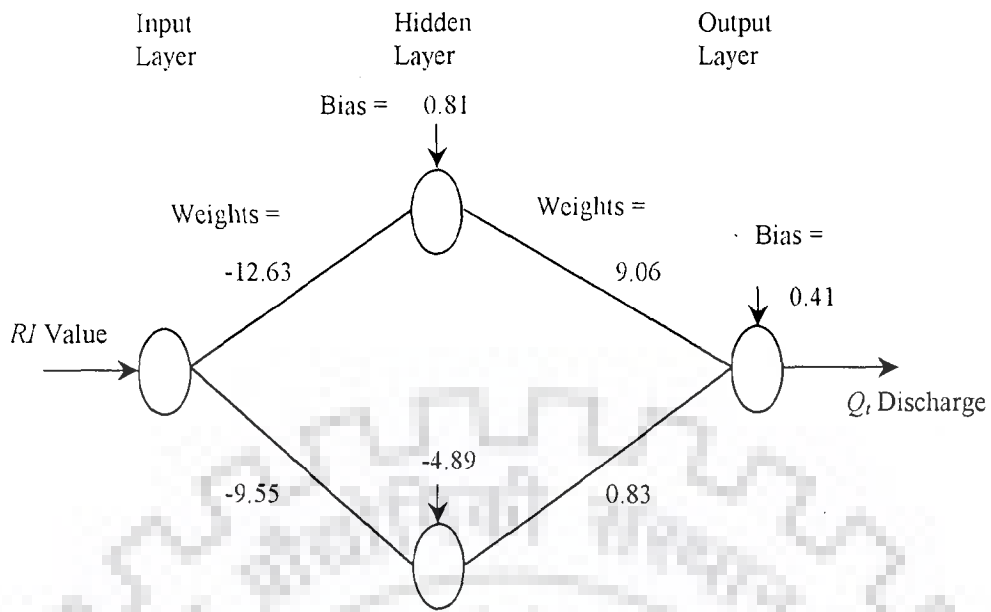


Bird Creek Catchment (1-3-1)

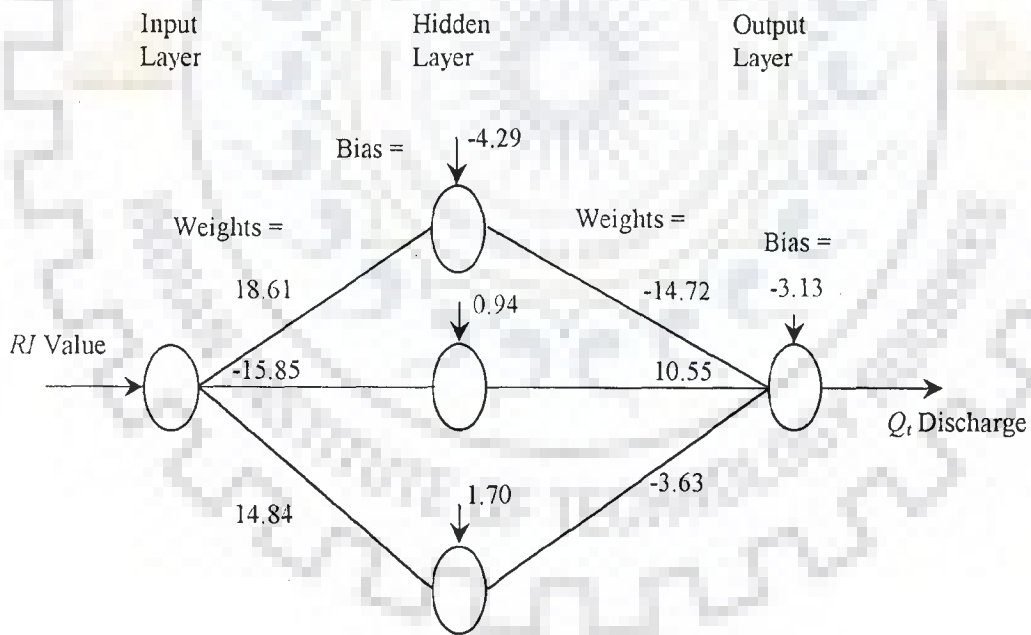


Brosna Catchment (1-2-1)

Fig. 6.15(a) The ANN Structures For Bird Creek and Brosna Catchments

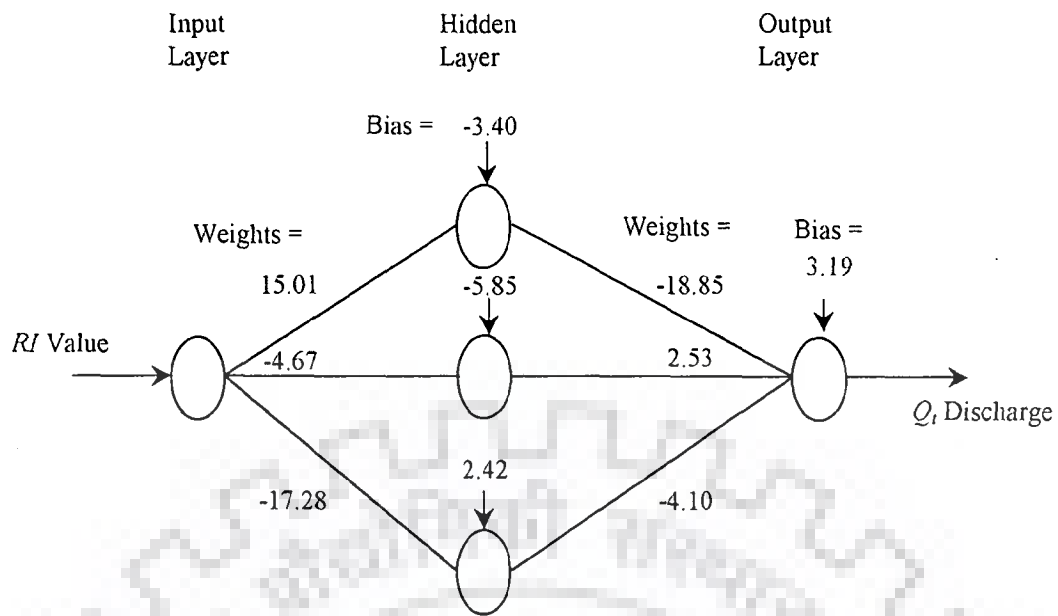


Garrapatas Catchment (1-2-1)

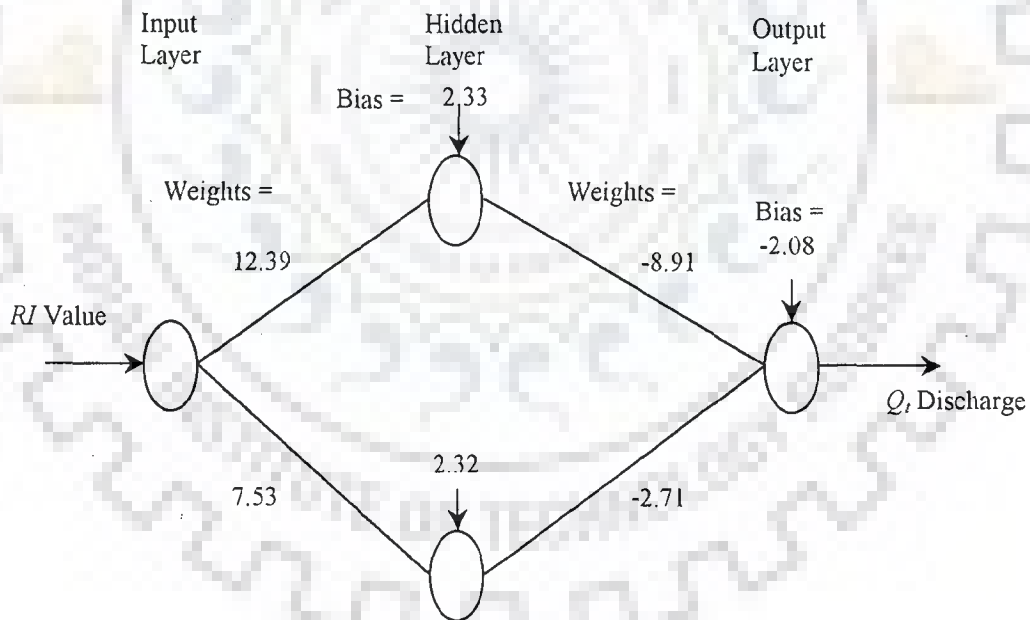


Kizu Catchment (1-3-1)

Fig. 6.15(b) The ANN Structures For Garrapatas and Kizu Catchments

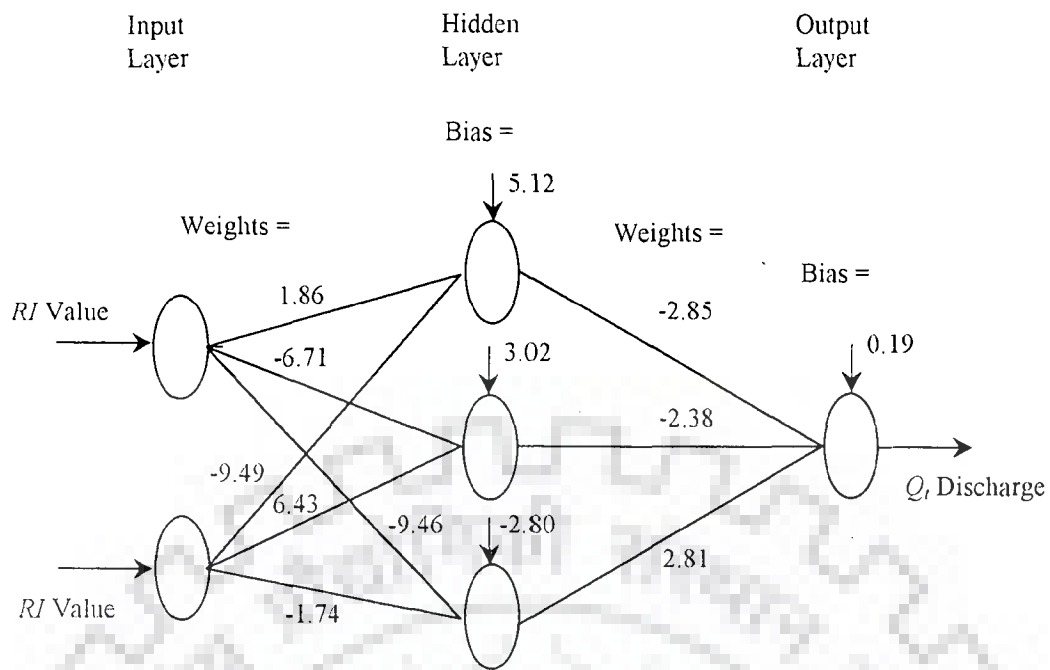


Pampanga Catchment (1-3-1)

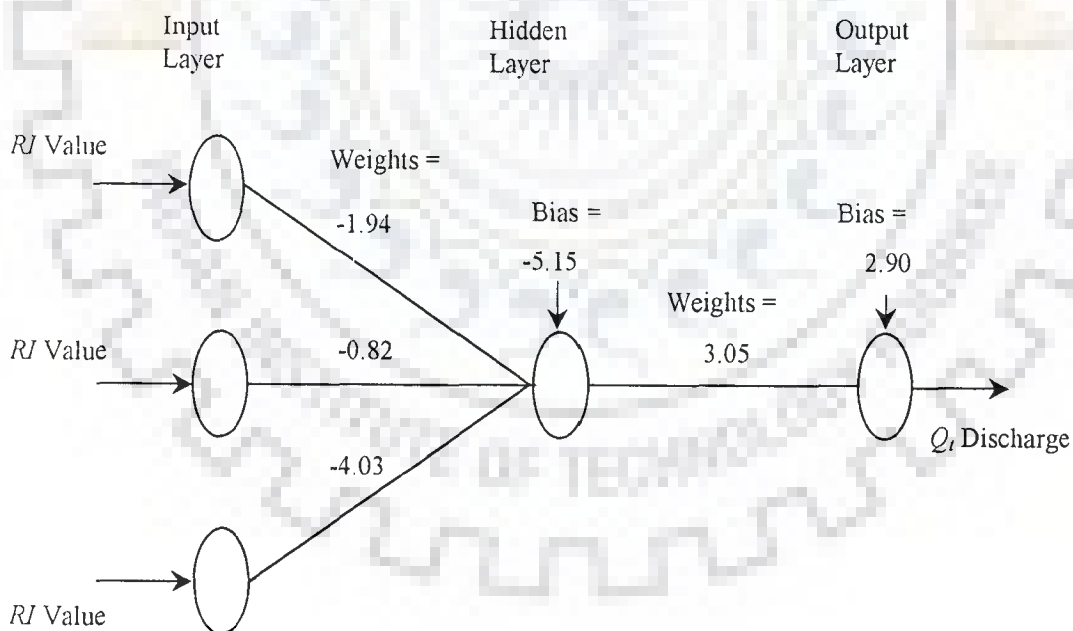


Narmada Catchment (No Sub-Division) (1-2-1)

Fig. 6.15(c) The ANN Structures For Pampanga Catchment and Narmada Catchment (No Sub-Division)

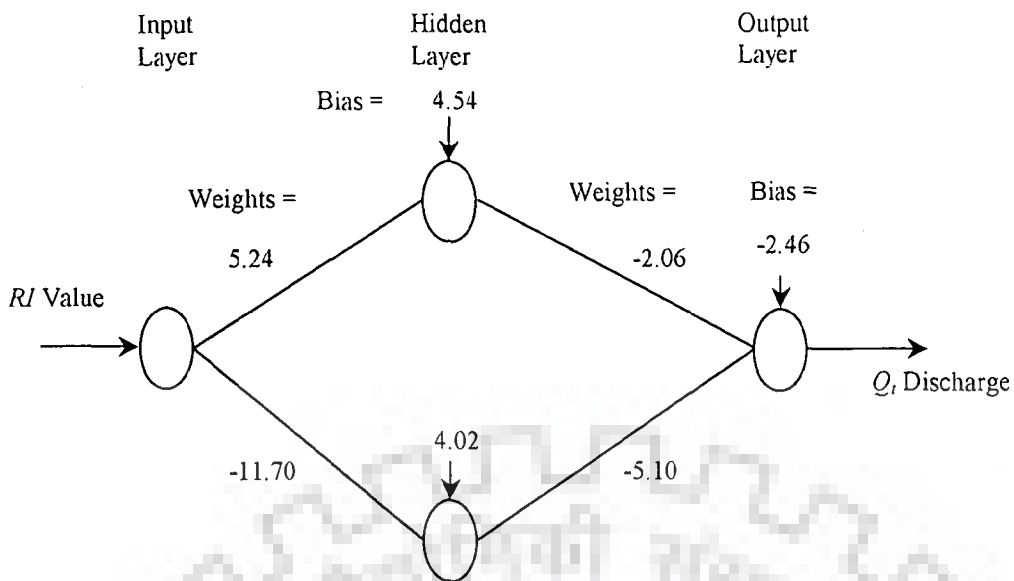


Narmada Catchment (Two Sub-Divisions) (2-3-1)

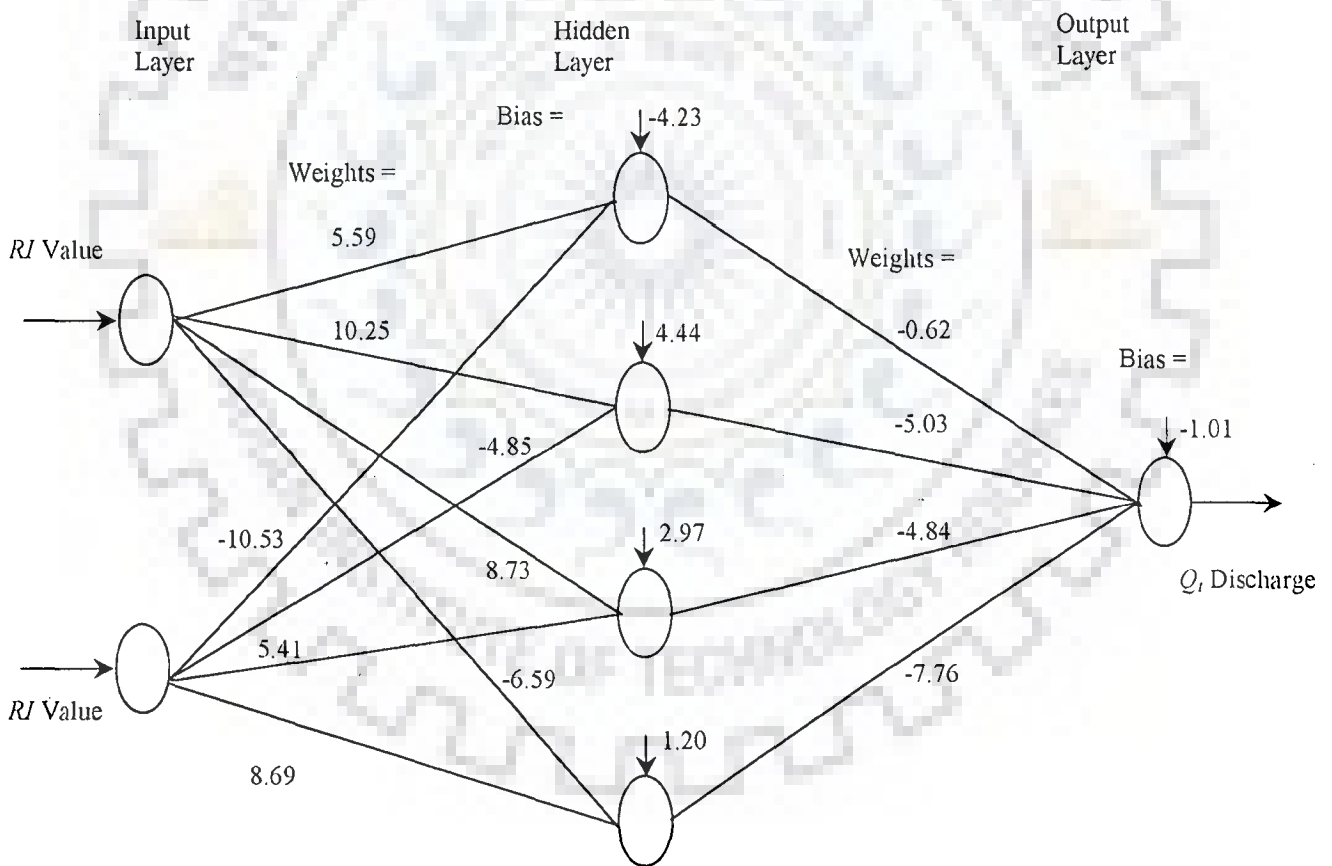


Narmada Catchment (Three Sub-Divisions) (3-1-1)

Fig. 6.15(d) The ANN Structures For Narmada Catchment (Two and Three Sub-Divisions)



Krishna Catchment (No Sub-Division) (1-2-1)



Krishna Catchment (Two Sub-Divisions) (2-4-1)

Fig. 6.15(e) The ANN Structures For Krishna Catchments (One and Two Sub-Divisions)

7.1 INTRODUCTION

An approach for modeling the rainfall-runoff process based on the application of an *ANN* is developed. The proposed approach couples the system based linear/nonlinear model and an *ANN* model. The advantages of the proposed approach include low cost and simplicity over the complex physically based models for the reason that measurement of precipitation and discharge can be obtained easily and cost effectively compared with the parameters such as soil characteristics, initial soil moisture, infiltration, ground water characteristics *etc.* required for most of the physically based and conceptual models. As the *ANN* model is calibrated using automated calibration techniques, it eliminates subjectivity involved in calibration and subsequent application of the conventional models.

While it is well established that the inclusion of the observed discharges in previous time periods with the current and antecedent rainfalls as inputs to the *ANN* greatly enhances its runoff forecasting ability in the updating case, the present study establishes convincingly that realistic estimates of runoff are obtainable using the *ANN* even without making use of the observed discharge/water level data of previous time periods. The flow simulation efficiency of the proposed approach is high for the non-updating flow simulation cases. Thus, present study demonstrates use of the *ANN* in a context that has not been used before. The broad and specific conclusions drawn on the basis of the study are stated below.

7.2 BROAD CONCLUSIONS

The study carried out with the objectives mentioned in chapter 1 lead to the broad conclusions as mentioned below.

- ☞ An approach for rainfall-runoff modeling on daily scale is proposed that uses *ANN* in a new perspective being coupled with the system based linear/nonlinear models for flow simulation in non-updating mode.
- ☞ The modeling of daily rainfall-runoff process presented in the study eliminates the subjectivity in determination of excess rainfall and base flow separation involved

in the *UH* based procedures used conventionally. This has been possible by consideration of rainfall for the memory length of a catchment as one of the inputs to the *ANN* based model. Thus, the rainfall-runoff process is modeled in such a way that the inputs supplied to the *ANN* have some relevance with the physical process being modeled.

- ☞ Losses due to evaporation and evapotranspiration have been accounted for as the rainfall-runoff modeling is carried out on daily scale and the simulated runoff events are spread over several days.
- ☞ The capability and effectiveness of the proposed methodology in sparse data scenario is demonstrated by using the daily rainfall and runoff data from seven catchments located in different parts of the world, two of which are relatively large in size.
- ☞ A viable alternative of providing the information about the soil moisture state of the catchment to the *ANN* in the form of the output of an auxiliary system based linear/nonlinear models is suggested.
- ☞ The *ANN*, when supplied with different inputs in two large sized catchments studied by way of sub-dividing these catchments into smaller areas resulted in improvement in the performance with the number of sub-divisions, thus demonstrating the capability of the *ANN* in understanding the distributed nature of inputs and producing appropriate results.
- ☞ The results obtained from the *ANN* model application in case of large size catchments prove that it is worthwhile to consider separate parallel inputs from the sub-catchments in order to account for the heterogeneity present in spatial distribution of rainfall data.

7.3 SPECIFIC CONCLUSIONS

The following specific conclusions are drawn on the basis of the study carried out.

A. Non-Linearity Analysis

- ☞ The non-linearity analysis based on the *SPDD* measure carried out for daily runoff shows that all the catchments studied are hydrologically nonlinear, thus the application of the *ANN* to these is justified.

B. Auxiliary Model Application

- ☞ The response functions of the auxiliary linear/nonlinear models obtained in all the catchments are physically realistic.
- ☞ The results from the application of auxiliary linear/nonlinear models indicate that such models are able to provide first approximate estimates for the runoff. The time to the peak of daily flows has been mostly well reproduced. However, the peak flows are either underestimated or overestimated by these models. Thus these models can very well serve as the auxiliary models, as they have ably reproduced the trend existing in the data.
- ☞ Parameterization of the response functions of auxiliary linear model by using the discrete gamma function lead to establishment of the relations, albeit qualitative, between these parameters and the catchment characteristics.

C. The ANN Model Application

- ☞ The results obtained demonstrate that the proposed alternative for discharges observed in the past being used as one of the input to the *ANN*, in the form of the output of the auxiliary system based linear/nonlinear models, provides better system theoretical representation of the rainfall-runoff relationship on catchments from varying climates investigated in the study.
- ☞ When the output of the linear model (*RIL*) in combination with rainfall (*P*) or the output of a nonlinear model (*RIN*) in combination *P* is supplied as input to the *ANN*, its performance is clearly superior to the case when the output of a linear or nonlinear model alone is given as input to the *ANN*.
- ☞ The coupled *SLM - ANN* model with *RIL* in combination with *P* as input is capable of producing reasonably satisfactory non-updated estimates of the outflows on most of the catchments.
- ☞ Replacing the linear model with a nonlinear model does not result in substantial improvement in the final results of the *ANN*, thus validating the capability of the *ANN* in taking care of the non-linearity existing in the input-output relationship.

- ☞ The coupled *SLM-ANN* model when supplied with the input *RIL* in combination with *P* has accurately estimated the time to peak runoff for various runoff events in all the catchments. The values of the peak and volume of runoff are also well simulated for most of the runoff events in all the catchments.
- ☞ Accurate results could also be obtained through the proposed methodology for large sized catchments by sub-dividing them into smaller homogeneous areas to account for the heterogeneity in spatial distribution of rainfall. The application of the *ANN* in the context of disaggregated rainfall indicates that the model results improve with increase in the number of sub-divisions. However, the maximum number of sub-divisions attempted in the present study were limited because of the limited number of rain gauge stations in a catchment resulting in some error in the areal averaging of rainfall.
- ☞ The research work carried out leads to the development of a cost effective methodology for runoff prediction that is simple to use, not catchment specific, and is capable of producing results with good accuracy.
- ☞ The algorithm used for training the *ANN* in the present study is widely available and used, so the proposed approach has no restrictions on its applicability and can be used almost in all the cases as desired.

7.4 SCOPE FOR FUTURE WORK

Several issues arise from this research that can be explored further. These issues can be stated as

1. Alternative *ANN* structures can be used and their performance with the new inputs proposed in the study can be examined and compared with the feedforward *ANN* used in the present study.
2. More efforts could be directed towards applying this approach to large number of catchments so that a more general relationship between the gamma function parameters and the catchment characteristics as attempted in the study could be established which may be helpful in extension of this approach to the ungauged catchments. For this purpose, the hypothesis that, the *ANN* model trained on hydrologically similar catchment can be applied to the catchment that is ungauged for discharge shall require thorough testing.

REFERENCES

- Abbott, M.B., Bathurst, J.C., Cunge, J.A., O'Connell, P.E., and Rasmussen, J. (1986 *a*) An introduction to the European hydrological system-Syste'me Hydrologique Europe'en, 'SHE' 1: History and philosophy of physically based distributed modeling system. *J. Hydrol.*, 87, 45 -59.
- Abbott, M.B., Bathurst, J.C., Cunge, J.A., O'Connell, P.E., and Rasmussen, J. (1986 *b*) An introduction to the European hydrological system-Syste'me Hydrologique Europe'en, 'SHE' 2: Structure of a physically based distributed modeling system. *J. Hydrol.*, 87, 61-77.
- Ahsan, M., and O'Connor, K.M. (1994) A simple nonlinear rainfall-runoff model with a variable gain factor. *J. Hydrol.*, 155, 151-183.
- Aitken, A.P. (1973) Assessing systematic errors in rainfall-runoff models. *J. Hydrol.*, 20, 121-136.
- Amorocho, J. (1963) Measures of the linearity of hydrologic system. *J. Geophys. Res.*, 68(8), 2237-2249.
- Amorocho, J. (1973) Nonlinear hydrologic analysis. *Advances in Hydrosociences*, 9, Academic Press, NY, 203-251.
- Amorocho, J., and Brandstetter, A. (1971) Determination of nonlinear response function in rainfall-runoff processes. *Water Resour. Res.*, 7(5), 1087-1101.
- Amorocho, J., and Hart, W.E. (1965) The use of laboratory catchments in the study of hydrologic systems. *J. Hydrol.*, 3, 106-123.
- Amorocho, J., and Orlob, G.T. (1961) Nonlinear analysis of hydrologic systems. Water Resources Center, University of California (Berkeley), USA, Contribution No. 40.
- Anmala, J., Zhang, B., and Govindaraju, R.S. (2000) Comparison of ANNs and empirical approaches for predicting watershed runoff. *J. Water Resour. Plng. and Mgmt.*, ASCE, 126(3), 156-166.
- ASCE Task Committee on Application of Artificial Neural Networks in Hydrology, (2000 *a*) Artificial neural networks in hydrology I: Preliminary concepts. *J. Hydrologic Engrg.* ASCE, 5(2), 115-123.

- ASCE Task Committee on Application of Artificial Neural Networks in Hydrology, (2000)
b) Artificial neural networks in hydrology II: Hydrologic applications. *J. Hydrologic Engrg.*, ASCE, 5(2), 124-137.
- Bender, D.L., and Roberson, J.A. (1961) The use of a dimensionless unit hydrograph to derive unit hydrographs from some Pacific Northwest basins. *J. Geophys. Res.*, 66, 521-527.
- Beven, K.J., and Kirkby, M.J. (1979) A physically based variable contributing area model of basin hydrology. *Hydrol. Sci. Bull.*, 24(1), 43-69.
- Beven, K.J. (1985) Distributed models. In *Hydrological Forecasting* M.G. Anderson and T.P. Burt (eds.), John Wiley and Sons Ltd., 405-435.
- Beven, K.J. (1987) Towards a new paradigm in hydrology. *IAHS Pub. No. 164*, 393-403.
- Beven, K.J. (1989) Changing ideas in hydrology-The case of physically based models. *J. Hydrol.*, 105, 157-172.
- Beven, K.J., Calver, A., and Morris, E.M. (1987) *The Institute of Hydrology Distributed Model*. Inst. Hydrol., Rep. No. 98, Wallingford (U.K.).
- Birikundavyi, S., Labib, R., Trung, H.T., and Rousselle, J. (2002) Performance of neural networks in daily streamflow forecasting. *J. Hydrologic Engrg.*, ASCE, 7(5), 392-398.
- Bishop, C.M. (1994) Neural networks and their applications. *Rev. Sci. Instrum.*, 65, 1803-1832.
- Bishop, C.M. (1995) *Neural networks for pattern recognition*. Clarendon Press, Oxford.
- Blank, D., Delleur, J.W., and Giorgini, A. (1971) Oscillatory kernel functions in linear hydrologic models. *Water Resour. Res.*, 7(5), 1102-1117.
- Bree, T. (1978) The stability of parameter estimation in the general linear model. *J. Hydrol.*, 37, 47-66.
- Brion, G.M., and Lingireddy, S. (1999) A neural network approach to identifying non point sources of microbial contamination. *Water Research*, 33(14), 3099-3106.
- Bruen, M., and Dooge, J.C.I. (1984) An efficient and robust method of estimating unit hydrograph ordinates. *J. Hydrol.*, 70, 1-24.
- Bruen, M., and Dooge, J.C.I. (1992 *a*) Unit hydrograph estimation with multiple events and prior information I: Theory and a computer program. *Hydrol. Sci. J.*, 37(5), 429-443.

- Bruen, M., and Dooge, J.C.I. (1992 *b*) Unit hydrograph estimation with multiple events and prior information II: Evaluation of the method. *Hydrol. Sci. J.*, 37(5), 445-462.
- Burian, S.J., Durrans, S.T., Pimmel, R.L., and Wai, C.N. (2000) Rainfall disaggregation using artificial neural networks. *J. Hydrologic Engrg., ASCE*, 5(3), 299-307.
- Burnash, J.R.E., Ferral, R.L., and McGuire, R.A. (1973) A generalized streamflow simulation system. Report, Joint Fed. – State River Forecast Centre, Sacramento, CA.
- Campolo, M., Andreussi, P., and Soldati, A. (1999) River flood forecasting with a neural network model. *Water Resour. Res.*, 35(4), 1191-1197.
- Carpenter, G.A., and Grossberg, S. (1987) ART2 Self organization of stable category of analog input patterns. *Applied Optics*, 26(3), 4919-4930.
- Carriere, P., Mohagheghs, S., and Gaskari, R. (1996) Performance of a virtual runoff hydrograph system. *J. Water Resour. Plng. and Mgnt., ASCE*, 122(6), 421-427.
- Caudill, M. (1987) Neural networks primer: Part I. *AI Expert*, December, 46-52.
- Chandramauli, V., and Raman, H. (2001) Multireservoir modeling with dynamic programming and neural networks. *J. Water Resour. Plng. and Mgnt., ASCE*, 127(2), 89-98.
- Chow, V.T. (1964) *Handbook of applied hydrology*. New York, McGraw Hill.
- Chow, V.T., Maidment, D.R., and Mays, L.W. (1988) *Applied hydrology*. McGraw Hill Book Co. Singapore.
- Clark, C.O. (1944) Flood storage accounting. *Trans. American Geophy. Union*, 25, 1014 - 1039.
- Clark, C.O. (1945) Storage and the unit hydrograph. *Trans. ASCE*, 110, 1419-1446.
- Clarke, R.T. (1971) The use of the term linearity as applied to hydrological models. *J. Hydrol.*, 13, 91-95.
- Clarke, R.T. (1973) A review of some mathematical models used in hydrology with observations on their calibration and use. *J. Hydrol.*, 19, 1-19.
- Collins, W.T. (1939) Runoff distribution graphs from precipitation occurring in more than one time unit, *Civil Engrg.*, 9(9), 559-561.
- Coulibaly, P., Anctil, F., and Bobee, B. (2000) Daily reservoir inflow forecasting using artificial neural networks with stopped training approach. *J. Hydrol.*, 230, 244 – 257.

- Crawford, N.H., and Linsley, R.K. (1966) Digital simulation of hydrology: The Stanford Watershed Model IV. Technical Report 39, Department of Civil Engineering, Stanford University, Palo Alto, California, USA.
- Dawson, C.W., and Wilby, R. (1998) An artificial neural network approach to rainfall runoff modeling. *Hydrol. Sci. J.*, 43(1), 47-66.
- Deininger, R.A. (1969) Linear programming for hydrologic analysis. *Water Resour. Res.*, 5(5), 1105-1109.
- Delleur, J.W., and Rao, A.R. (1971) Linear system analysis hydrology, the transform approach, the kernel oscillations and the effect of noise. In *Systems Approach to Hydrology*, V. Yevjevich (eds.), Fort Collins, Water Resour. Pub., 116-130.
- De Villars, S.J., and Bernard, E. (1993) Backpropagation neural nets with one and two hidden layers. *IEEE Trans. Neural Networks*, 4(1), 136-141.
- Diskin, M.H., and Boneh, A. (1973) Determination of optimal kernels for second order stationary surface runoff systems. *Water Resour. Res.*, 9(2), 311-325.
- Diskin, M.H., and Boneh, A. (1975) Determination of an optimal IUH for linear, time invariant systems from multistorm records. *J. Hydrol.*, 24, 57-76.
- Diskin, M.H., and Boneh, A. (1980) Discussion on 'Optimization of unit hydrograph determination' by Mays and Coles, (1980). *J. Hydr. Engrg., ASCE*, 106(11), 1951-1954.
- Diskin, M.H., Boneh, A., and Golan, A. (1984) Identification of a Volterra series conceptual model based on a cascade of nonlinear reservoirs. *J. Hydrol.*, 68, 231-245.
- Dooge, J.C.I. (1959) A general theory of the unit hydrograph. *J. Geophys. Res.* 64(2), 241-256.
- Dooge, J.C.I. (1965) Analysis of linear systems by means of Laguerre functions. *SIAM J. Control*, 2(3), 396-408.
- Dooge, J.C.I. (1973) Linear theory of hydrologic systems. Tech. Bull. No. 1468, Agril. Res. Service, USDA, Washington, D.C.
- Dooge, J.C.I. (1977) Problems and methods of rainfall-runoff modeling. In T.A. Giriani, V. Maione, and J.R. Wallis (eds.) *Mathematical Models for Surface Water Hydrology*, John Wiley, NY, 71-108.
- Dooge, J.C.I., and Bruen M. (1989) Unit hydrograph stability and linear algebra. *J. Hydrol.*, 111, 377-390.

- Duan, Q., Sorooshain, S., and Gupta, V.K. (1992) Effective and efficient global optimization of conceptual rainfall-runoff models. *Water Resour. Res.*, 28(4), 1015-1031.
- Eagelson, P.S.R., Mejia-R., and March, F. (1966) Computation of optimum realizable unit hydrographs. *Water Resour. Res.*, 2(4), 755-764.
- Elshorbagy, A., and Simonovic, S.P., (2000) Performance evaluation of artificial neural networks for runoff prediction. *J. Hydrologic Engrg., ASCE*, 5(4), 424-427.
- Engman, E.T., and Rogowski, A.S. (1974) A partial area model for storm flow synthesis. *Water Resour. Res.*, 10(3), 464-472.
- Fahlman, S.E., and Leberie, C. (1991) The cascade-correlation learning architecture. CMU Tech. Rep., CMU-CS-90-100, Carnegie Mellon University, Pittsburgh, PA.
- Fausett, L. (1994) Fundamentals of neural networks. Prentice Hall, Englewood Cliffs, NJ.
- Fernando, D.A.K., and Jayawardena, A.W. (1998) Runoff forecasting using RBF networks with OLS algorithm. *J. Hydrologic Engrg., ASCE*, 3(3), 203-209.
- French, M.N., Krajewski, W. F., and Cuykendall, R.R. (1992) Rainfall forecasting in space and time using a neural network. *J. Hydrol.*, 137, 1-31.
- Gautam, M.R., Watanabe, K., and Saegusa, H. (2000) Runoff analysis in humid forest catchment with artificial neural network. *J. Hydrol.*, 235, 117-136.
- Gray, D.M. (1961) Synthetic unit hydrographs for small watersheds. *J. Hydr. Engrg., ASCE*, 87(4), 33-54.
- Gupta, H.V., Hsu, K.L., and Sorooshian, S. (1997) Superior training of artificial neural networks using weight space partitioning. Proc. IEEE Intl. Conf. on Neural Networks, June 9-12, Houston, Texas (USA).
- Gupta, V.K., and Sorooshian, S. (1985) the relationship between data and the precision of parameter estimates of hydrologic models. *J. Hydrol.* 81, 57-77.
- Gupta, V.K., Waymire, E., and Wang, C.T. (1980) A representation of an instantaneous unit hydrograph from geomorphology. *Water Resour. Res.*, 16(5), 855-862.
- Halff, A.H., Halff, H.M., and Azmoodeh, M. (1993) Predicting runoff from rainfall using neural networks. Proc. Engrg. Hydrol., ASCE, NY, 760-765.
- Hall, M. J., and Minns, A.W. (1998) Regional flood frequency analysis using artificial neural networks. Proc. Hydroinformatics, Copenhagen, Vol. 2, 759-763.
- Hall, M.J., and Minns, A.W. (1999) The classification of hydrologically homogeneous regions. *Hydrol. Sci. J.*, 44(5), 693-704.

- Hall, M.J., Minns, A.W., and Ashrafuzzaman, A.K.M. (2000) Regional flood frequency analysis using artificial neural networks: A case study. Proc. Hydroinformatics, Cedar Rapids.
- Hassoun, M.H. (1995) Fundamentals of artificial neural networks. MIT Press.
- Haykin, S. (1994) Neural networks a comprehensive foundation. Macmillan, NY.
- Hebb, D.O. (1949) The organization of behavior: A neurophysical theory. Wiley, New York.
- Hecht-Nielsen, R. (1987) Counter propagation networks. J. App. Optics, 26(3), 4979-4984.
- Hecht-Nielsen, R. (1990) Neurocomputing. Addison-Wesley Publ. Co., Reading, Mass.
- Heggen, R.J. (1995) Discussion on 'Neural networks for river flow prediction' by Karunanithi *et al.* (1994). J. Comp. Civil Engrg., ASCE, 9(5), 293.
- Helweg, O.J., Amorocho, J., and Finch, R.H. (1982) Improvements of nonlinear rainfall runoff model. J. Hydr. Engrg., ASCE, 108(7), 813-822.
- Hinton, G.E. (1989) Connectionist learning procedures. Artificial Intelligence, 40, 185-234.
- Hjelmfelt, A.T., and Wang, M. (1993) Artificial neural networks as unit hydrograph applications. Proc. Engrg. Hydrol., ASCE, NY, 745-759.
- Hjelmfelt, A.T., and Wang, M. (1996) Predicting runoff using artificial neural networks. Surface Water Hydrol., 233-244.
- Hopfield, J.J. (1982) Neural networks and physical system with emergent collective conceptual abilities. Proc. National Academy of Science, 79, 2554-2558.
- Hornik, K., Stinchcombe, M., and White, M. (1989) Multilayer feedforward networks are universal approximators. Neural Networks, 2, 359-366.
- Hsu, K. L., Gupta, H.V., and Sorooshian, S. (1995) Artificial neural network modeling of the rainfall-runoff process. Water Resour. Res., 31(10), 2517-2530.
- Hsu, K.L., Gupta, H.V., and Sorooshian, S. (1997 *a*) Precipitation estimation from remotely sensed information using artificial neural networks. J. App. Meteorology, 36(9), 1176-1190.
- Hsu, K.L., Gupta, H.V., and Sorooshian, S. (1997 *b*) Application of recurrent neural network to rainfall-runoff modeling. Proc. Conf. Aesthetics in Constructed Envir., ASCE, NY, 68 -73.

- Hsu, K.L., Gupta, H.V., and Sorooshian, S. (1998) Streamflow forecasting using artificial neural networks, Proc. Conf. Water Res. Engrg., ASCE, Memphis, Tennessee, 967-972.
- Hsu, K.L., Gupta, H.V., Gao, X., and Sorooshian, S. (1999) Estimation of physical variables from multichannel remotely sensed imagery using a neural network: Application to rainfall estimation. *Water Resour. Res.*, 35(5), 1605-1618.
- Hu, T.S., Lam, K.C., Ng, S.T. (2001) River flow time series prediction with a range dependent neural network. *Hydrol. Sci. J.*, 46(5), 729-745.
- Imrie, C.E., Durucan, S., and Korre, A. (2000) River flow prediction using artificial neural networks: generalization beyond the calibration range. *J. Hydrol.*, 233, 138-153.
- Islam, S., and Kothari, R. (2000) Artificial neural networks in remote sensing of hydrologic processes. *J. Hydrologic Engrg., ASCE*, 5(2), 138-144.
- Jain, S.K., and Chalisgaonkar, D. (2000) Setting up stage-discharge relations using ANN. *J. Hydrologic Engrg., ASCE*, 5(4), 428-433.
- Jain, S.K., Das, D., and Shrivastava, D.K. (1999) Application of ANN for reservoir inflow prediction and operation, *J. Water Resour. Plng. Mgnt., ASCE*, 125(5), 263-271.
- Johnson, V.M., and Rogers, L.L. (1995) Location analysis in groundwater remediation using neural networks. *Groundwater*, 33(5), 749-758.
- Kachroo, R.K. (1992) River flow forecasting Part 1: A discussion of the principles. *J. Hydrol.*, 133, 1-15.
- Kachroo, R.K., and Liang, G.C. (1992) River flow forecasting Part 2: Algebraic development of linear modeling techniques. *J. Hydrol.*, 133, 17-40.
- Kachroo, R.K., and Natale, L. (1992) Nonlinear modeling of rainfall-runoff transformation. *J. Hydrol.*, 135, 341-369.
- Kachroo, R.K., Sea, C.H., Warsi, M.S., Jemener, H., and Saxena, R.P. (1992) River flow forecasting Part 3: Application of linear techniques in modeling rainfall-runoff transformation. *J. Hydrol.*, 133, 41-97.
- Kartalopoulos, S.T. (2000) Understanding neural networks and fuzzy logic: Basic concepts and applications. Prentice-Hall of India Pvt. Ltd., New Delhi.
- Karunanithi, N., Grenney, W.J., Whitley, D., and Bovee, K. (1994) Neural networks for river flow prediction. *J. Comp. Civil Engrg., ASCE*, 8(2), 201-220.
- Khalil, M., Panu, U.S., and Lennox, W.C. (2001) Groups and neural networks based streamflow data infilling procedures. *J. Hydrol.*, 241, 153-176.

- Kitanidis, P.K., and Bras, R.L. (1979) Collinearity and stability in the estimation of rainfall-runoff model parameters. *J. Hydrol.*, 42, 91-108.
- Klemes, V. (1982) Empirical and causal models in hydrology. Chapter 8 in *Scientific Basis of Water Resource Management*, Washington, D.C., National Academy Press, 95-104.
- Kohonen, T. (1989) *Self organization and associative memory*. Springer Verlag, NY.
- Kohonen, T. (1990) The self organizing map. *Proc. IEEE*, 78, 1464-1480.
- Kothyari, U.C., and Singh, V.P. (1999) Multiple input single output model for flow forecasting. *J. Hydrol.*, 220, 12-26.
- Kothyari, U.C., Aravamuthan, V., and Singh, V.P. (1993) Monthly runoff generation using the linear perturbation model. *J. Hydrol.*, 144, 371-379.
- Kulandaiswamy, V.C. (1964) A basic study of the rainfall excess surface runoff relationship in a basin system. Ph. D. dissertation, University Illinois, Urbana.
- Kumar, A., and Minocha, V.K. (2001) Discussion on 'Rainfall runoff modeling using artificial neural networks' by Tokar and Johnson (1999). *J. Hydrologic Engrg., ASCE*, 6(3), 176-177.
- Kumar, M., Raghuwanshi, N.S., Singh, R., Wallender, W.W., and Pruitt, W.O. (2002) Estimating evapotranspiration using artificial neural networks. *J. Irrig. and Drg. Engrg., ASCE*, 128(4), 224-233.
- Kutchment, L.S. (1967) Solution to inverse problem for linear flow models. *Sov. Hydrol. Select. Pap.*, 2, 194-199.
- Kutchment, L.S. (1980) A two-dimensional rainfall-runoff model: Identification of parameters and possible use for hydrological forecasts. In *Hydrological Forecasting*, IAHS Pub., 129, 215-219.
- Laurenson, E.M., and O'Donnell, T. (1969) Data error effects in unit hydrograph derivation. *J. Hydr. Engrg., ASCE*, 95(6), 1899-1917.
- Levi, E., and Valdes, E. (1964) A method for direct analysis of hydrographs. *J. Hydrol.*, 2, 182-190.
- Liang, G.C. (1988) Identification of multiple input single output linear time invariant model for hydrological forecasting. *J. Hydrol.*, 101, 251-262.
- Liang, G.C., and Nash, J.E. (1988) Linear models for river flow routing on large catchments. *J. Hydrol.*, 103, 153-188.

- Liang, G.C., O'Connor, K.M., and Kachroo, R.K. (1994) A multiple input single output variable gain factor model. *J. Hydrol.*, 155, 185-198.
- Linsley, R.K. (Jr.), Kohler, M.A., and Paulhus, J.L. (1958) *Hydrology for engineers*. McGraw - Hill Book Co. Inc., NY.
- Loague, K.M., and Freeze, R.A. (1985) A comparison of rainfall-runoff modeling techniques on small upland catchments. *Water Resour. Res.*, 21(2), 229-248.
- Lorrai, M., and Sechi, G.M. (1995) Neural nets for modeling rainfall-runoff transformations. *Water Resour. Mgnt.*, 9, 299-313.
- Maier, H.R., and Dandy, G.C. (1996) The use of artificial neural networks for prediction of water quality parameters. *Water Resour. Res.*, 32(4), 1013-1022.
- Mason, J.C., Price, R.K., and Tem'ne, A. (1996) A neural network model for rainfall-runoff using radial basis functions. *J. Hydr. Res., Proc. IAHR*, 34(4), 537-548.
- Mawdsley, J.A., and Tagg, A.F. (1981) Identification of unit hydrographs from multi-event analysis. *J. Hydrol.*, 49, 315-327.
- Mays, L.W., and Coles, L. (1980) Optimization of unit hydrograph determination. *J. Hydr. Engrg., ASCE*, 106(1), 85-97.
- Mays, L.W., and Taur, C.K. (1982) Unit hydrographs via nonlinear programming. *Water Resour. Res.*, 18(4), 744-752.
- McCuen, R.H. (1993) *Statistical hydrology*. Prentice Hall, Englewood Cliffs, NJ.
- McCuen, R.H. (1997) *Hydrologic analysis and design*. 2nd Ed., Prentice-Hall, Upper Saddle River, NJ.
- McCuen, R.H., and Snyder, W.M. (1986) *Hydrological modeling: Statistical methods and applications*. Prentice-Hall Inc., Englewood Cliffs, NJ.
- McCulloch, W.S., and Pitts, W. (1943) A logic calculus of the ideas immanent in nervous activity. *Bull. Math. Biophys.*, 5, 115-133.
- Mimikou, M. (1983) A study of drainage basin linearity and nonlinearity. *J. Hydrol.*, 64, 113-134.
- Minns, A.W., and Hall, M.J. (1996) Artificial neural networks as rainfall-runoff models. *Hydrol. Sci. J.*, 41(3), 399-417.
- Minshall, N.E. (1960) Predicting storm runoff on small experimental watersheds, *J. Hydr. Engrg., ASCE*, 86(8), 17-38.
- Muftuoglu, R.F. (1984) New models for nonlinear catchment analysis. *J. Hydrol.*, 73, 335-357.

- Muftuoglu, R.F. (1991) Monthly runoff generation by nonlinear models. *J. Hydrol.*, 125, 277-291.
- Mulvany, T.J. (1850) On the use of self-registering rain and flood gauges. *Proc. Inst. of Civil Engineers, Dublin, Ireland*, 4(2), 1-8.
- Muttaih, R.S., Srinivasan, R., and Allen, P.M. (1997) Prediction of two-year peak stream discharges using neural networks. *J. American Water Resour. Assoc.*, 33(3), 625-630.
- Nash, J.E. (1957) The form of the instantaneous unit hydrograph. In: *General Assembly of Toronto, 3-14 September 1957, Vol. III, Surface Water, Prevision, Evaporation*, IASH Pub. 45(3), 114-121.
- Nash, J.E. (1959) Systematic determination of unit hydrograph parameters. *J. Geophy. Res.*, 64(1), 111-115.
- Nash, J.E. (1960) A unit hydrograph study, with particular reference to British catchments. *Proc. of the Institution of Civil Engineers, London*, 17, 249-282.
- Nash, J.E., and Barsi, B.I. (1983) A hybrid model for flow forecasting on large catchments. *J. Hydrol.*, 65, 125-137.
- Nash, J.E., and Foley, J.J. (1982) Linear models of rainfall-runoff system. In V.P. Singh (eds.) *Rainfall-Runoff Relationship*, Water Resour. Pub., 51-66.
- Nash, J.E., and Sutcliffe, J.V. (1970) River flow forecasting through conceptual models, part 1 - a discussion of principles. *J. Hydrol.*, 10, 282-290.
- Navone, H.D., and Ceccatto, H.A. (1994) Predicting Indian monsoon rainfall: A neural network approach. *Climate Dynamics*, 10, 305-312.
- Newton, D.W., and Vinyard, J.W. (1967) Computer determined unit hydrograph from floods. *J. Hydr. Engrg., ASCE*, 93(5), 19-35.
- O'Connor, K.M., and Ahsan, M. (1991) Estimation of the gain factor for a discrete linear time-invariant system when input and output series each have zero mean. *J. Hydrol.*, 128, 335-355.
- O'Donnell, T. (1960) Instantaneous unit hydrograph derivation by harmonic analysis. *IASH Pub. No. 51*, 546-557.
- O'Kelly, J.J. (1955) The employment of unit hydrograph to determine the flows of Irish arterial drainage channels. *Proc. of the Institution of Civil Engineers, Dublin, Ireland*, 4(3), 365-412.

- Ooyen, A.V., and Nichhuis, B. (1992) Improving the convergence of backpropagation problem. *Neural Networks*, 5, 465-471.
- Papamichail, D.M., and Papazafiriou, Z.G. (1992) Multiple input single output functional models for river flow routing. *J. Hydrol.*, 133, 365-377.
- Papazafiriou, Z.G. (1976) Linear and nonlinear approaches for short-term runoff estimations in time-invariant open hydrologic systems. *J. Hydrol.*, 30, 63-80.
- Powell, M.J.D. (1985) Radial basis function for multi variable interpolation: A review. *Proc. IMA Conf. Algorithm for the approximation of function and data*, RMCS, Shrivenham.
- Raman, H., and Chandramouli, V. (1996) Deriving a general operating policy for reservoirs using neural networks. *J. Water Resour. Plng. and Mgnt.*, ASCE, 122(5), 342-347.
- Raman, H., and Sunilkumar, N. (1995) Multivariate modeling of water resources time series using artificial neural networks. *Hydrol. Sci. J.*, 40, 145-163.
- Ranjithan, S., Eheast, J.W., and Garrett, J.H. (Jr.) (1993) Neural network based screening for groundwater reclamation under uncertainty. *Water Resour. Res.*, 29(3), 563-574.
- Rao, A.R., and Tirtotjondro, W. (1995) Computation of unit hydrograph by a Bayesian method. *J. Hydrol.* 164, 325-344.
- Rao, K.N., George, C.J., and Ramasastri, K.S. (1976) The climatic water balance of India. *India Meteorological Department*, Vol. XXXII, Part III.
- Ray, C., and Kindworth, K.K. (2000) Neural networks for agrochemical vulnerability assessment of rural private wells. *J. Hydrologic Engrg.*, ASCE, 5(2), 162-171.
- Refsgaard, J.C., Seth, S.M., Bathurst, J.C., Erlich, M., Storm, B., Jorgensen, G.H., and Chandra, S. (1992) Application of the SHE to catchments in India, part 1: general results. *J. Hydrol.*, 140, 1-23.
- Rockwood, D.M. (1982) Theory and practice of the SSARR model as related to analyzing and forecasting the response of hydrologic systems. *Applied Modeling of Catchment Hydrology*, V.P. Singh (eds.) *Water Resources Pub.*, Littleton, Colo., 87-106.
- Rodriguez-Iturbe, I., and Valdes, J.B. (1979) The geomorphologic structure of hydrologic responses. *Water Resour. Res.*, 15(6), 1409-1420.

- Rogers, L.L., and Dowla, F.U. (1994) Optimization of groundwater remediation using artificial neural networks with parallel solute transport modeling. *Water Resour. Res.*, 30(2), 457-481.
- Rogers, W.F. (1980) A practical model for linear and nonlinear runoff. *J. Hydrol.*, 46, 51-78.
- Rogers, W.F. (1982) Some characteristics and implications of drainage basin linearity and nonlinearity. *J. Hydrol.*, 55, 247-265.
- Rogers, W.F., and Zia, H.A. (1982) Linear and nonlinear runoff from large drainage basins. *J. Hydrol.*, 55, 267-278.
- Rosenblatt, F. (1958) The perceptron: A probabilistic model for information storage and organization in the brain. *Psychological Review*, 65, 386-407.
- Ross, B.B., Contractor, D.N., and Shanholz, V.O. (1979) A finite element model of overland and channel flow for assessing the hydrological impact of land use change. *J. Hydrol.*, 41, 11-30.
- Rumelhart, D.E., Hinton, G.E., and Williams, R.J. (1986) Learning internal representation by error propagation. In D.E. Rumelhart, and J.L. McClelland (eds.) *Parallel Distributed Processing Explorations in the Microstructure of Cognition, Vol. I*, MIT Press, Cambridge, MA 318-362.
- Rumelhart, D.E., Widrow, B., and Lehr, M.A. (1994) The basic idea in neural networks. *Communications of ACM*, 37(3), 87-92.
- Sajikumar, N., and Thandaveswara, B.S. (1999) A nonlinear rainfall-runoff model using an artificial neural network. *J. Hydrol.*, 216, 32-55.
- Sarma, P.B.S., Delleur, J.W., and Rao, A.K. (1973) Comparison of rainfall-runoff models for urban areas. *J. Hydrol.*, 18, 329-367.
- Shamseldin, A.Y. (1997) Application of a neural network technique to rainfall-runoff modeling. *J. Hydrol.*, 199, 272-294.
- Shamseldin, A.Y., and O'Connor, K.M. (1999) A real-time combination method for the outputs of different rainfall-runoff models. *Hydrol. Sci. J.*, 44(6), 895-912.
- Shamseldin, A.Y., O'Connor, K.M., and Liang, G.C. (1997) Methods for combining the outputs of different rainfall-runoff models. *J. Hydrol.*, 199, 203-229.
- Sherman, L.K. (1932) Streamflow from rainfall by the unit graph method. *Engrg. News Record*, 108, 501-505.

- Shin, H.S., and Salas, J.D. (2000) Regional drought analysis based on neural networks. *J. Hydrologic Engrg.*, ASCE, 5(2), 145-155.
- Singh, K.P. (1964) Nonlinear instantaneous unit hydrograph theory. *J. Hydr. Engrg.*, ASCE, 90(2), 313-347.
- Singh, K.P. (1976) Unit hydrographs: a comparative study. *Water Resour. Bull.*, 12(2), 381-392.
- Singh, V.P. (1982) A survey of water yield. *Proc. Intl. Symp. on Hydrological Aspects of Mountainous Watersheds*, University of Roorkee, Roorkee (India), Nov. 4-6, III-9 – III-18.
- Singh, V.P. (1988) *Hydrologic systems, vol. 1: rainfall-runoff modeling*. Prentice Hall, Englewood Cliffs, NJ.
- Singh, V.P. (1994) *Elementary hydrology*. Prentice Hall of India, New Delhi.
- Singh, V.P., and Aminian, H. (1986) An empirical relation between volume and peak of direct runoff. *Water Resour. Bull.*, AWRA, 22(5), 725-730.
- Singh, V.P., and Woolhiser, D.A. (2002) Mathematical modeling of watershed hydrology. ASCE 150th Anniversary Paper, *J. Hydrologic Engrg.*, ASCE, 7(4), 270-292.
- Sivakumar, B., Jayawardena, A.W., and Fernando, T.M.K.G. (2002) River flow forecasting: use of phase-space reconstruction and artificial neural networks approaches. *J. Hydrol.*, 265, 225-245.
- Sivapalan, M., Jothityangkoon, C., and Menabde, M. (2002) Linearity and nonlinearity of basin response as a function of scale: discussion of alternative definitions. *Water Resour. Res.*, 38(2), 4-1 – 4-5.
- Smith, J., and Eli, R.N. (1995) Neural network models of rainfall-runoff process. *J. Water Resour. Plng. Mgnt.*, ASCE, 121(6), 499-508.
- Smith, R.E., and Woolhiser, D.A. (1971) Overland flow on an infiltrating surface. *Water Resour. Res.*, 7(4), 899-913.
- Snyder, F.F. (1938) Synthetic unit graphs. *Trans. American Geophy. Union*, 19, 447-454.
- Snyder, W.M. (1955) Hydrograph analysis by the method of least squares. *J. Hydr. Engrg.*, ASCE, 81, Paper No. 793.
- Soil Conservation Service (SCS) (1972) Travel time, time of concentration, and lag. *National Engineering Handbook*, 15-1 to 15-16, USDA, Washington, D.C.

- Sorooshian, S., Hsu, K.L., Gao, X., Gupta, H.V., Imam, B., and Braithwaite, D. (2000) Evaluation of PERSIANN system satellite based estimates of tropical rainfall. *Bull. Amer. Meteorol. Soc.*, 81(9), 2035-2046.
- Sudheer, K.P., Gosain, A.K., Nayak, P.C., and Rangam, D.M. (2000) River flow forecasting through artificial neural network approach. *Proc. Recent Advances in Hydraulics and Water Resources Engrg.*, (HYDRO, 2000), Kurukshetra, (India), 79-86.
- Sugawara, M.I., Watanabe, I., Ozaki, E., and Katsuyame, Y. (1983) Reference manual for the Tank model. Report, National Resources Center for Disaster Prevention, Tokyo, Japan.
- Thandaveswara, B.S., and Sajikumar, N. (2000) Classification of river basins using artificial neural network. *J. Hydrologic Engrg.*, ASCE, 5(3), 290-298.
- Thirumalaih, K., and Deo, M.C. (2000) Hydrological forecasting using neural networks. *J. Hydrologic Engrg.*, ASCE, 5(2), 180-189.
- Tingsanchali, T., and Gautam, M.R. (2000) Application of Tank, NAM, ARMA and neural network models to flood forecasting. *Hydrol. Process.*, 14(14), 2473-2487.
- Todini, E. (1988) Rainfall-runoff modeling - past, present and future. *J. Hydrol.*, 100, 341-352.
- Tokar, A.S., and Johnson, P.A. (1999) Rainfall-runoff modeling using artificial neural networks. *J. Hydrologic Engrg.*, ASCE, 4(3), 232-239.
- Tokar, A.S., and Markus, M. (2000) Precipitation runoff modeling using artificial neural networks and conceptual models. *J. Hydrologic Engrg.*, ASCE, 5(2), 156-161.
- Turner, J.E., Dooge, J.C.I, and Bree, T. (1989) Deriving the unit hydrograph by root selection. *J. Hydrol.*, 110, 137-152.
- Unver, O., and Mays, L.W. (1984) Optimal determination of loss rate functions and unit hydrographs. *Water Resour. Res.*, 20(2), 203-214.
- Wen, C.G., and Lee, C.S., (1998) A neural network approach to multiobjective optimization for water quality management in a river basin. *Water Resour. Res.*, 34(3), 427-436.
- Werbos, P. (1974) Beyond regression: New tools for prediction and analysis in the behavioral sciences. Ph.D. Dissertation, Harvard University, Cambridge, Mass.
- Wilkinson, J.H. (1965) *The Algebraic-Eigenvalue problem*. Oxford University Press, Oxford.

- WMO (1975) Intercomparison of conceptual models used in operational hydrological forecasting. Operational Hydrol. Rep. No. 7, WMO No. 429, Geneva, 172 pp.
- Wood, E.F., and O'Connell, P.E. (1985) Real time forecasting. In Hydrological Forecasting M.G. Anderson and T.P. Burt (eds.), John Wiley and Sons Ltd., 505-558.
- Wright, N.G., and Dastorani, M.T. (2001) Effects of river basin classification on artificial neural networks based ungauged catchment flood prediction. Proc. Intl. Symp. Environ. Hydraulics.
- Xiong, L., O'Connor, K.M., and Goswami, M. (2001) Application of the artificial neural network in flood forecasting on a Karstic catchment, Proc. XXIX IAHR Congress, China, 29-35.
- Zealand, C., Burn, D.H., and Simonovic, S.P. (1999) Short-term streamflow forecasting using artificial neural networks. J. Hydrol., 214, 32-48.
- Zhang, B., and Govindaraju, R.S. (2000) Prediction of watershed runoff using Bayesian concepts and modular neural networks. Water Resour. Res., 36(3), 753-762.
- Zhang, Q., and Stanley, S.J. (1997) Forecasting raw water quality parameters for the north Saskatchewan river by neural network modeling. Water Research, 31(9), 2340-2350.
- Zhao, B., Tung, Y.K., and Yang, J.C. (1995) Estimation of unit hydrograph by ridge least squares method. J. Irrig. and Drg. Engrg., ASCE, 121(3), 253-259.
- Zhu, M.L., and Fujitha, M. (1994) Comparison between fuzzy reasoning and neural network methods to forecast runoff discharge. J. Hydrosoci. Hydr. Engrg., 12(2), 131-141.

PUBLICATIONS FROM THE THESIS

International Journals

1. **Rajurkar M. P.**, Kothyari, U.C., and Chaube U.C. (2002) “Artificial Neural Network for Daily Rainfall-Runoff Modeling”, Hydrological Sciences Journal, 47(6), Dec. Issue.
2. **Rajurkar M. P.**, Kothyari, U.C., and Chaube U.C. “Modeling of The Daily Rainfall-Runoff Relationship with an Artificial Neural Network” Tentatively accepted in the Journal of Hydrology, Elsevier, The Netherlands, (Review Communicated).

International Conference

1. **Rajurkar M. P.**, Kothyari, U.C., and Chaube U.C. (2002) “Daily Rainfall-Runoff Modeling using Artificial Neural Network”, Proc. of 13th APD-IAHR International Congress, Singapore, August 6-8, Vol. 2, 702-707.